frontiers | Research Topics

Women in parasitology

2021

Edited by
Alessia Libera Gazzonis, Simona Gabrielli and Serena Cavallero

Published in
Frontiers in Veterinary Science

ISSN 1664-8714
ISBN 978-2-83252-144-1
DOI 10.3389/978-2-83252-144-1

About Frontiers

Frontiers is more than just an open access publisher of scholarly articles: it is a pioneering approach to the world of academia, radically improving the way scholarly research is managed. The grand vision of Frontiers is a world where all people have an equal opportunity to seek, share and generate knowledge. Frontiers provides immediate and permanent online open access to all its publications, but this alone is not enough to realize our grand goals.

Frontiers journal series

The Frontiers journal series is a multi-tier and interdisciplinary set of open-access, online journals, promising a paradigm shift from the current review, selection and dissemination processes in academic publishing. All Frontiers journals are driven by researchers for researchers; therefore, they constitute a service to the scholarly community. At the same time, the *Frontiers journal series* operates on a revolutionary invention, the tiered publishing system, initially addressing specific communities of scholars, and gradually climbing up to broader public understanding, thus serving the interests of the lay society, too.

Dedication to quality

Each Frontiers article is a landmark of the highest quality, thanks to genuinely collaborative interactions between authors and review editors, who include some of the world's best academicians. Research must be certified by peers before entering a stream of knowledge that may eventually reach the public - and shape society; therefore, Frontiers only applies the most rigorous and unbiased reviews. Frontiers revolutionizes research publishing by freely delivering the most outstanding research, evaluated with no bias from both the academic and social point of view. By applying the most advanced information technologies, Frontiers is catapulting scholarly publishing into a new generation.

What are Frontiers Research Topics?

Frontiers Research Topics are very popular trademarks of the *Frontiers journals series*: they are collections of at least ten articles, all centered on a particular subject. With their unique mix of varied contributions from Original Research to Review Articles, Frontiers Research Topics unify the most influential researchers, the latest key findings and historical advances in a hot research area.

Find out more on how to host your own Frontiers Research Topic or contribute to one as an author by contacting the Frontiers editorial office: frontiersin.org/about/contact

Women in parasitology: 2021

Topic editors

Alessia Libera Gazzonis — University of Milan, Italy

Simona Gabrielli — Sapienza University of Rome, Italy

Serena Cavallero — Sapienza University of Rome, Italy

Citation

Gazzonis, A. L., Gabrielli, S., Cavallero, S., eds. (2023). *Women in parasitology: 2021*. Lausanne: Frontiers Media SA. doi: 10.3389/978-2-83252-144-1

Table of contents

frontiers | Frontiers in Veterinary Science

TYPE Editorial
PUBLISHED 28 March 2023
DOI 10.3389/fvets.2023.1153126

OPEN ACCESS

EDITED AND REVIEWED BY
Antoinette Marsh,
The Ohio State University, United States

*CORRESPONDENCE
Alessia Libera Gazzonis
✉ alessia.gazzonis@unimi.it

SPECIALTY SECTION
This article was submitted to Parasitology, a section of the journal Frontiers in Veterinary Science

RECEIVED 08 February 2023
ACCEPTED 16 March 2023
PUBLISHED 28 March 2023

CITATION
Gazzonis AL, Cavallero S and Gabrielli S (2023) Editorial: Women in parasitology: 2021. *Front. Vet. Sci.* 10:1153126. doi: 10.3389/fvets.2023.1153126

Editorial: Women in parasitology: 2021

Alessia Libera Gazzonis[1]*, Serena Cavallero[2] and Simona Gabrielli[2]

[1]Department of Veterinary Medicine and Animal Sciences, Università degli Studi di Milano, Milan, Italy, [2]Department of Public Health and Infectious Diseases, Sapienza University of Rome, Rome, Italy

KEYWORDS

parasitology, women, gender equality, diversity, inclusion

Editorial on the Research Topic
Women in parasitology: 2021

Inclusion and gender balance in science have received increasing attention in recent years, as evidenced by the present "Women in Parasitology" Research Topic included in the Frontiers collection of articles "Women in Sciences."

The participation of women in academia and scientific research remains underrepresented, with <30% of researchers being women worldwide (1). Women are even less represented in high-ranking academic positions, particularly in the Science, Technology, Engineering, and Mathematics (STEM) fields.

Various barriers, primarily of socio-cultural nature, are at the basis of the "leaky pipeline," for which there is a disproportion in career advancement between men and women. Long-standing stereotypes historically discouraged women from entering the STEM world. Furthermore, there are still difficulties in reconciling an academic career with personal and family life, particularly during the highly demanding transition phase from early career to independent researcher, which frequently coincides with the will of motherhood. The COVID-19 pandemic has exacerbated this phenomenon, with the burden of family responsibilities increasing mostly for women; furthermore, the resulting economic losses have had a greater impact on women's employment, accounting for the largest number of job losses.

While more women are entering academia as junior researchers, only a small number hold senior positions. Similarly, in scientific publishing, women are underrepresented on editorial boards, accounting for 14% of editors and an even lower percentage of editors-in-chief (8%) (2). As a result of the lower representation of women in leadership positions, there are fewer female role models to inspire young female researchers.

Parasitology also aligns with other STEM-related fields, with women underrepresented among peer reviewers, editorial boards, and research councils, as recently reported (3). To promote the achievements of women parasitologists, Frontiers in Parasitology launched the Research Topic "*Women in Science: Parasitology*." This Research Topic accepted eight original articles and one case report from a wide variety of research focuses and, to date, has over 10,000 total views and 1,258 article downloads. More than half of the 62 authors who participated in the Research Topic identified themselves as female. In particular, the participation of female researchers in their first career position should be emphasized, with the first position held by female authors in all included articles. Finally, there are four female researchers in senior positions, holding the last positions among the authors of the manuscripts. In the one-health perspective of parasitology, the current Research Topic includes articles focusing on parasites with great public health relevance and high

zoonotic potential, or causative agents of important food-borne diseases (e.g., *Toxoplasma gondii, Taenia solium*, and *Echinococcus multilocularis*), as well as parasites affecting animal health and productivity. The main aspects were investigated with the aim of filling the gap in knowledge about complex host-parasite interactions and the actual limits of treatments and control strategies.

Rezende-Gondim et al. described an immunomagnetic separation (IMS) method for the purification of *T. gondii* and *Hammondia* spp. tissue cysts generated in cell culture. This method finds useful application in proteomic studies on *T. gondii* and other related parasites. Furthermore, given the large number of *in vitro* generated tissue cysts obtained, IMS also represents a promising alternative for *in vivo* generated cysts, thus helping to reduce the number of animals used for experimental purposes.

With similar potential outcomes, Li et al. carried out a comparative proteomic analysis of *T. solium* larval (cysticerci) and adult stages, providing reference values for studying the pathogenic mechanism of the two stages and the interaction with the host. Such studies are of great relevance, accounting for the ability of cysticerci to infect humans as well as adults.

With the aim of investigating novel alternative treatments against alveolar echinococcosis, Chaudhry et al. focused on the mitochondrial energy metabolism of *E. multilocularis,* among novel targetable pathways. The *in vitro* activity of 13 endochin-like quinolones against metacestodes and isolated germinal layer cells was screened. The results suggested a promising novel treatment approach for alveolar echinococcosis and other helminthiases, with implications for both human health and livestock production.

Meng et al. investigated the molecular mechanisms underlying the host-parasite interactions of a protein within the rhoptry kinase family of *Eimeria tenella*, one of the most pathogenic species among those causing avian coccidiosis. The transcriptomic analysis revealed that *E. tenella* rhoptry kinase family protein 17 (EtROP17) has several potential roles, including the modulation of parasite replication and contributing to defense against microbial infections.

Another important parasitic disease afflicting the poultry industry is avian trichomonosis caused by the flagellated protozoan *Trichomonas gallinae*. With the emergence of strains that are resistant to the standard treatment, alternative therapies for control are required. Bailén et al. studied the efficacy of several essential oils from Lamiaceae and Asteraceae plants against *T. gallinae*. The demonstration of good *in vitro* anti-trichomonal activity in the absence of cytotoxicity of the tested essential oils suggested their potential application in the control of this protozoan in avian production.

Nápravníková et al. addressed drug resistance with a study on the efficacy of the most commonly used drugs in the control of strongylid infections in horses, by means of fecal egg count reduction tests conducted on a large population of equines from the Czech Republic. While the macrocyclic lactones demonstrated excellent efficacy, the authors highlighted a resistance of strongylids against pyrantel embonate and fenbendazole, suggesting the urgency to review current practices used in parasitic control to slow or limit the spread of anthelmintic resistance.

In the field of companion animals, Györke et al. reported an intriguing clinical case of co-infection by *Notoedres cati* and *Aelurostrongylus abstrusus* in two domestic cats from Romania. The clinical symptomatology, the parasitological methodologies for the diagnosis of notoedric mange and aelurostrongylosis and the complementary laboratory tests, and the pharmacological treatment and management of the animals were described. The follow-up, with the complete resolution of symptoms in both subjects, confirmed the validity of the case management scheme.

Finally, studies by Zhang et al. and Hu et al. addressed aspects concerning the epidemiology of pathogens that cause important economic losses in the livestock sector worldwide. In the first study, the genetic diversity of *Enterocytozoon bieneusi*, a common opportunistic intestinal pathogen and cause of enteric disorders in immunosuppressed humans and animals, was investigated in Chinese pigs, with the identification of 15 known genotypes and the description of one novel genotype genetically closely related to the zoonotic genotype EbpB. The obtained genetic data on this Microsporidia, with both zootechnical relevance and zoonotic potential, provided the baseline data for the prevention and control of *E. bieneusi* in the pig industry. The seroepidemiological study by Hu et al. on *T. gondii* and *Neospora caninum* infections in goats from Southwestern China highlighted different patterns of distribution relating to geographical variables and factors regarding farm management. The findings suggested the need to implement tailored control measures to reduce the distribution of these protozoa, which cause reproductive failure and production losses in the caprine species worldwide.

The editors would like to thank the contributors and reviewers, who made it possible to produce a Research Topic of high scientific quality highlighting the impact of women researchers in the field of Parasitology and providing a space to disseminate science, especially in light of the International day of Women and Girls in Science (11 February). Here, young researchers driven by curiosity and highly scientific rigor have had the opportunity to promote their research activity; moreover, authors at different career levels represent role models for young female researchers. We, therefore, hope that this Research Topic has provided an opportunity to create new collaborations and networks of female researchers and to attract attention to the issues of gender equality, diversity, and inclusion in parasitology and in science in general.

Author contributions

All authors listed have made a substantial, direct, and intellectual contribution to the work and approved it for publication.

Conflict of interest

The authors declare that the research was conducted in the absence of any commercial or financial relationships that could be construed as a potential conflict of interest.

Publisher's note

References

1. UNESCO (2021). *UNESCO Science Report: The Race Against Time for Smarter Development* (Schneegans S, Straza T, Lewis J, editors). Paris: UNESCO.

2. Liu F, Holme P, Chiesa M, AlShebli B, Rahwan T. Gender inequality and self-publication are common among academic editors. *Nat Hum Behav*. (2023). doi: 10.1038/s41562-022-01498-1

3. Calvani NED, De Marco Verissimo C, Cantacessi C, Clark E, Kanduma E. Herminthology: promoting gender equity in science and parasitology. *Trends Parasitol*. (2023) 39:73–9. doi: 10.1016/j.pt.2022.11.013

frontiers in Veterinary Science

ORIGINAL RESEARCH
published: 21 February 2022
doi: 10.3389/fvets.2022.833204

Total Failure of Fenbendazole to Control Strongylid Infections in Czech Horse Operations

Jana Nápravníková[1]*, *Marián Várady*[2] and *Jaroslav Vadlejch*[1]

[1] Department of Zoology and Fisheries, Czech University of Life Sciences Prague, Prague, Czechia, [2] Institute of Parasitology, Slovak Academy of Sciences, Košice, Slovakia

The control of strongylid infections has become challenging globally for equine practitioners due to the development of anthelmintic resistance. Comprehensive information on anthelmintic resistance in the Czech Republic, however, is still lacking. This study monitored the current efficacy of fenbendazole, pyrantel embonate, ivermectin and moxidectin. Forty-eight of 71 operations met the criteria (≥6 horses with ≥200 eggs per gram), with 969 fecal egg count reduction tests performed. Anthelmintic resistance was evaluated on an operation level based on fecal egg count reduction (FECR) and the lower limit of the 95% credible interval (LLCI) using Bayesian hierarchical models. General anthelmintic efficacy across all operations was assessed by posterior FECRs and the occurrence of sub-zero efficacies. Ivermectin and moxidectin demonstrated excellent efficacy (FECR 99.8–100%; 99.4–100 LLCI) in 45 and 23 operations, respectively, pyrantel embonate demonstrated sufficient efficacy in 15 operations and resistance was suspected in seven operations (FECR 88.1–99.1%; 72.5–98.5 LLCI). Fenbendazole, however, was not effective in a single operation (FECR 19.1–77.8%; 8.1–50.1 LLCI) out of 18. Fenbendazole had the highest probability of sub-zero efficacy (29.1%), i.e., post-treatment fecal egg counts exceeded the pre-treatment counts. Our data indicate an increase in the development of anthelmintic resistance, resulting in total failure of fenbendazole and a reduced efficacy of pyrantel embonate. Introducing advanced approaches of parasite control in the Czech Republic to slow the spread of anthelmintic resistance is thus needed.

Keywords: equine strongyles, anthelmintic resistance, fecal egg count reduction test, Mini-FLOTAC, anthelmintic drug

OPEN ACCESS

Edited by:
Alessia Libera Gazzonis, University of Milan, Italy

Reviewed by:
Muthusamy Raman, Tamil Nadu Veterinary and Animal Sciences University, India
Tetiana Kuzmina, National Academy of Sciences of Ukraine (NAN Ukraine), Ukraine

***Correspondence:**
Jana Nápravníková
napravnikovaj@af.czu.cz

Specialty section:
This article was submitted to Parasitology, a section of the journal Frontiers in Veterinary Science

Received: *10 December 2021*
Accepted: *28 January 2022*
Published: *21 February 2022*

Citation:
Nápravníková J, Várady M and Vadlejch J (2022) Total Failure of Fenbendazole to Control Strongylid Infections in Czech Horse Operations. Front. Vet. Sci. 9:833204. doi: 10.3389/fvets.2022.833204

INTRODUCTION

Strongylid nematodes, particularly cyathostomins, are ubiquitous in equine operations and are currently considered to be the main equine parasites at risk of developing anthelmintic resistance (AR) and causing associated health consequences (1, 2). The spread of AR is in the spotlight for both parasitologists and equine practitioners around the world. Strongylid resistance has been recorded for all equine anthelmintics currently used (3), so the control of these infections has become challenging.

AR is characterized by the genetically transmitted loss of sensitivity to a formerly effective drug in the parasite population at the dose recommended by the manufacturer. The development of AR is based on the selection of specific alleles under drug pressure (4). Fenbendazole (FBZ)

resistance is currently the rule rather than the exception in Europe (5–12), the USA (13–15), Chile (16), Cuba (17) and Brazil (18, 19). Resistance to pyrantel (PYR) has progressively spread (4, 7–11, 13, 18, 20–23), but macrocyclic lactones (MLs) usually maintain sufficient efficacy. Early signs of resistance to MLs, such as shortened periods of egg reappearance (24–26) or fully developed AR confirmed by fecal egg count reduction tests (FECRTs), however, have been reported (8, 11, 18).

Four anthelmintics belonging to three classes based on chemical structure and pharmacological behavior are used for controlling strongylid infections in the Czech Republic: FBZ, a benzimidazole (BZ); pyrantel embonate (PYR), a tetrahydropyrimidine and two MLs, ivermectin (IVM), an avermectin, and moxidectin (MOX), a milbemycin. Limited data on the resistance of strongylids to these drugs, however, are available. Several AR studies have been conducted in the Czech Republic but were local studies and small-scale studies. No nationwide studies evaluating all anthelmintics registered for the control of strongylid infections have yet been performed. BZ resistance and sufficient IVM efficacy have been reported (27–29), but limited data on PYR (30) resistance and no data on MOX efficacy in the Czech Republic are available.

In the first nationwide study, we evaluated the efficacy of all anthelmintics currently used in the Czech Republic to control strongylid infections in horses.

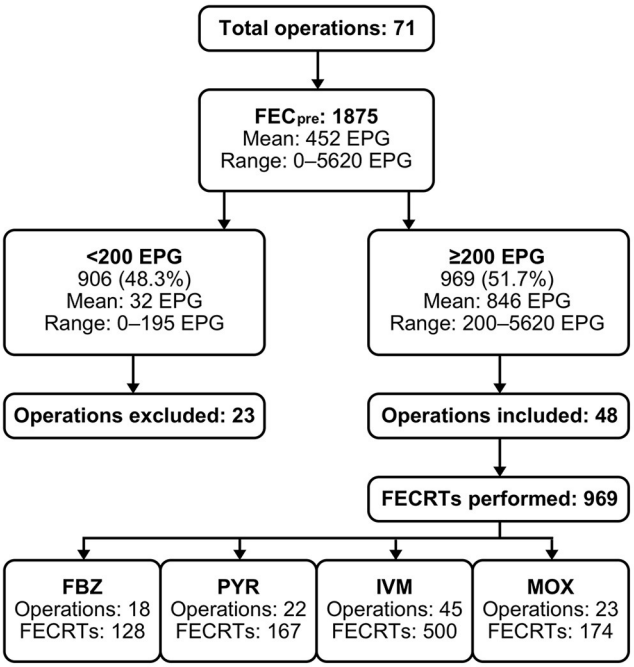

FIGURE 1 | Flow diagram of the study design and FEC_{pre} results represented by EPG prior to the statistical analysis of the FECRTs for FBZ, PYR, IVM and MOX. EPG, eggs per gram; FBZ, fenbendazole; FEC_{pre}, initial pre-treatment fecal egg count; FECRT, fecal egg count reduction test; IVM, ivermectin; MOX, moxidectin; PYR, pyrantel embonate.

MATERIALS AND METHODS

Equine Operations

The data presented in this study were obtained in 2019 and 2020 from equine operations across the Czech Republic. Out of a total of 71 operations, 48 met the criteria for resistance testing (2–4 operations in each of the 14 regions). Mares, geldings and stallions aged 2–28 years with diverse functions (stud, show, leisure, therapy) were included. Operations followed a routine plan of treatment frequency (2–4/year) and anthelmintic choice determined by local veterinary practitioners. Only operations with a minimum of a 16-week period since the previous treatment were included. The flow diagram in **Figure 1** shows the design of the study and the selection of operations based on our criteria.

Parasitological Procedures

The efficacies of FBZ, PYR, IVM and MOX were estimated using the fecal egg count reduction test (FECRT), the estimation of anthelmintic efficacy *via* post-treatment egg reduction (31–33). The Mini-FLOTAC technique (34) with the Fill-FLOTAC (35) apparatus was used following the protocol recommended for fresh herbivore feces (5 g feces; 45 ml flotation solution at a specific gravity of 1.28; multiplication factor of 5). This technique is based on the passive flotation of eggs in flotation chambers with total volumes of 2 ml and is characterized by a revolving reading disc that provides improved readability. The disk were examined by an experienced technician using an Olympus BX51 microscope at a magnification of 100×. The eggs were then morphologically identified (36).

Initial fecal egg counts (FEC_{pre}) for all horses from each operation were performed to determine whether the operation met the criteria for the FECRT, i.e., a minimum of six horses with ≥200 eggs per gram (EPG). Operations that did not fulfill these requirements were excluded. A subsequent fecal egg count (FEC_{post}) followed 14 days after anthelmintic application and was performed in a selected group of horses (≥200 EPG). Individual fecal samples were collected immediately after defecation, placed into airtight zip-lock bags, transported to the laboratory, refrigerated (4°C) and processed within 24 h after collection.

Anthelmintic Treatment

Registered anthelmintics available in the Czech Republic (FBZ: Panacur, Intervet International, Boxmeer, Netherlands; PYR: EQUISTRONG, Bioveta, Ivanovice na Hané, Czech Republic; IVM: NOROMECTIN, Norbrook Laboratories, Monaghan, Ireland; MOX: EQUIMOXIN, Bioveta, Ivanovice na Hané, Czech Republic) were administered per os by an authorized person in a single dose recommended by the manufacturer (FBZ 7.5 mg/kg body weight (BW); PYR 19 mg/kg BW; IVM 0.2 mg/kg BW; MOX 0.4 mg/kg BW) based on estimates of body weight (tape measurements). The expiry dates were checked before application. The number of anthelmintics tested in one operation varied depending on the total number of horses in the operation, the number of horses with sufficient FECs and the common local practices such as the number of anthelmintic treatments per year.

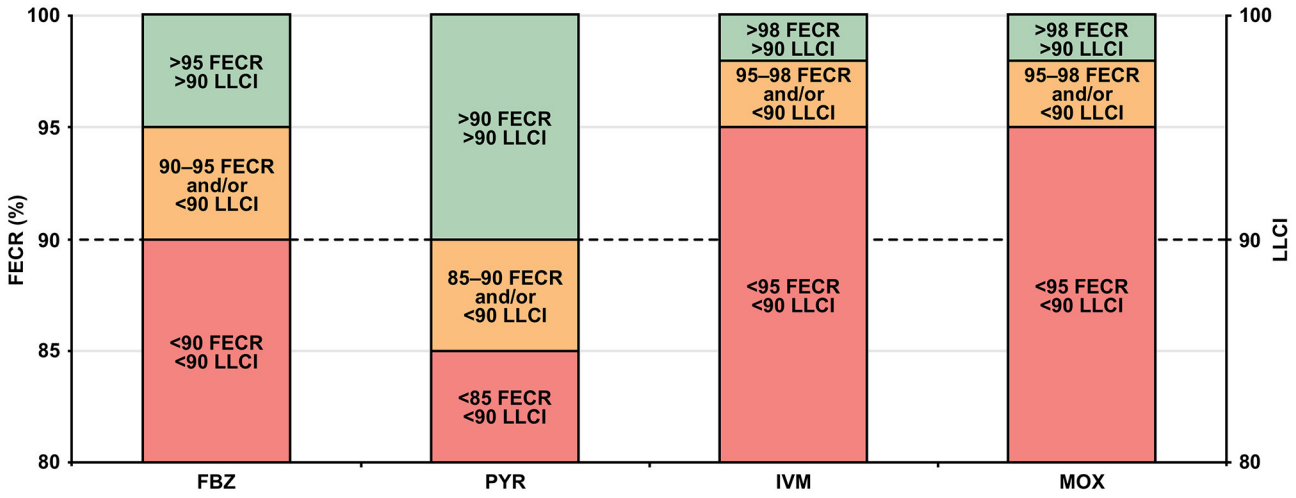

FIGURE 2 | Criteria for determining the efficacies of FBZ, PYR, IVM and MOX: FECR% (normal, green; suspected, orange; reduced, red) and 95% LLCI. FBZ, fenbendazole; FECR%, mean fecal egg count reduction; IVM, ivermectin; 95% LLCI, lower limit of the 95% credible interval; MOX, moxidectin; PYR, pyrantel embonate.

TABLE 1 | Estimated efficacies of fenbendazole (FBZ), pyrantel embonate (PYR), ivermectin (IVM) and moxidectin (MOX) at the operation and horse levels.

Efficacy	*n*		Reduced		Suspected		Normal	
	Operations	Horses	Operations	Horses	Operations	Horses	Operations	Horses
FBZ	18	128	18 (100%)	122 (95.3%)	–	1 (0.8%)	–	5 (3.9%)
PYR	22	167	–	10 (6.0%)	7 (31.8%)	3 (1.8%)	15 (68.2%)	154 (92.2%)
IVM	45	500	–	–	–	–	45 (100%)	500 (100%)
MOX	23	174	–	–	–	–	23 (100%)	174 (100%)

Statistical Analyses

The FECRs for individual horses were calculated by a Bayesian hierarchical model analysis of the data using an estimate of mean FECR and 95% credible intervals (CIs) (37, 38). FECR (%) was calculated for each horse, and mean FECRs, 95% CIs and the means and ranges of FEC_{pre} and FEC_{post} were calculated for each operation. Data representing the anthelmintic efficacy in horses and particular operations are displayed in the tables and column graphs attached as **Supplementary Material** (unabridged tables).

Drug efficacy (normal, suspected and reduced) at the operation level was determined using mean FECR (%) and the lower limit of the 95% CIs (LLCI) (**Figure 2**) (33, 39).

General efficacy was also calculated for each anthelmintic regardless of affiliations with individual operations (subsamples) and is graphed as the posterior distribution of FECR. An analysis of sub-zero efficacies (FECR <0%) with confidence intervals in individual horses was performed with restriction efficacies to interval 0 to 1 and random variabilities between operations.

RESULTS

FEC_{pre} was performed in 71 operations and 1,875 horses, of which 48.3% can be considered low (0–195 EPG), 19.7% moderate (200–500 EPG), and 32.0% high (>505 EPG) contaminators. Horses with 0 EPG represented 23.3% of the total.

Twenty-three operations were excluded from resistance testing for not meeting the condition of the sufficient number of horses with sufficient FEC_{pre}. Therefore, 969 FECRTs were performed in the remaining 48 operations (**Figure 1** and **Table 1**).

Operation-Level Efficacy

The estimates of efficacy of the four anthelmintics in individual equine operations were visualized using column graphs (**Figure 3**) with cut-off values (horizontal dashed line) highlighted. The columns represent mean FECR (%) and are arranged in descending order for clarity. Unabridged data are attached in the **Supplementary Material**.

FBZ demonstrated reduced efficacy (mean FECR 19.1–77.8%; 8.1–50.1 LLCI) in all operations, PYR predominantly demonstrated normal efficacy with suspected resistance in seven operations (mean FECR 88.1–99.1%; 72.5–98.5 LLCI) and IVM (mean FECR 99.8–100%; 99.4–100 LLCI) and MOX (mean FECR 99.8–100%; 99.5–100 LLCI) demonstrated normal efficacies in all operations. Dual-drug resistance (FBZ resistance and suspected PYR resistance) was suspected in five operations (21, 22, 37, 43 and 48).

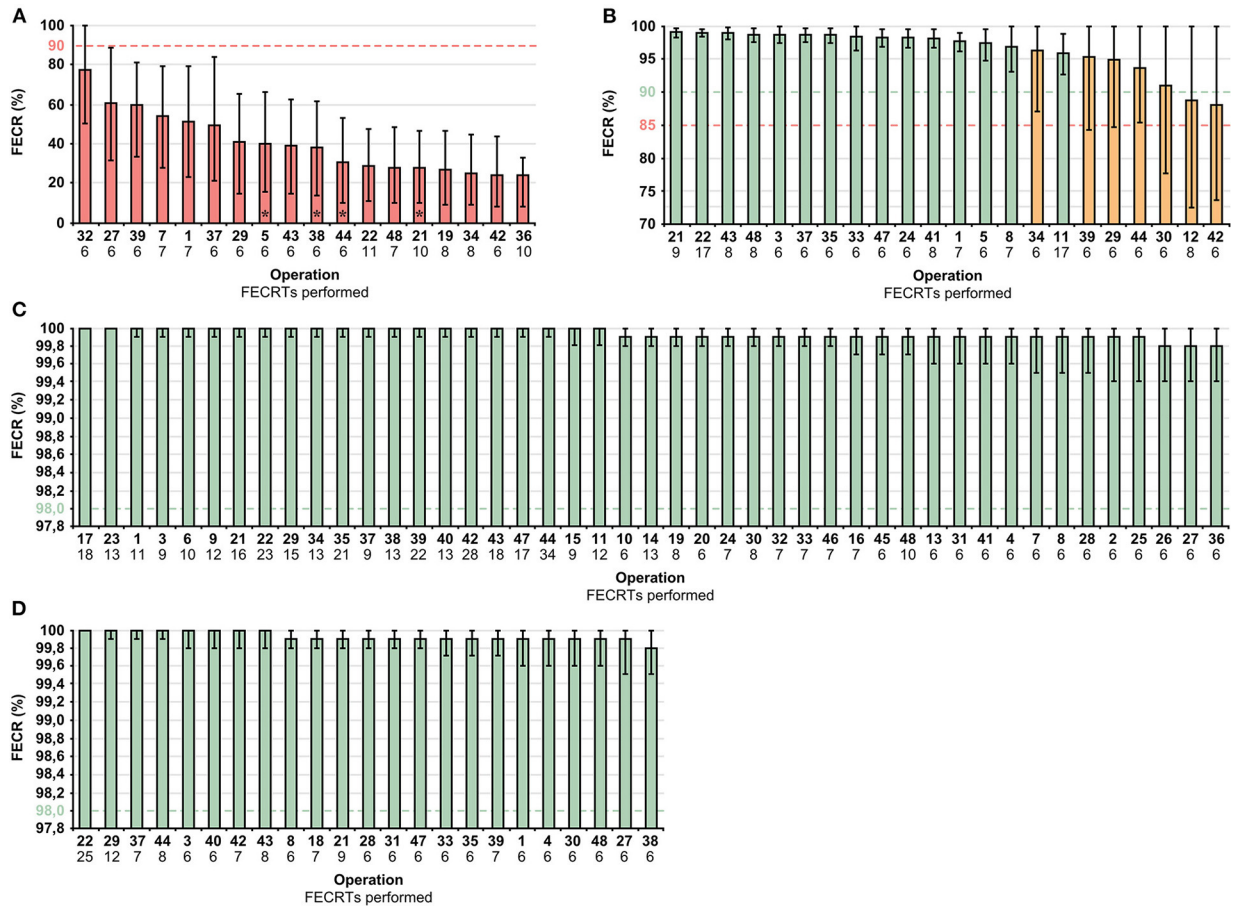

FIGURE 3 | Estimated efficacies of FBZ **(A)**, PYR **(B)**, IVM **(C)** and MOX **(D)** (normal, green; suspected, orange; reduced, red) based on FECR% and 95% LLCI at the operation level. The dashed lines represent the criteria for estimating FECR% efficacy for each anthelmintic, error bars 95% CI (credible interval), *sub-zero efficacy at operation level (mean FECRT < 0%). FBZ, fenbendazole; FECR%, mean fecal egg count reduction; IVM, ivermectin; MOX, moxidectin; PYR, pyrantel embonate; 95% LLCI, lower limit of 95% credible interval.

General Efficacy

Figure 4 presents the general efficacies of the anthelmintics visualized as the posterior distribution of fecal egg reduction. Almost one-third (29.1%; CI 21.9–37.6) of the FBZ treatments resulted in sub-zero efficacies (individual FEC_{post} exceeding FEC_{pre}), and the occurrence of sub-zero efficacies was minimal for PYR (0.6%; CI 0.1–4.2) and absent for the MLs. The probability of occurrence of sub-zero efficacies for FBZ and PYR compared to the MLs differed significantly (p <0.0001) among the horses.

DISCUSSION

The equine industry in the Czech Republic is growing, with the number of registered equines in 2021 exceeding the 100,000 mark for the first time. This study provides the first comprehensive data on the efficacy of all anthelmintic compounds used in Czech horse operations. All equine anthelmintics in the Czech Republic are available only with a prescription, and their distribution strictly relies on veterinary practitioners. Individual horses maintain their shedding potential, and the majority of eggs are produced by a small portion of herd individuals (40, 41), but the strategic approach lacking adequate measures to determine the need to administer anthelmintics and verify the efficacy to avoid ineffective drugs is still commonly practiced in the Czech Republic. Nearly half of the horses in our study were considered low contaminators, because they shed fewer than 200 EPG. Most of the horses, however, still received treatment using the customary approach to treat all horses at fixed times of the year. In contrast, treatment twice a year could be insufficient for high shedders to avoid the excessive contamination of pastures. The threshold for the selective-treatment approach has not been precisely determined for horses and could vary depending on individual conditions. Horses classified as moderate (200–500 EPG) and high (>500 EPG) contaminators generally shed the majority of eggs and require anthelmintic treatment (28).

A high level of resistance was confirmed for FBZ, resistance was suspected for PYR due to the sporadic incidence of reduced efficacy in individual horses in an operation and MLs remained fully effective.

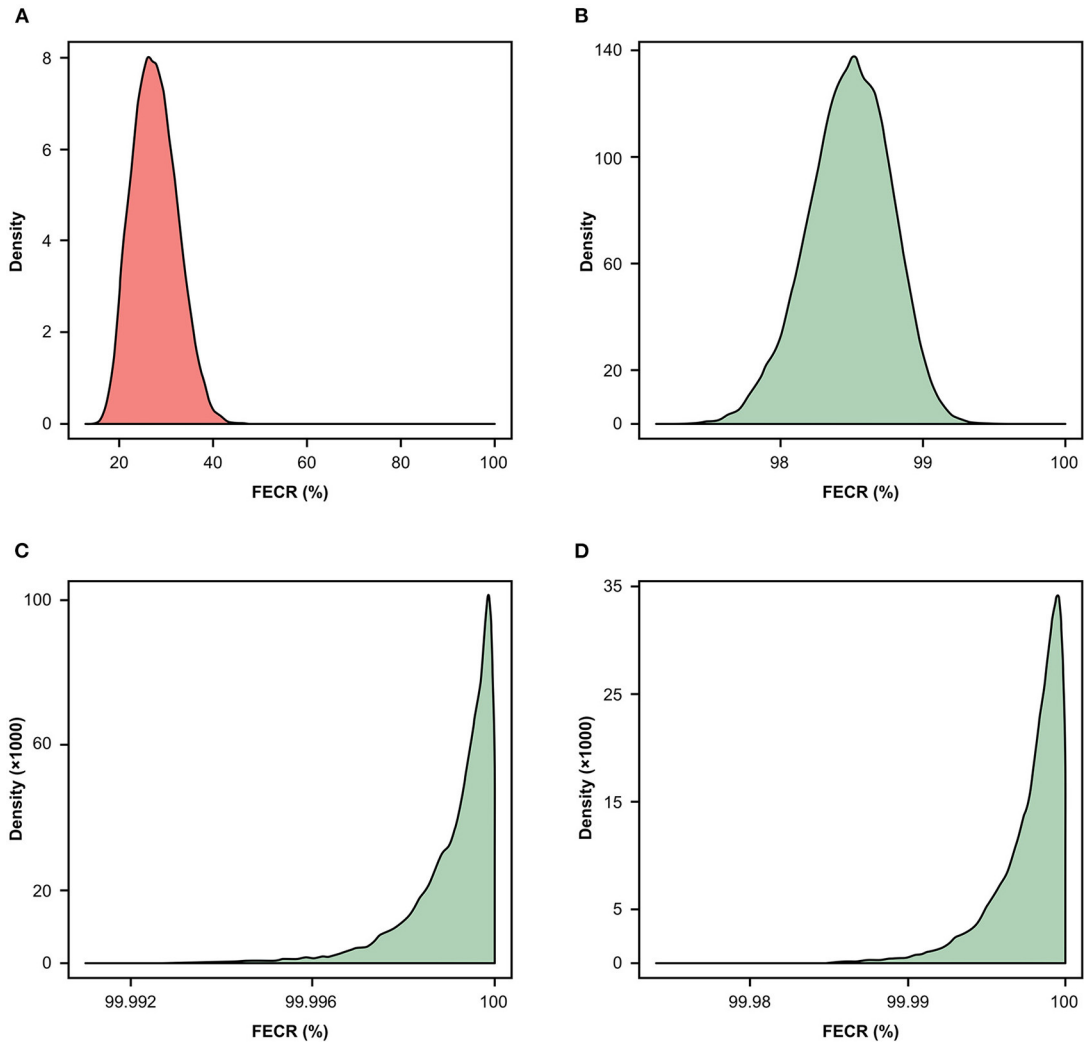

FIGURE 4 | Posterior probability distribution of FECR% for FBZ **(A)**, PYR **(B)**, IVM **(C)** and MOX **(D)** at the horse level. FBZ, fenbendazole; FECR%, fecal egg count reduction; IVM, ivermectin; MOX, moxidectin; PYR, pyrantel embonate.

Our results suggest that although MLs are currently used the most frequently (IVM 42%, MOX 21%), compared to PYR (20%) and FBZ (17%), they remain highly effective, and the development of AR is slow. The importation of horses and ineffective quarantine measures, however, can strongly affect the spread of ML-resistant strongylids (42). Reports of resistance to MLs in Europe (8, 11, 33, 43) indicate the potential risk of ML-resistant strongylids. Our results nevertheless indicated excellent efficacy for the MLs and confirmed the results of previous studies (27–29). These results may be due to the uncommon use of the interval strategy in the Czech Republic. The overuse of anthelmintics and the minimal use of refugia are known factors for the development of AR (1).

We did not detect fully developed resistance to PYR, but 32% (7 of 22) of the operations demonstrated suspected resistance, because some horses had decreased FECRs (8% of the horses had FECRs <90%). The data obtained from our study highlight the need to verify the efficacy of regular PYR treatment (32) for the early detection of AR. FBZ resistance is ubiquitous, so potential multidrug resistance can lead to the exclusive use of MLs associated with the risk of accelerating the emergence of resistance.

BZ-resistant strongylids are pervasive in the Czech Republic. The value of the FECRT continues to decrease over time, and the incidence of individual sub-zero efficacies is increasing compared to previous studies (27–30). Avoiding the use of FBZ to control strongylid infections is essential for preventing economic and health consequences. FBZ was introduced to the Czech market in 1976, and IVM was introduced 10 years later (personal communication). Both anthelmintics were used under similar conditions, but FBZ lacks efficacy and IVM remains fully effective. Other factors possibly affecting AR need to be considered. Product formulation and the size of the packaging may indirectly influence the exact dosage. Powder and granules (FBZ) mixed with grain are not willingly accepted by all horses, and repeated underdosing may occur (44). The dose of a

drug in an applicator insufficient for standard warm-blooded animals (e.g., 450 kg BW mebendazole, a BZ) could tempt horse owners, due to economic reasons, to administer only one paste to a horse requiring a larger amount. Finally, the variety of concurrently marketed products of the same anthelmintic class (e.g., FBZ and mebendazole) could substantially increase the use of one anthelmintic class with a false impression of rotation of anthelmintics with different modes of action (45).

Various approaches for analyzing anthelmintic efficacy make the comparison of the results among studies challenging. FECRT is currently a gold standard in AR detection, but it still has limitations such as low sensitivity, variable reliability of the coprological FEC methods used (46), the lack of standardization and cut-off values for horses and the difficulty of interpretation. The high species diversity of equine strongylids is also an important factor.

In conclusion, this study provides comprehensive information about the current situation of the resistance of equine strongylids to anthelmintics in the Czech Republic. FBZ is no longer effective for strongylid control. PYR resistance was suspected in some operations and should therefore be used with caution due to the potential risk of the development dual resistance. In contrast, the MLs still had sufficient efficacy, which must be maintained as long as possible for detecting early signs of AR (e.g., period of egg reappearance). Modern approaches to strongylid control, e.g., non-chemical approaches or selective anthelmintic treatment, need to be implemented but will require educating both horse owners and veterinarians. Identifying the risk factors that accelerate the development of AR, and further research oriented in this direction, are essential.

DATA AVAILABILITY STATEMENT

The original contributions presented in the study are included in the article/**Supplementary Material**, further inquiries can be directed to the corresponding author.

ETHICS STATEMENT

Ethical review and approval was not required for the animal study because this study involved the examination of naturally excreted fecal samples. Written informed consent was obtained from the owners for the participation of their animals in this study.

AUTHOR CONTRIBUTIONS

JN designed the study, collected the samples, performed the laboratory work, analyzed the data, interpreted the results, and prepared the manuscript. MV interpreted the results and reviewed the manuscript. JV designed the study, supervised the project, and reviewed the manuscript. All authors contributed to the article and approved the submitted version.

FUNDING

This research was partially supported by the Ministry of Education, Youth and Sports INTER-EXCELLENCE project (INTER-COST LTC19018) and was performed within the initiative of the Center for Infectious Animal Diseases (CINeZ).

ACKNOWLEDGMENTS

The authors are grateful to the horse owners for their willingness to participate in this study and to Dr. William Blackhall for his proofreading services.

SUPPLEMENTARY MATERIAL

The Supplementary Material for this article can be found online at: https://www.frontiersin.org/articles/10.3389/fvets.2022.833204/full#supplementary-material

REFERENCES

1. Matthews JB. Anthelmintic resistance in equine nematodes. *Int J Parasitol Drugs Drug Resist.* (2014) 4:310–5. doi: 10.1016/j.ijpddr.2014.10.003
2. Love S, Murphy D, Mellor D. Pathogenicity of cyathostome infection. *Vet Parasitol.* (1999) 85:113–22. doi: 10.1016/S0304-4017(99)00092-8
3. Raza A, Qamar AG, Hayat K, Ashraf S, Williams AR. Anthelmintic resistance and novel control options in equine gastrointestinal nematodes. *Parasitology.* (2019) 146:425–37. doi: 10.1017/S0031182018001786
4. Köhler P. The biochemical basis of anthelmintic action and resistance. *Int J Parasitol.* (2001) 31:336–45. doi: 10.1016/S0020-7519(01)00131-X
5. Craven J, Bjørn H, Barnes EH, Henriksen SA, Nansen P. A comparison of *in vitro* tests and a faecal egg count reduction test in detecting anthelmintic resistance in horse strongyles. *Vet Parasitol.* (1999) 85:49–59. doi: 10.1016/S0304-4017(99)00113-2
6. Várady M, Königová A, Corba J. Benzimidazole resistance in equine cyathostomes in Slovakia. *Vet Parasitol.* (2000) 94:67–74. doi: 10.1016/S0304-4017(00)00366-6
7. Lind EO, Kuzmina T, Uggla A, Waller PJ, Höglund J. A field study on the effect of some anthelmintics on cyathostomins of horses in Sweden. *Vet Res Commun.* (2007) 31:53–65. doi: 10.1007/s11259-006-3402-5
8. Traversa D, von Samson-Himmelstjerna G, Demeler J, Milillo P, Schürmann S, Barnes H, et al. Anthelmintic resistance in cyathostomin populations from horse yards in Italy, United Kingdom and Germany. *Parasit Vectors.* (2009) 2:1–7. doi: 10.1186/1756-3305-2-S2-I1
9. Traversa D, Castagna G, von Samson-Himmelstjerna G, Meloni S, Bartolini R, Geurden T, et al. Efficacy of major anthelmintics against horse cyathostomins in France. *Vet Parasitol.* (2012) 188:294–300. doi: 10.1016/j.vetpar.2012.03.048
10. Lester HE, Spanton J, Stratford CH, Bartley DJ, Morgan ER, Hodgkinson JE, et al. Anthelmintic efficacy against cyathostomins in horses in Southern England. *Vet Parasitol.* (2013) 197:189–96. doi: 10.1016/j.vetpar.2013.06.009
11. Relf VE, Lester HE, Morgan ER, Hodgkinson JE, Matthews JB. Anthelmintic efficacy on UK Thoroughbred stud farms. *Int J Parasitol.* (2014) 44:507–14. doi: 10.1016/j.ijpara.2014.03.006
12. Stratford CH, Lester HE, Pickles KJ, McGorum BC, Matthews JB. An investigation of anthelmintic efficacy against strongyles on equine yards in Scotland. *Equine Vet J.* (2014) 46:17–24. doi: 10.1111/evj.12079
13. Tarigo-Martinie JL, Wyatt AR, Kaplan RM. Prevalence and clinical implications of anthelmintic resistance in cyathostomes of horses. *J Am Vet Med Assoc.* (2001) 218:1957–60. doi: 10.2460/javma.2001.218.1957
14. Rossano MG, Smith AR, Lyons ET. Shortened strongyle-type egg reappearance periods in naturally infected horses treated with moxidectin

and failure of a larvicidal dose of fenbendazole to reduce fecal egg counts. *Vet Parasitol.* (2010) 173:349–52. doi: 10.1016/j.vetpar.2010.07.001
15. Bellaw JL, Krebs K, Reinemeyer CR, Norris JK, Scare JA, Pagano S, et al. Anthelmintic therapy of equine cyathostomin nematodes – Larvicidal efficacy, egg reappearance period, and drug resistance. *Int J Parasitol.* (2018) 48:97–105. doi: 10.1016/j.ijpara.2017.08.009
16. von Witzendorff C, Quintana I, Sievers G, Schnieder T, von Samson-Himmelstjerna G. Estudio sobre resistencia frente a los bencimidazoles de pequeños estrongilos (Cyathostominae) del equino en el sur de Chile. *Arch Med Vet*. (2003) 35:187–94. doi: 10.4067/S0301-732X2003000200006
17. Salas-Romero J, Gómez-Cabrera KA, Salas JE, Vázquez R, Arenal A, Nielsen MK. First report of anthelmintic resistance of equine cyathostomins in Cuba. *Vet Parasitol Reg Stud Reports*. (2018) 13:220–3. doi: 10.1016/j.vprsr.2018.07.005
18. Canever RJ, Braga PR, Boeckh A, Grycajuck M, Bier D, Molento MB. Lack of Cyathostomin sp. reduction after anthelmintic treatment in horses in Brazil. *Vet Parasitol.* (2013) 194:35–9. doi: 10.1016/j.vetpar.2012.12.020
19. Vera JHS, Fachiolli DF, Ramires LM, Saes, LI, Yamada PH, Gonçalves JA, et al. Eficacy of ivermectin, moxidectin and febendazole in equine in Brazil. *Vet Parasitol Reg Stud Reports.* (2020) 20:100374. doi: 10.1016/j.vprsr.2020.100374
20. Chapman MR, French DD, Monahan CM, Klei TR. Identification and characterization of a pyrantel pamoate resistant cyathostome population. *Vet Parasitol.* (1996) 66:205–12. doi: 10.1016/S0304-4017(96)01014-X
21. Slocombe JOD, de Gannes RV. Cyathostomes in horses in Canada resistant to pyrantel salts and effectively removed by moxidectin. *Vet Parasitol.* (2006) 140:181–4. doi: 10.1016/j.vetpar.2006.03.019
22. Näreaho A, Vainio K, Oksanen A. Impaired efficacy of ivermectin against *Parascaris equorum*, and both ivermectin and pyrantel against strongyle infections in trotter foals in Finland. *Vet Parasitol.* (2011) 182:372–7. doi: 10.1016/j.vetpar.2011.05.045
23. Dauparaite E, Kupčinskas T, von Samson-Himmelstjerna G, Petkevičius S. Anthelmintic resistance of horse strongyle nematodes to ivermectin and pyrantel in Lithuania. *Acta Vet Scand.* (2021) 63:1–7. doi: 10.1186/s13028-021-00569-z
24. von Samson-Himmelstjerna G, Fritzen B, Demeler J, Schürmann S, Rohn K, Schnieder T, et al. Cases of reduced cyathostomin egg-reappearance period and failure of *Parascaris equorum* egg count reduction following ivermectin treatment as well as survey on pyrantel efficacy on German horse farms. *Vet Parasitol.* (2007) 144:74–80. doi: 10.1016/j.vetpar.2006.09.036
25. Lyons ET, Tolliver SC, Ionita M, Lewellen A, Collins SS. Field studies indicating reduced activity of ivermectin on small strongyles in horses on a farm in Central Kentucky. *Parasitol Res.* (2008) 103:209–15. doi: 10.1007/s00436-008-0959-7
26. Daniels SP, Proudman CJ. Shortened egg reappearance after ivermectin or moxidectin use in horses in the UK. *Vet J.* (2016) 218:36–9. doi: 10.1016/j.tvjl.2016.11.003
27. Chroust K. Occurrence of anthelmintic resistance in strongylid nematodes of sheep and horses in the Czech Republic. *Vet Med.* (2000) 45:233–9.
28. Langrová I, Borovský M, Jankovská I, Navrátil J, Slavík V. The benzimidazole resistance of cyathostomes on five horse farms in the Czech Republic. *Helminthologia.* (2002) 39:211–6.
29. Bodeček Š, Vavrouchová E. Monitoring of anthelmintic resistance in small strongyles in the Czech Republic in the years 2006–2009. *Acta Vet Brno.* (2013) 82:243–8. doi: 10.2754/avb201382030243
30. Bodeček S, Světlíková J, Hargitaiová K, Kecerová Z, Mráčková M. Monitoring the avermectin and pyrantel resistance status of nematode parasites of horses in the Czech Republic. *Vet Med.* (2018) 63:299–305. doi: 10.17221/125/2017-VETMED
31. Coles GC, Jackson F, Pomroy WE, Prichard RK, von Samson-Himmelstjerna G, Silvestre A, et al. The detection of anthelmintic resistance in nematodes of veterinary importance. *Vet Parasitol.* (2006) 136:167–85. doi: 10.1016/j.vetpar.2005.11.019
32. ESCCAP. *A Guide to the Treatment and Control of Equine Gastrointestinal Parasite Infections.* (2019). Available online at: https://www.esccap.org/uploads/docs/70ep8j2z_0796_ESCCAP_Guideline_GL8_v8_1p.pdf (accessed October 20, 2021).
33. AAEP. *AAEP Internal Parasite Control Guidelines.* (2019). Available online at: https://aaep.org/sites/default/files/2021-03/Internal_Parasite_Guidelines.pdf (accessed October 20, 2021).
34. Barda BD, Rinaldi L, Ianniello D, Zepherine H, Salvo F, Sadutshang T, et al. Mini-FLOTAC, an innovative direct diagnostic technique for intestinal parasitic infections: experience from the field. *PLoS Negl Trop Dis.* (2013) 7:e2344. doi: 10.1371/journal.pntd.0002344
35. Cringoli G, Maurelli MP, Levecke B, Bosco A, Vercruysse J, Utzinger J, et al. The Mini-FLOTAC technique for the diagnosis of helminth and protozoan infections in humans and animals. *Nat Protoc.* (2017) 12:1723. doi: 10.1038/nprot.2017.067
36. Cernea M, de Carvalho LM, Cozma V. *Atlas of Diagnosis of Equine Strongylidosis.* Cluj-Napoca: Editura Academic Press (2008). p. 118.
37. Torgerson PR, Paul M, Furrer R. Evaluating faecal egg count reduction using a specifically designed package "eggCounts" in R and a user friendly web interface. *Int J Parasitol.* (2014) 44:299–303. doi: 10.1016/j.ijpara.2014.01.005
38. Wang C, Torgerson PR, Kaplan RM, George MM, Furrer R. Modelling anthelmintic resistance by extending eggcounts package to allow individual efficacy. *Int J Parasitol Drugs Drug Resist.* (2018) 8:386–93. doi: 10.1016/j.ijpddr.2018.07.003
39. Levecke B, Kaplan RM, Thamsborg SM, Torgerson PR, Vercruysse J, Dobson RJ. How to improve the standardization and the diagnostic performance of the fecal egg count reduction test? *Vet Parasitol.* (2018) 253:71–8. doi: 10.1016/j.vetpar.2018.02.004
40. Kaplan RM, Nielsen MK. An evidence-based approach to equine parasite control: it ain't the 60s anymore. *Equine Vet Educ.* (2010) 22:306–16. doi: 10.1111/j.2042-3292.2010.00084.x
41. Nápravníková J, Vadlejch J. *The Distribution of Family Strongylidae Nematodes in Czech Horse Farms*. 9th Workshop on Biodiversity, Jevany (2017).
42. Nielsen MK, Banahan M, Kaplan RM. Importation of macrocyclic lactone resistant cyathostomins on a US thoroughbred farm. *Int J Parasitol Drugs Drug Resist.* (2020) 14:99–104. doi: 10.1016/j.ijpddr.2020.09.004
43. Milillo P, Boeckh A, Cobb R, Otranto D, Lia RP, Perrucci S, et al. Faecal cyathostomin egg count distribution and efficacy of anthelmintics against cyathostomins in italy: a matter of geography? *Parasit Vectors.* (2009) 2:1–7. doi: 10.1186/1756-3305-2-S2-S4
44. Smith G, Grenfell BT, Isham V, Cornell S. Anthelmintic resistance revisited: under-dosing, chemoprophylactic strategies, and mating probabilities. *Int J Parasitol.* (1999) 29:77–91. doi: 10.1016/S0020-7519(98)00186-6
45. Coles GC. The biochemical mode of action of some modern anthelmintics. *Pestic Sci.* (1977) 8:536–43. doi: 10.1002/ps.2780080518
46. Nápravníková J, Petrtýl M, Stupka R, Vadlejch J. Reliability of three common fecal egg counting techniques for detecting strongylid and ascarid infections in horses. *Vet Parasitol.* (2019) 272:53–7. doi: 10.1016/j.vetpar.2019.07.001

Conflict of Interest: The authors declare that the research was conducted in the absence of any commercial or financial relationships that could be construed as a potential conflict of interest.

Publisher's Note: All claims expressed in this article are solely those of the authors and do not necessarily represent those of their affiliated organizations, or those of the publisher, the editors and the reviewers. Any product that may be evaluated in this article, or claim that may be made by its manufacturer, is not guaranteed or endorsed by the publisher.

frontiers | Frontiers in Veterinary Science

CASE REPORT
published: 01 June 2022
doi: 10.3389/fvets.2022.849525

Case Report: Notoedric Mange and Aelurostrongylidosis in Two Domestic Cats From Rural Environment in Romania

Adriana Györke[1,2]*, *Mirabela Oana Dumitrache*[1,2], *Aurora Livia Ursache*[2], *Gianluca D'Amico*[1] and *Viorica Mircean*[1,2]

[1] Parasitology and Parasitic Diseases Department, Faculty of Veterinary Medicine, University of Agricultural Sciences and Veterinary Medicine, Cluj-Napoca, Romania, [2] Dermatology Clinic, Faculty of Veterinary Medicine, University of Agricultural Sciences and Veterinary Medicine, Cluj-Napoca, Romania

This article describes two cases of notoedric mange concurrent with aelurostrongylidosis in two domestic-owned cats from a rural environment in Romania. Two European shorthair cats originating from the same litter were referred to our clinic, at 2 months apart, with a history of skin lesions, pruritus, weight loss, and respiratory signs. Cats lived mainly outdoor together with the queen and a third littermate. The latter two expressed the same clinical signs and had died before the presentation of the first cat. None of the four cats was vaccinated, dewormed, or treated for external parasites. Coat brushing, skin scrapings, skin cytology, earwax direct microscopic examination, and coproparasitological techniques (flotation and Baermann methods) were used as laboratory procedures. A blood sample was also collected for hematology, blood biochemistry, and feline immunodeficiency virus/feline leukemia virus (FIV/FeLV) test. *Notoedres cati* mites in high numbers were identified by all complementary tests, alongside fleas and *Aelurostrongylus abstrusus* first-stage larvae. The blood analysis revealed neutrophilia, and the FIV/FeLV fast test was negative. The cats were successfully treated off-label with selamectin spot-on formulation (Stronghold®, Zoetis) three times at 1- or 4-week intervals. Furthermore, they were treated with amoxicillin trihydrate/clavulanic acid, housed indoor, and fed with a commercial diet. Before presentation to the clinic, the female cat was unsuccessfully treated with a combination of fipronil, S-methoprene, eprinomectin, and praziquantel. During this period, the female cat remained outdoor and fed with home wastes. The cats become negative for *A. abstrusus* L1 larvae after 2–4 months of treatment. The owners developed pruritic skin lesions 1 month after introducing the first cat in the house. In conclusion, notoedric mange and aelurostrongylidosis can be treated successfully with selamectin as a spot-on formulation and the treatment must be continued until no parasite will be detected through specific techniques. The success of treatment depends on improving the quality of animal life (nutrition and hygiene) and treatment of secondary complications.

Keywords: cat, mange, lungworm, *Notoedres*, *Aelurostrongylus*

OPEN ACCESS

Edited by:
Serena Cavallero, Sapienza University of Rome, Italy

Reviewed by:
Leucio Camara Alves, Federal Rural University of Pernambuco, Brazil
Ibrahim Abbas, Mansoura University, Egypt

***Correspondence:**
Adriana Györke
adriana.gyorke@usamvcluj.ro

Specialty section:
This article was submitted to Parasitology, a section of the journal Frontiers in Veterinary Science

Received: *06 January 2022*
Accepted: *20 April 2022*
Published: *01 June 2022*

Citation:
Györke A, Dumitrache MO, Ursache AL, D'Amico G and Mircean V (2022) Case Report: Notoedric Mange and Aelurostrongylidosis in Two Domestic Cats From Rural Environment in Romania. Front. Vet. Sci. 9:849525. doi: 10.3389/fvets.2022.849525

INTRODUCTION

Notoedric mange is a pruritic and contagious skin disease caused by the burrowing mites belonging to the *Notoedres* genus (family Sarcoptidae). Nowadays, more than forty-one species are recognized in the *Notoedres* genus (1). *Notoedres* mites affect mammals belonging to Rodentia, Carnivora, Chiroptera, and Lagomorpha orders (2). *Notoedres cati* is the first species from the genus described by Hering in 1838 (2). *Notoedres cati* affects mainly cats, but it was found in more than 18 host mammal species (insectivores, rodents, lagomorphs, bobcats, procyonids, and viverrids), including humans (3). It is transmitted by direct contact and rarely indirectly from the contaminated environment (4). All stages (eggs, larvae, nymphs, and adults) of the mite live in the skin and do not survive out of the host (3, 4). The life cycle of *N. cati* is similar to *Sarcoptes scabiei*, but a detailed description is not available (5). The larvae, nymphs, and adults of *N. cati* borrow tunnels in the superficial epidermis, on the face and ears, and sometimes on the legs and genital regions (3, 6). After mating on the skin surface, female mites burrow tunnels within the horny layer of the skin, where they lay 2–3 eggs a day. The life cycle lasts 14–21 days, in favorable environmental conditions.

Notoedric mange is considered a rare skin condition in cats and is mainly diagnosed in stray cats (4). Little information is available on this topic, represented mainly by case reports and therapeutical trials, and few epidemiological studies. In Romania, the parasite was previously reported in 3 out of 24, and in 1 out of 389 cats with skin lesions (7, 8). More recently, a case report of notoedric mange in association with otodectic mange and roundworm infection was reported (9).

Cats with notoedric mange present intense pruritus and skin lesions such as papules, alopecia, erythema, excoriations, scales, crusts, and lichenification (4, 6). The first lesions appear on the edge of the ear pinna and they spread fast on the head and neck, and sometimes on the legs and perineum facilitated by the cat's habits of self-grooming and of sleeping in a curled position (10). Untreated diseases can be fatal both in young and adult cats (4). Notoedric mange is successfully treated with macrocyclic lactones (11).

Aelurostrongylidosis is a common verminous pneumonia caused by metastrongyloid lungworm *Aelurostrongylus abstrusus* in cats worldwide (12). The clinical presentation varies from subclinical to severe diseases, but most of the animals present mild to moderate respiratory signs such as sneezing and nasal discharge, cough, dyspnea, tachypnea, and abdominal breathing (13). Macrocyclic lactones and fenbendazole are commonly used to treat aelurostrongylidosis (11, 13).

This report describes two cases of notoedric mange concurrent with aelurostrongylidosis in domestic-owned cats from a rural environment in Romania.

CASE HISTORY

Two European shorthair cats originating from the same litter were referred to the Faculty of Veterinary Medicine Cluj-Napoca, at the Dermatology Clinic, at 2 months apart, with a history of skin lesions, weight loss, and respiratory signs (sneezing and cough). Both cats lived in a rural area (Alba County), mainly outdoor together with the queen and a third littermate. The latter two died a month before the consultation of the first cat in our clinic, and they had expressed the same clinical signs. None of the four cats was vaccinated, dewormed, or treated for external parasites. Each case will be presented below.

Case 1

In January 2021, an 18-months-old male cat was submitted to the clinic. The physical examination revealed poor body condition (body score 3/9, 1.5 kg), a body temperature of 37.0°C, skin lesions, excessive earwax, moderate head pruritus, fleas, and flea feces. Alopecia, erythema, scales, crusts, and lichenification were found on the head (face and ears pinna), dorsal thorax, right hind limb, tail, and ventral part of the tail (**Figure 1**). Based on the history and clinical examination, the main differential diagnoses were flea allergy dermatitis and ectoparasitic infestation such as lice (*Felicola subrostrata*) and/or mites (*Otodectes cynotis*, *N. cati*, *Cheiletiella* spp.). Coat brushing, skin scrapings, skin cytology (scotch test), earwax direct microscopic examination, and coproparasitological techniques (flotation and Baermann methods) were used as laboratory procedures. A blood sample was also collected for hematology, blood biochemistry, and feline immunodeficiency virus/feline leukemia virus (FIV/FeLV) test (SNAP FIV/FeLV Combo Test, IDEXX).

A stereomicroscope examination of the coat brushing revealed the presence of fleas (adults and flea feces), adult mites, and eggs of *Notoedres cati* in high numbers (**Figure 2**). *N. cati* mites were morphologically identified based on the presence of concentric rings on the dorsal idiosoma and subterminal anus (**Figure 3**) (4). Furthermore, eggs and adult mites of *N. cati* were detected by the skin scrapings, cytology, and coproparasitological examination by flotation technique (**Figure 3**). The microscopic examination of the earwax was negative. *Aelurostrongylus abstrusus* first stage larvae (L1) and *N. cati* mites were identified by the Baermann technique. The presence of *A. abstrusus* L1 was confirmed by multiplex PCR (mPCR) of internally transcribed spacer 2 (ITS2) region on recovered larvae by Baerman technique following the protocol previously described (14). Coci were identified to the cytology. A blood analysis revealed neutrophilia. The FIV/FeLV fast test was negative.

After diagnosis, the cat was housed indoor in a different location (Cluj County), and the current diet (leftover food) was changed with a commercial dry food. The cat was off-label treated with selamectin (Stronghold®, Zoetis) three administration (**Supplementary File 1**), amoxicillin trihydrate/clavulanic acid (Kesium®, Ceva) for 10 days, and single administration of praziquantel and pyrantel embonate (Cestal Cat®, Ceva). The skin scrapings and coproparasitological examination by flotation and Baermann technique were repeated 2 weeks after the first treatment and 4 weeks after the second and third treatments, respectively (**Supplementary File 1**).

Clinical improvement was noticed at 2 weeks after the first treatment with selamectin; the cat gained weight (body score 4/9), the pruritus decreased, and alopecia and scales was noticed on the head and right hind limb. *Notoedres cati*

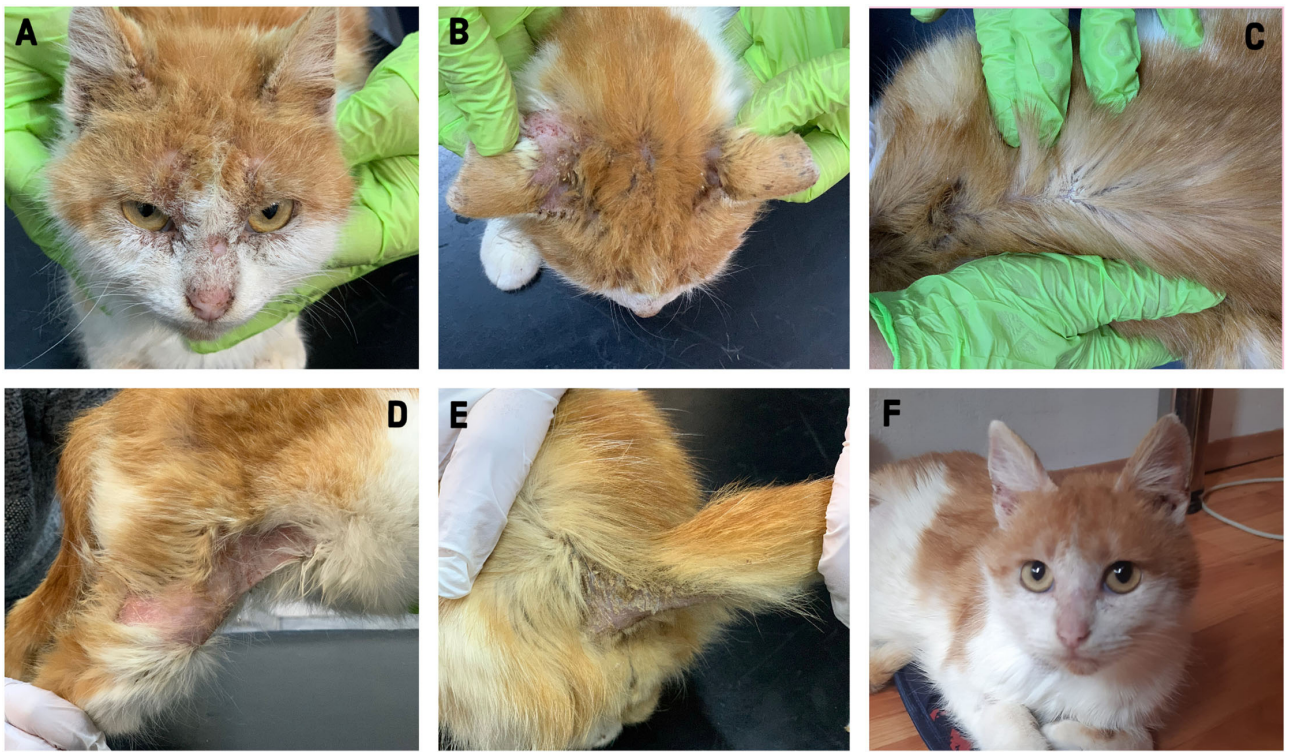

FIGURE 1 | Clinical aspect of the 18-month-old male cat (case 1) before **(A–E)** and after **(F)** treatment.

mites were detected by the skin scrapings and flotation in low numbers. The Baermann technique revealed an increased number of *A. abstrusus* larvae compared with the first examination (**Supplementary File 1**). After a month from the second treatment, skin lesions were observed only on the ear pinna (diffuse alopecia, hyperpigmented macules, and scales) and no pruritus was present. A single mite was detected by skin scraping. Although in a low number, larvae of *A. abstrusus* were still detected by the Baermann technique. After 4 weeks from the third treatment, the cat had no clinical signs or lesions (**Figure 1**). Both the skin scrapings and the Baermann technique were negative (**Supplementary File 1**). One month after the cat was diagnosed with notoedric mange, the onset of pruritic skin lesions (papules) on the chest were reported by the owners.

Case 2

Due to the contagious character of the notoedric mange, and considering the epidemiological characteristics of *A. abstrusus* as well as the similar clinical manifestations, it was presumed that the surviving littermate was suffering from the same conditions. A combination of labeled fipronil, S-methoprene, eprinomectin, and praziquantel (Broadline®, Boehringer Ingelheim) two times monthly was administrated at our recommendation.

In March 2021, the surviving littermate, a 20-month-old female was referred to our clinic because no clinical improvement was obtained after the treatment with fipronil, S-methoprene, eprinomectin, and praziquantel (Broadline®, Boehringer Ingelheim). The clinical examination of the second cat revealed poor body condition (3/9, weight 900 g), cough, sneeze, pruritus, and skin lesions such as diffuse alopecia, scales, crusts, erosions, and lichenification (**Figure 4**). The skin lesions were distributed on the head (face, ear pinna), lateral neck, lateral thorax, ventrum, hind limbs, lumbosacral area, and ventral part of the tail. The same diagnostic techniques as for the first cat were used. Large numbers of *N. cati* and *A. abstrusus* L1 larvae were identified. After the first consultation, the cat was housed indoors, the diet was changed with a commercial food, and she was treated with selamectin (Stronghold®, Zoetis) every 2 weeks, for 6 weeks, and then monthly until negative results to the Baermann technique (**Supplementary File 2**). An antibiotic (amoxicillin trihydrate/clavulanic acid; Kesium®, Ceva) was prescribed for 10 days. Clinical improvement was registered after 2 weeks from the first treatment and a complete clinical cure in a month (**Figure 4**). Skin scrapings became negative after 4 weeks (**Supplementary File 2**). The cat became negative for *A. abstrusus* in 4 months (**Supplementary File 2**).

DISCUSSION

The most common primary pruritic skin conditions in cats are represented by ectoparasites and allergies that are frequently complicated by bacterial or fungal infections (15). Our

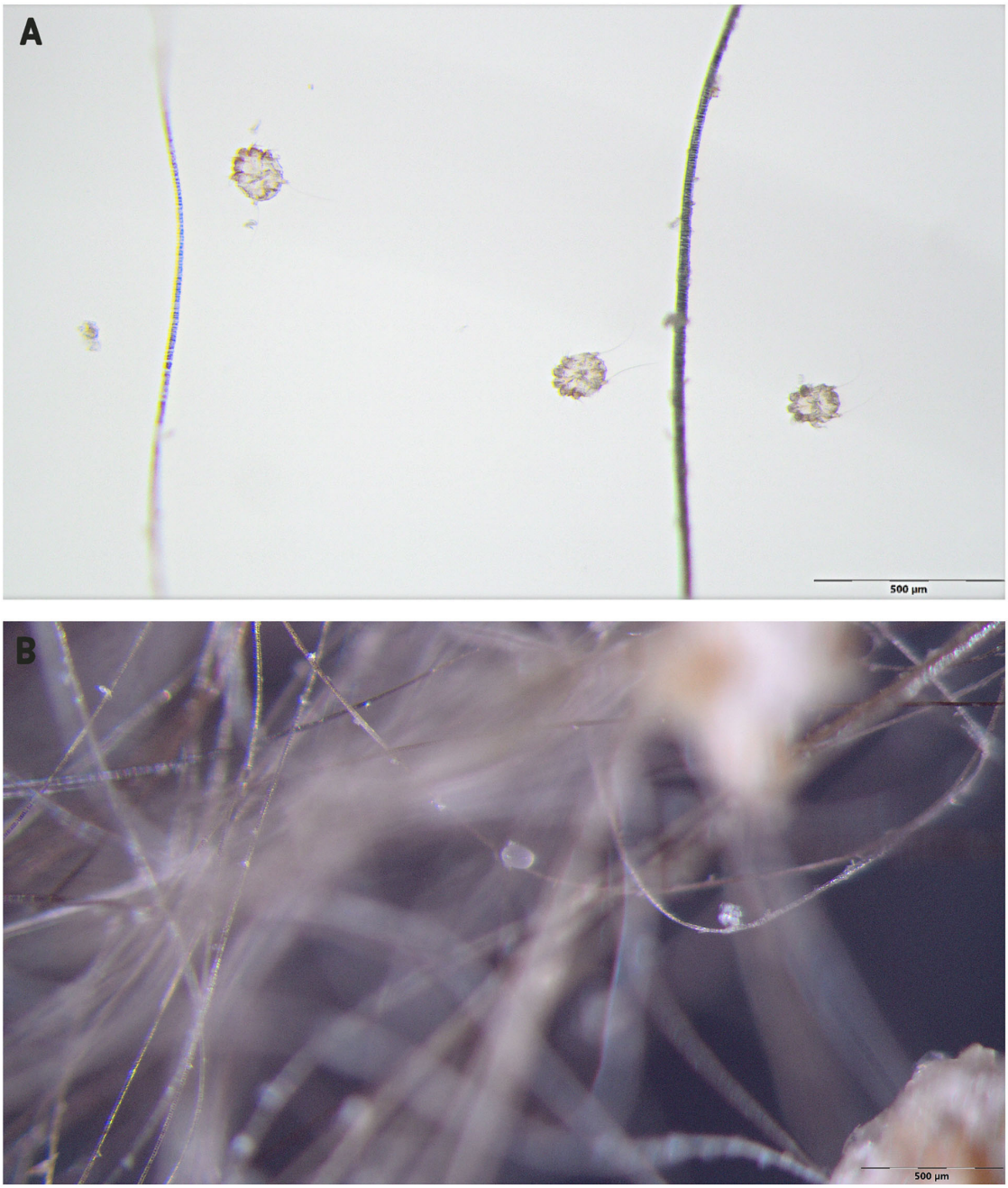

FIGURE 2 | *Notoedres cati* identified through an stereomicroscope examination of the coat brushing (**A**, adults; **B**, egg).

littermate cats presented pruritic skin lesions and respiratory signs. They had outdoor access, lived in a rural area, and they did not benefit from any vaccination and parasite prevention treatment.

Notoedres cati affects both the health and wellbeing of cats. The pruritic skin lesions can rapidly aggravate as a consequence of scratching (up to self-mutilation) and secondary bacterial infections. If it is left untreated in kittens and immunosuppressed individuals, notoedric mange can cause death in 4–5 months (3, 4, 10). Clinically, cases are rare and are diagnosed mainly in cats kept or living in poor hygienic conditions, with malnutrition, and with concurrent diseases (4). In Europe, the prevalence of the diseases varies between 0.2% in owned cats and 2.4% in stray ones (16–18).

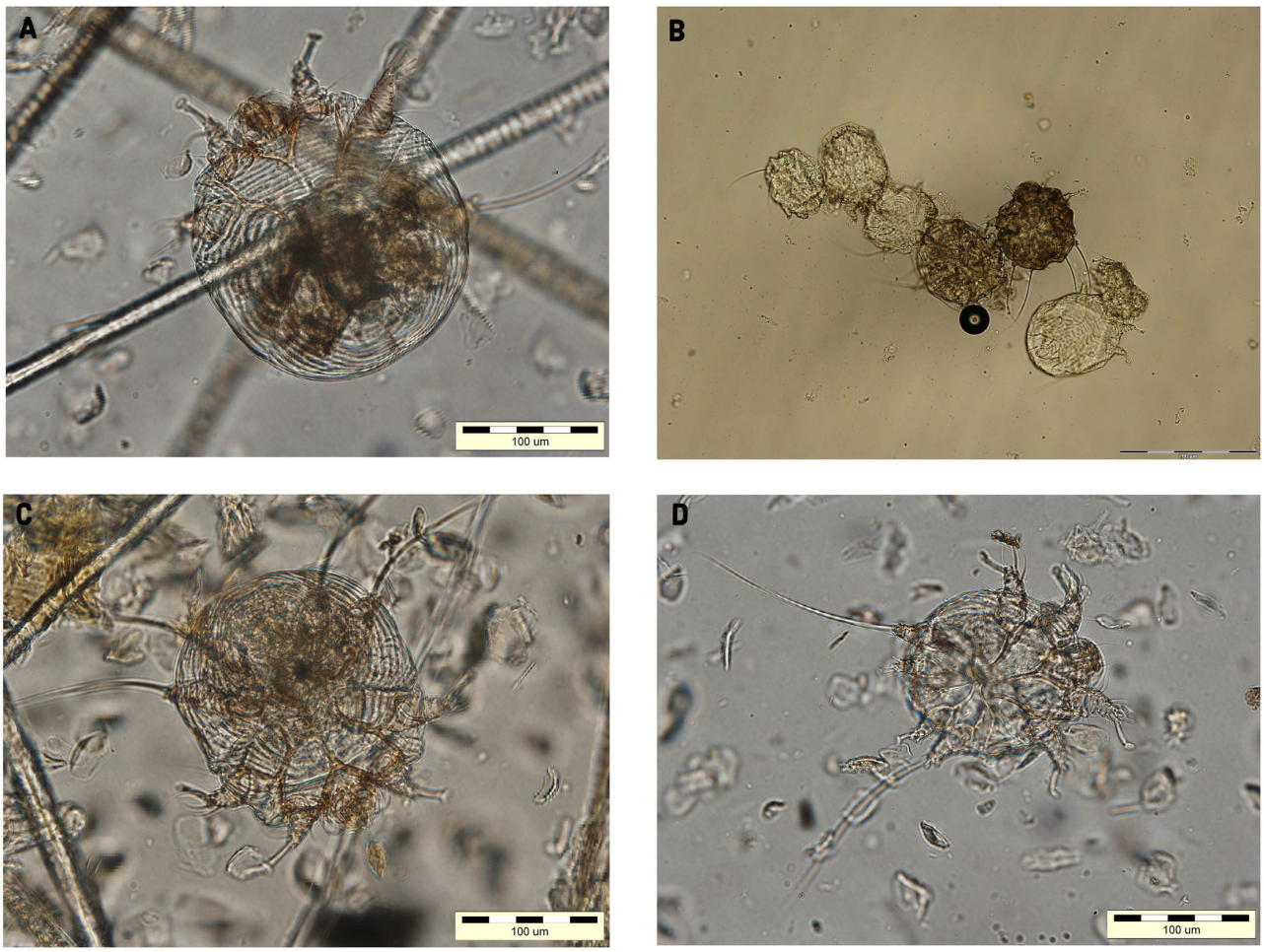

FIGURE 3 | *Notoedres cati* (x100) identified through skin scraping **(A,C,D)** and flotation **(B)**.

The cats from this report presented a generalized clinical form and most probably got the infection from their queen who died together with a littermate. Although, due to the history and epidemiological context, we might presume that the cause of death for the later two was the notoedric mange associated with aelurostrongylidosis, no confirmation was possible as no necropsy was performed. Both our patients were in poor body condition and their food consisted mainly of household waste and probably supplemented by game meat. Usually, most of the cats infected with *A. abstrusus* present mild to moderate respiratory signs. However, there are reports of fatal cases in kittens (19).

Notoedres cati mites are detected mainly by skin scraping and examination under the light microscope. In these cases, *N. cati* mites were identified in high numbers through skin scraping, coat brushing, acetate tape impression, flotation, and Baermann techniques. The acetate tape impression was found to have similar results with skin scraping, and it was able to isolate the mite from cats with negative skin scrapings (20). Cats can ingest accidentally ectoparasites during grooming and thereafter can be identified in the feces. Thus, a fecal flotation can add value to the diagnosis of ectoparasites when they are not identified to the specific methods as it was already demonstrated for other ectoparasites as *Demodex* spp., *Cheyletiella* spp., *Leporacarus* spp., and *Otodectes cynostic* (21, 22). Also, *N. cati* mites were identified by fecal flotation in asymptomatic stray cats from the USA (22, 23).

Macrocyclic lactones are the treatment of choice for mites, but these molecules can be used also for the treatment of metastrongyloid lungworms (11, 24). Selamectin belongs to this drug group and it is licensed for the treatment of sarcoptic and otodectic manges in dogs and cats. It was also successfully used in the treatment of notoedric mange in different hosts, including cats (25–28). The present cases were treated off-label with selamectin spot-on formulation three times every 2- or 4-week interval. The cats were completely cured for notoedric mange after application of

FIGURE 4 | Clinical aspect of the 20-month-old female cat (case 2) before **(A)** and after **(B)** treatment.

the third treatment. The *A. abstrusus* infection was treated at the same time with notoedric mange in one of the cats, while in the other case, 5 applications of selamectin were needed. The spot-on labeled formulation of fipronil/(S)-methoprene/eprinomectin/praziquantel applied twice monthly before the treatment with selamectin was not effective in treating the notoedric mange or aelurostrongylidosis. According to previous studies, this topical formulation applied once has high efficacy in the treatment of notoedric mange (>99%) and aelurostrongylidosis (90.5%) (29, 30). The failure of the treatment with this product could be attributed to the incorrect application of the product by the owner, the lack of absorption to the skin level, the secondary bacterial infection or the immunosuppression caused by the bad diet, and improper hygienic conditions.

The cats' owners developed pruritic skin lesions after 1 month from the moment when the male cat was housed indoor. It was already demonstrated that *N. cati* has zoonotic potential being diagnosed in humans after close contact with infected cats (31–33). It is a self-limiting, transient infestation characterized by papulovesicular lesions with intense pruritus secondary to hypersensitivity developed to the acarian bite. Generally, the lesions disappear within 2-3 weeks if the contact with the infected cat is interrupted, as the parasite does not multiply on the human skin (32).

In conclusion, notoedric mange and aelurostrongylidosis can be treated successfully with selamectin as a spot-on formulation and the treatment must be continued until no parasite will be detected through specific techniques. However, the success of treatment is conditioned by the improvement of the life quality (nutrition and hygiene) and the treatment of secondary complications.

DATA AVAILABILITY STATEMENT

The original contributions presented in the study are included in the article/**Supplementary Material**, further inquiries can be directed to the corresponding authors.

ETHICS STATEMENT

Written informed consent was obtained from the owners for the participation of their animals in this study.

AUTHOR CONTRIBUTIONS

AG wrote the manuscript. MOD revised the manuscript and made important suggestions. VM and AU performed the clinical examination of the cats and laboratory methods. AG, GD'A, and

MOD collected the parasites and took and prepared the photos for the manuscript. VM designed the manuscript. All authors contributed to the article and approved the submitted version.

FUNDING

The work of AG, MOD, AU, and VM was carried out under the frame of the USAMV Cluj-Napoca Internal Grant number 6270/2017. Also, this project was funded by the Ministry of Research and Innovation of Romania, Contract no. PFE/546.

SUPPLEMENTARY MATERIAL

The Supplementary Material for this article can be found online at: https://www.frontiersin.org/articles/10.3389/fvets.2022.849525/full#supplementary-material

REFERENCES

1. Klompen JSH. *Phylogenetic Relationships in the Mite Family Sarcoptidae (Acari: Astigmata)*. Miscellaneous Publications Museum of Zoology, University Of Michigan No. 180 (1992). 164 p.
2. Lavoipierre MMJ. Mange mites of the genus notoedres (Acari: Sarcoptidae) with descriptions of two new species and remarks on notoedric mange in the squirrel and the vole. *J Med Entomol.* (1964) 1:5–17. doi: 10.1093/jmedent/1.1.5
3. Foley J, Serieys LE, Stephenson N, Riley S, Foley C, Jennings M, et al. A synthetic review of notoedres species mites and mange. *Parasitology*. (2016) 143:1847–61. doi: 10.1017/S0031182016001505
4. Deplazes P, Eckert J, Mathis A, Samson-Himmelstjerna Gv, Zahner H. *Parasitology in Veterinary Medicine*. Wageningen: Wageningen Academic Publishers (2016). 653 p. doi: 10.3920/978-90-868 6-274-0
5. Kraabøl M, Gundersen V, Fangel K, Olstad K. The taxonomy, life cycle and pathology of *Sarcoptes scabiei* and *Notoedres cati* (Acarina, Sarcoptidae): a review in a Fennoscandian wildlife perspective. *Fauna Norvegica*. (2015) 35:21–33. doi: 10.5324/fn.v35i0.1652
6. Taylor MA, Coop RL, Wall RL. *Veterinary parasitology. 3rd Edn*. Oxford: Blackwell Pub. (2007). 2080 p.
7. Dărăbuș GH. Incidența dermatomicozelor și a altor afecțiuni cutanate, la câine și pisică, în vestul României [Incidence of dermatophytosis and other skin diseases in dogs and cats from Western Romania]. *Sci Parasitol.* (2003) 1–2:9–13.
8. Draghici AK, Draghici F. Clinical and microscopical aspects in cutaneous polyparasitism in cats. *Bull UASVM Vet Med*. (2008) 65:80–3.
9. Deak G, Dumitrache MO. Therapeutic efficacy of topical treatment with selamectin and sarolaner against notoedric mange in a domestic cat: case report. *Rev Rom Med Vet.* (2021) 31:41–4.
10. Miller WH, Griffin CE, Campbell KL. *Muller and Kirk's Small Animal Dermatology. 7nth Edn*. St. Louis, MO: Elsevier (2017). 950 p.
11. Nolan TJ, Lok JB. Macrocyclic lactones in the treatment and control of parasitism in small companion animals. *Curr Pharm Biotechnol.* (2012) 13:1078–94. doi: 10.2174/138920112800399167
12. Giannelli A, Capelli G, Joachim A, Hinney B, Losson B, Kirkova Z, et al. Lungworms and gastrointestinal parasites of domestic cats: a European perspective. *Int J Parasitol.* (2017) 47:517–28. doi: 10.1016/j.ijpara.2017.02.003
13. Morelli S, Diakou A, Colombo M, Di Cesare A, Barlaam A, Dimzas D, et al. Cat respiratory nematodes: current knowledge, novel data and warranted studies on clinical features, treatment and control. *Pathogens.* (2021) 10:454. doi: 10.3390/pathogens10040454
14. Di Cesare A, Veronesi F, Frangipane di Regalbono A, Iorio R, Traversa D. Novel molecular assay for simultaneous identification of neglected lungworms and heartworms affecting cats. *J Clin Microbiol.* (2015) 53:3009–13. doi: 10.1128/JCM.00901-15
15. Hill PB, Lo A, Eden CA, Huntley S, Morey V, Ramsey S, et al. Survey of the prevalence, diagnosis and treatment of dermatological conditions in small animals in general practice. *Vet Rec.* (2006) 158:533–9. doi: 10.1136/vr.158.16.533
16. Genchi M, Vismarra A, Zanet S, Morelli S, Galuppi R, Cringoli G, et al. Prevalence and risk factors associated with cat parasites in Italy: a multicenter study. *Parasit Vectors.* (2021) 14:475. doi: 10.1186/s13071-021-04981-2
17. Beugnet F, Bourdeau P, Chalvet-Monfray K, Cozma V, Farkas R, Guillot J, et al. Parasites of domestic owned cats in Europe: co-infestations and risk factors. *Parasit Vectors.* (2014) 7:291. doi: 10.1186/1756-3305-7-291
18. Lefkaditis MA, Sossidou AV, Panorias AH, Koukeri SE, Paştiu AI, Athanasiou LV. Urban stray cats infested by ectoparasites with zoonotic potential in Greece. *Parasitol Res.* (2015) 114:3931–4. doi: 10.1007/s00436-015-4688-4
19. Gavrilovic P, Jovanovic M, Gavrilovic A, Nesic S. Fatal aelurostrongylosis in a kitten in Serbia. *Acta Parasitol.* (2017) 62:488–91. doi: 10.1515/ap-2017-0058
20. Sampaio KO, de Oliveira LM, Burmann PM, Sousa Filho RP, Evangelista JS, Cunha MG. Acetate tape impression test for diagnosis of notoedric mange in cats. *J Feline Med Surg.* (2017) 19:702–5. doi: 10.1177/1098612X16632279
21. Moskvina TV, Shchelkanov MY, Begun MA. Fecal flotation in the detection of canine Demodex mites. *Vet Dermatol.* (2018) 29:263–4. doi: 10.1111/vde.12540
22. Milley C, Dryden M, Rosenkrantz W, Griffin J, Reeder C. Comparison of parasitic mite retrieval methods in a population of community cats. *J Feline Med Surg.* (2017) 19:657–64. doi: 10.1177/1098612X16650717
23. Wyrosdick HM, Chapman A, Martinez J, Schaefer JJ. Parasite prevalence survey in shelter cats in Citrus County, Florida. *Vet Parasitol Reg Stud Rep.* (2017) 10:20–4. doi: 10.1016/j.vprsr.2017.07.002
24. Pennisi MG, Hartmann K, Addie DD, Boucraut-Baralon C, Egberink H, Frymus T, et al. Lungworm disease in cats: ABCD guidelines on prevention and management. *J Feline Med Surg.* (2015) 17:626–36. doi: 10.1177/1098612X15588455
25. Fisher MA, Shanks DJ. A review of the off-label use of selamectin (Stronghold/Revolution) in dogs and cats. *Acta Vet Scand.* (2008) 50:46. doi: 10.1186/1751-0147-50-46
26. Olivieri L, Nardini G, Leopardi S, Abramo F. Mite infection in a masked palm civet (Paguma larvata) treated by selamectin (Stronghold®, Pfizer ltd.). *J Zoo Wildl Med.* (2015) 46:592–5. doi: 10.1638/2014-0152.1
27. Itoh N, Muraoka N, Aoki M, Itagaki T. Treatment of Notoedres cati infestation in cats with selamectin. *Vet Rec.* (2004) 154:409.
28. Leone F. Canine notoedric mange: a case report. *Vet Dermatol.* (2007) 18:127–9. doi: 10.1111/j.1365-3164.2007.00577.x
29. Knaus M, Capári B, Visser M. Therapeutic efficacy of Broadline against notoedric mange in cats. *Parasitol Res.* (2014) 113:4303–6. doi: 10.1007/s00436-014-4126-z
30. Giannelli A, Brianti E, Varcasia A, Colella V, Tamponi C, Di Paola G, et al. Efficacy of Broadline® spot-on against Aelurostrongylus abstrusus and Troglostrongylus brevior lungworms in naturally infected cats from Italy. *Vet Parasitol.* (2015) 209:273–7. doi: 10.1016/j.vetpar.2015.02.037
31. Sivajothi S, Sudhakara Reddy B, Rayulu VC, Sreedevi C. Notoedres cati in cats and its management. *J Parasit Dis.* (2015) 39:303–5. doi: 10.1007/s12639-013-0357-7
32. Chakrabarti A. Human notoedric scabies from contact with cats infested with Notoedres cati. *Int J Dermatol.* (1986) 25:646–8. doi: 10.1111/j.1365-4362.1986.tb04527.x

33. Ross IC. Notoedres cati: its possible transmission to man. *Med J Aust.* (1923) 2:246–9. doi: 10.5694/j.1326-5377.1923.tb118888.x

Conflict of Interest: The authors declare that the research was conducted in the absence of any commercial or financial relationships that could be construed as a potential conflict of interest.

Publisher's Note: All claims expressed in this article are solely those of the authors and do not necessarily represent those of their affiliated organizations, or those of the publisher, the editors and the reviewers. Any product that may be evaluated in this article, or claim that may be made by its manufacturer, is not guaranteed or endorsed by the publisher.

frontiers | Frontiers in Veterinary Science

ORIGINAL RESEARCH
published: 15 July 2022
doi: 10.3389/fvets.2022.933691

Molecular Detection and Genotyping of *Enterocytozoon bieneusi* in Pigs in Shanxi Province, North China

Zhen-Huan Zhang[1], *Rui-Lin Qin*[1], *Ya-Ya Liu*[1], *Yang Zou*[2], *Jin-Jin Mei*[1], *Qing Liu*[1], *Wen-Wei Gao*[1], *Xing-Quan Zhu*[1,3,4], *Yu-Hong Ren*[1]* *and Shi-Chen Xie*[1,3]*

[1] College of Veterinary Medicine, Shanxi Agricultural University, Jinzhong, China, [2] Heilongjiang Key Laboratory for Zoonosis, College of Veterinary Medicine, Northeast Agricultural University, Harbin, China, [3] Research Center for Parasites & Vectors, College of Veterinary Medicine, Hunan Agricultural University, Changsha, China, [4] Key Laboratory of Veterinary Public Health of Higher Education of Yunnan, College of Veterinary Medicine, Yunnan Agricultural University, Kunming, China

Enterocytozoon bieneusi is a common opportunistic intestinal pathogen that can cause acute diarrhea in immunosuppressed humans and animals. Though *E. bieneusi* has been widely detected in pigs around the world, little is known of its prevalence and genotype distribution in pigs in Shanxi province, north China. In this study, a total of 362 fecal samples were collected from pigs in three representative counties in north, south, and central Shanxi province, China. The prevalence and genotypes of *E. bieneusi* were investigated by nested PCR amplification of the ribosomal internal transcribed spacer (ITS) region of the ribosomal RNA (rRNA) gene. Overall, the prevalence of *E. bieneusi* in pigs in Shanxi province was 54.70% (198/362). Statistical analysis showed the difference in prevalence was statistically significant between regions ($\chi^2 = 41.94$, df = 2, $P < 0.001$) and ages ($\chi^2 = 80.37$, df = 1, $P < 0.001$). In addition, 16 genotypes of *E. bieneusi* were identified in this study by sequence analysis of the ITS region, including 15 known genotypes (EbpC, EbpA, EbpB, pigEb4, PigEBITS5, I, Henan-I, G, WildBoar 7, SH10, EbpD, CHC5, PigSpEb1, PigSpEb2, and CHG19) and one novel genotype (designated as PigSX-1). Phylogenetic analysis revealed that 14 known genotypes and the novel genotype were clustered into Group 1, whereas genotype I belonged to Group 2. To the best of our knowledge, this is the first report on the prevalence and genotypes of *E. bieneusi* in pigs in Shanxi province. These findings enrich the genetic diversity of *E. bieneusi* and provide the baseline data for the prevention and control of *E. bieneusi* in pigs in the study regions.

Keywords: *Enterocytozoon bieneusi*, pigs, prevalence, genotypes, Shanxi province

OPEN ACCESS

Edited by:
Simona Gabrielli,
Sapienza University of Rome, Italy

Reviewed by:
Iraj Mohammadpour,
Shiraz University of Medical Sciences, Iran
Lei Deng,
National University of Singapore, Singapore
Yujuan Shen,
National Institute of Parasitic Diseases, China

***Correspondence:**
Yu-Hong Ren
renyuhong1963@163.com
Shi-Chen Xie
xieshichen221@163.com

Specialty section:
This article was submitted to Parasitology, a section of the journal Frontiers in Veterinary Science

Received: *01 May 2022*
Accepted: *16 June 2022*
Published: *15 July 2022*

Citation:
Zhang Z-H, Qin R-L, Liu Y-Y, Zou Y, Mei J-J, Liu Q, Gao W-W, Zhu X-Q, Ren Y-H and Xie S-C (2022) Molecular Detection and Genotyping of Enterocytozoon bieneusi in Pigs in Shanxi Province, North China. Front. Vet. Sci. 9:933691. doi: 10.3389/fvets.2022.933691

INTRODUCTION

The phylum Microsporidia contains a large group of single-celled, obligate intracellular spore-forming parasites (more than 220 genera and 1,700 species). Of which, *Enterocytozoon bieneusi* is the most frequently detected species in humans (1). Although *E. bieneusi* infection in immunocompetent individuals is usually asymptomatic (2), acute diarrhea can occur in immunocompromised individuals, such as patients with AIDS (3). In addition, *E. bieneusi* has also been detected in a variety of mammals and birds (4). Humans and animals can be infected by *E. bieneusi* through contact with infected hosts or by ingesting spore-contaminated water or food (5).

Genotyping of *E. bieneusi* is based on amplification and sequencing of the ribosomal internal transcribed spacer (ITS) region of the rRNA gene, which has high single nucleotide polymorphisms (SNPs) (6). At present, over 500 genotypes of *E. bieneusi* have been identified, which are divided into 11 phylogenetic groups (5). Group 1 is the largest human-pathogenic group containing more than 300 genotypes (5). The prevalence of *E. bieneusi* in pigs varied, ranging from 10 to 93.70% worldwide (5). A number of genotypes within Group 1 identified in humans have also been found in pigs, suggesting that pigs could serve as a potential reservoir for *E. bieneusi* transmission to humans (5, 7, 8).

According to data from the National Bureau of Statistics of China, approximately 8 million pigs were produced and consumed in Shanxi province annually (http://www.stats.gov.cn/tjsj/ndsj/2019/indexeh.htm). However, little is known about the epidemiology of *E. bieneusi* in pigs in Shanxi province. In this study, the prevalence and genotypes of *E. bieneusi* in pigs in Shanxi province were investigated by using nested PCR amplification of the ribosomal ITS region. Meanwhile, phylogenetic analysis was conducted to evaluate the zoonotic potential of the *E. bieneusi* isolates.

MATERIALS AND METHODS

Collection of Samples

In November 2020, with the permission of the farm owners, a total of 362 fresh fecal samples were randomly collected from pigs in three farms each in Shanyin county (39°52′ N, 112°81′ E) located in northern Shanxi province, Qi county (37°35′ N, 112°33′ E) located in central Shanxi province, and Jishan county (35°59′ N, 110°97′ E) located in southern Shanxi province. Approximately, 5–15% of samples were collected from each farm. All fecal samples were transported to the laboratory in a styrofoam box with ice packs immediately and stored at −20°C until genomic DNA extraction.

DNA Extraction and PCR Amplification

The genomic DNA was extracted from each fecal sample (approximately 200 mg) using the E.Z.N.A.® Stool DNA Kit (Omega Bio-tek Inc., Norcross, GA, USA) and stored at −20°C until used for subsequent PCR amplification. A nested PCR was performed to amplify the ITS region by using *E. bieneusi*-specific primers described in a previous study (9). Briefly, the reaction mixture (25 μl) contained 2.5 μl of 10×PCR Buffer (Mg^{2+} free), 1.5 mM of $MgCl_2$, 2 μl of dNTP mixture (2.5 mM each), 1.25 U of *Ex*-Taq polymerase (Takara, Dalian, China), 1 μM of each primer, 14.75 μl of ddH_2O, and 2 μl of DNA template. The conditions and cycling parameters were as follows: initial denaturation at 94°C for 5 min, followed by 35 cycles at 94°C for 30 s, annealing at 55°C for 30 s, 72°C for 40 s, and a final extension at 72°C for 10 min. To ensure the reliability of the results, each PCR amplification included a negative control (reagent-grade water) and a positive control (DNA of the *E. bieneusi* BEB6 genotype from sheep). Then, secondary products were checked by using 2.5% agarose gel and visualized under UV light after staining in ethidium bromide.

Sequencing and Phylogenetic Analysis

All PCR products were sent to Sangon Biotech Co. Ltd (Shanghai, China) for two-directional sequencing on an ABI PRISM DNA Analyzer (Applied Biosystems, Foster City, CA, USA) using relevant internal primers for PCR amplification. The obtained sequences were aligned with the relevant sequences available in the GenBank database using Basic Local Alignment Search Tool (BLAST) and Clustal X to determine the genotypes of *E. bieneusi*. All samples with novel genotypes were sequenced two times to ensure the reliability of the data. The novel genotype was denominated according to the nomenclature established by Santin and Fayer (6). The phylogenetic tree was constructed by MEGA 7 using the Neighbor-Joining (NJ) method and Kimura 2-parameter model with 1,000 bootstraps (9).

Statistical Analysis

In this study, the software SPSS V26.0 (SPSS Inc., Chicago, IL, USA) was used to analyze the correlation between prevalence and risk factors of *E. bieneusi* in pigs by Chi-square (χ^2) test. Odds ratios (ORs) and their 95% confidence intervals (95%CIs) were calculated to identify risk factors. There was a significant difference in prevalence when the p-value was <0.05.

RESULTS

Prevalence of *E. bieneusi* in Pigs in Shanxi Province

In this study, 198 of 362 fecal samples were detected to be positive for *E. bieneusi*, and the prevalence of *E. bieneusi* in pigs in Shanxi province was 54.70% (**Table 1**). Statistical analysis showed that the prevalence of *E. bieneusi* in pigs aged <6 months was 71.73% (170/237), which was significantly higher than that in pigs aged more than 6 months (22.40%, 28/125) ($\chi^2 = 80.37$, df = 1, $P < 0.001$). The prevalence of *E. bieneusi* in Qi county (22.06%, 15/68) was significantly lower than that of Shanyin county (53.15%, 59/111) and Jishan county (67.76%, 124/183) ($\chi^2 = 41.94$, df = 2, $P < 0.001$), respectively.

Genotype Distribution of *E. bieneusi* in Pigs

A total of 16 genotypes were identified by ITS sequence analysis, including 15 known genotypes (EbpC, EbpA, EbpB, pigEb4, PigEBITS5, I, Henan-I, G, WildBoar7, SH10, EbpD, CHC5, PigSpEb1, CHG19, and PigSpEb2) and one novel genotype (named as PigSX-1) (**Table 2**). Of which, EbpA (5.05%, 10/198), EbpC (34.34%, 68/198), and PigSpEb2 (22.22%, 44/198) were the predominant genotype in Qi county, Jishan county, and Shanyin county, respectively. Notably, genotype PigSpEb2 was detected in Shanyin county (55.70%, 44/79) and Jishan county (44.30%, 35/79), but not in Qi county. A comparison between the two age groups showed that PigSpEb2 was mainly distributed in young pigs (<6 months) (94.94%, 75/79). Almost all the genotypes identified in Jishan county were EbpC (98.55%, 68/69), which was mainly detected in young pigs (91.30%, 63/69). In addition, the novel genotype pigSX-1 (2.53%, 5/198) was only detected in pigs in Jishan county. Sequence analysis revealed that the novel genotype pigSX-1 showed a 98.71% similarity to the genotype EbpB (AF076041), with five SNPs.

TABLE 1 | Factors associated with prevalence of *Enterocytozoon bieneusi* in pigs in Shanxi province, China.

Factor	Category	No. tested	No. positive	Prevalence% (95%CI)	OR (95%CI)	*P*-value
Region	Jishan	183	124	67.76 (60.99–74.53)	7.43 (3.87–14.25)	<0.001
	Qi	68	15	22.06 (12.20–31.91)	1	
	Shanyin	111	59	53.15 (43.87–62.44)	4.01 (2.02–7.94)	
Age	0 < month ≤ 6	237	170	71.73 (66.00–77.46)	8.79 (5.30–14.59)	<0.001
	6 > month	125	28	22.40 (15.09–29.71)	1	
Total		362	198	54.70 (49.57–59.82)		

TABLE 2 | Genotype distribution of *Enterocytozoon bieneusi* in pigs in Shanxi province, China.

Factor	Category	No. tested	No. positive	Genotypes (*n*)
Location	Jishan	183	124	EbpC (68), PigSpEb2 (35), PigSX-1 (5), Henan-I (3), pigEb4 (3), I (3), WildBoar7 (2), PigEBITS5 (2), EbpA (1), CHG19 (1), CHC5 (1)
	Qi	68	15	EbpA (10), EbpB (4), EbpD (1)
	Shanyin	111	59	PigSpEb2 (44), EbpA (8), G (2), SH10 (2), EbpC (1), PigEBITS5 (1), PigSpEb1 (1)
Age	0 < month < 6	237	170	PigSpEb2 (75), EbpC (63), EbpA (16), PigSX-1 (5), EbpB (4), Henan-I (1), CHG19 (1), CHC5 (1), G (1), PigEBITS5 (1), PigSpEb1 (1), SH10 (1)
	month > 6	125	28	EbpC (6), PigSpEb2 (4), EbpA (3), pigEb4 (3), I (3), WildBoar7 (2), PigEBITS5 (2), Henan-I (2), EbpD (1), G (1), SH10 (1)
Total		362	198	PigSpEb2 (79), EbpC (69), EbpA (19), PigSX-1 (5), EbpB (4), pigEb4 (3), PigEBITS5 (3), I (3), Henan-I (3), G (2), WildBoar7 (2), SH10 (2), EbpD (1), CHC5 (1), PigSpEb1 (1), CHG19 (1)

Phylogenetic Relationship Based on ITS Locus

A phylogenetic tree was used to evaluate the genetic relationship of the 16 genotypes of *E. bieneusi* obtained in this study. The results showed that all 15 genotypes were clustered into Group 1, except for genotype I, which belonged to Group 2 (**Figure 1**).

Nucleotide Sequence Accession Numbers

The 16 representative ITS sequences of *E. bieneusi* obtained in this study were deposited in the GenBank database under accession numbers OM219033-OM219048.

DISCUSSION

E. bieneusi has caused economic losses to the pig industry worldwide since it was detected in Sweden in 1996 for the first time (10). The results obtained in this study showed that the overall prevalence of *E. bieneusi* in pigs in Shanxi province was 54.70% (198/362), which was higher than that in pigs in most provinces in China (11–17) (**Table 3**), Thailand (14.75%, 36/244) (18), Japan (33.33%, 10/30) (19), Spain (22.58%, 42/186) (20), Massachusetts, USA (31.68%, 64/202) (21), and Malaysia (40.67%, 183/450) (22). However, the prevalence of *E. bieneusi* in pigs in Shanxi province was lower than that in two provinces in China (23, 24) (**Table 3**) and Brazil (59.34%, 54/91) (25). Regional differences in the prevalence of *E. bieneusi* may be related to geographical locations, sample volumes, breeding management, and ecological factors.

There were significant differences in *E. bieneusi* prevalence between the two age groups, which was consistent with the results of a previous study (14). Some researchers argue that the probable reason for the higher prevalence of *E. bieneusi* in young pigs (<6 months) might be due to their imperfect immune system (23). However, a high prevalence of *E. bieneusi* was also found in older pigs in different areas of China (12, 14). The difference in *E. bieneusi* prevalence among these age groups indicated that geoecology, rearing conditions, and stocking density may be partially responsible for the variations in prevalence.

In this study, 15 known genotypes (PigSpEb2, EbpC, EbpA, EbpB, pigEb4, PigEBITS5, I, Henan-I, G, WildBoar7, SH10, EbpD, CHC5, PigSpEb1, and CHG19) and a novel genotype (PigSX-1) were identified in pigs in Shanxi province. Of which, genotype PigSpEb2 (39.90%, 79/198) was the predominant genotype, followed by EbpC (34.85%, 69/198) (synonyms: E, WL13, WL17, and Peru4) and EbpA (9.60%, 19/198) (synonym: F). This finding was not consistent with the results of previous studies, in which EbpC was detected as the predominate genotype in pigs in Zhejiang province, Guangdong province, Jilin province, and Tibet Autonomous Region in China (13, 14, 26). So far, the reasons for the difference in predominate genotypes of *E. bieneusi* in pigs from different study regions are still unknown. We reasoned that the geographical locations, pig breeds, and hygiene conditions might be responsible for the variations in predominate genotypes. Hence, more samples from diverse

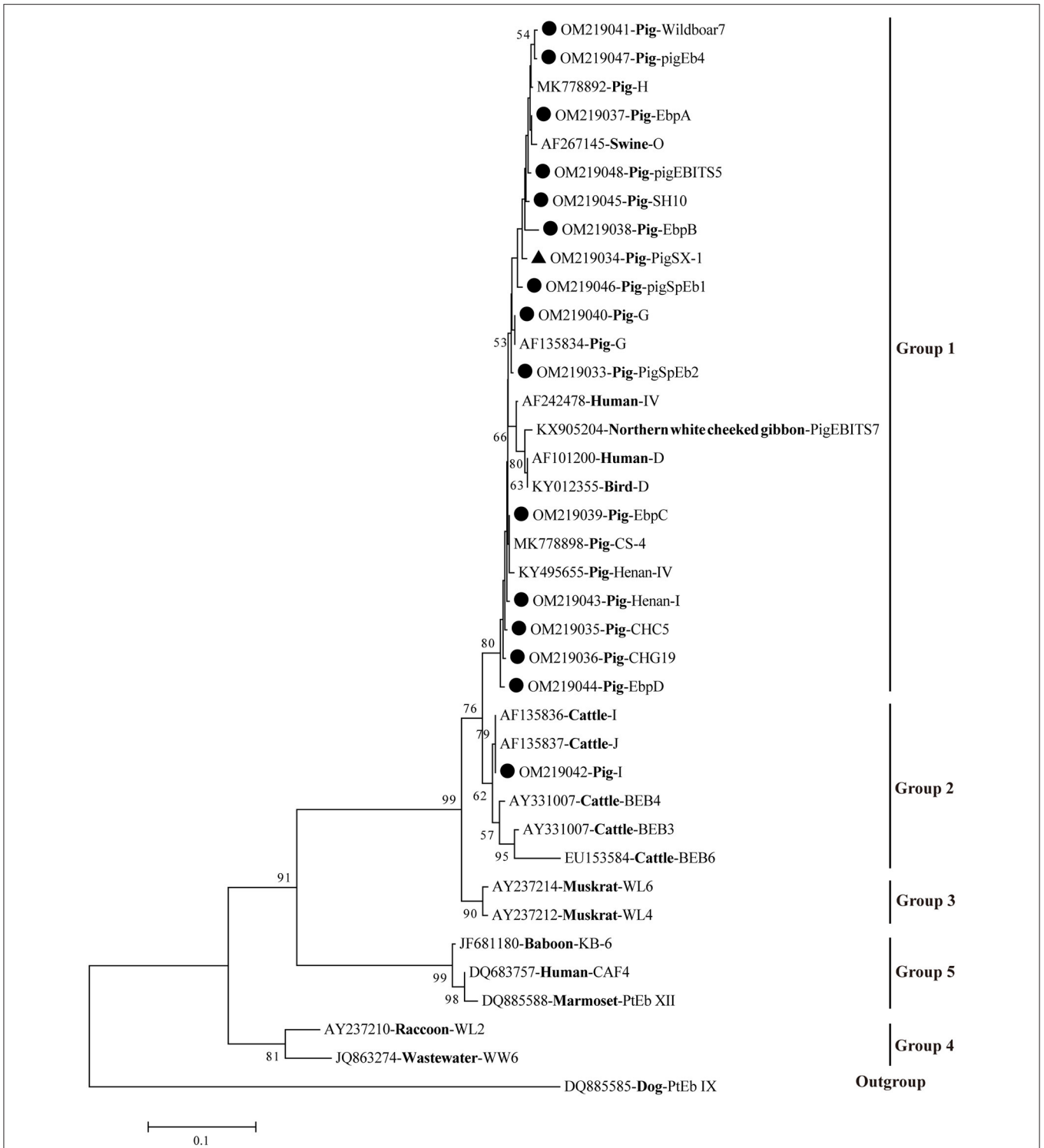

FIGURE 1 | Phylogenetic relationships of *E. bieneusi* genotypes based on ITS sequences. Obtained ITS sequences in the present study were marked with black circles (• known genotypes) and black triangle (▲ novel genotype), respectively. The bootstrap value <50% was hide.

hosts in the study areas should be examined in the future to further clarify the possible patterns of prevalent genotypes of *E. bieneusi*.

Of those 16 identified genotypes, seven known genotypes (EbpC, EbpA, EbpB, PigEBITS5, I, EbpD, and CHG19) were commonly observed in humans (27), livestock (7, 28–30),

TABLE 3 | *Enterocytozoon bieneusi* occurrence and genotypes identification in pigs in China.

District	No. Positive/Total	Prevalence (%)	Genotypes	Year	References
Beijing	108/257	42.02	**EbpC**, CAM5, wildboar12, CHS12, CM8, CTS3, Henan-IV, pigEBITS5	2020	(15)
Fujian	177/725	24.41	**EbpC**, EbpA, FJF, CHN-RR2, KIN-1, CHG7, CHS5, CM11, FJS, CHG23, G, PigEBITS, D	2019	(11)
Guangdong	19/72	26.39	**EbpC**, CHS5, GD1	2018	(14)
Hainan	88/188	46.81	**CS-4**, MJ14, CHG19, EbpA, HNP-I, HNP-II, HNP-III, HNP-IV	2020	(17)
Heilongjiang	267/563	47.42	**EbpC**, O, CS-4, EbpA, Henan-IV, PigEBITS5, EbpB, CC-1, CS-1, CS-3, CHN7, CS-10	2016	(12)
Henan	186/246	75.61	**EbpC**, EbpA, CHC5, CHG19, H, Henan-III	2019	(24)
Shaanxi province	442/560	78.93	**SZZD1**, SLTC2, SYLA5, CHG19, CHC5, SLTC3, SZZA2, EbpA, PigEBITS5, SHZA1, SZZC1, H, PigEB4, SYLC1, Henan-IV, SLTC1, SYLA1, SYLA2, CHS5, D, CHN7, CM6, SMXB1, SMXC1, SZZB1, SZZA1, SYLA3, SMXD1, SYLA4, SYLD1, CHG3, SZZD2, SHZC1, SMXD2	2018	(23)
Tibet autonomous Region	41/345	11.88	**EbpC**, CHS12, EbpD, PigEBITS5, GB11, GB31	2019	(13)
Xinjiang Uygur Autonomous region	389/801	48.56	**EbpC**, CHC5, CS-1, CS-4 CS-7, CS-9, D, EbpA, EbpD, H, PigEb4, PigEBITS5, WildBoar8, XJP-II, XJP-III	2019	(16)
Yunnan	58/200	29.00	**EbpC**, EbpA, YN1, Henan-IV, YN3, G, H, PigEBITS5, YN2, D	2018	(14)
Zhejiang	48/124	38.71	**EbpC**, EbpA, ZJ1, ZJ2, KIN-1, PigEBITS5	2018	(14)

Prevalent genotypes of E. bieneusi in that study are shown in bold.

non-human primates (NHPs) (31), wild animals (32), and water (33), posing a great threat to the public health. Particularly, genotypes EbpC and I were also found in squirrels and pet rabbits in China, respectively, which have close contact with humans (34, 35). Genotypes PigSpEb1 and PigSpEb2 were first identified in pigs in Spain in 2020 and 2021, respectively, but there was no data regarding the age patterns of the two genotypes in pigs (20, 36). Although our results revealed that younger pigs (<6 months) were more susceptible to PigSpEb1 and PigSpEb2, more investigations are still needed to confirm this in the future. A few studies have reported the presence of PigEb4, Henan-I, CHC5, Wildboar7, and SH10 in pigs, and further studies are warranted to clarify the host specificity and public health implications of these genotypes (24, 30, 37, 38). Phylogenetic analysis showed that 15 known genotypes were clustered into Group 1 and Group 2 (**Figure 1**). The novel genotype (PigSX-1) was clustered into Group 1, and was genetically closely related to zoonotic genotype EbpB, suggesting its importance and zoonotic potential.

CONCLUSION

This study reported, for the first time, the prevalence of *E. bieneusi* (54.70%) in pigs in Shanxi province, north China, and a higher prevalence was observed in young pigs. Fifteen known *E. bieneusi* genotypes and one novel genotype (PigSX-1) were identified. Fifteen genotypes were clustered into Group 1, suggesting that these infections may not only be a veterinary issue but also a public health concern. These findings enriched the global genetic diversity of *E. bieneusi* and provided baseline data for the prevention and control of *E. bieneusi* infection in pigs in the study regions.

DATA AVAILABILITY STATEMENT

The original contributions presented in the study are included in the article/supplementary material, further inquiries can be directed to the corresponding authors.

ETHICS STATEMENT

Ethical review and approval was not required for the animal study because this is not applicable. Written informed consent was obtained from the owners for the participation of their animals in this study.

AUTHOR CONTRIBUTIONS

S-CX, X-QZ, and Y-HR conceived and designed the experiments. Z-HZ performed the experiments, analyzed the data, and wrote the paper. J-JM, R-LQ, and Y-YL participated in the collection of fecal samples. W-WG and Y-HR participated in the implementation of the study. S-CX, QL, YZ, and X-QZ critically revised the manuscript. All authors have read and approved the final version of the manuscript.

FUNDING

Project support was provided by Fund for Shanxi 1331 Project (Grant No. 20211331-13), the Special Research Fund

of Shanxi Agricultural University for High-level Talents (Grant No. 2021XG001), the Yunnan Expert Workstation (Grant No. 202005AF150041), and the Veterinary Public Health Innovation Team of Yunnan Province (Grant No. 202105AE160014).

REFERENCES

1. Han B, Pan G, Weiss LM. Microsporidiosis in humans. *Clin Microbiol Rev.* (2021) 34:e0001020. doi: 10.1128/CMR.00010-20
2. Sak B, Brady D, Pelikánová M, Květonová D, Rost M, Kostka M, et al. Unapparent microsporidial infection among immunocompetent humans in the Czech Republic. *J Clin Microbiol.* (2011) 49:1064–70. doi: 10.1128/JCM.01147-10
3. Matos O, Lobo ML, Xiao L. Epidemiology of *Enterocytozoon bieneusi* infection in humans. *J Parasitol Res.* (2012) 2012:981424. doi: 10.1155/2012/981424
4. Santin M, Fayer R. Microsporidiosis: *Enterocytozoon bieneusi* in domesticated and wild animals. *Res Vet Sci.* (2011) 90:363–71. doi: 10.1016/j.rvsc.2010.07.014
5. Li W, Feng Y, Santin M. Host specificity of *Enterocytozoon bieneusi* and public health implications. *Trends Parasitol.* (2019) 35:436–51. doi: 10.1016/j.pt.2019.04.004
6. Santin M, Fayer R. *Enterocytozoon bieneusi* genotype nomenclature based on the internal transcribed spacer sequence: a consensus. *J Eukaryot Microbiol.* (2009) 56:34–8. doi: 10.1111/j.1550-7408.2008.00380.x
7. Hu Y, Feng Y, Huang C, Xiao L. Occurrence, source, and human infection potential of *Cryptosporidium* and *Enterocytozoon bieneusi* in drinking source water in Shanghai, China, during a pig carcass disposal incident. *Environ Sci Technol.* (2014) 48:14219–27. doi: 10.1021/es504464t
8. Leelayoova S, Piyaraj P, Subrungruang I, Pagornrat W, Naaglor T, Phumklan S, et al. Genotypic characterization of *Enterocytozoon bieneusi* in specimens from pigs and humans in a pig farm community in central Thailand. *J Clin Microbiol.* (2009) 47:1572–4. doi: 10.1128/JCM.00187-09
9. Ma YT, Zou Y, Liu Q, Xie SC, Li RL, Zhu XQ, et al. Prevalence and multilocus genotypes of *Enterocytozoon bieneusi* in alpacas (*Vicugna pacos*) in Shanxi province, northern China. *Parasitol Res.* (2019) 118:3371–5. doi: 10.1007/s00436-019-06503-7
10. Deplazes P, Mathis A, Muller C, Weber R. Molecular epidemiology of *Encephalitozoon cuniculi* and first detection of *Enterocytozoon bieneusi* in faecal samples of pigs. *J Eukaryot Microbiol.* (1996) 43:93S. doi: 10.1111/j.1550-7408.1996.tb05018.x
11. Zhang N, Wu R, Ji T, Cui LL, Cao HX, Li D, et al. Molecular detection, multilocus genotyping, and population genetics of *Enterocytozoon bieneusi* in pigs in southeastern China. *J Eukaryot Microbiol.* (2020) 67:107–14. doi: 10.1111/jeu.12759
12. Wan Q, Lin Y, Mao Y, Yang Y, Li Q, Zhang S, et al. High prevalence and widespread distribution of zoonotic *Enterocytozoon bieneusi* genotypes in swine in northeast China: implications for public health. *J Eukaryot Microbiol.* (2016) 63:162–70. doi: 10.1111/jeu.12264
13. Zou Y, Zheng WB, Song HY, Xia CY, Shi B, Liu JZ, et al. Prevalence and genetic characterization of *Enterocytozoon bieneusi* and *Giardia duodenalis* in Tibetan pigs in Tibet, China. *Infect Genet Evol.* (2019) 75:104019. doi: 10.1016/j.meegid.2019.104019
14. Zou Y, Hou L, Li FC, Zou FC, Lin RQ, Ma JG, et al. Prevalence and genotypes of *Enterocytozoon bieneusi* in pigs in southern China. *Infect Genet Evol.* (2018) 66:52–6. doi: 10.1016/j.meegid.2018.09.006
15. Feng S, Jia T, Huang J, Fan Y, Chang H, Han S, et al. Identification of *Enterocytozoon bieneusi* and *Cryptosporidium* spp. in farmed wild boars (Sus scrofa) in Beijing, China. *Infect Genet Evol.* (2020) 80:104231. doi: 10.1016/j.meegid.2020.104231
16. Li DF, Zhang Y, Jiang YX, Xing JM, Tao DY, Zhao AY, et al. Genotyping and zoonotic potential of *Enterocytozoon bieneusi* in pigs in Xinjiang, China. *Front Microbiol.* (2019) 10:2401. doi: 10.3389/fmicb.2019.02401
17. Zhou HH, Zheng XL, Ma TM, Qi M, Zhou JG, Liu HJ, et al. Molecular detection of *Enterocytozoon bieneusi* in farm-raised pigs in Hainan province, China: infection rates, genotype distributions, and zoonotic potential. *Parasite.* (2020) 27:12. doi: 10.1051/parasite/2020009
18. Thathaisong U, Siripattanapipong S, Leelayoova S, Mungthin M. Prevalence and molecular characterization of *Enterocytozoon bieneusi* among pigs in Chonburi province, eastern Thailand. *Am J Trop Med Hyg.* (2019) 101:1392–6. doi: 10.4269/ajtmh.19-0569
19. Abe N, Kimata I. Molecular survey of *Enterocytozoon bieneusi* in a Japanese porcine population. *Vector Borne Zoonotic Dis.* (2010) 10:425–7. doi: 10.1089/vbz.2009.0039
20. Dashti A, Rivero-Juárez A, Santín M, López-López P, Caballero-Gómez J, Frías-Casas M, et al. *Enterocytozoon bieneusi* (Microsporidia): identification of novel genotypes and evidence of transmission between sympatric wild boars (*Sus scrofa ferus*) and Iberian pigs (*Sus scrofa domesticus*) in southern Spain. *Transbound Emerg Dis.* (2020) 67:2869–80. doi: 10.1111/tbed.13658
21. Buckholt MA, Lee JH, Tzipori S. Prevalence of *Enterocytozoon bieneusi* in swine: an 18-month survey at a slaughterhouse in Massachusetts. *Appl Environ Microbiol.* (2002) 68:2595–9. doi: 10.1128/AEM.68.5.2595-2599.2002
22. Ruviniyia K, Abdullah DA, Sumita S, Lim YAL, Ooi PT, Sharma RSK. Molecular detection of porcine *Enterocytozoon bieneusi* infection in Peninsular Malaysia and epidemiological risk factors associated with potentially zoonotic genotypes. *Parasitol Res.* (2020) 119:1663–74. doi: 10.1007/s00436-020-06648-w
23. Wang SS, Li JQ, Li YH, Wang XW, Fan XC, Liu X, et al. Novel genotypes and multilocus genotypes of *Enterocytozoon bieneusi* in pigs in northwestern China: a public health concern. *Infect Genet Evol.* (2018) 63:89–94. doi: 10.1016/j.meegid.2018.05.015
24. Li D, Zheng S, Zhou C, Karim MR, Wang L, Wang H, et al. Multilocus typing of *Enterocytozoon bieneusi* in pig reveals the high prevalence, zoonotic potential, host adaptation and geographical segregation in China. *J Eukaryot Microbiol.* (2019) 66:707–18. doi: 10.1111/jeu.12715
25. Fiuza VR, Oliveira FC, Fayer R, Santín M. First report of *Enterocytozoon bieneusi* in pigs in Brazil. *Parasitol Int.* (2015) 64:18–23. doi: 10.1016/j.parint.2015.01.002
26. Li W, Diao R, Yang J, Xiao L, Lu Y, Li Y, et al. High diversity of human-pathogenic *Enterocytozoon bieneusi* genotypes in swine in northeast China. *Parasitol Res.* (2014) 113:1147–53. doi: 10.1007/s00436-014-3752-9
27. Wang SS, Wang RJ, Fan XC, Liu TL, Zhang LX, Zhao GH. Prevalence and genotypes of *Enterocytozoon bieneusi* in China. *Acta Trop.* (2018) 183:142–52. doi: 10.1016/j.actatropica.2018.04.017
28. Li J, Luo N, Wang C, Qi M, Cao J, Cui Z, et al. Occurrence, molecular characterization and predominant genotypes of *Enterocytozoon bieneusi* in dairy cattle in Henan and Ningxia, China. *Parasit Vectors.* (2016) 9:142. doi: 10.1186/s13071-016-1425-5
29. Shi K, Li M, Wang X, Li J, Karim MR, Wang R, et al. Molecular survey of *Enterocytozoon bieneusi* in sheep and goats in China. *Parasit Vectors.* (2016) 9:23. doi: 10.1186/s13071-016-1304-0
30. Li W, Li Y, Li W, Yang J, Song M, Diao R, et al. Genotypes of *Enterocytozoon bieneusi* in livestock in China: high prevalence and zoonotic potential. *PLoS ONE.* (2014) 9:e97623. doi: 10.1371/journal.pone.0097623
31. Karim MR, Dong H, Li T, Yu F, Li D, Zhang L, et al. Predomination and new genotypes of *Enterocytozoon bieneusi* in captive nonhuman primates in zoos in China: high genetic diversity and zoonotic significance. *PLoS ONE.* (2015) 10:e0117991. doi: 10.1371/journal.pone.0117991
32. Lin X, Xin L, Cao Y, Hou M, Qiao F, Li J, et al. Common occurrence of *Enterocytozoon bieneusi* genotypes SHR1 and PL2 in farmed masked palm civet (*Paguma larvata*) in China. *Int J Parasitol Parasites Wildl.* (2021) 16:99–102. doi: 10.1016/j.ijppaw.2021.08.009
33. Ye J, Ji Y, Xu J, Ma K, Yang X. Zoonotic *Enterocytozoon bieneusi* in raw wastewater in Zhengzhou, China. *Folia Parasitol.* (2017) 64:2017.002. doi: 10.14411/fp.2017.002
34. Deng L, Chai Y, Luo R, Yang L, Yao J, Zhong Z, et al. Occurrence and genetic characteristics of *Cryptosporidium* spp. and enterocytozoon bieneusi in pet red squirrels (Sciurus vulgaris) in China. *Sci Rep.* (2020) 10:1026. doi: 10.1038/s41598-020-57896-w

35. Deng L, Chai Y, Xiang L, Wang W, Zhou Z, Liu H, et al. First identification and genotyping of *Enterocytozoon bieneusi* and *Encephalitozoon* spp. in pet rabbits in China. *BMC Vet Res.* (2020) 16:212. doi: 10.1186/s12917-020-02434-z
36. Dashti A, Rivero-Juárez A, Santín M, George NS, Köster PC, López-López P, et al. Diarrhoea-causing enteric protist species in intensively and extensively raised pigs (*Sus scrofa domesticus*) in southern Spain. part I: prevalence and genetic diversity. *Transbound Emerg Dis.* (2021). doi: 10.1111/tbed.14388. [Epub ahead of print].
37. Rinder H, Thomschke A, Dengjel B, Gothe R, Löscher T, Zahler M. Close genotypic relationship between *Enterocytozoon bieneusi* from humans and pigs and first detection in cattle. *J Parasitol.* (2000) 86:185–8. doi: 10.1645/0022-3395(2000)086[0185:CGRBEB]2.0.CO;2
38. Liu H, Ni H, Xu J, Wang R, Li Y, Shen Y, et al. Genotyping and zoonotic potential of *Cryptosporidium* and *Enterocytozoon bieneusi* in pigs transported across regions in China. *Microb Pathog.* (2021) 154:104823. doi: 10.1016/j.micpath.2021.104823

Conflict of Interest: The authors declare that the research was conducted in the absence of any commercial or financial relationships that could be construed as a potential conflict of interest.

frontiers | Frontiers in Veterinary Science

TYPE Original Research
PUBLISHED 05 August 2022
DOI 10.3389/fvets.2022.981664

OPEN ACCESS

EDITED BY
Serena Cavallero,
Sapienza University of Rome, Italy

REVIEWED BY
Jun-Jun He,
Chinese Academy of Agricultural Sciences (CAAS), China
David Smith,
Moredun Research Institute, United Kingdom

*CORRESPONDENCE
Britta Lundström-Stadelmann
britta.lundstroem@vetsuisse.unibe.ch

†These authors have contributed equally to this work

SPECIALTY SECTION
This article was submitted to Parasitology, a section of the journal Frontiers in Veterinary Science

RECEIVED 29 June 2022
ACCEPTED 18 July 2022
PUBLISHED 05 August 2022

CITATION
Chaudhry S, Zurbriggen R, Preza M, Kämpfer T, Kaethner M, Memedovski R, Scorrano N, Hemphill A, Doggett JS and Lundström-Stadelmann B (2022) Dual inhibition of the *Echinococcus multilocularis* energy metabolism. *Front. Vet. Sci.* 9:981664. doi: 10.3389/fvets.2022.981664

Dual inhibition of the *Echinococcus multilocularis* energy metabolism

Sheena Chaudhry[1†], Raphael Zurbriggen[1†], Matías Preza[1], Tobias Kämpfer[1,2], Marc Kaethner[1,2], Roman Memedovski[1], Nathalie Scorrano[1], Andrew Hemphill[1], Joseph Stone Doggett[3,4] and Britta Lundström-Stadelmann[1*]

[1]Institute of Parasitology, Vetsuisse Faculty, University of Bern, Bern, Switzerland, [2]Graduate School for Cellular and Biomedical Sciences, University of Bern, Bern, Switzerland, [3]Department of Infectious Diseases and Pathobiology, Oregon Health and Science University, Portland, OR, United States, [4]Department of Infectious Diseases and Pathobiology, Veterans Affairs Portland Health Care System, Portland, OR, United States

Alveolar echinococcosis is caused by the metacestode stage of the zoonotic parasite *Echinococcus multilocularis*. Current chemotherapeutic treatment options rely on benzimidazoles, which have limited curative capabilities and can cause severe side effects. Thus, novel treatment options are urgently needed. In search for novel targetable pathways we focused on the mitochondrial energy metabolism of *E. multilocularis*. The parasite relies hereby on two pathways: The classical oxidative phosphorylation including the electron transfer chain (ETC), and the anaerobic malate dismutation (MD). We screened 13 endochin-like quinolones (ELQs) *in vitro* for their activities against two isolates of *E. multilocularis* metacestodes and isolated germinal layer cells by the phosphoglucose isomerase (PGI) assay and the CellTiter Glo assay. For the five most active ELQs (ELQ-121, ELQ-136, ELQ-271, ELQ-400, and ELQ-437), EC_{50} values against metacestodes were assessed by PGI assay, and IC_{50} values against mammalian cells were measured by Alamar Blue assay. Further, the gene sequence of the proposed target, the mitochondrial cytochrome *b*, was analyzed. This allowed for a limited structure activity relationship study of ELQs against *E. multilocularis,* including analyses of the inhibition of the two functional sites of the cytochrome *b*. By applying the Seahorse XFp Extracellular Flux Analyzer, oxygen consumption assays showed that ELQ-400 inhibits the *E. multilocularis* cytochrome bc_1 complex under normoxic conditions. When tested under anaerobic conditions, ELQ-400 was hardly active against *E. multilocularis* metacestodes. These results were confirmed by transmission electron microscopy. ELQ-400 treatment increased levels of parasite-released succinate, the final electron acceptor of the MD. This suggests that the parasite switched to MD for energy generation. Therefore, MD was inhibited with quinazoline, which did not induce damage to metacestodes under anaerobic conditions. However, it reduced the production of succinate compared to control treated parasites (i.e., inhibited the MD). The combination treatment with quinazoline strongly improved the activity of the bc_1 inhibitor ELQ-400 against *E. multilocularis* metacestodes under anaerobic conditions. We conclude that simultaneous targeting of the ETC and the MD of *E. multilocularis* is a

possible novel treatment approach for alveolar echinococcosis, and possibly also other foodborne diseases inflicted by platyhelminths, which cause substantial economic losses in livestock industry.

KEYWORDS

mitochondrium, ELQ, endochin-like quinolone, malate dismutation, cytochrome bc_1, electron transfer chain, drug repurposing

Introduction

Alveolar Echinococcosis (AE) is a lethal disease caused by infections with the fox tapeworm *Echinococcus multilocularis*, which is endemic to the Northern hemisphere. AE is the highest ranked food-borne parasitic disease in Europe (1) causing at least 18'500 new human cases of AE each year and more than 666,400 disability-adjusted life years (DALYs) with case numbers rising (2). AE is a neglected and emerging disease and until now, AE is an uncontrolled health problem of particular concern in developing and resource-poor regions (3).

The natural life cycle of *E. multilocularis* includes foxes and other canids as definitive hosts. In these definite hosts adult tapeworms grow in the intestines and release parasite eggs into the environment *via* the host's feces. Intermediate hosts, such as small rodents, are infected upon accidental oral uptake of these eggs. Also humans and other accidental hosts such as monkeys, pigs and dogs, can get infected by the parasite *via* oral uptake of eggs. This may lead to the establishment of a multivesicular larval stage, the metacestode, which grows mainly in the liver, thereby causing the disease AE (4). Metacestodes are surrounded by a protective carbohydrate-rich laminated layer (LL). Adjacent to the LL, the germinal layer (GL) is formed, which consists of muscle cells, nerve cells, glycogen storage cells, connective tissue sub-tegumentary cytons, and undifferentiated stem cells (5). Eventually, metacestodes form brood capsules and protoscoleces which, when taken up by a suitable final host, will grow into adult tapeworms in the final host's intestines.

AE is a chronic disease characterized by a tumor-like growth of the metacestodes with the potential for metastasis formation (3). In the progressive stage of AE, non-specific symptoms such as abdominal pain, jaundice, cholestasis, hepatomegaly, fever, anemia, weight loss, and pleural pain appear (3). If untreated, the infection will reach a final advanced stage, during which severe hepatic dysfunction occurs. If not treated properly, or if treatment fails, the infection leads to death due to malfunction of the liver or other affected organs (6).

Surgical removal is the only curative option for treatment of AE, but it cannot always be applied. Drug treatment is based on albendazole or mebendazole, but these drugs are not always effective, often act parasitostatically, and they have to be taken daily and life-long. Although benzimidazole treatment has significantly increased the 10-year survival rate for patients, it poses a considerable burden to patients, also, because side-effects frequently occur (7). All these shortcomings make it urgent to develop alternative chemotherapeutic options against AE (6).

As AE is a neglected disease, development of treatment options receives hardly any financial or industrial attention. Therefore, drug repurposing is a valuable method, which can allow for the identification of potential new drugs by use of already known drugs and drug-classes from other fields of disease (8). The advancements in the *in vitro* culture of *E. multilocularis* metacestodes, as well as the establishment of reliable *in vitro* drug testing systems, allow for screening and characterization of repurposed drugs against AE (6). This makes *E. multilocularis* an excellent model to study basic concepts of drug-treatment against liver-infecting platyhelminths *in vitro*. In the future, findings could be transferred to related parasites, such as *E. granulosus*, *Fasciola* spp., and others, which cause substantial economic losses in livestock industries (9, 10).

The energy metabolism of *E. multilocularis* might provide a valuable future target, because the generation of energy is central to any organism. Like any eukaryotic life form, also *E. multilocularis* uses glucose as a prime energy source, and metabolizes it through glycolysis and, to a small extent, fermentation, as well as through mitochondrial pathways. Interestingly, *E. multilocularis* applies two mitochondrial pathways for energy generation: (i) the classical electron transfer chain (ETC) coupled to oxidative phosphorylation and (ii) the malate dismutation (MD) (11). In the classical pathway pyruvate produced through glycolysis is imported into the mitochondria and metabolized through the citric acid cycle. Further, electrons are passed through the ETC consisting of complexes I-IV and this finally leads to the generation of ATP, which is depending on oxygen as an electron acceptor. Thus, this classical pathway can only function in the presence of oxygen. The second pathway, the MD, is an oxygen-independent pathway found in all helminths, marine invertebrates and euglenids, *Trypanosoma* spp. and bacteria (12–15), but it is absent from mammals. This difference in energy metabolism compared to mammalian host species renders the MD an interesting drug target.

MD includes a partial inversion of the citric acid cycle with complex II working as a fumarate reductase rather than a succinate dehydrogenase, and instead of ubiquinone,

rhodoquinone is used to transfer electrons between complexes I and II. Complex I hereby translocates protons across the inner mitochondrial membrane, which finally leads to the generation of ATP by ATP synthase even in the absence of oxygen. Succinate is released as a final electron acceptor. In addition, MD also includes the oxidation of malate to pyruvate and acetate. Thus, the final electron acceptors of MD are succinate in one branch, and acetate in the other branch, and these products are strongly released by many helminths, also *E. multilocularis* (11, 15).

Few studies have tackled the energy metabolism of *E. multilocularis* in the past: Enkai *et al.* showed that a combined inhibition of mitochondrial complexes II and III by atpenin A5 and atovaquone, respectively, killed protoscoleces *in vitro* (16). It was also shown that buparvaquone efficiently inhibited complex III (also called cytochrome bc_1 complex) and it was effective against metacestodes *in vitro* (17). The same study also identified the endochin-like quinolone (ELQ) ELQ-400 as highly active against *E. multilocularis* metacestodes *in vitro*, but the compound was not further characterized at that time (17). ELQs are potent inhibitors of the cytochrome bc_1 complex of a variety of apicomplexan parasites like *Plasmodium falciparum* (18, 19), *Toxoplasma gondii* (20–22), *Neospora caninum* (23, 24), *Babesia* spp. and *Theileria equi* (25–27), and *Besnoitia besnoiti* (28). One study examined the MD of *E. multilocularis* and showed that quinazolines can inhibit the complex I, and thereby the MD, of protoscoleces (29).

As these above-mentioned studies pointed toward the big potential of inhibitors of the mitochondrial energy pathways of *Echinococcus*, the present paper laid further focus on the comparative testing of a series of ELQs against two different isolates of *E. multilocularis*, and a combined inhibition of the classical ETC and the MD, to treat *E. multilocularis* metacestodes.

Materials and methods

All chemicals were purchased from Sigma-Aldrich (St. Louis, Mo, USA), if not stated otherwise. Dulbeccos's modified Eagle medium (DMEM) and fetal bovine serum (FBS) were purchased from Biochrom GmbH (Berlin, Germany). Trypsin/ EDTA (Trypsin 0.05%/ EDTA 0.02%) was bought from LuBioScience GmbH (Luzern, Switzerland). Penicillin and Streptomycin (10'000 Units/mL Penicillin, 10'000 µg/mL Streptomycin) was supplied by Gibco (Fisher Scientific AG, Reinach, Switzerland). The 13 ELQs (ELQ-100, ELQ-121, ELQ-127, ELQ-136, ELQ-271, ELQ-300, ELQ-316, ELQ-400, ELQ-433, ELQ-434, ELQ-435, ELQ-436, and ELQ-437) were synthetized as described before (22) and prepared as 10 mM solutions in DMSO, stored as aliquots at minus 20°C. Before use, compounds were shaken for 10 min at 45°C and vortexed well. The structures of ELQs were prepared in ACD/ChemSketch (ACD Labs, Toronto, Canada, Version 2020.2.1) and they are given in Figure 1.

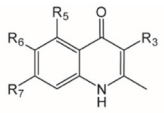

ELQ	R_3	R_5	R_6	R_7
100	C_7H_{15}	-	-	OCH_3
121	C_7H_{15}	F	-	F
127	C_7H_{15}	-	-	-
136	C_7H_{15}	F	-	-
271	DAE	-	-	-
300	DAE	-	Cl	OCH_3
316	DAE	-	F	OCH_3
400	DAE	F	-	F
433	C_7H_{15}	-	F	OCH_3
434	$C_{11}H_{23}$	-	Cl	OCH_3
435	$C_{11}H_{23}$	-	F	OCH_3
436	$C_{11}H_{23}$	-	-	-
437	$C_{11}H_{23}$	F	-	F

FIGURE 1
Structures of endochin-like quinolones (ELQs). Core structure of ELQs with numbered residues for each of the here tested ELQs. ELQ numbers are given in the first column, and the substituents (R3, R5, R6, and R7) are given in the following columns. DAE, diaryl ether.

Mice and ethics statement

For parasite maintenance animals were purchased from Charles River Laboratories (Sulzheim, Germany) and used for experimentation after 2 weeks of acclimatization. Female BALB/c mice were maintained in a 12 h light/dark cycle, controlled temperature of 21–23°C, and a relative humidity of 45–55%. Food and water was provided *ad libitum*. All animals were treated in compliance with the Swiss Federal Protection of Animals Act (TSchV, SR455), and experiments were approved by the Animal Welfare Committee of the canton of Bern under the license number BE30/19.

In vitro culture of *E. multilocularis* metacestodes

E. multilocularis metacestodes were maintained as previously described by Rufener *et al.* (17). Metacestodes [isolates H95 (30) and Sval (31)] were grown in intraperitoneally infected mice and parasite material was resected after 4 months of parasite growth. *In vitro* cultures were initiated and cultured as described by Rufener *et al.* (17) in DMEM containing 10% FBS, 100 U/mL penicillin, 100 µg/mL streptomycin and

10 μg/mL tetracycline, and in co-culture with Reuber rat hepatoma (Rh) cells at 37°C with 5% CO_2 under humid atmosphere.

In vitro drug testing against *E. multilocularis* metacestodes

To assess the *in vitro* efficacy of ELQs against *E. multilocularis*, (a) the damage-marker phosphoglucose isomerase (PGI) assay was applied against metacestodes, and (b) the germinal layer (GL) cell viability assay was applied to measure effects on isolated GL cells. Both assays are described in more detail below. The drug testing strategy was as follows: PGI assay was first conducted for overview screening at 10 μM with the parasite isolates H95 and Sval. The GL cell viability assay was performed at 0.1 μM with both isolates H95 and Sval. For active compounds (PGI > 20% activity compared to Tx-100 positive control; GL cell viability < 30% of DMSO negative control), PGI assay was applied for EC_{50} measurements based on the H95 isolate.

In vitro testing of ELQs against *E. multilocularis* metacestodes by PGI assay

The PGI assay measures the amount of PGI that metacestodes release into the medium when damaged (17, 32). The purification and *in vitro* drug incubation of *E. multilocularis* metacestodes was conducted according to Stadelmann *et al.* (32). In short, cultures were applied for *in vitro* drug testing at the age of 6-8 weeks. *E. multilocularis* metacestodes were therefore purified by the addition of 2% saccharose and washed extensively with PBS. Purified metacestodes were suspended 1:3 with DMEM (without phenol red, supplemented with 100 U/mL penicillin, 100 μg/mL streptomycin) and distributed in 48-well plates (1 mL/well, thus 300 μL pure metacestode vesicles per well). ELQs were added to the wells to the desired concentrations (10 μM for screening, 30–0.12 μM in 1:2 dilution steps for EC_{50} measurements) in 0.1% DMSO. The corresponding DMSO concentration was used as negative control and Tx-100 (0.1% final concentration) was used for total damage (positive control). The plates were incubated for 5 days under normoxic conditions (37°C; 5% CO_2, 21% O_2, humid atmosphere). After 5 days, relative PGI activities were measured and calculated as percentage of the Tx-100 control as described previously in Rufener *et al.* (17). They were calculated as mean values and standard deviations for each triplicate. EC_{50} calculations were calculated based on logit-log transformed values in Microsoft Office Excel 2010. EC_{50} measurements were performed twice, and averages and standard deviations of these repeated tests are given.

In vitro testing of ELQs against *E. multilocularis* GL cells by viability assay

The isolation of *E. multilocularis* GL cells was done as described previously (17) with minor modifications. Fifteen units of GL cells were distributed to each well of a 384 well plate in a total volume of 12.5 μL conditioned medium. The different ELQs were added to the wells to 0.1 μM, in quadruplicates. As a negative control 0.1% DMSO was used. The 384-well plate was incubated for 5 days at 37°C under humid nitrogen atmosphere. Thereafter, viability of the GL cells under different drug treatments was assessed by CellTiter-Glo® (Promega AG, Dübendorf, Switzerland). The CellTiter-Glo reagent was complemented with 1% Tx-100. The luciferase bioluminescence was measured at 530 nm by using the Enspire multilabel reader (PerkinElmer Life Sciences, Schwerzenbach, Switzerland). Using Microsoft Excel, the blank values were subtracted from the experimental values and the relative viability compared to DMSO was calculated. Viabilities were calculated as mean values and standard deviations for each quadruplicate. Calculations were made based on logit-log transformed values in Microsoft Office Excel 2010.

Mammalian cell toxicity assay

For the compounds with activity against *E. multilocularis* (ELQ-121, ELQ-136, ELQ-271, ELQ-400, and ELQ-437), the toxicity against mammalian cells was assessed according to Rufener *et al.* (17) by Alamar Blue assay on Rh cells, at confluent and pre-confluent state. Compounds were added in a serial dilution (30–0.23 μM, 1:2 dilution steps) and in triplicates. Plates were incubated at 37°C, 5% CO_2 and humid atmosphere for 5 days. Resazurin was added to a final concentration of 10 mg/L to each well, and fluorescence measured at 530 nm on an Enspire multilabel plate reader over 3 h. By using Microsoft Office Excel 2010 and a logit-log transformation of the relative growth, IC_{50} values were calculated. The test was performed twice for each compound, and respective averages and standard deviations are given.

Transmission electron microscopy (TEM)

E. multilocularis metacestodes treated with ELQ-400 (0.2, 1 and 2 μM, 5 days of incubation) under normoxic (37°C, 21% O_2, 5% CO_2, humid atmosphere) and anaerobic conditions (37°C, 80% N_2, 10% CO_2, and 10% H_2, humid atmosphere) were processed for TEM as previously described (17). Metacestodes were washed in 100 mM sodium cacodylate buffer (pH 7.3), and were fixed in 2% glutaraldehyde in cacodylate buffer overnight at 4°C. Following several washes in cacodylate buffer, metacestodes were post-fixed in 2% osmium tetroxide in cacodylate buffer for 3–4 h, washed in water, and

samples were treated with Uranyless^{TM} solution (EMS, Hatfield, PA, USA) for 20 min, followed by several washes in distilled water. Specimens were dehydrated in a graded series of ethanol and were embedded in EPON-812 epoxy resin. Polymerization of the resin was carried out at 60°C for 24 h. Ultrathin sections were cut on a Reichert and Jung (Vienna) microtome, and were allowed to settle onto 400 mesh formvar carbon coated grids (Plano GmbH, Wetzlar, Germany). Specimens were contrasted with Uranyless and lead citrate, and were viewed on a FEI Morgagni Transmission Electron Microscope operating at 80 kV.

Seahorse assay

To measure effects of ELQ-400 on the oxygen consumption rate (OCR), Seahorse assay was conducted according to the method established by Rufener *et al.* (17) and according to the manual for Seahorse XFp Extracellular Flux Analyzer (Agilent Technologies, Bucher Biotec, Basel, Switzerland). *E. multilocularis* GL cells were isolated and prepared the day before. Cells were centrifuged and resuspended in Mitochondrial Assay Solution (MAS) solution (220 mM mannitol, 70 mM sucrose, 10 mM KH_2PO_4, 5 mM $MgCl_2$, 2 mM HEPES, and 1 mM EGTA pH 7.2). This cell suspension was centrifuged again and the pellet was resuspended in assay-buffer (MAS, 10 mM succinate, 2 µM rotenone, 4 mM ADP, and 3.6 nM PMP). 100 units of GL cells were distributed to each well of a Seahorse XFp miniplate (Agilent Technologies) pre-coated with CellTak according to the instruction manual (Fisher Scientific, Schwerte, Germany). Two wells were used as blanks with assay buffer without cells. ELQ-400 (1 µM) was diluted in MAS solution and loaded to the delivery ports of the sensor cartridge of the first injection (or DMSO as a control). In the second injection, succinate (10 mM), glycerol 3-phosphate (10 mM), or ascorbate (20 mM) with TMPD (0.6 mM) was added. Subsequently, the measurement on the Seahorse machine (Agilent Technologies) was started with three measurements for the base line, four after the first injection, and 10 after the second injection. For each measurement 30 s mix, 30 s delay, and 2 min measure was applied. Each drug setup was tested in triplicates and the read-out and analysis was done using the software Wave (Agilent Technologies, Bucher Biotec, Basel, Switzerland). The test was repeated two times independently.

Sequence comparisons

Sequences of cytochrome *b* were obtained from Uniprot (33) for *E. multilocularis* (C6L2E3), *T. gondii* (S8EQL3) and *P. falciparum* (Q02768) and *H. sapiens* (P00156), and from WormBase ParaSite (34) version 16 for *E. granulosus* (EgrG_900000100). Alignments were performed with Clustal (35), using the program Bioedit (36). The Qo and Qi sites of the complex were identified based on previous literature (22).

In vitro drug testing against *E. multilocularis* metacestodes by combination treatments

For double inhibition of the mitochondrial energy pathways of *E. multilocularis*, quinazoline as an inhibitor of the anaerobic MD (29) was applied in combination with ELQ-400 as an inhibitor of the ETC. Both compounds were tested either alone or in combination at 10 µM with the above-described PGI assay for 5 days for their activity against *E. multilocularis* metacestodes. PGI assays were done in triplicates and two times independently. Drug incubations were performed at three different conditions for the PGI assay: normoxic (37°C, 21% O_2, 5% CO_2, humid atmosphere) and anaerobic conditions (37°C, 80% N_2, 10% CO_2, and 10% H_2, humid atmosphere). Results of the assays were calculated as mean values and standard deviations for each biological triplicate were calculated as relative percentage to the Tx-100 control. To assess direct effects on the MD, succinate levels were measured in the supernatants of the PGI assay, as described below. To determine whether differences between groups were significant, data was subjected to student's *t*-test analysis and *P*-values below 0.05 are given.

Assessment of succinate concentrations in culture supernatants

Succinate measurements in supernatants of drug-treated *E. multilocularis* metacestodes was performed with the "Succinic Acid Assay Kit" (Megazyme, Bray, Ireland). For the standard curve, a serial dilution (1:2) from 0.125 to 4 µg succinate per well was prepared. 20 µL of each diluted (1:20) sample or standard was used in triplicate for succinate measurements in 96-well plates (flat bottom, Greiner Bio-One GmbH, Frickenhausen, Germany). The reaction mix buffer was prepared as described in the supplier manual: per well 180 µL H_2O, 20 µL solvent 1 (buffer, pH 8.4, sodium azide 0.02% w/v), 20 µL solvent 2 (NADH plus stabilizer), 20 µL solvent 3 (ATP, PEP, and CoA) and 2 µL solvent 4 (pyruvate kinase plus L-lactate dehydrogenase suspension) were added. After a 180 s pre-incubation time, a first measurement at 340 nm was done on an EnSpire multilabel plate reader (PerkinElmer Life Sciences, Schwerzenbach, Switzerland). 10 µL solvent 5 (succinyl-CoA synthetase suspension; 1:10 diluted) were then added to each well and the plate was read at 340 nm for 1 h every minute. Calculation of succinate concentrations was done by regression analysis using Microsoft Office Excel 2010. Succinate levels are shown as mean values with standard deviations of biological

TABLE 1 *In vitro* efficacy of ELQs against metacestodes and GL cells of two isolates of *E. multilocularis*.

ELQ	Isolate Sval		Isolate H95	
	Metacestodes	GL cells	Metacestodes	GL cells
100	0 (0.4)	57.9 (5.7)	1.4 (0.1)	100.1 (8.3)
121	20.9 (15.3)	7.3 (3.8)	15.2 (4.0)	1.0 (0.3)
127	2.5 (0.8)	40.4 (2.7)	11.7 (0.2)	17.2 (9.5)
136	7 (7.6)	15.1 (4.7)	21.4 (2.2)	8.4 (11.7)
271	56.9 (4.3)	25.4 (7.2)	33 (1.7)	2.7 (1.6)
300	7.6 (1.1)	46.9 (9.6)	6.6 (2.2)	84.0 (7.0)
316	4.6 (1.3)	58 (5.3)	21.4 (0.1)	81.1 (9.5)
400	27 (10.5)	14.6 (8.6)	21.4 (2.5)	8.4 (4.8)
433	1.8 (1.6)	62.1 (6.3)	4.3 (4.2)	96.4 (17.7)
434	0.6 (1.1)	81.3 (5.8)	0.4 (0.4)	33.3 (6.4)
435	0 (0.9)	80.1 (13.1)	2.6 (1.6)	15.6 (14.0)
436	3.1 (2.6)	16.4 (1.8)	3.4 (1.2)	14.0 (9.7)
437	33.1 (7.2)	19.1 (5.7)	37.6 (0.5)	19.7 (13.3)

ELQ numbers are given in the first column. The two parasite isolates Sval and H95 were tested. Efficacy against metacestodes was assessed by PGI assay (relative to the positive control Tx-100), and against GL cells by viability assessment via ATP measurements (relative to the DMSO control) in μM. Compounds were considered to be active, if they reached a threshold of >20% against metacestodes, and <30% against GL cells. This overview screen was performed once in triplicates, and respective mean relative values are given with standard deviations in parentheses.

TABLE 2 Halfmaximal activities of ELQs against *E. multilocularis* metacestodes and Reuber rat hepatoma cells.

ELQ	EC_{50} metacestodes	IC_{50} Rh preconfluent	IC_{50} Rh confluent
121	1.19 (0.52)	>30	>30
136	0.22 (0.03)	>30	>30
271	0.24 (0.13)	8.64 (1.05)	>30
400	1.06 (0.60)	1.46 (0.17)	>30
437	1.71 (0.01)	>30	>30

The first number indicates the ELQ numbers. Efficacy against metacestodes (isolate H95) was assessed by PGI assay (relative to the positive control Tx-100) and EC_{50} values are given in μM (concentration range tested: 30–0.12 μM). Activity against mammalian cells (Reuber rat hepatoma cells, Rh) was assessed by Alamar blue assay (relative to the DMSO control), and IC_{50} values are given for preconfluent and confluent cells is given in μM (range tested: 30–0.23 μM). All tests were performed twice with triplicates for each concentration, and respective mean relative values are given with standard deviations in parentheses.

triplicates. To determine whether differences between groups were significant, data was subjected to student's *t*-test analysis and *P*-values below 0.05 are given.

Results

ELQs show activity against *E. multilocularis* metacestodes and GL cells

Results of the overview screening of 13 different ELQs against *E. multilocularis* isolates H95 and Sval is shown in Table 1. Tested against the Sval isolate, the PGI assay, which measures the overall damage to metacestodes, showed an activity for compounds ELQ-121, ELQ-271, ELQ-400, and ELQ-437 at 10 μM. Against the H95 isolate, ELQ-136, ELQ-271, ELQ-316, ELQ-400, and ELQ-437 were active. In the GL cell viability assay, which measures the activity of compounds against the viability of isolated GL cells of *E. multilocularis*, the compounds ELQ-121, ELQ-136, ELQ-271, ELQ-400, ELQ-436, and ELQ-437 were active against the Sval isolate. For the H95 isolate, the same compounds were active, and in addition also ELQ-127, ELQ-435, and ELQ-436.

Thus, overall, several compounds were active against both parasite isolates, and in both assays. Compounds that showed activity in three out of four assays were selected as positive hits and further characterized. These are: ELQ-121, ELQ-136, ELQ-271, ELQ-400, and ELQ-437. EC_{50}s were calculated for metacestodes, IC_{50}ies for the cytotoxicity assessed on confluent and pre-confluent Rh cell lines. Results are given in Table 2. All five ELQs showed an EC_{50} of around 0.2–2 μM against intact metacestodes (Table 2). None of the compounds was toxic on

confluent Rh cells within the tested range of concentrations, whereas ELQ-271 and ELQ-400 exhibited some toxicity on pre-confluent Rh cells (8.64 and 1.46 μM, respectively). ELQ-400 was chosen for further characterization, as it was the most active compound that was previously characterized against *E. multilocularis* and applied in *in vivo* studies in mice (22), albeit other compounds tested here promised a potentially better therapeutic window based on *in vitro* data.

Morphological effects induced by ELQ-400 on *E. multilocularis* metacestodes

Transmission electron microscopy showed that exposure of *E. multilocularis* metacestodes to ELQ-400 under normoxic conditions exerted detrimental effects, apparently in a dose-dependent manner. Metacestodes treated with 0.2 μM ELQ-400 did not show obvious ultrastructural alterations compared to non-treated parasites (Figures 2A,B). A closer look at the mitochondria, which are found within the GL tissue, and which are prominent within the cytoplasm of undifferentiated cells (Figure 2B), revealed that they exhibited different shapes and sizes. Mitochondria were filled with a relatively electron-dense matrix, and contained fine-structured cristae, which were not very prominent but nevertheless clearly discernible. In some metacestodes exposed to 0.2 μM ELQ-400, lipid droplets had formed (Figure 2C). However, this changed upon treatments with 1 μM ELQ-400 (Figures 3A,B), as the overall structural organization of the parasites, especially of the GL, was partially compromised, and mitochondria appeared rounded. Microtriches were still visible being embedded in the LL after 1 μM ELQ-400 treatments (Figure 3A) but not evident anymore after 2 μM treatments (Figure 3C). In addition, the progressive structural damage lead to partial separation of the GL and the LL (Figure 3C), and the presence of rounded mitochondria lacking an electron dense matrix and cristae, which was especially evident in undifferentiated cells (Figure 3D).

ELQ-400 inhibits the mitochondrial bc_1 complex

Direct effects of ELQ-400 on isolated GL cells were also assessed by measurement of the OCR in these cells (Figure 4). The addition of ELQ-400 (but not of DMSO) led to an immediate reduction of the OCR of GL cells, and feeding of electrons *via* ascorbate and TMPD, which donate electrons downstream of the bc_1 complex, could restore this effect (Figure 4A). The electron donors succinate or glycerol 3-phosphate, which donate electrons upstream of the bc_1 complex, could not restore the ELQ-400 induced OCR drop (Figures 4B,C). Thus, ELQ-400 inhibits the bc_1 complex of the mitochondrial ETC of *E. multilocularis* GL cells.

Cytochrome *b* sequence alignments

Cytochrome *b* sequences of the apicomplexan parasites *T. gondii* and *P. falciparum*, as well as *Homo sapiens* were aligned with the sequences of *E. multilocularis* and *E. granulosus* (Supplementary Figure 1). Interestingly, *Echinococcus*, like most eukaryotes, has a lysine at position 229, which was previously shown to reduce Qi site inhibition by ELQs with OCH_3 at R7 (22) (Figure 5), explaining the lack of activity of these ELQs against *E. multilocularis*.

Double-treatment of the bc_1 complex and the malate dismutation

ELQ-400 was active in the PGI assay when tested against *E. multilocularis* metacestodes at standard normoxic conditions, and its activity was significantly reduced at anaerobic conditions ($P = 0.0316$, Figure 6A). Morphological characterization by TEM confirmed the loss of activity of ELQ-400 under anaerobic conditions: In contrast to the damage exerted by ELQ-400 at 1 and 2 μM under normoxic conditions (Figures 2, 3), metacestodes inspected upon ELQ-400 treatment under anaerobic conditions did not exhibit such alterations, and were largely similar to non-treated metacestodes (Figure 7).

E. multilocularis is known to employ also an alternative mitochondrial energy-generating pathway that works oxygen independently, the MD. This pathway leads to the release of succinate as a final electron acceptor, thus succinate is an indicator of MD activity. Succinate levels were significantly increased when metacestodes were incubated under anaerobic conditions ($P = 0.0038$, Figure 6B). ELQ-400 treatment significantly enhanced the release of succinate by metacestodes when compared to the DMSO control ($P = 0.0249$ normoxic, $P = 0.0151$ anaerobic, Figure 6B). Concluding, both anaerobic incubation and ELQ-400 treatment of metacestodes induced the MD.

As a consequence, we then also employed quinazoline the published inhibitor of MD (29), which led to a significant reduction of succinate release under anaerobic conditions ($P = 0.0006$, Figure 6B). Quinazoline treatment alone led only to no PGI release by metacestodes under anaerobic conditions (Figure 6A). The combined treatment of metacestodes with ELQ-400 and quinazoline, thus double inhibition of two mitochondrial pathways ETC and MD simultaneously, led to a significantly increased PGI release, as compared to single treatments under anaerobic conditions ($P = 0.0009$).

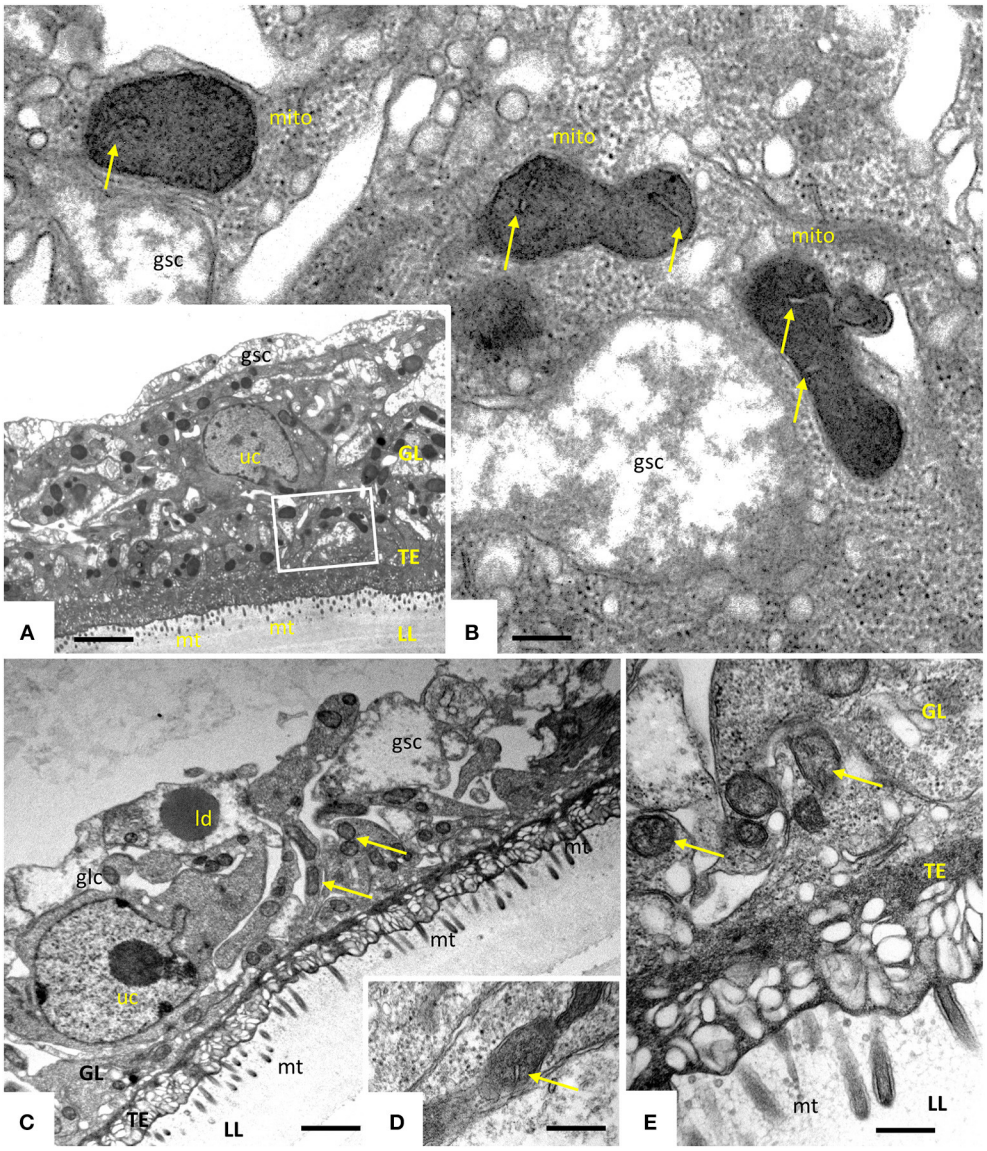

FIGURE 2
Transmission electron microscopy (TEM) of *E. multilocularis* metacestodes treated with 0.2 μM ELQ-400. TEM of non-treated metacestodes **(A,B)** and metacestodes treated with 0.2 μM ELQ-400 **(C,D)** under normoxic (21% O_2) conditions. The boxed area in **(A)** is shown at higher magnification in **(B)**. Parasites are comprised of an outer laminated layer (LL), a tegument (TE) with numerous microtriches (mt) protruding into the LL, and the GL comprised of various cell types, including glycogen storage cells (gsc) and undifferentiated cells (uc). Structures remain largely unaltered in the presence of 0.2 μM ELQ-400 **(C,D)**. Note the presence of mitochrondria (mito) **(B–D)** with a rather electron-dense matrix and cristae (arrows); ld, lipid droplet. Bars in **(A)** = 2.4 μm; **(B)** = 0.25 μm; **(C)** = 1.2 μm; **(D,E)** = 0.40 μm.

Discussion

This study was investigating novel alternative treatment options against the foodborne disease AE, which is currently treated with benzimidazoles that only act parasitostatic. Other related food-transmitted flatworms that also affect the liver, and are likewise treated by benzimidazoles, are cystic echinococcosis, caused by *E. granulosus*, fasciolosis caused by *Fasciola hepatica* and *F. gigantica*, clonorchiasis caused by *Clonorchis sinensis* or opisthorchiasis caused by *Opisthorchis viverrini* and *O. felineus*. Whereas, AE is of major concern for humans, captive monkeys and dogs, cystic echinococcosis and fasciolosis are additionally also highly relevant diseases in livestock worldwide causing substantial economic losses (9, 10). Thus, novel treatment options against foodborne platyhelminth-infections are needed.

In search for novel treatment options against AE, and possibly other helminth-diseases, we repurposed ELQs that have been shown previously to be highly effective inhibitors

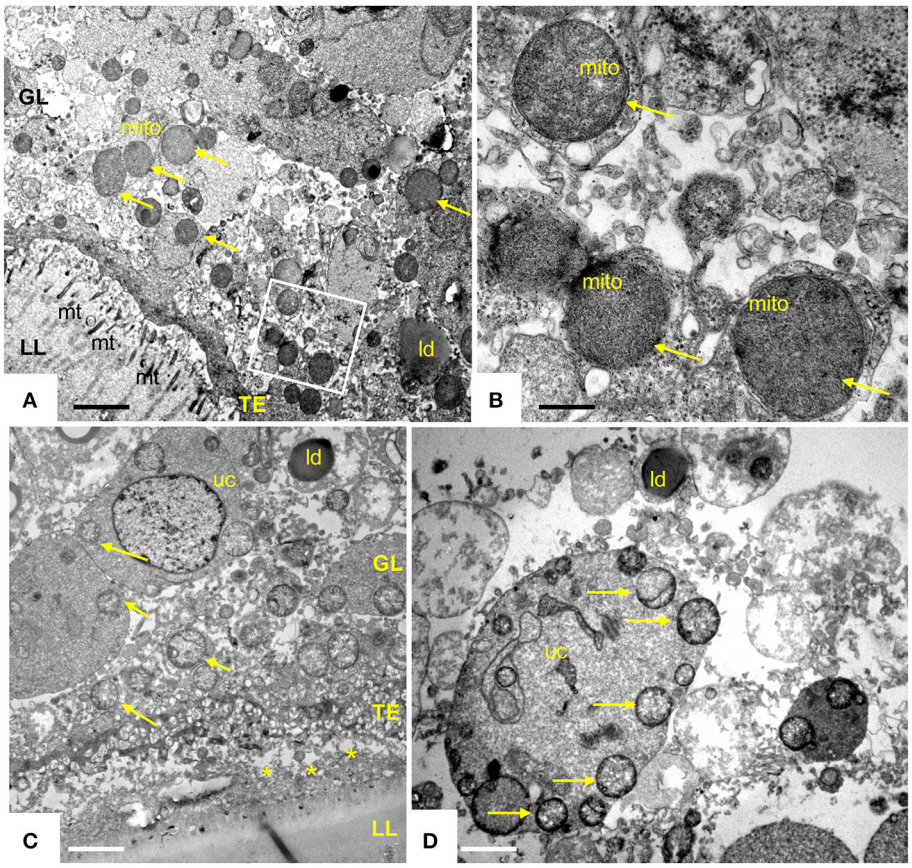

FIGURE 3
Transmission electron microscopy (TEM) of *E. multilocularis* metacestodes treated with 1 and 2 μM ELQ-400. TEM of metacestode tissue treated with 1 μM **(A,B)** and 2 μM **(C,D)** of ELQ-400 under normoxic (21% O_2) conditions. The boxed area in **(A)** is shown at higher magnification in **(B)**. Mitochondria (mito) are rounded, progressively less electron dense, on both the GL tissue [**(C)** as well as in undifferentiated cells (uc)] **(D)**, as indicated by the arrows; *indicates separated LL and GL; mt, microtriches; ld, lipid droplet. Bars in **(A)** = 1.2 μm; **(B)** = 0.28 μm; **(C)** = 2.2 μm; **(D)** = 1.8 μm.

of apicomplexan parasites (22). The activities of 13 different ELQs were assessed against metacestodes and isolated GL cells of two isolates of *E. multilocularis*. This small screen revealed that activities of ELQs correlated well between the two parasite isolates, one of which is kept in laboratory mice since the year 1995 (H95) and the other one since at least 2012 (Sval). The data allowed for a small structure activity relationship (SAR) study of the tested ELQs with respect to anti-echinococcal activity. Our data indicates that ELQs with a fluorine at position 5 or 5 and 7 were active, whereas a methoxy group at position 7 led to reduced activity against *Echinococcus*. This is true for the compounds ELQ-121, ELQ-136, ELQ-400, and ELQ-437. The cytochrome bc_1 complex was previously shown to be the target of ELQs (21). The bc_1 complex can be inhibited at two sites that are responsible for building up a proton gradient across the inner mitochondrial membrane: the ubiquinol oxidation site (Qo) or the quinone reduction site (Qi) (22). The Qo site of Apicomplexan bc_1 is inhibited with 5,7-difluoro- or 7 fluoro-position substituents (19), which is in line with the above-mentioned active ELQs against *E. multilocularis*. In contrast, ELQ-271 does not have substituents at positions 5 or 7 and is a Qi site inhibitor (21, 26). The Qi site of the mitochondrial cytochrome bc_1 complex of apicomplexans is also inhibited by compounds with an electron-withdrawing substituent (like a halogen) at position 6, or a 7-methoxy group (19). ELQ-271 was shown to inhibit both human and apicomplexan cytochrome bc_1, whereas ELQs with a 7-methoxy group selectively inhibited the apicomplexan cytochrome bc_1. A better understanding of ELQ selectivity for apicomplexans came from experiments demonstrating that a mutation of the threonine at position 222 of the Qi binding site in *T. gondii* led to resistance to ELQs with a methoxy group at position 7 (22, 37). The *E. multilocularis* cytochrome *b* gene sequence shows a lysine residue at this position, like other eukaryotes, which is well in line with the

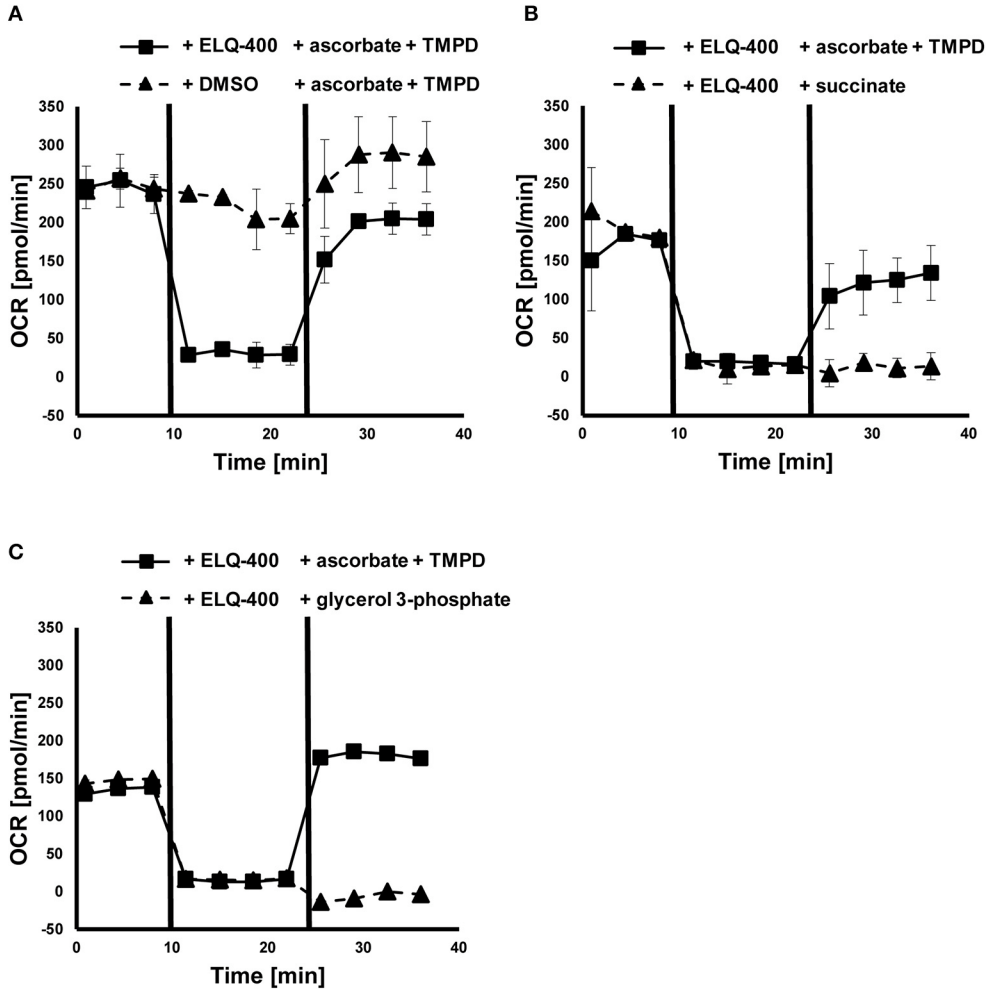

FIGURE 4
Effects of ELQ-400 on the mitochondrial respiration of *E. multilocularis* germinal layer (GL) cells. The oxygen consumption rate (OCR) of *E. multilocularis* GL cells was measured by Seahorse XFp Extracellular Flux Analyzer. Succinate was given as an initial electron donor. After addition of 1 μM ELQ-400 (but not DMSO), the OCR dropped, but recovered after addition of 20 mM ascorbate and 0.6 mM TMPD, which donate electrons to the mitochondrial respiration chain complex IV, thus downstream of the bc_1 complex **(A)**. OCR dropped after ELQ-400 treatment, but did not recover upon addition of 10 mM succinate **(B)**, nor 10 mM glycerol-3-phosphate (G3P, **C**), both electron-donors which donate electrons upstream of the bc_1 complex. The experiment was repeated two times independently, and one representative plot is shown. Measurements were performed in triplicates, and mean values with standard deviations are shown.

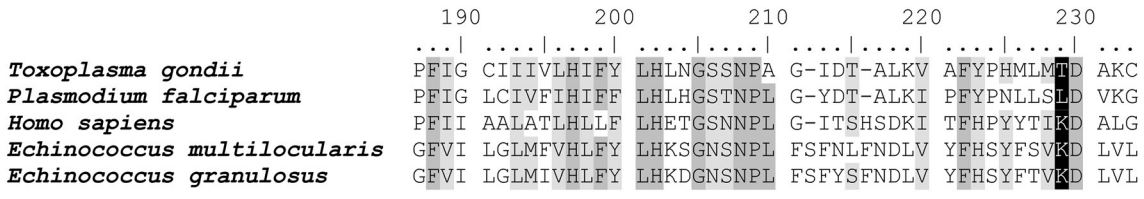

FIGURE 5
Sequence comparisons of the cytochrome *b* of *Echinococcus* spp. and apicomplexan parasites. Sequence alignment of the Qi site of cytochrome *b* between *E. multilocularis* (C6L2E3), *T. gondii* (S8EQL3) and *P. falciparum* (Q02768), and *H. sapiens* (P00156; EgrG_900000100). The *T. gondii* position 222 is highlighted in black. Conserved sites are marked in gray (four out of five amino acids same) and in light gray (three out of five amino acids same). Position 222 is labeled in black. The entire sequence alignment is given in Supplementary Figure 1.

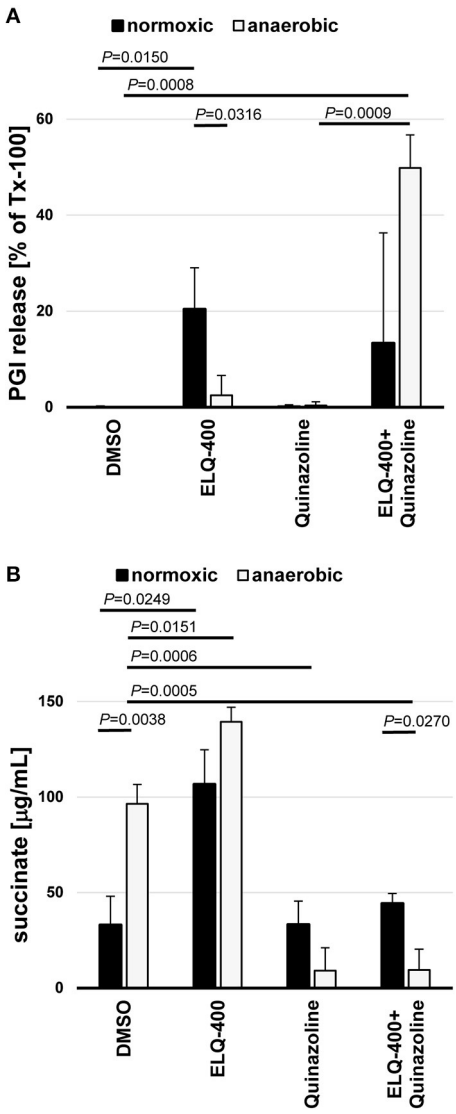

FIGURE 6
Double-inhibition of the bc_1 complex and the malate dismutation of *E. multilocularis* metacestodes and GL cells. *E. multilocularis* metacestodes were treated with ELQ-400 (10 µM) and or quinazoline (10 µM) for 5 days and PGI release assessed as a quantifiable damage marker in relation to meteacestodes treated with the internal positive control Tx-100 **(A)**. From the same setup, released succinate levels were assessed for each condition by Succinic Acid Assay Kit. Incubations were performed under normoxic (21% O_2) and anaerobic (0% O_2) conditions in parallel. DMSO treatment was used a negative control **(B)**. Experiments were performed in biological triplicates, and mean values with standard deviations are given for the relative PGI release **(A)** and the succinate levels **(B)**. *P*-values are given for significant differences with $P < 0.05$.

lack of activity of all ELQs carrying a 7-methoxy group. Within the group of ELQs that are active against *Echinococcus*, this holds true for ELQ-271 and ELQ-400. Thus, Qi inhibitors that are not selective for apicomplexans may be active against *E. multilocularis*. Sequence comparisons with *E. granulosus* suggest that these Qi inhibitors might also be active against this related parasite. However, experimental testing of ELQs against *E. granulosus* and other platyhelminths infecting the liver has yet to be performed.

Past studies in apicomplexan parasites showed that buparvaquone (alike atovaquone) is a Qo site inhibitor, whereas ELQ-400 is primarily a Qo site inhibitor, but may inhibit both the Qo and the Qi site (38).This might also be the case in *E. multilocularis*, but cannot be further confirmed, as mutagenesis studies cannot be performed to date. Simultaneous treatment of the Qo and the Qi site was shown to be a treatment strategy against *Babesia microti,* and *Plasmodium* infections (26, 39). Our studies demonstrate that the Qi site inhibitor, ELQ-271, also is a potent inhibitor of *E. multilocularis* and had a greater therapeutic index than ELQ-400.

Electron microscopy showed that exposure of *E. multilocularis* metacestodes to ELQ-400 under normoxic conditions exerts detrimental effects in a dose-dependent manner, which closely aligns to the results of the PGI measurements. While 0.2 µM ELQ-400 treatment did not lead to clear-cut changes in the parasite ultrastructure, higher concentrations clearly affected the overall structural organization of the metacestode tissue. In parallel, the mitochondria rounded up, lost their characteristic electron dense matrix, and cristae were dramatically reduced or absent after ELQ-400 treatment. Basically, the observed effects mirrored those seen earlier with the hydroxynaphthoquinone buparvaquone, another cytochrome bc_1 inhibitor (17). However, buparvaquone affected the parasite ultrastructure already at 0.3 µM, by impacting the electron dense mitochondrial matrix.

Our further experiments clearly showed that ELQ-400 affects the mitochondria of *E. multilocularis*, and that it inhibits the bc_1 complex of the mitochondrial ETC. Its activity was depending on the availability of oxygen. Importantly, in the liver of naturally infected hosts, *E. multilocularis* metacestodes do not grow at normoxic conditions, but encounter rather microaerobic conditions (40). This prompted us to include additional experiments targeting a second energy-generating mitochondrial pathway, which functions independent of oxygen: the MD. Even though present in all helminths, and not in mammalian hosts, this pathway has been only little explored for future anthelminthic treatment options. Most of the past studies focused on the free-living nematode *Caenorhabditis elegans* (41, 42) or on parasitic nematodes like *Ascaris suum* and the inhibition of the MD (complex II) by harzianopyridone and atpenin a5 (43) or flutolanil and derivatives (44, 45), or *A. suum* and *Haemonchus contortus* by nafuredin (46). The MD of *E. multilocularis* protoscoleces was described previously, and inhibition of the MD in mitochondria of protoscoleces was achieved by quinazoline and derivatives (29). Furthermore, several benzimidazoles were suggested to interfere with MD of different cestodes (47–50).

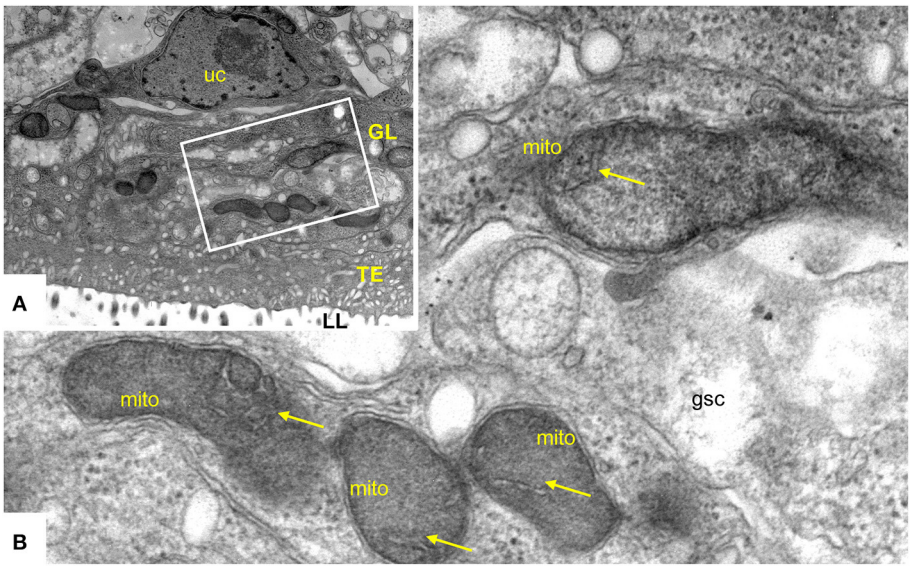

FIGURE 7
Transmission electron microscopy (TEM) of *E. multilocularis* metacestodes treated with 2 μM ELQ-400 under anaerobic conditions. **(A)** Is a lower magnification view, the boxed area is enlarged in **(B)**. LL, laminated layer; TE, tegument; GL, germinal layer; uc, undifferentiated cell; gsc, glyocogen storage cell; mito, mitochondrion. Arrows point toward mitochondrial cristae which are clearly visible. Bars in **(A)** = 2.4 μm; **(B)** = 0.25 μm.

We here report for the first time on the direct measurements of MD activity in metacestodes of *E. multilocularis* by measuring succinate, the end product of MD, in this parasite. Succinate production was induced upon anaerobic incubation. ELQ-400 treatment of metacestodes induced succinate production, which could be an indication of an increased MD activity when the bc_1 complex of the ETC is blocked. MD inhibition by quinazoline led to a reduction of succinate production by *E. multilocularis* metacestodes under anaerobic conditions, but did not affect the viability of the parasite. Only a combined treatment approach of the MD inhibitor quinazoline together with the bc_1 inhibitor ELQ-400 led to a strong damage to metacestodes also under anaerobic conditions.

Concluding, this study provides the first proof of concept of a dual inhibition of the mitochondria of *E. multilocularis* metacestodes as a promising approach for future treatment of AE and potentially other helminthiases, in particular the ones caused by platyhelminths. Future studies should aim at the identification of optimized inhibitors that are not toxic to mammalian cells, and exhibit good aqueous solubility and oral bioavailability.

Data availability statement

The original contributions presented in the study are included in the article/Supplementary material, further inquiries can be directed to the corresponding author.

Ethics statement

The animal study was reviewed and approved by Amt für Veterinärwesen, Kanton Bern.

Author contributions

BL-S and JD: conceptualization, project administration, and funding acquisition. SC, RZ, MP, TK, MK, RM, NS, and BL-S: performed experiments with the parasite and extracts. SC and AH performed electron microscopy. JD synthesized the compounds. SC, RZ, MP, AH, JD, and BL-S: performed data analysis. BL-S: writing—original draft preparation and supervision. SC, RZ, MP, TK, MK, RM, NS, AH, JD, and BL-S: contributed in review and editing and approval of manuscript. TK, MP, AH, and BL-S: visualization. All authors contributed to the article and approved the submitted version.

Funding

This work was supported by a grant from the Novartis Research Foundation to BL-S, the Swiss National Science Foundation (SNSF) grant no. 192072 to BL-S, and VA Merit Review Award BX004522 to JD from the U.S. Department of Veterans Affairs Biomedical Laboratory Research and Development.

Conflict of interest

The authors declare that the research was conducted in the absence of any commercial or financial relationships that could be construed as a potential conflict of interest.

Publisher's note

All claims expressed in this article are solely those of the authors and do not necessarily represent those of their affiliated organizations, or those of the publisher, the editors and the reviewers. Any product that may be evaluated in this article, or claim that may be made by its manufacturer, is not guaranteed or endorsed by the publisher.

Supplementary material

The Supplementary Material for this article can be found online at: https://www.frontiersin.org/articles/10.3389/fvets.2022.981664/full#supplementary-material

SUPPLEMENTARY FIGURE 1
Alignment of cytochrome *b* sequences. Sequence alignment of cytochrome b between *E. multilocularis* (C6L2E3), *T. gondii* (S8EQL3), *P. falciparum* (Q02768), and *H. sapiens* (P00156; EgrG_900000100). Conserved sites are marked in gray (four out of five amino acids same) and in light gray (three out of five amino acids same). Dotted rectangles indicate the Qo site, solid lined rectangles the Qi site.

References

1. Bouwknegt M, Devleesschauwer B, Graham H, Robertson LJ, Giessen JW. The Euro-Fbp workshop participants. Prioritisation of food-borne parasites in Europe, 2016. *Euro Surveill Bull Eur Sur Mal Transm Eur Commun Dis Bull.* (2018) 23:161. doi: 10.2807/1560-7917.ES.2018.23.9.17-00161

2. Torgerson PR, Macpherson CNL. The socioeconomic burden of parasitic zoonoses: global trends. *Vet Parasitol.* (2011) 182:79–95. doi: 10.1016/j.vetpar.2011.07.017

3. Kern P, Menezes da Silva A, Akhan O, Müllhaupt B, Vizcaychipi KA, Budke C, et al. The echinococcoses: diagnosis, clinical management and burden of disease. *Adv Parasitol.* (2017) 96:259–369. doi: 10.1016/bs.apar.2016.09.006

4. Romig T, Deplazes P, Jenkins D, Giraudoux P, Massolo A, Craig PS, et al. Ecology and life cycle patterns of echinococcus species. *Adv Parasitol.* (2017) 95:213–314. doi: 10.1016/bs.apar.2016.11.002

5. Koziol U, Rauschendorfer T, Zanon Rodríguez L, Krohne G, Brehm K. The unique stem cell system of the immortal larva of the human parasite *Echinococcus multilocularis*. *Evodevo.* (2014) 5:10. doi: 10.1186/2041-9139-5-10

6. Lundström-Stadelmann B, Rufener R, Ritler D, Zurbriggen R, Hemphill A. The importance of being parasiticidal: an update on drug development for the treatment of alveolar echinococcosis. *Food Waterborne Parasitol.* (2019) 15:e00040. doi: 10.1016/j.fawpar.2019.e00040

7. Grüner B, Kern P, Mayer B, Gräter T, Hillenbrand A, Barth TFE, et al. Comprehensive diagnosis and treatment of alveolar echinococcosis: a single-center, long-term observational study of 312 patients in Germany. *GMS Infect Dis.* (2017) 2017:1–12. doi: 10.3205/id000027

8. Andrews KT, Fisher G, Skinner-Adams TS. Drug repurposing and human parasitic protozoan diseases. *Int J Parasitol Drugs Drug Resist.* (2014) 4:95–111. doi: 10.1016/j.ijpddr.2014.02.002

9. Siles-Lucas M, Becerro-Recio D, Serrat J, González-Miguel J. Fascioliasis and fasciolopsiasis: current knowledge and future trends. *Res Vet Sci.* (2021) 134:27–35. doi: 10.1016/j.rvsc.2020.10.011

10. Woolsey ID, Miller AL. *Echinococcus granulosus* sensu lato and *Echinococcus multilocularis*: a review. *Res Vet Sci.* (2021) 135:517–22. doi: 10.1016/j.rvsc.2020.11.010

11. Ritler D, Rufener R, Li JV, Kämpfer U, Müller J, Bühr C, et al. *In vitro* metabolomic footprint of the *Echinococcus multilocularis* metacestode. *Sci Rep.* (2019) 9:19438. doi: 10.1038/s41598-019-56073-y

12. Besteiro S, Biran M, Biteau N, Coustou V, Baltz T, Canioni P, et al. Succinate secreted by *Trypanosoma brucei* is produced by a novel and unique glycosomal enzyme, NADH-dependent fumarate reductase. *J Biol Chem.* (2002) 277:38001–12. doi: 10.1074/jbc.M201759200

13. Kita K, Nihei C, Tomitsuka E. Parasite mitochondria as drug target: diversity and dynamic changes during the life cycle. *Curr Med Chem.* (2003) 10:2535–48. doi: 10.2174/0929867033456549

14. Komuniecki R, Harris BG. Carbohydrate and energy metabolism in helminths. In: Marr JJ, Muller M, editors. *Biochemistry and Molecular Biology of Parasites*. San Diego, CA: Academic Press Inc (1995). p. 2. doi: 10.1016/B978-012473345-9/50005-2

15. Tielens AG. Energy generation in parasitic helminths. *Parasitol Today Pers Ed.* (1994) 10:346–52. doi: 10.1016/0169-4758(94)90245-3

16. Enkai S, Inaoka DK, Kouguchi H, Irie T, Yagi K, Kita K. Mitochondrial complex III in larval stage of *Echinococcus multilocularis* as a potential chemotherapeutic target and *in vivo* efficacy of atovaquone against primary hydatid cysts. *Parasitol Int.* (2020) 75:102004. doi: 10.1016/j.parint.2019.102004

17. Rufener R, Dick L, D'Ascoli L, Ritler D, Hizem A, Wells TNC, et al. Repurposing of an old drug: *in vitro* and *in vivo* efficacies of buparvaquone against *Echinococcus multilocularis*. *Int J Parasitol Drugs Drug Resist.* (2018) 8:440–50. doi: 10.1016/j.ijpddr.2018.10.011

18. Nilsen A, Miley GP, Forquer IP, Mather MW, Katneni K, Li Y, et al. Discovery, synthesis, and optimization of antimalarial 4(1H)-quinolone-3-diarylethers. *J Med Chem.* (2014) 57:3818–34. doi: 10.1021/jm500147k

19. Stickles AM, de Almeida MJ, Morrisey JM, Sheridan KA, Forquer IP, Nilsen A, et al. Subtle changes in endochin-like quinolone structure alter the site of inhibition within the cytochrome bc1 complex of *Plasmodium falciparum*. *Antimicrob Agents Chemother.* (2015) 59:1977–82. doi: 10.1128/AAC.04149-14

20. Doggett JS, Schultz T, Miller AJ, Bruzual I, Pou S, Winter R, et al. Orally bioavailable endochin-like quinolone carbonate ester prodrug reduces *Toxoplasma gondii* brain cysts. *Antimicrob Agents Chemother.* (2020) 64:e00535–20. doi: 10.1128/AAC.00535-20

21. Doggett JS, Nilsen A, Forquer I, Wegmann KW, Jones-Brando L, Yolken RH, et al. Endochin-like quinolones are highly efficacious against acute and latent experimental toxoplasmosis. *Proc Natl Acad Sci USA.* (2012) 109:15936–41. doi: 10.1073/pnas.1208069109

22. McConnell EV, Bruzual I, Pou S, Winter R, Dodean RA, Smilkstein MJ, et al. Targeted structure-activity analysis of endochin-like quinolones reveals potent Qi and Qo site inhibitors of *Toxoplasma gondii* and *Plasmodium falciparum* cytochrome bc1 and identifies ELQ-400 as a remarkably effective compound against acute experimental toxoplasmosis. *ACS Infect Dis.* (2018) 4:1574–84. doi: 10.1021/acsinfecdis.8b00133

23. Anghel N, Imhof D, Winzer P, Balmer V, Ramseier J, Haenggeli K, et al. Endochin-like quinolones (ELQs) and bumped kinase inhibitors (BKIs): synergistic and additive effects of combined treatments against *Neospora caninum* infection *in vitro* and *in vivo*. *Int J Parasitol Drugs Drug Resist.* (2021) 17:92–106. doi: 10.1016/j.ijpddr.2021.08.007

24. Anghel N, Balmer V, Müller J, Winzer P, Aguado-Martinez A, Roozbehani M, et al. Endochin-like quinolones exhibit promising efficacy against *Neospora caninum in vitro* and in experimentally infected pregnant mice. *Front Vet Sci.* (2018) 5:285. doi: 10.3389/fvets.2018.00285

25. Chiu JE, Renard I, Pal AC, Singh P, Vydyam P, Thekkiniath J, et al. Effective therapy targeting cytochrome bc1 prevents babesia erythrocytic development

and protects from lethal infection. *Antimicrob Agents Chemother.* (2021) 65:e0066221. doi: 10.1128/AAC.00662-21

26. Lawres LA, Garg A, Kumar V, Bruzual I, Forquer IP, Renard I, et al. Radical cure of experimental babesiosis in immunodeficient mice using a combination of an endochin-like quinolone and atovaquone. *J Exp Med.* (2016) 213:1307–18. doi: 10.1084/jem.20151519

27. Silva MG, Bastos RG, Stone Doggett J, Riscoe MK, Pou S, Winter R, et al. Endochin-like quinolone-300 and ELQ-316 inhibit *Babesia bovis*, *B. bigemina, B caballi* and *Theileria equi*. *Parasit Vectors.* (2020) 13:606. doi: 10.1186/s13071-020-04487-3

28. Eberhard N, Balmer V, Müller J, Müller N, Winter R, Pou S, et al. Activities of endochin-like quinolones against *in vitro* cultured *Besnoitia besnoiti* Tachyzoites. *Front Vet Sci.* (2020) 7:96. doi: 10.3389/fvets.2020.00096

29. Matsumoto J, Sakamoto K, Shinjyo N, Kido Y, Yamamoto N, Yagi K, et al. Anaerobic NADH-fumarate reductase system is predominant in the respiratory chain of *Echinococcus multilocularis*, providing a novel target for the chemotherapy of alveolar echinococcosis. *Antimicrob Agents Chemother.* (2008) 52:164–70. doi: 10.1128/AAC.00378-07

30. Spiliotis M, Tappe D, Sesterhenn L, Brehm K. Long-term *in vitro* cultivation of *Echinococcus multilocularis* metacestodes under axenic conditions. *Parasitol Res.* (2004) 92:430–2. doi: 10.1007/s00436-003-1046-8

31. Knapp J, Staebler S, Bart JM, Stien A, Yoccoz NG, Drögemüller C, et al. *Echinococcus multilocularis* in Svalbard, Norway: microsatellite genotyping to investigate the origin of a highly focal contamination. *Infect Genet Evol J Mol Epidemiol Evol Genet Infect Dis.* (2012) 12:1270–4. doi: 10.1016/j.meegid.2012.03.008

32. Stadelmann B, Scholl S, Müller J, Hemphill A. Application of an *in vitro* drug screening assay based on the release of phosphoglucose isomerase to determine the structure–activity relationship of thiazolides against *Echinococcus multilocularis* metacestodes. *J Antimicrob Chemother.* (2010) 65:512–9. doi: 10.1093/jac/dkp490

33. The UniProt Consortium. UniProt: a worldwide hub of protein knowledge. *Nucleic Acids Res.* (2019) 47:D506–15. doi: 10.1093/nar/gky1049

34. Howe KL, Bolt BJ, Shafie M, Kersey P, Berriman M. WormBase ParaSite – a comprehensive resource for helminth genomics. *Mol Biochem Parasitol.* (2017) 215:2–10. doi: 10.1016/j.molbiopara.2016.11.005

35. Thompson JD, Gibson TJ, Plewniak F, Jeanmougin F, Higgins DG. The CLUSTAL_X windows interface: flexible strategies for multiple sequence alignment aided by quality analysis tools. *Nucleic Acids Res.* (1997) 25:4876–82. doi: 10.1093/nar/25.24.4876

36. Hall T. *Bioedit: A User-Friendly Biological Sequence Alignment Editor and Analysis Program for Windows 95/98/ NT*. (1999)

37. Alday PH, Bruzual I, Nilsen A, Pou S, Winter R, Ben Mamoun C, et al. Genetic evidence for cytochrome b Qi site inhibition by 4(1H)-Quinolone-3-Diarylethers and Antimycin in *Toxoplasma gondii*. *Antimicrob Agents Chemother.* (2017) 61:e01866–16. doi: 10.1128/AAC.01866-16

38. Song Z, Iorga BI, Mounkoro P, Fisher N, Meunier B. The antimalarial compound ELQ-400 is an unusual inhibitor of the bc1 complex, targeting both Qo and Qi sites. *FEBS Lett.* (2018) 592:1346–56. doi: 10.1002/1873-3468.13035

39. Stickles AM, Smilkstein MJ, Morrisey JM, Li Y, Forquer IP, Kelly JX, et al. Atovaquone and ELQ-300 combination therapy as a novel dual-site cytochrome bc1 inhibition strategy for malaria. *Antimicrob Agents Chemother.* (2016) 60:4853–9. doi: 10.1128/AAC.00791-16

40. Bryant C. Electron transport in parasitic helminths and protozoa. *Adv Parasitol.* (1970) 8:139–72. doi: 10.1016/S0065-308X(08)60253-5

41. Del Borrello S, Lautens M, Dolan K, Tan JH, Davie T, Schertzberg MR, et al. Rhodoquinone biosynthesis in *C. elegans* requires precursors generated by the kynurenine pathway. *eLife.* (2019) 8:e48165. doi: 10.7554/eLife.48165

42. Lautens MJ, Tan JH, Serrat X, Del Borrello S, Schertzberg MR, Fraser AG. Identification of enzymes that have helminth-specific active sites and are required for Rhodoquinone-dependent metabolism as targets for new anthelmintics. *PLoS Negl Trop Dis.* (2021) 15:e0009991. doi: 10.1371/journal.pntd.0009991

43. Miyadera H, Shiomi K, Ui H, Yamaguchi Y, Masuma R, Tomoda H, et al. Atpenins, potent and specific inhibitors of mitochondrial complex II (succinate-ubiquinone oxidoreductase). *Proc Natl Acad Sci USA.* (2003) 100:473–7. doi: 10.1073/pnas.0237315100

44. Inaoka DK, Shiba T, Sato D, Balogun EO, Sasaki T, Nagahama M, et al. Structural insights into the molecular design of flutolanil derivatives targeted for fumarate respiration of parasite mitochondria. *Int J Mol Sci.* (2015) 16:15287–308. doi: 10.3390/ijms160715287

45. Osanai A, Harada S, Sakamoto K, Shimizu H, Inaoka DK, Kita K. Crystallization of mitochondrial rhodoquinol-fumarate reductase from the parasitic nematode *Ascaris suum* with the specific inhibitor flutolanil. *Acta Crystallograph Sect F Struct Biol Cryst Commun.* (2009) 65:941–4. doi: 10.1107/S1744309109031352

46. Omura S, Miyadera H, Ui H, Shiomi K, Yamaguchi Y, Masuma R, et al. An anthelmintic compound, nafuredin, shows selective inhibition of complex I in helminth mitochondria. *Proc Natl Acad Sci USA*. (2001) 98:60–2. doi: 10.1073/pnas.98.1.60

47. Cumino AC, Elissondo MC, Denegri GM. Flubendazole interferes with a wide spectrum of cell homeostatic mechanisms in *Echinococcus granulosus* protoscoleces. *Parasitol Int.* (2009) 58:270–7. doi: 10.1016/j.parint.2009.03.005

48. Vinaud MC, Ferreira CS, Lino Junior R de S, Bezerra JCB. *Taenia crassiceps*: energetic and respiratory metabolism from cysticerci exposed to praziquantel and albendazole *in vitro*. *Exp Parasitol.* (2008) 120:221–6. doi: 10.1016/j.exppara.2008.07.008

49. Wani JH, Srivastava VM. Effect of cations and anthelmintics on enzymes of respiratory chains of the cestode *Hymenolepis diminuta*. *Biochem Mol Biol Int.* (1994) 34:239–50.

50. Xiao SH, Feng JJ, Guo HF, Jiao PY, Yao MY, Jiao W. Effects of mebendazole, albendazole, and praziquantel on succinate dehydrogenase, fumarate reductase, and malate dehydrogenase in *Echinococcus granulosus* cysts harbored in mice. *Zhongguo Yao Li Xue Bao.* (1993) 14:151–4.

frontiers | Frontiers in Veterinary Science

TYPE Original Research
PUBLISHED 09 August 2022
DOI 10.3389/fvets.2022.956040

OPEN ACCESS

EDITED BY
Simona Gabrielli,
Sapienza University of Rome, Italy

REVIEWED BY
Madhu Sudhana Saddala,
The Johns Hopkins Hospital,
United States
Yang Zou,
Lanzhou Veterinary Research Institute, China
Serena Cavallero,
Sapienza University of Rome, Italy

*CORRESPONDENCE
Qing Liu
lqsxau@163.com

SPECIALTY SECTION
This article was submitted to Parasitology, a section of the journal Frontiers in Veterinary Science

RECEIVED 29 May 2022
ACCEPTED 18 July 2022
PUBLISHED 09 August 2022

CITATION
Meng Y-J, Mu B-J, Liu X-X, Yu L-M, Zheng W-B, Xie S-C, Gao W-W, Zhu X-Q and Liu Q (2022) Transcriptional changes in LMH cells induced by *Eimeria tenella* rhoptry kinase family protein 17. *Front. Vet. Sci.* 9:956040. doi: 10.3389/fvets.2022.956040

Transcriptional changes in LMH cells induced by *Eimeria tenella* rhoptry kinase family protein 17

Yi-Jing Meng[1], Bing-Jin Mu[1], Xiao-Xin Liu[1], Lin-Mei Yu[1], Wen-Bin Zheng[1], Shi-Chen Xie[1], Wen-Wei Gao[1], Xing-Quan Zhu[1,2] and Qing Liu[1]*

[1]College of Veterinary Medicine, Shanxi Agricultural University, Jinzhong, China, [2]Key Laboratory of Veterinary Public Health of Higher Education of Yunnan Province, College of Veterinary Medicine, Yunnan Agricultural University, Kunming, China

Though a number of *Eimeria tenella* rhoptry kinase family proteins have been identified, little is known about their molecular functions. In the present study, the gene fragment encoding the matured peptide of *E. tenella* rhoptry kinase family protein 17 (EtROP17) was used to construct a recombinant vector, followed by transfection into leghorn male hepatoma (LMH) cells. Then, the transcriptional changes in the transfected cells were determined by RNA-seq. The expression of EtROP17 in LMH cells was validated by both Western blot and indirect immunofluorescence analysis. Our analysis showed that EtROP17 altered the expression of 309 genes (114 downregulated genes and 195 upregulated genes) in LMH cells. The quantitative real-time polymerase chain reaction (qRT-PCR) results of the selected differentially expressed genes (DEGs) were consistent with the RNA-seq data. Kyoto Encyclopedia of Genes and Genomes (KEGG) analysis showed that DEGs were significantly enriched in nine pathways, such as toll-like receptor signaling pathway, ECM-receptor interaction, intestinal immune network for IgA production and focal adhesion. These findings reveal several potential roles of EtROP17, which contribute to understanding the molecular mechanisms underlying the host-parasite interplay.

KEYWORDS

***Eimeria tenella*, rhoptry kinase family protein 17, LMH cells, overexpression, transcriptome**

Introduction

Avian coccidiosis is an economically significant disease of the poultry industry caused by intracellular intestinal parasites of the genus *Eimeria*, with a worldwide distribution (1, 2). Seven *Eimeria* species, namely *Eimeria maxima*, *Eimeria acervulina*, *Eimeria necatrix*, *Eimeria brunetti*, *Eimeria mitis*, *Eimeria tenella* and *Eimeria praecox*, are recognized to infect chickens (3). *E. tenella* is one of the most pathogenic species, causing caecal coccidiosis of chickens (4, 5).

Twenty-eight rhoptry kinase family proteins (ROPs) have been predicted in *E. tenella* through genomic analysis, such as *E. tenella* ROP 17 (EtROP17), EtROP21 and EtROP30

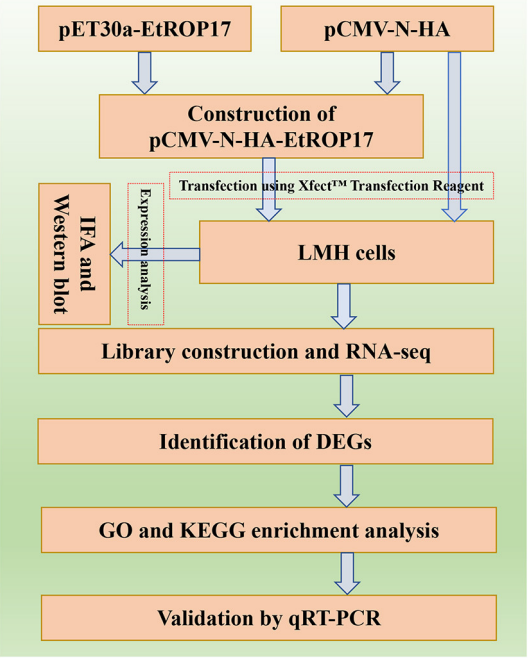

FIGURE 1
Flow chart of the performed research work.

(6). Subsequently, the expression patterns of these genes during the *E. tenella* life-cycle have been studied by quantitative real-time polymerase chain reaction (qRT-PCR) (7). Meanwhile, EtROP30 was reported to localize to the nucleus and possibly play an important role during parasite reinvasion and development (8). Additionally, a previous study showed that Et-ROPK-Eten5-A may be a potential candidate for the development of new vaccines against *E. tenella* (9). To date, however, the roles of the majority of EtROPs remain unknown.

Toxoplasma gondii ROP17 (TgROP17) was reported to be an important effector molecule, which is associated with maintaining *T. gondii* proliferation in host cells through regulating the Bcl-2-Beclin 1 pathway (10). Moreover, TgROP17 contributes to *T. gondii* dissemination (11). Additionally, transcriptomic analysis showed that TgROP17 plays a pivotal role in the survival of *T. gondii* within host cells by inhibiting the innate immune response (12).

The aim of the present study was to determine the biological function of EtROP17, which shares homology with TgROP17. To achieve this, the fragment of the ROP17 gene of the *E. tenella* SD-01 strain was used to construct the recombinant vector. Then, the role of EtROP17 was determined by transcriptomic analysis of leghorn male hepatoma (LMH) cells transfected with the recombinant vector. The workflow of the research is illustrated in Figure 1.

Materials and methods

Cell line

An epithelial cell line, LMH, was used for transfection, which was often used in studies of avian pathogens (13, 14). LMH cells were grown in Dulbecco's modified eagle medium (DMEM) containing 10% (vol/vol) fetal bovine serum (FBS), 100 U/mL penicillin, and 100 μg/mL streptomycin. The cell culture was maintained at 37°C in an incubator with 5% CO_2, and cells were passaged every 2 days (15).

Construction of the recombinant vector

The pCMV-N-HA vector and the previously constructed pET30a-EtROP17 were double digested with BamHI and EcoRI (16), and the nucleotide sequence encoding the matured peptide of EtROP17 (Figure 2A) was ligated into the linearized vector pCMV-N-HA using the T4 DNA Ligase (Takara, Dalian, China). Following transformation into *Escherichia coli* DH5α competent cells (Transgen Biotech, China), single bacterial colony was randomly selected for PCR analysis. The positive colony was cultured in Luria-Bertani (LB) medium, and the recombinant vector (designated pCMV-N-HA-EtROP17) was extracted using the PhasePrep EndoFree Maxi Kit (Aidlab, Beijing, China) according to the manufacturer's specifications. The extracted vector was verified by double restriction enzyme digestion and sequencing (Sangon Biotech, Shanghai, China). The quality and quantity of yielded vector were determined by a spectrophotometer (NanoDrop One/One^c, Thermo Scientific).

Transfection of LMH cells

The Xfect^{TM} Transfection Reagent (Takara, Dalian, China) was used for transfection of LMH cells (∼ 80% confluent). For immunofluorescence analysis, 1 day prior to the transfection, the LMH cells were seeded in 24-well plate. Then, 0.75 μg PCMV-N-HA-EtROP17 and PCMV-N-HA were diluted separately with Xfect reaction buffer to a final volume of 25 μL. Afterwards, 0.225 μL Xfect polymer was added and incubated for 10 min at room temperature to allow nanoparticle complexes to form. The mixture was then added to the cell culture medium and incubated for 4 h. Subsequently, the medium was replaced with 500 μL fresh DMEM plus 10% FBS.

For Western blot analysis and RNA-seq, the LMH cells were seeded in T-25cm^2 cell culture flasks, and 12.5 μg PCMV-N-HA-EtROP17 and PCMV-N-HA were used separately for transfection. Meanwhile, each plasmid was diluted with Xfect

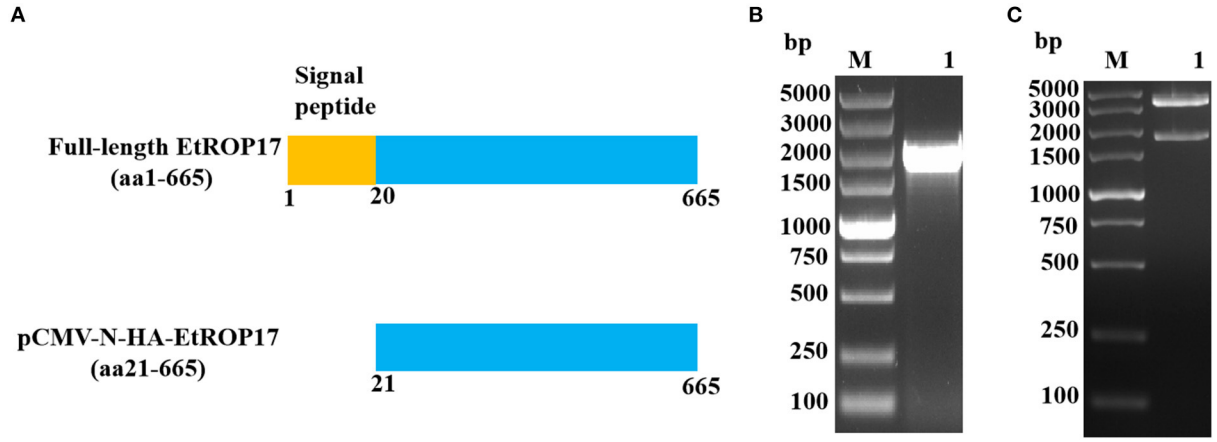

FIGURE 2
(A) Schematic illustration of full-length EtROP17 and the region of EtROP17 used in the present study. **(B)** The gel electrophoresis of the PCR products. Lane M, DL5000 DNA Marker; lane 1, the gene fragment of EtROP17 amplified from cDNA of *E. tenella* SD-01 strain. **(C)** Digestion of the resultant vector with BamHI and EcoRI restriction enzymes.

reaction buffer to a final volume of 250 μL, and 3.75 μL Xfect polymer was used.

Indirect immunofluorescence assay

The cells were fixed at 48 h post-transfection with 2% paraformaldehyde for 10 min, followed by incubation with 0.1% Triton X-100 for 10 min. After blocking with 5% bovine serum albumin, mouse anti-HA tag antibody (Invitrogen, CA, USA) was added to each well and incubated for 1 h. Following washing for three times with PBS, each well was incubated with FITC-conjugated goat anti-mouse IgG (Abcam, UK) at 37 °C for 1 h. The cells were observed under a Nikon fluorescence microscope (Nikon, Japan).

Western blot

Forty-eight hours post transfection, the cells were lysed by treatment with RIPA lysis buffer (Beyotime, China). Protein extracts were electrophoretically separated under denaturing conditions with 10% Expressplus™ PAGE Gels (GenScript, China), and then blotted onto a polyvinylidene fluoride (PVDF) membrane (Millipore, USA). After blocking, the membrane was incubated with mouse anti-HA tag antibody for 2 h. After washing thrice with TBST buffer (20 mM Tris-HCl, 150 mM NaCl, 0.05% Tween 20), the membrane was incubated with HRP-conjugated goat anti-mouse IgG antibody for 1 h. The band was visualized with an enhanced chemiluminescent (ECL) reagent (Thermo Scientific, USA).

Transcriptome sequencing and read alignment

We performed transcriptomic analysis of LMH cells transfected with PCMV-N-HA-EtROP17 or PCMV-N-HA, and the RNA-seq service was provided by Novogene Corporation (Beijing, China). Three biological replicates were included for each condition, and the TRIzol reagent (Invitrogen, CA, USA) was used for extraction of total RNA. The Agilent 2100 Bioanalyzer (Agilent Technologies, CA, USA) was used to evaluate the quality of the extracted RNA. mRNA was purified with poly-T oligo-attached magnetic beads and segmented into small fragments using divalent cations under elevated temperature, followed by cDNA synthesis. After adenylation, NEBNext Adaptor with hairpin loop structure was ligated to the cDNA fragments. Then, these fragments were subjected to purification and PCR amplification. Following purification of PCR products, quality assessment and cluster generation, the libraries were sequenced using an Illumina Novaseq platform. After removal of low quality reads and reads containing adaptor or poly-N, clean data with high quality were aligned to the chicken (*Gallus gallus*) genome (https://www.ncbi.nlm.nih.gov/genome/?term=Gallus+gallus) using Hisat2 (v2.0.5) (17).

Bioinformatics analysis

Differential expression analysis of two groups was carried out by using the DESeq2 R package (v1.20.0) (18). Differential gene screening was performed under the condition of both P value <0.05 and $|\log_2$ fold change (FC)$|>1.0$.

TABLE 1 Sequences of the primers used for the qRT-PCR assay.

Gene ID	Gene name	Forward primer (5′-3′)	Reverse primer (5′-3′)
374193	GAPDH	CTGGGGCTCATCTGAAGGGT	GGACGCTGGGATGATGTTCT
395908	OASL	GGTGCTCTTCATCAACTGCTTCTCCA	TCGTAAGCAGGCAGGATGTC
403120	IFI6	TCCTTCTGGAGGGACTACTGCTA	TGGACCGCTGCTTCTTTCTATT
418982	MMP1	TTGATGAGGAGGAAACCTGGAC	GGTCTGTGTAGGCATAGTTTGGATA
428310	HSPB9	ACGCAGAACACGGACGAGAA	TTTGCTGACAGCTCCATCCTT
428650	RSAD2	TGCCGAGATTATGCTGTTGCT	CAATGATTAGGCACTGGAACACC
395313	MX1	CTCTGCCAAAGTTGAAGAAATCG	CCTCAAATGTCCAGTAGCTGATAAAG
417964	EMP1	GTTTGGATGGTGGGTAGGAGTT	TGATGGCTCCAGTGATGTAGAAAC
428431	GPNMB	GAAGACCTTTCCCTCATTATCCT	CCGAGAGTGATATTTGCAGTGTT

Gene Ontology (GO) annotation and Kyoto Encyclopedia of Genes and Genomes (KEGG) pathway enrichment analysis were performed by using the clusterProfiler R package (v3.8.1) (19). A P value <0.05 was set as the cut-off threshold to identify the significantly enriched GO terms or pathways.

Validation of RNA-seq data by qRT-PCR

RNA-seq results were verified by qRT-PCR, which was performed on a CFX Connect Real-Time PCR Detection System (Bio-Rad, CA, USA). Eight DEGs were selected for validation. For normalizing the expression of gene, GAPDH was used as the endogenous reference gene, and the control was used as a reference sample, which was set to one. The qRT-PCR cycling conditions included 95°C for 30 s, followed by 40 cycles of 95°C for 15 s, and 60°C for 30 s. The temperatures of the melting curve analysis ranged from 65°C to 95°C. The qRT-PCR reactions were carried out in triplicates. All the primers are shown in Table 1. Normalized FC ($2^{-\Delta\Delta Ct}$) in expression was determined based on ΔCt ($Ct_{target\ gene} - Ct_{GAPDH}$) and ΔΔCt ($\Delta Ct_{experimental\ group} - \Delta Ct_{control\ group}$) (20), and then the $\log_2$ FC value was calculated.

Results

Confirmation of the resultant vector

As shown in Figure 2B, the gene fragment of EtROP17 was obtained by PCR amplification. Digestion of the resultant vector with BamHI and EcoRI restriction enzymes was carried out to confirm the presence of the gene fragment of EtROP17. Two bands were observed, indicating that the recombinant vector was successfully constructed (Figure 2C).

Expression analysis of EtROP17 in LMH cells

Successful transfection was determined by means of the indirect immunofluorescence assay. As shown in Figure 3A, mouse anti-HA tag antibody clearly labeled the LMH cells transfected with pCMV-N-HA-EtROP17. Meanwhile, no fluorescent signal was observed in null plasmid transfected cells. Western blot analysis showed that LMH cells transfected with pCMV-N-HA-EtROP17 expressed a protein at a size of approximately 57 kDa (Figure 3B, lane 1), which was not observed in LMH cells transfected with the empty control vector (Figure 3B, lane 2).

Analysis of differential gene expression

RNA integrity of all samples was evaluated, with RNA integrity number (RIN) values ranging from 8.9 to 10 (Supplementary Table 1). Compared with the control group, 309 genes were found to be differentially expressed in LMH cells transfected with EtROP17 (Figure 4). Of which, 195 DEGs were upregulated, and 114 DEGs were downregulated. Details of the DEGs are provided in Supplementary Table 2.

GO enrichment

GO analysis showed that the DEGs were categorized into 323 GO terms. Eighteen significantly enriched terms were identified based on a P value <0.05 as a cutoff, including six GO biological process terms (regulation of catalytic activity, regulation of molecular function, lipid biosynthetic process, immune system process, immune response, and response to chemical), seven GO cellular component terms (mitochondrion, cytoskeletal part, cytoskeleton, extracellular region, intermediate filament, intermediate filament cytoskeleton, and polymeric cytoskeletal fiber), and five GO molecular function terms

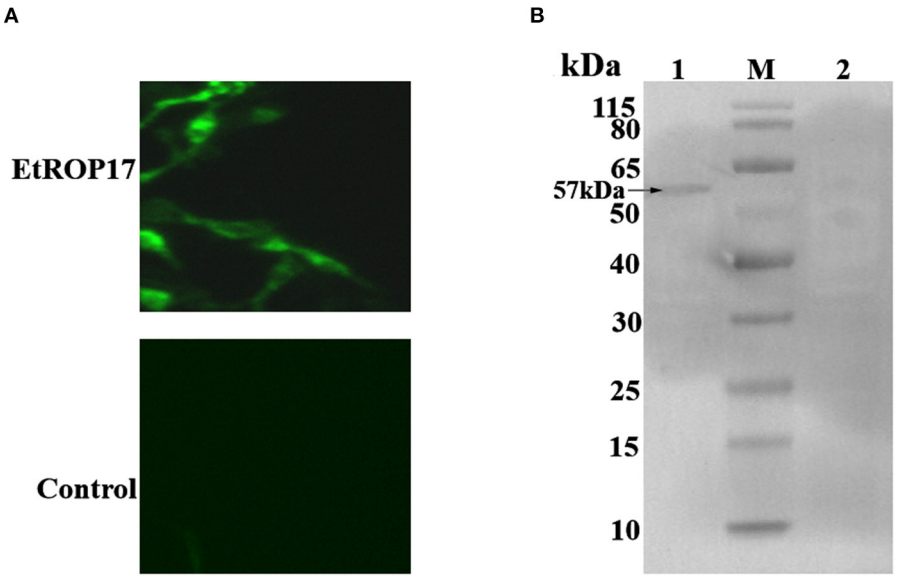

FIGURE 3
(A) Immunofluorescent analysis of PCMV-N-HA-EtROP17-transfected cells and PCMV-N-HA-transfected control cells. **(B)** Western blot analysis of PCMV-N-HA-EtROP17-transfected cells and PCMV-N-HA-transfected control cells. Lane 1, total protein extracted from PCMV-N-HA-EtROP17-transfected LMH cells; lane 2, total protein extracted from PCMV-N-HA-transfected control cells; the arrow indicates the position of a 57-kDa EtROP17 band.

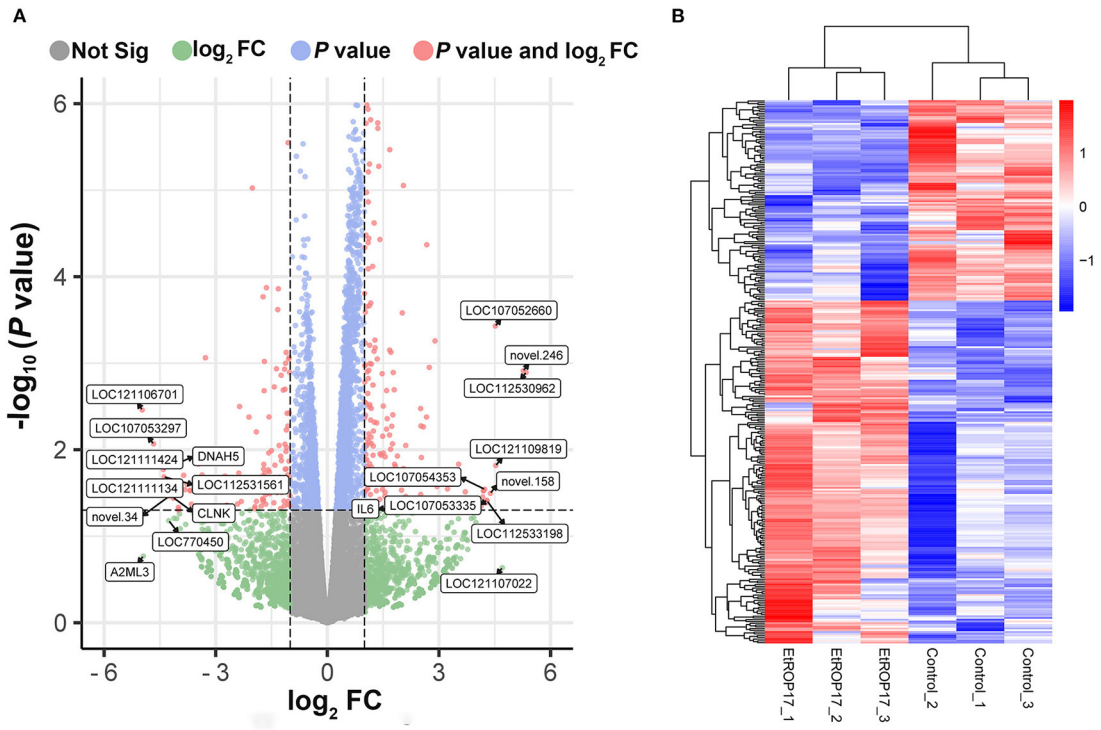

FIGURE 4
Effect of EtROP17 on gene transcription in LMH cells. **(A)** Volcano plot showing the DEGs in EtROP17-expressing LMH cells compared to the control group. **(B)** Heatmap of 309 DEGs. Rows: DEGs; columns: samples.

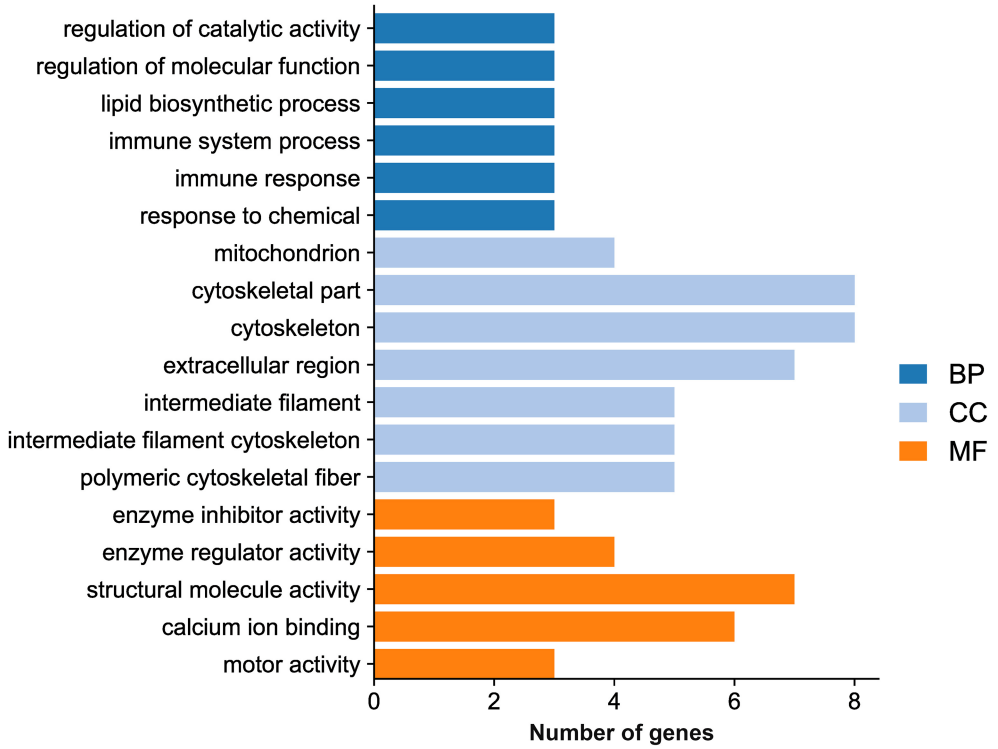

FIGURE 5
Histogram of the significantly enriched GO terms.

(enzyme inhibitor activity, enzyme regulator activity, structural molecule activity, calcium ion binding, and motor activity) (Figure 5; Supplementary Table 3).

KEGG analysis

KEGG analysis of DEGs was conducted to determine the affected pathways. As shown in Figure 6, nine significantly enriched pathways were found on the basis of a *P* value <0.05 as a cutoff, namely mRNA surveillance pathway, toll-like receptor signaling pathway, influenza A, ECM-receptor interaction, intestinal immune network for IgA production, focal adhesion, tight junction, cytosolic DNA-sensing pathway, and ribosome.

Validation of DEGs by qRT-PCR

The transcript expression patterns derived from RNA-Seq were validated by examining the level of expression of selected DEGs from each group using qRT-PCR. An agreement between the results obtained by RNA-seq and qRT-PCR was found (Figure 7; Supplementary Table 4).

Discussion

E. tenella was reported to manipulate many signaling pathways of host cells (21, 22). To date, however, the roles of *E. tenella* proteins in host-parasite interactions remain incompletely understood. In a previous study, we confirmed the expression of EtROP17 in the merozoite stage of *E. tenella* (16). The present study aimed to provide a comprehensive picture of transcriptomic changes in host cells in response to EtROP17 based on an overexpression mode in conjunction with RNA-seq, by which the functions of several genes of *T. gondii* have been characterized (12, 23, 24). The expression of EtROP17 in LMH cells was confirmed by immunofluorescence measurements and Western blot analysis. All RNA samples showed high RIN values, and the transcriptomic data were validated by qRT-PCR. Clustering analysis showed that distinct changes in the expression genes were observed between the two groups.

A previous study revealed the roles of TgROP17 in regulation of the host immune response (12). Though the number of DEGs in LMH cells in response to EtROP17 was lower than that in HEK293T cells in response to TgROP17 (12), several DEGs identified in the present study were also involved in immune responses, such as CCL4, IL6 and IL12B. Meanwhile, GO analysis uncovered that several significantly

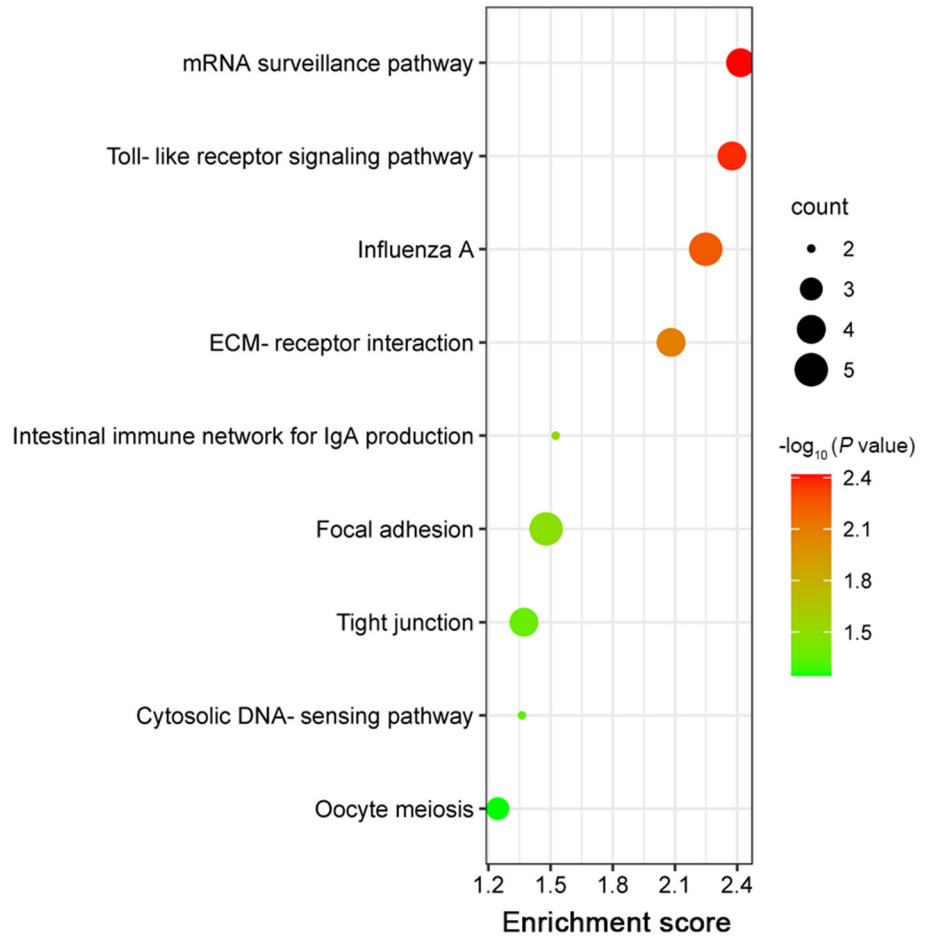

FIGURE 6
The nine significantly enriched KEGG pathways for the DEGs.

enriched GO terms were related to immune responses, such as cytokine activity, cytokine receptor binding, immune system process, and immune response.

The host innate and adaptive immune responses, relying on a complex network of various immune cells and their signals, are involved in fighting against *E. tenella* infection (25, 26). A previous study showed that TgROP17 could negatively regulate toll-like receptor signaling pathway, which is one of the innate host defense mechanisms against pathogens (12, 27). Also, our analysis showed that toll-like receptor signaling pathway in EtROP17-expressing LMH cells was downregulated, and the related genes were CCL4 and IL12B. This indicated that *E. tenella* may negatively regulate toll-like receptor signaling pathway to inhibit innate immune responses by using EtROP17. Additionally, three downregulated DEGs (RSAD2, MX1 and IL12B) were enriched in influenza A, which is also associated with innate immune response (28).

Using RNA-seq, a previous study reported that *E. tenella* could affect intestinal immune network for IgA production in chicken cecal epithelia (29). Meanwhile, *E. maxima* was reported to be able to alter the expression of immune network for IgA production-associated genes (30). Given that IgA production may not play an important role in combating coccidian infection (29), EtROP17 is possibly involved in defense against bacterial and viral infections through affecting intestinal immune network for IgA production (31).

High-throughput sequencing results revealed that focal adhesion and ECM-receptor interaction were significantly enriched. ECM is a complex mixture composed of structural proteins, and attachment to ECM is essential for survival of epithelial cells (32, 33). Focal adhesion is involved in mediating the regulatory effects of a cell in response to ECM adhesion (34). This indicated that EtROP17 may play a crucial role in parasite replication within chicken intestinal epithelial cells. Moreover, the cell to ECM interaction can form physical barriers to prevent invasion of pathogens (35). This indicated that, besides affecting intestinal immune network for IgA production, EtROP17 may contribute to defense

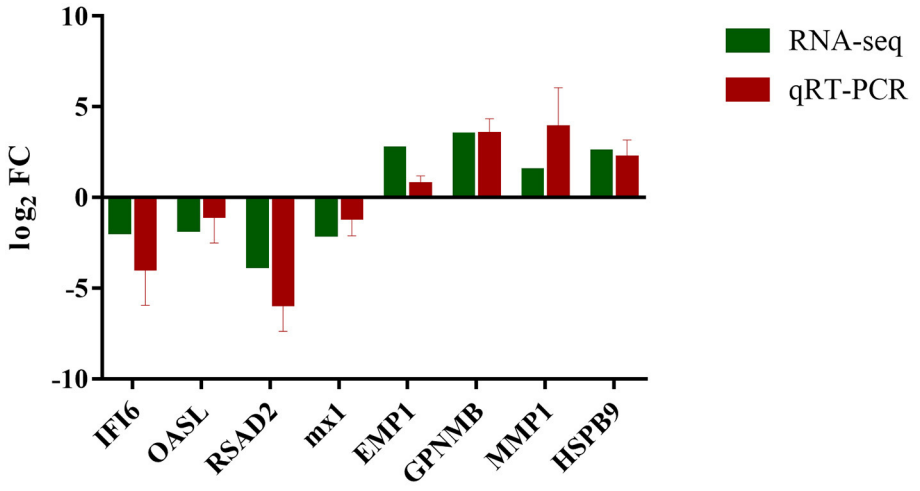

FIGURE 7
Expression verification of eight genes in RNA-seq using qRT-PCR. Green color refers to the result of RNA-seq; red color refers to the result of qRT-PCR.

against microbial infections through affecting ECM-receptor interaction.

Conclusion

The present research revealed gene expression in LMH cells in response to EtROP17 expression. A total of 114 downregulated genes and 195 upregulated genes were identified in EtROP17-expressing LMH cells, which were significantly enriched in nine signaling pathways. These data reveal several potential roles of EtROP17 and contribute to better understanding of the molecular mechanisms underlying the host-parasite interactions.

Data availability statement

The datasets presented in this study can be found in online repositories. The names of the repository/repositories and accession number(s) can be found below: https://www.ncbi.nlm.nih.gov/bioproject/PRJNA831776.

Author contributions

QL and X-QZ conceived and designed the experiments. Y-JM performed the experiments, analyzed the data, and wrote the paper. B-JM, X-XL, L-MY, S-CX, and W-WG participated in the implementation of the study. W-BZ, QL, and X-QZ critically revised the manuscript. All authors contributed to the article and approved the submitted version.

Funding

Project support was provided by the National Natural Science Foundation of China (Grant No. 31902298), the Fund for Shanxi 1331 Project (Grant No. 20211331-13), the Research Fund for Introduced High-level Leading Talents of Shanxi Province, the Special Research Fund of Shanxi Agricultural University for High-level Talents (Grant No. 2021XG001) and Yunnan Expert Workstation (Grant No. 202005AF150041).

Conflict of interest

The authors declare that the research was conducted in the absence of any commercial or financial relationship that could be construed as a potential conflict of interest.

Publisher's note

All claims expressed in this article are solely those of the authors and do not necessarily represent those of their affiliated organizations, or those of the publisher, the editors and the reviewers. Any product that may be evaluated in this article, or claim that may be made by its manufacturer, is not guaranteed or endorsed by the publisher.

Supplementary material

The Supplementary Material for this article can be found online at: https://www.frontiersin.org/articles/10.3389/fvets.2022.956040/full#supplementary-material

References

1. Song X, Yang X, Zhang T, Liu J, Liu Q. Evaluation of 4 merozoite antigens as candidate vaccines against *Eimeria tenella* infection. *Poult Sci.* (2021) 100:100888. doi: 10.1016/j.psj.2020.12.001

2. Li C, Zhao Q, Zhu S, Wang Q, Wang H, Yu S, et al. *Eimeria tenella Eimeria*-specific protein that interacts with apical membrane antigen 1 (EtAMA1) is involved in host cell invasion. *Parasit Vectors.* (2020) 13:373. doi: 10.1186/s13071-020-04229-5

3. Kundu K, Garg R, Kumar S, Mandal M, Tomley FM, Blake DP, et al. Humoral and cytokine response elicited during immunization with recombinant Immune Mapped protein-1 (EtIMP-1) and oocysts of *Eimeria tenella*. *Vet Parasitol.* (2017) 244:44–53. doi: 10.1016/j.vetpar.2017.07.025

4. Mouafo AN, Richard F, Entzeroth R. Observation of sutures in the oocyst wall of *Eimeria tenella* (Apicomplexa). *Parasitol Res.* (2000) 86:1015–7. doi: 10.1007/PL00008521

5. Shen X, Wang C, Zhu Q, Li T, Yu L, Zheng W, et al. Effect of the diclazuril on Hsp90 in the second-generation merozoites of *Eimeria tenella*. *Vet Parasitol.* (2012) 185:290–5. doi: 10.1016/j.vetpar.2011.10.018

6. Reid AJ, Blake DP, Ansari HR, Billington K, Browne HP, Bryant J, et al. Genomic analysis of the causative agents of coccidiosis in domestic chickens. *Genome Res.* (2014) 24:1676–85. doi: 10.1101/gr.168955.113

7. Ribeiro E. Silva A, Sausset A, Bussière FI, Laurent F, Lacroix-Lamandé S, Silvestre A. Genome-wide expression patterns of rhoptry kinases during the *Eimeria tenella* life-cycle. *Microorganisms.* (2021) 9:1621. doi: 10.3390/microorganisms9081621

8. Wang B, Zhao N, Wang Y, Sun L, Li H, Zhang X, et al. Characterization of the *Eimeria tenella* rhoptry protein with a nuclear localization sequence (EtROP30). *Parasitol Res.* (2022) 121:1507–16. doi: 10.1007/s00436-022-07499-3

9. Song X, Yang X, Zhang T, Liu J, Liu Q, A. novel rhoptry protein as candidate vaccine against *Eimeria tenella* infection. *Vaccines.* (2020) 8:452. doi: 10.3390/vaccines8030452

10. Guo M, Sun J, Wang WT, Liu HY, Liu YH, Qin KR, et al. *Toxoplasma gondii* ROP17 promotes autophagy *via* the Bcl-2-Beclin 1 pathway. *Folia Parasitol.* (2021) 68:2021.016. doi: 10.14411/fp.2021.016

11. Drewry LL, Jones NG, Wang Q, Onken MD, Miller MJ, Sibley LD. The secreted kinase ROP17 promotes *Toxoplasma gondii* dissemination by hijacking monocyte tissue migration. *Nat Microbiol.* (2019) 4:1951–63. doi: 10.1038/s41564-019-0504-8

12. Li JX, He JJ, Elsheikha HM, Chen D, Zhai BT, Zhu XQ, et al. *Toxoplasma gondii* ROP17 inhibits the innate immune response of HEK293T cells to promote its survival. *Parasitol Res.* (2019) 118:783–92. doi: 10.1007/s00436-019-06215-y

13. Zhang L, Katselis GS, Moore RE, Lekpor K, Goto RM, Lee TD, et al. Proteomic analysis of surface and endosomal membrane proteins from the avian LMH epithelial cell line. *J Proteome Res.* (2011) 10:3973–82. doi: 10.1021/pr200179r

14. Hériveau C, Dimier-Poisson I, Lowenthal J, Naciri M, Quéré P. Inhibition of *Eimeria tenella* replication after recombinant IFN-gamma activation in chicken macrophages, fibroblasts and epithelial cells. *Vet Parasitol.* (2000) 92:37–49. doi: 10.1016/S0304-4017(00)00275-2

15. Sato M, Kawashima T, Aosasa M, Horiuchi H, Furusawa S, Matsuda H. Excision of foreign gene product with cathepsin D in chicken hepatoma cell line. *Biochem Biophys Res Commun.* (2005) 330:533–9. doi: 10.1016/j.bbrc.2005.03.008

16. Liu X, Mu B, Zheng W, Meng Y, Yu L, Gao W, et al. Identification and protective efficacy of *Eimeria tenella* rhoptry kinase family protein 17. *Animals.* (2022) 12:556. doi: 10.3390/ani12050556

17. Kim D, Langmead B, Salzberg SL. HISAT: a fast spliced aligner with low memory requirements. *Nat Methods.* (2015) 12:357–60. doi: 10.1038/nmeth.3317

18. Love MI, Huber W, Anders S. Moderated estimation of fold change and dispersion for RNA-seq data with DESeq2. *Genome Biol.* (2014) 15:550. doi: 10.1186/s13059-014-0550-8

19. Yu G, Wang LG, Han Y, He QY. clusterProfiler: an R package for comparing biological themes among gene clusters. *OMICS.* (2012) 16:284–7. doi: 10.1089/omi.2011.0118

20. Livak KJ, Schmittgen TD. Analysis of relative gene expression data using real-time quantitative PCR and the 2(-Delta Delta C(T)) Method. *Methods.* (2001) 25:402–8. doi: 10.1006/meth.2001.1262

21. Sandholt AKS, Wattrang E, Lilja T, Ahola H, Lundén A, Troell K, et al. Dual RNA-seq transcriptome analysis of caecal tissue during primary *Eimeria tenella* infection in chickens. *BMC Genomics.* (2021) 2:660. doi: 10.1186/s12864-021-07959-7

22. Sandholt AKS, Xu F, Söderlund R, Lundén A, Troell K, Svärd SG, et al. Dual RNA-seq transcriptome analysis of chicken macrophage-like cells (HD11) infected *in vitro* with *Eimeria tenella*. *Parasitology.* (2021) 148:712–25. doi: 10.1017/S0031182021000111

23. Li JX, He JJ, Elsheikha HM, Ma J, Xu XP, Zhu XQ. ROP18-mediated transcriptional reprogramming of HEK293T cell reveals new roles of ROP18 in the interplay between *Toxoplasma gondii* and the host cell. *Front Cell Infect Microbiol.* (2020) 10:586946. doi: 10.3389/fcimb.2020.586946

24. Liu Q, Gao WW, Elsheikha HM, He JJ, Li FC, Yang WB, et al. Transcriptomic analysis reveals *Toxoplasma gondii* strain-specific differences in host cell response to dense granule protein GRA15. *Parasitol Res.* (2018) 117:2785–93. doi: 10.1007/s00436-018-5966-8

25. Vazquez MI, Catalan-Dibene J, Zlotnik A. B cells responses and cytokine production are regulated by their immune microenvironment. *Cytokine.* (2015) 74:318–26. doi: 10.1016/j.cyto.2015.02.007

26. Dalloul RA, Lillehoj HS. Poultry coccidiosis: recent advancements in control measures and vaccine development. *Expert Rev Vaccines.* (2006) 5:143–63. doi: 10.1586/14760584.5.1.143

27. Haunshi S, Cheng HH. Differential expression of Toll-like receptor pathway genes in chicken embryo fibroblasts from chickens resistant and susceptible to Marek's disease. *Poult Sci.* (2014) 93:550–5. doi: 10.3382/ps.2013-03597

28. Yu S, Mao H, Jin M, Lin X. Transcriptomic analysis of the chicken MDA5 response genes. *Genes.* (2020) 11:308. doi: 10.3390/genes11030308

29. Guo A, Cai J, Gong W, Yan H, Luo X, Tian G, et al. Transcriptome analysis in chicken cecal epithelia upon infection by *Eimeria tenella in vivo*. *PLoS ONE.* (2013) 8:e64236. doi: 10.1371/journal.pone.0064236

30. Li C, Yan X, Lillehoj HS, Oh S, Liu L, Sun Z, et al. *Eimeria maxima*-induced transcriptional changes in the cecal mucosa of broiler chickens. *Parasit Vectors.* (2019) 12:285. doi: 10.1186/s13071-019-3534-4

31. Rodríguez A, Tjärnlund A, Ivanji J, Singh M, García I, Williams A, et al. Role of IgA in the defense against respiratory infections IgA deficient mice exhibited increased susceptibility to intranasal infection with *Mycobacterium bovis* BCG. *Vaccine.* (2005) 23:2565–72. doi: 10.1016/j.vaccine.2004.11.032

32. Engin AB, Nikitovic D, Neagu M, Henrich-Noack P, Docea AO, Shtilman MI, et al. Mechanistic understanding of nanoparticles' interactions with extracellular matrix: the cell and immune system. *Part Fibre Toxicol.* (2017) 14:22. doi: 10.1186/s12989-017-0199-z

33. Buchheit CL, Weigel KJ, Schafer ZT. Cancer cell survival during detachment from the ECM: multiple barriers to tumour progression. *Nat Rev Cancer.* (2014) 14:632–41. doi: 10.1038/nrc3789

34. He C, Ma T, Shi J, Zhang Z, Wang J, Zhu K, et al. Melatonin and its receptor MT1 are involved in the downstream reaction to luteinizing hormone and participate in the regulation of luteinization in different species. *J Pineal Res.* (2016) 61:279–90. doi: 10.1111/jpi.12345

35. Memon FU, Yang Y, Leghari IH, Lv F, Soliman AM, Zhang W, et al. Transcriptome analysis revealed ameliorative effects of bacillus based probiotic on immunity, gut barrier system, and metabolism of chicken under an experimentally induced *Eimeria tenella* infection. *Genes.* (2021) 12:536. doi: 10.3390/genes12040536

frontiers | Frontiers in Veterinary Science

TYPE Original Research
PUBLISHED 09 September 2022
DOI 10.3389/fvets.2022.981763

OPEN ACCESS

EDITED BY
Alessia Libera Gazzonis,
University of Milan, Italy

REVIEWED BY
Iolanda Moretta,
University of Perugia, Italy
Abdelaziz Ed-Dra,
Zhejiang University, China

*CORRESPONDENCE
María Teresa Gómez-Muñoz
mariateg@ucm.es
Azucena González-Coloma
azu@ica.csic.es

†These authors share last authorship
‡Deceased

SPECIALTY SECTION
This article was submitted to Parasitology, a section of the journal Frontiers in Veterinary Science

RECEIVED 29 June 2022
ACCEPTED 23 August 2022
PUBLISHED 09 September 2022

CITATION
Bailén M, Díaz-Castellanos I, Azami-Conesa I, Alonso Fernández S, Martínez-Díaz RA, Navarro-Rocha J, Gómez-Muñoz MT and González-Coloma A (2022) Anti-*Trichomonas gallinae* activity of essential oils and main compounds from Lamiaceae and Asteraceae plants. *Front. Vet. Sci.* 9:981763. doi: 10.3389/fvets.2022.981763

Anti-*Trichomonas gallinae* activity of essential oils and main compounds from Lamiaceae and Asteraceae plants

María Bailén[1], Irene Díaz-Castellanos[1,2], Iris Azami-Conesa[2], Sara Alonso Fernández[1], Rafael A. Martínez-Díaz[1‡], Juliana Navarro-Rocha[3], María Teresa Gómez-Muñoz[2*†] and Azucena González-Coloma[4*†]

[1]Department of Preventive Medicine, Public Health and Microbiology, Faculty of Medicine, Autonomous University of Madrid, Madrid, Spain, [2]Department of Animal Health, Faculty of Veterinary Sciences, University Complutense of Madrid, Madrid, Spain, [3]Centro de Investigación y Tecnología Agroalimentaria de Aragón, Unidad de Recursos Forestales, Zaragoza, Spain, [4]Instituto de Ciencias Agrarias, Centro Superior de Investigaciones Científicas (CSIC), Madrid, Spain

Trichomonas gallinae is a flagellated protozoan that parasitizes the upper digestive tract of various bird species and causes avian trichomonosis. The emergence of resistant strains to the standard treatment, based on nitroimidazoles, increases the need to find alternative therapies. In this study, 36 essential oils (EOs) from Lamiaceae and Asteraceae plant families were tested against *T. gallinae* trophozoites using the 3-(4,5-dimethylthiazol-2-yl-)-2,5-diphenyltetrazolium bromide (MTT) reduction assay. Among them, EOs from distinct species of Lamiaceae, including the genera *Lavandula*, *Salvia*, *Thymus, Origanum*, and *Satureja* were the ones reporting better anti-trichomonal activity, and were selected for further analysis, including chemical composition and *in vitro* assays. The chemical composition of the selected EOs was determined by gas chromatography followed by mass spectrometry and 19 pure compounds were tested against the protozoa, according to their higher abundance in the active EOs. Pure compounds which displayed the highest activity against *T. gallinae* trophozoites, ordered by highest to lowest activity, were α and β-thujones, camphene, β-pinene, linalyl acetate, thymol, 4-terpineol, γ-terpinene, α-pinene, p-cymene, D-fenchone and β-caryophyllene. A dose dependent effect was observed in most of the EOs and pure compounds tested. The toxicity test conducted in eukaryotic cell cultures with the anti-trichomonal active pure compounds showed that β-caryophyllene, camphene, α-pinene, and β-pinene were slightly toxic for Vero cells, and the selectivity index was calculated. Based on the anti-trichomonal activity and the absence of cytotoxicity results, natural products from Lamiaceae plants could be useful as alternative therapy against avian trichomonosis, mainly those containing linalyl acetate, thymol, 4-terpinenol, γ-terpinene, p-cymene and D-fenchone.

KEYWORDS

natural products, *Salvia*, *Satureja montana*, *Lavandula luisieri*, linalyl acetate, thymol, 4-terpineol, γ-terpinene

Introduction

Trichomonas gallinae (*T. gallinae*) is a flagellated parasite of the oropharynx and causes a potentially life-threatening disease, oral trichomonosis. The main reservoirs are Columbiformes, but many avian species, including domestic and wild birds, can be infected (1). Nitroimidazoles are the drugs of choice for treatment, but several studies reported resistant strains, both, *in vivo* (2–5) and *in vitro* (3, 4, 6–8). Since the ban of the use of nitroimidazoles for prevention in the EU and the USA, there is no alternative to prevent the disease (9).

Natural products are compounds obtained from living organisms that contain secondary metabolites that help them to survive in adverse environments or even to defend against pathogens. Among them, Essential Oils (EOs) are one of the more frequently employed for diverse uses, including antioxidant, anti-inflammatory and antimicrobial activity, which encompass virus, bacteria, fungi, and parasites (10, 11). Their composition is variable depending on the species, soil conditions, fertilizers, origin, climate, and mode of extraction, as examples, and for that reason it is difficult to assess their effects. Between 10 and 60 components are usually found in their composition, although up to 200–400 different substances are described in some of them (10, 11). However, only the major components, usually 2–4, are thought to be responsible for the attributed properties. Terpenes, especially monoterpenes and sesquiterpenes, are considered the most important components of EOs.

There is little information on the use of natural products against *T. gallinae* and few reports were found in the literature, including some EOs from the Asteraceae and Geraniaceae families (12, 13) but also from other medicinal plants such as *Cymbopogon flexuosus* (14) and *Dennetia tripetala* (15). Besides EOs, aqueous, alkaloid and ethanol and methanol extracts from different plants have been tested against *T. gallinae*, including plants from Lamiaceae and Asteraceae families, such as *Lavandula angustifolia*, *Rosmarinus officinalis* and *Artemisia annua*, and also extracts from other plants: *Allium sativum*, *Harungana madagascariensis*, *Zingiber officinale*, *Myrtus commuis*, *Zataria multiflora*, *Quercus persica*, *Lycopus europaeus*, *Pulycaria disenterica*, *Eugenia uniflora*, *Murraya koenigii*, *Peganum harmala*, *Clausena lansium* (15–24). However, while EOs displayed activity against *T. gallinae*, most of the above cited extracts were less active, and only four publications mention anti-trichomonal (AT) activity of alcoholic or alkaloid extracts comparable to that of metronidazole at a similar dose, extracts from *Clausena lansium* (18), *Peganum harmala* (19), *Eugenia uniflora* (20), *Lavandula angustifolia,* and *Zingiber officinale* (24).

The research of natural products against *Trichomonas vaginalis* (*T. vaginalis*) is a little wider, and EOs from several plant genera, such as *Lavandula*, *Nectandra* and *Nigella* were tested with satisfactory anti-trichomonal effects, and around 30 compounds from potatoes, tomatoes, and several medicinal plants have been identified having anti-protozoal activities in different bioassays [revised in Friedman et al. (25)].

EOs components from the families Lamiaceae and Asteraceae have shown antimicrobial and insect repellent properties (11), but only a scarce number of publications proved their activity against trichomonads. In this study, we have analyzed the potential use as anti-*T. gallinae* of 36 EOs obtained by two classical methods of EOs extraction: hydrodistillation (HD) and steam distillation (SD). We have also evaluated the main compounds from these EOs against the avian parasite *Trichomonas gallinae* and their cytotoxic effects on African green monkey kidney cells (Vero cells).

Materials and methods

Plants and essential oil extraction

The EOs employed in this study were obtained from 17 species from the Lamiaceae plant family and three species from the Asteraceae plant family selected for their medicinal properties, mainly antimicrobial properties. The plant species were cultivated in distinct locations of Spain. *Ditrichia graveolens* in Castilla-La Mancha, and the rest of plants in Aragon: *Santolina chamaecyparissus, Lavandula lanata, Lavandula angustifolia, Lavandula x intermedia* "Abrial", *Lavandula x intermedia* "Super", *Lavandula mallete, Origanum majorana, Rosmarinus officinalis*, *Satureja montana*, *Mentha suaveolens, Salvia officinalis, Salvia hibrida, Salvia sclarea, Thymus vulgaris*, *Thymus zygis, Origanum virens*, and *Lavandula luisieri* populations "1" and "2", this last two populations were predomesticated from two origins, west and center of the Iberian Peninsula. The seeds from the 17 species were deposited in the germplasm of CITA (Centro de Investigación y Tecnología Agroalimentaria de Aragón, Unidad de Recursos Forestales, Zaragoza, Spain).

The plant species used were identified by Dr. Daniel Gomez, IPE-CSIC (see Voucher numbers at Supplementary Table S1). The *Salvia* hybrid (*S. officinalis* L. × *S. lavandulifolia* Vahl) used in this work was obtained by J. Burillo (CITA) (Supplementary Table S1). Aerial plant parts were collected at the flowering stage during the years 2016–2019. Approximately 100 g of aerial parts, maintained at room temperature and preserved from the light at the laboratory for 7 days, were submitted to hydrodistillation. The hydrodistillation was carried out in triplicate with 100 g of dried aerial plant parts and 2 l of water for 2 h in a Clevenger-type apparatus according to the method recommended by the European Pharmacopoeia (26). The oils were dried over MgSO4, filtered and stored at 4°C until used in 2021 for activity and determination of EOs composition, as previously described. (27). Pilot plant steam distillation was carried out on the fresh biomass of the plants (60 Kg total fresh

plant biomass) harvested at the flowering stage. A stainless-steel pilot extraction plant equipped with a pressure reducing valve was used as described (28). The pressure of work was 0.5 bar. The hydrolate (aqueous phase) was decanted from the essential oil collected in the condensation section and filtered.

EOs analysis and pure compounds identification

The EOs from the studied plants were analyzed and the main compounds determined. The analysis was performed by gas chromatography-mass spectrometry (GC-MS) using a Shimadzu GC-2010 Plus coupled to a Shimadzu GCMS-QP2010-Ultra mass detector with an electron impact ionization source at 70 eV and a Single Quadrupole analyzer and employing Helium as carrier gas. Chromatography was carried out with a Teknokroma TRB-5 (95%) Dimethyl- (5%) diphenylpolysiloxane capillary column, 30 m x 0.25 mm ID and 0.25 μm phase thickness. The working conditions used were: Split mode injection using 1 μl of sample with a split ratio (20:1) employing a Shimadzu AOC-20i automatic injector, injector temperature 300°C, transfer line temperature connected to the mass spectrometer 250°C, and ionization source temperature 220°C. The initial column temperature was 70°C, heating up to 290°C at 6°C /min and leaving at 290°C for 15 min. All the samples (4g/μl) were previously dissolved in 100% dichloromethane (DCM) for injection.

The mass spectra, retention time, and retention indexes were used to identify the compounds by comparison with those found in the Wiley database (Wiley 275 Mass Spectra Database, 2001) and NIST 17 (NIST/EPA/NIH Mass Spectral Library), while the relative area percentages of all peaks obtained in the chromatograms were used for quantification. Identification of trans-α-necrodyl acetate from *L. luisieri* was preformed using a standard compound previously isolated.

Pure compounds

After analyzing the composition of the EOs by GC-MS, products that fulfill the following criteria were selected to study their antitrichomonal activity *in vitro*: three more abundant in each of the selected active EO, abundance higher than 5%, and availability. Some of the major compounds that were excluded were not identified, not commercially available or not easy to obtain or isolate. Pure compounds (monoterpenes and sesquiterpenes) were obtained from commercial sources, except camphor that was previously isolated in our laboratory (ICA, CSIC). Linalool, thymol, α-pinene, α-terpineol, β-pinene, camphene, β- caryophyllene and caryophyllene oxide were obtained from Sigma Aldrich (Madrid, Spain); linalyl acetate, γ-terpinene, and p-cymene from Acros Organics (Madrid, Spain); 4-terpineol from Merck Life Sciences (Madrid, Spain); α and β thujone from Phytolab: borneol, 1,8-cineole, carvacrol and D-fenchone from Fluka (Madrid, Spain).

Anti-trichomonal activity *in vitro*

The AT activity assay was performed using round bottom microwell plates in quadruplicate. Each well had 150 μl of *T. gallinae* trophozoites in Trypticase-Yeast Extract-Maltose medium (TYM) with 10% fetal calf serum (Sigma, Madrid, Spain) at 500.000 trophozoites/ml (29). EOs and pure compounds were solved in DMSO (Sigma, Madrid, Spain) (<1% final concentration). The EOs were tested under concentrations of 800, 400, and 200 μg/ml, and in those cases that showed moderate antitrichomonal activity (>50%) at the lowest concentration, the assay was done also at lower concentrations: 100, 50, and 25 μg/ml. Trophozoite viability was analyzed using the modified MTT colorimetric assay method as previously described in literature (29). Briefly, after incubating the plate for 24 h at 37°C with the EOs and compounds to be tested, the plates were centrifuged at 750 x *g*, the medium was eliminated and 100 μl of a solution of MTT (Sigma, Madrid, Spain) (1.25 μg/ml) and PMS (Sigma, Madrid, Spain) (0.1 μg/ml) in PBS (Sigma, Madrid, Spain) was added to each well. The plate was incubated for 45 min in dark conditions to allow the reduction of MTT to formazan salts. Prior to reading, 100 μl of DMSO was added to each well to dissolve the formazan crystals. The plate was read in a spectrophotometer using a wavelength of 570 nm.

The percentage of AT activity was calculated as growth inhibition using the following formula:

$$\%\, \boldsymbol{AT} = \boldsymbol{100} - \left[\left(\boldsymbol{Ap} - \boldsymbol{Ab}\right) \div \left(\boldsymbol{Ac} - \boldsymbol{Ab}\right)\right] \times 100$$

Where Ap is the absorbance of the tested product, Ab the absorbance of the blank and Ac the absorbance of the control wells (culture without treatment).

Pure compounds were assayed using the same method described above, although the concentrations tested were 100, 75, 50, 25, 10, and 1 μg/ml. Metronidazole (Acros Organics, Madrid Spain) was used as a reference drug for antitrichomonal activity.

Cytotoxicity of active pure compounds

African green monkey kidney cells (Vero cells) were grown in Dulbecco's modified Eagle's minimal essential medium (DMEM, Avantor, Llinars del Vallès, Barcelona) supplemented with 10% fetal calf serum (Sigma, Madrid, Spain) and 1% penicillin/streptomycin (Fisher Scientific, Madrid, Spain) at 37°C under a humidified atmosphere of 5% CO_2/95% air.

Cells seeded in 96-well flat-bottom microplates with 100 μL medium per well (initial densities 10^4 cells per well) were exposed for 48 h to serial dilutions of the test compounds in DMSO (<1% final concentration). Cell viability was analyzed by the MTT colorimetric assay method, and the purple-colored formazan precipitate was dissolved with 100 μL of DMSO (30). The cell viability was tested with each compound in a dose-response experiment to calculate their relative potency (CC_{50}) value, the effective dose to give 50% cell viability, employing the concentrations of 100, 75, 50, 25, 10, and 1 μg/ml.

IC_{50} (μg/ml) reflects the dose needed to produce 50% mortality of *T. gallinae* trophozoites. Selectivity index was calculated for the AT active products that showed cytotoxicity, using the formula SI = CC_{50}/IC_{50}. Compounds with SI higher than 1 were considered as potential antitrichomonal compounds since they are more toxic for trichomonads than for mammalian cells.

Statistical analysis

The data was analyzed using STATGRAPHICS Centurion XIX (https://www.statgraphics.com).

IC_{50} anti-trichomonal activity and CC_{50} cytotoxic activity were determined from the dose-response experiment, employing a linear regression analysis (% cell viability on log dose).

Parametric bivariate correlation analysis was performed between the main components of the EOs and the AT activity. The chemical composition of the 36 EOs studied was analyzed and those components in proportion higher than 5% were correlated with the IC_{50} of the EOs.

Results

Anti-trichomonal activity of EOs from Lamiaceae and Asteraceae plants

The activity against *T. gallinae* trophozoites of a total of 36 EOs belonging to 17 different plant species was evaluated in this study, including species of the Lamiaceae genera *Lavandula*, *Origanum*, *Salvia*, *Satureja, Mentha*, and *Thymus*, and the Asteraceae genera *Ditrichia* and *Santolina* (Table 1). From the tested EOs, 17 were extracted by steam distillation (SD), while the remaining 19 were obtained by hydrodistillation (HD).

In general, all the tested EOs, except two (EOs from *L. lanata* and *L. angustifolia*), displayed good anti-trichomonal activity (higher than 80%), especially at the highest concentration (800 μg/ml), although the results vary depending on the plant and the extraction method used in each case (Figure 1; Supplementary Figure 1).

A total of 13 EOs from five species of *Lavandula* were analyzed (Figure 1; Supplementary Figure 1), of which seven EOs from three species showed high activity (80–100%) at the highest concentration. These belong to the species *L. luisieri*, *L. x intermedia* "Abrial" and "Super" and *L. mallete*. It is remarkable that *L. luisieri* was the only one that showed high activity in all the tested EOs coming from two populations and two extraction methods, although in both populations the best results were reported by the EOs extracted by SD. EOs from *L. luisieri* presented moderate activity (above 50%) even at lower concentrations, 200 μg/ml in the case of population 1, and 100 μg/ml in population 2, being the EOs with the highest activity among the *Lavandula* species.

All the tested EOs from *Salvia* species showed activity above 90% at the highest dose (800 μg/ml) except the EO from *S. sclarea* obtained by SD, which displayed 54.5% AT activity (Figure 1). By contrast, the EO obtained by HD from the same species, *S. sclarea*, maintained a high activity, close to 100%, even at lower concentration (200 μg/ml). On the contrary, the EOs of *S. officinalis* and *S. hibrida* obtained by SD displayed better AT activity than EOs obtained by HD, keeping moderate activity even at 200 μg/ml.

All the EOs from *Thymus* spp. and *Origanum* spp. (Figure 1) presented AT activity over 80% at the highest concentration (800 μg/ml). The activity was maintained at intermediate concentrations (400 μg/ml) with EOs from *T. vulgaris* and *T. zygis* obtained by HD, as well as for EOs from *O. majorana* obtained by both methods. It is noteworthy that the EO from this last species obtained by HD kept AT activity over 70% at 200 μg/ml.

In the same manner, the EOs from the other Lamiaceae tested, *R. officinalis*, *S. montana* and *M. suaveolens*, (Figure 1; Supplementary Figure S1) showed high activity (80–100%) at the highest concentration employed (800 μg/ml), except for *M. suaveolnes* obtained by SD, whose AT activity was close to 70%. The best result was obtained with EO from *S. montana* extracted by SD, which maintained an activity close to 70% at 200 μg/ml.

Finally, all the EOs from Asteraceae tested in this study (Supplementary Figure S1) showed AT activity over 90% at the highest concentration tested (800 μg/ml). This activity downed close to 60% at 400 μg/ml in both samples of *D. graveolens* and declined drastically in the EO from *S. chamaecyparissus*.

The IC_{50} from the tested EOs was calculated (Table 1), and those having a IC_{50} lower than 200 μg/ml were selected for further analysis ($n = 13$), together with the EOs obtained from the alternative extraction method to compare their composition. Among all the plants, those with EOs showing the highest AT activity were *L. luisieri* (2 populations), *S. officinalis*, *S. hibrida*, *S. sclarea*, *T. vulgaris*, *T. zygis*, *O. majorana*, and *S. montana*.

From the 13 EOs, eight were obtained by SD while five were obtained from HD. Among the selected species, most of them rendered better results with EOs obtained by SD than EOs obtained from HD (*L. luisieri* 1 and 2, *O. majorana*, *O. virens*, *S.*

10.3389/fvets.2022.981763

TABLE 1 Effects of the tested essential oils on *Trichomonas gallinae* (IC_{50})[a].

Family	Genus	Species	Extraction method	IC_{50} (μg/ml)
Asteraceae	*Santolina*	*Santolina chamaecyparissus*	HD	394.3 (316.8–490.7)
	Ditrichia	*Ditrichia graveolens*	SD	261.0 (203.7–334.5)
		Ditrichia graveolens	HD	259.7 (233.9–288.2)
Lamiaceae	*Lavandula*	*Lavandula lanata*	HD	731.7 (546.1–980.2)
		Lavandula luisieri 1	SD	189.8 (170.0–212.0)
		Lavandula luisieri 1	HD	331.4 (278.8–394.0)
		Lavandula luisieri 2	SD	103.4 (77.7–137.7)
		Lavandula luisieri 2	HD	455.2 (434.5–476.8)
		Lavandula angustifolia	SD	600.4 (480.6–749.9)
		Lavandula angustifolia	HD	823.4 (612.1–1.107.8)
		Lavandula x intermedia "Abrial"	SD	406.8 (286.3–578.0)
		Lavandula x intermedia "Abrial"	HD	452.7 (370.9–552.6)
		Lavandula x intermedia "Super"	SD	583.7 (445.8–764.2)
		Lavandula x intermedia "Super"	HD	321.2 (263.4–391.6)
		Lavandula mallete	SD	702.1 (558.3–883.0)
		Lavandula mallete	HD	373.9 (318.4–439.1)
	Origanum	*Origanum virens*	SD	175.4 (123.4–249.3)
		Origanum virens	HD	197.9 (106.2–368.8)
		Origanum majorana	SD	139.7 (109.1–178.9)
		Origanum majorana	HD	158.8 (129.9–194.0)
	Rosmarinus	*Rosmarinus officinalis*	SD	328.1 (292.8–367.8)
		Rosmarinus officinalis	HD	256.6 (227.6–289.4)
	Satureja	*Satureja montana*	SD	141.4 (128.9–155.0)
		Satureja montana	HD	321.3 (244.4–422.6)
	Mentha	*Mentha suaveolens*	SD	419.1 (355.5–494.0)
		Mentha suaveolnes	HD	303.0 (262.8–349.3)
	Salvia	*Salvia officinalis*	SD	139.6 (119.1–163.6)
		Salvia officinalis	HD	420.4 (396.4–445.9)
		Salvia hibrida	SD	134.6 (118.1–153.4)
		Salvia hibrida	HD	239.9 (196.9–292.3)
		Salvia sclarea	SD	712.3 (606.1–837.1)
		Salvia sclarea	HD	117.4 (99.4–138.6)
	Thymus	*Thymus vulgaris*	SD	193.3 (161.9–230.9)
		Thymus vulgaris	HD	166.0 (151.1–182.4)
		Thymus zygis	SD	274.5 (237.2–317.6)
		Thymus zygis	HD	133.1 (117.5–150.7)

[a]IC50 (μg/ml) = concentration needed to produce 50% trophozoite mortality. SD, steam distillation; HD, hydrodistillation.

hibrida, *S. officinalis*, and *S. montana*), and only three of them display better results with EOs obtained by HD (*S. sclarea*, *T. vulgaris* and *T. zygis*), although in some cases differences in the IC_{50} were scarce.

Composition of essential oils

The composition of the EOs with the highest AT activity was determined by GC-MS (Table 2) and compared with the composition of the EO extracted by the alternative method (SD or HD). In some of the active EOs, more than fifty compounds were identified, but only the major components (with a proportion higher than 5%) were considered.

Camphor, trans-α-necrodyl acetate and D-fenchone were the main compounds of *L. luisieri* EOs (both populations), with concentrations over 15% in any of the populations tested (Table 2). The extraction method influenced the composition of the oils, with D-fenchone being the major

10.3389/fvets.2022.981763

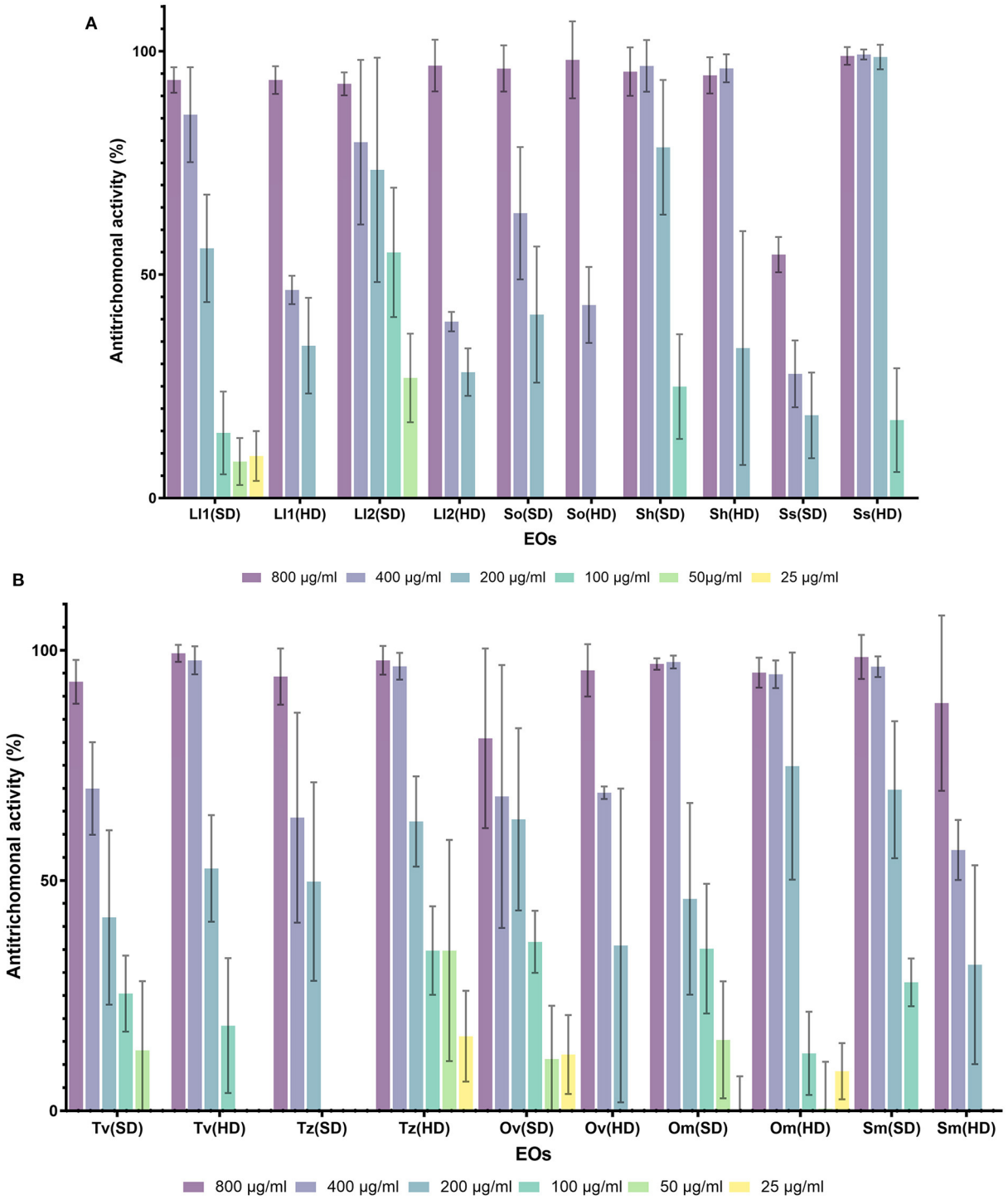

FIGURE 1
Percentage of antitrichomonal activity of EOs obtained by hydrodistillation (HD) and steam distillation (SD). **(A)** EOs from *L. luisieri* 1 and 2 (Ll1 and Ll2), *S. officinalis* (So), *S. hibrida* (Sh) and *S. sclarea* (Ss). **(B)** EOs from *T. zygis* (Tz), *T. vulgaris* (Tv), *O. virens* (Ov), *O. majorana* (Om) and *S. montana* (Sm).

component in the EO of population "2" obtained by HD and trans-α-necrodyl acetate in both EOs obtained by SD. Camphor was more variable with the extraction method, and appear at higher concentration in the EO from *L. luisieri* "1" obtained by SD and *L. luisieri* "2" obtained by HD.

TABLE 2 Chemical composition of the EOs from the most active species: *L. luisieri* (1 and 2) (Ll1 and Ll2), *S. montana* (Sjm); *S. officinalis* (So), *S. hibrida* (Sh), *S. sclarea* (Ss), *T. vulgaris* (Tv), *T. zygis* (Tz), *O. majorana* (Om) and *O. virens* (Ov). RI, Retention index; RT, Retention time; HD, EOs obtained by hydrodistillation; SD, EOs obtained by steam distillation.

Compounds	RI	RT	Ll 1		Ll 2		Sjm		Sh		So		Ss		Tv		Tz		Om		Ov	
			HD	SD	HD	SD	HD	SD	HD	SD	HD	SD	HD	SD	HD	SD	HD	SD	HD	SD	HD	SD
α-pinene	937	3.81	5.7	4.9	2.8	2.6	0.9	0.4	4.3	6.3	3.4	4.4	0.1	0.3	1.1	1.4	1.7	0.4	0.8	0.5	0.7	0.4
Camphene	950	4.02	0.6	1.1			0.5	0.2	6.6	7.6	2.8	3.5	0.6	0.4	0.5	1.1	2.1	0.5	0.1	0.4	0.3	0.2
Sabinene	974	4.34							0.7	1.4	0.2	0.5							5.8		2.7	1.1
β-pinene	982	4.40	0.2				0.4	0.2	10.9	18.4	7.5	12.0	0.1	1.5	0.5	0.5	0.4	0.2	0.6	0.3	0.5	0.3
β-myrcene	988	4.53					1.4	1.1	4.1	4.2	0.6	1.9	2.0	0.3	1.6	0.7	1.5	0.8	1.3	0.8	6.0	2.1
α-terpinene	1,020	5.00					2.6	1.9	0.1	0.3	0.1	0.3			1.4	1.0	1.6	0.5	5.9	1.0	3.1	2.3
p-cymene	1,026	5.15	0.7	0.6			18.5	11.8	2.4	1.6	0.7	0.9		0.7	22.3	31.7	18.3	8.0	5.5	21.0	12.2	3.3
1.8-cineole	1,034	5.24	4.5	1.1	0.9	2.0	0.9	0.9	20.6	13.4	18.0	12.8		0.7	2.3	2.3		1.5	3.4	2.1		1.2
Ocimene	1,043	5.48		0.5					0.1	0.2		0.1	0.4					0.4	5.4		2.7	1.9
γ-terpinene	1,060	5.72					11.7	12.4	0.4	2.3	0.2	1.3			5.7	2.8	9.0	1.9	10.7	1.2	22.4	15.4
D-fenchone	1,089	6.31	20.0	1.3	2.5	1.3																
Linalool	1,102	6.45	4.2	0.3	1.1	2.2	1.3	1.1	0.4	0.1	0.5	0.2	22.7	2.0	3.8	3.5	5.4	11.6	3.0	3.5	13.9	15.3
β-thujone	1,109	6.64							3.2	2.0	22.9	13.9		0.3								
α-thujone	1,143	6.86							0.6	0.4	6.0	4.2										
Camphor	1,148	7.44	13.4	35.0	49.2	4.6	0.1	0.1	14.2	6.4	5.0	4.7	0.2	1.2	0.5	0.9	1.0	2.7		1.0	0.1	2.4
Borneol	1,160	7.80			1.3	1.6	2.0	1.3						2.4	1.0	2.0	6.3	2.5		0.9	0.7	1.6
Trans-bornyl acetate	1,165	7.88							12.9	6.9	7.0	3.9		1.1					0.1			
4-terpinenol	1,181	8.19	0.7				1.5	0.9	0.7	0.2	0.5	0.2			1.5	0.8	0.8	1.4	29.7	0.9	2.6	1.5
α-terpineol	1,196	8.40					0.2	0.2			0.2		11.3	0.4	0.3	0.2	0.1	0.6	3.6	0.2	0.3	0.7
Carvacryl methyl ether	1,240	9.54																		3.5	5.7	2.3
Linalyl acetate	1,257	9.70											31.2	14.5		0.1		17.9			0.2	15.1
123/139/81/121/79/91/57/105/43/124*	1,282	10.47				5.6																
Trans-α-necrodyl acetate	1,283	10.47	12.4	18.8	13.2	18.1																
Lavandulyl acetate	1,285	10.53	5.6	6.2																		2.6
Lavandulol	1,286	10.54			5.9	7.9																
Thymol	1,287	10.58					17.3	7.1							43.8	28.2	39.5	21.2		32.7	6.6	4.6
Carvacrol	1,299	10.84					32.6	41.3							2.4	2.3	5.0	1.4		2.2	4.7	2.9
Neryl acetate	1,360	12.21											7.5	0.4			0.7					0.6
β-caryophyllene	1,421	13.55	0.4	0.6	0.1	3.7	2.1	6.1	3.9	8.0	6.4	10.3	3.0	12.2	2.4	5.8	1.4	4.0	5.2	7.3	2.1	4.3
α-humulene	1,458	14.29		0.5			0.1	0.3	1.0	1.7	4.3	5.6	0.2	2.9	0.1	0.3			0.6	0.8	0.2	
Germacrene D	1,484	14.87	0.4	0.6		7.5		0.3		0.1	0.1	0.1	6.0	3.5	0.1	0.1		1.3	2.5	0.3	0.4	2.4
Spatulenol	1,580	16.90				1.5		0.2	1.7	1.3		0.8	0.2	5.4			0.2		0.6	0.2	1.7	0.2
Caryophyllene oxide	1,587	17.02	0.4		0.1	1.2	1.0	1.4	1.1	1.0	0.9	0.7	0.6	6.5	1.1	1.7	0.9	0.8	1.5	3.7	1.1	0.3
Viridiflorol	1,594	17.20	1.7	1.4		2.1			3.8	4.9	7.4	7.8		15.0						0.5		
α -bisabolol	1,684	18.94																5.5				2.2
Epimanool	2,059	25.63		0.8					0.3	0.7	1.4	1.8	0.3	7.4						1.1		

*Mass spectra of a nonidentified compound.
% Area: 5–10% 10–15% >15%.

The main composition of the EOs of the three species of *Salvia* analyzed shows a large list of compounds (Table 2). Differences were observed between the species, as well as considering the extraction methods to obtain the EOs. The EOs of *S. officinalis* present β-pinene, 1,8-cineole, β-thujone and β-caryophyllene as the major components, representing over 10% in the composition depending on the extraction method. β-caryophyllene and β-pinene were the major components in the

SD extract, while β-pinene and 1,8-cineole were more abundant in the EO obtained by HD. Among the major compounds of the EOs from *S. hibrida*, 1,8-cineole, camphor, and borneol were present over 10%, mainly in the HD extract, while β-pinene camphene and β-caryophyllene were more abundant in the EOs extracted by SD. The EO from *S. sclarea* was the most different in composition compared to the other two species. Linalyl acetate stands out in the composition of both extracts, although they differ in the proportion, being more than double in the HD one. Linalool and α-terpineol were only majority in the HD extract and β-caryophyllene and viridiflorol in the SD oil.

Among the major components in the extracts of the genus *Thymus* (Table 2), p-cymene and thymol appeared in high proportions in the EOs of *T. vulgaris* and *T. zygis*, while linalool and linalyl acetate appeared in high proportions (over 10%) in the EO from *T. zygis* obtained by SD. The concentration of p-cymene varies among the extracts, among the species and among the extraction method, being higher in the EO of *T. vulgaris* obtained by SD and in the EO from *T. zygis* by HD. The concentration of thymol was over 20% in all the EOs, but the percentage varies according to the extraction method, appearing in higher concentration in the EO obtained by HD.

The composition of *Origanum* EOs (Table 2) varied depending on the species (*O. virens* and *O. majorana*) and the extraction technique used. In the EO obtained by SD, the major components were p-cymene and thymol, with concentrations over 20%. Thymol was the major component of the EO obtained by SD, with an abundance of 32.73%, while in the HD extract it did not even appear. On the other hand, γ-terpinene and 4-terpineol displayed an abundance over 10% in the EO from *O. majorana* obtained by HD. In the EO from *O. virens* obtained by SD, only linalyl acetate appeared at a concentration higher than 15%, while p-cymene, γ-terpinene, and linalool appeared at concentrations higher than 10% in the EO obtained by HD.

The main compound of *S. montana* EOs was carvacrol, representing over 30% in the EOs obtained from the two extraction methods. Other compounds with concentrations higher than 10% in any of the EOs were γ-terpinene, p-cymene and thymol (Table 2).

According to the extraction method and comparing the composition of the EOs obtained in the distinct species analyzed, EOs obtained by SD in comparison with EOs obtained by HD, showed systematically higher proportion of the following compounds: β-pinene, β-caryophyllene, viridiflorol, and trans-α-necrodyl acetate. The opposite was observed with the compounds D-fenchone, camphene, α-terpineol, α-terpinene, 4-terpineol, that were extracted in higher proportion with the HD method compared to the SD method. The rest of the compounds appeared with higher enrichment in one or another of the extraction methods used, but not systematically (i.e., thymol, p-cymene, camphor, linalool, linalyl acetate, γ-terpinene, α-pinene).

TABLE 3 Pearson correlation coefficients between main components of EOs and AT activity.

Compound	Pearson correlation coefficient	p
α-terpinene	−0.374	0.025
p-cymene	−0.385	0.020
1,8-cineole	0.413	0.012
γ-terpinene	−0.373	0.025
Linalool	0.334	0.047
Lavandulol	0.335	0.046
Thymol	−0.355	0.033

Parametric bivariate correlation analysis between the main components of the EOs and the AT activity showed seven significant correlations with AT ($p < 0.05$) (Table 3). Among the compounds included in the analysis, p-cymene, thymol, γ-terpinene, and α-terpinene were significantly associated with the AT activity of the EOs (negative correlation between compound abundance and IC_{50} of the EO). On the contrary, 1,8-cineole, linalool and lavandulol were significantly associated ($p < 0.05$) with lower AT activity (positive correlation between compound abundance and IC_{50} of the EO).

Antitrichomonal activity and cytotoxic activity of pure compounds

A total of 19 pure compounds, 17 monoterpenes and two sesquiterpenes, were tested against *T. gallinae* (Supplementary Figure S2). All of them were major components of the active EOs and fulfill the criteria previously described.

Among the tested products, seven did not showed AT activity at 100 μg/ml, including borneol, camphor, carvacrol, 1,8-cineole, caryophyllene oxide, linalool and α-terpineol. The rest of the tested compounds showed AT activity, and the IC_{50} was calculated. From higher to lower AT activity, these compounds were: α and β thujones, camphene, β-pinene, linalyl acetate, thymol, 4-terpinenol, γ-terpinene, α-pinene, p-cymene, D-fenchone, and β-caryophyllene (Table 4).

The cytotoxic activity of the 19 pure compounds was also evaluated. None of the products without AT activity displayed cytotoxic activity. From the AT active compounds, only four of them were slightly toxic for Vero cells: α-pinene, β-pinene, camphene and β-caryophyllene (Table 4).

Taking these results into account, an adjustment of the effective dose was calculated to equilibrate AT activity and cytotoxic effect. For that purpose, the selectivity index (SI) was applied (Table 4). The best results were obtained by camphene (SI = 3.12), linalyl acetate (SI = 3.11), thymol (SI = 2.6), 4-terpinenol (SI = 2.41), γ-terpinene (SI = 2.28), p-cymene

TABLE 4 Effects of the tested compounds on *Trichomonas gallinae* and Vero cells (IC_{50} and CC_{50} respectively).

Compound	Vero cells (CC_{50}[a])	*T. gallinae* (IC_{50}[b])	SI[c]
1,8 cineole	>100	>100	1.0
Linalool	>100	>100	1.0
Thymol	>100	38.4 (31.5–46.9)	2.6
Carvacrol	>100	>100	1.0
Linalyl acetate	>100	32.2 (27.2–38.2)	3.1
γ-terpinene	>100	43.8 (37.0–52.0)	2.3
p-cymene	>100	59.7 (49.3–72.4)	1.7
α-terpineol	>100	>100	1.0
Caryophyllene oxide	>100	≈100	1.0
α-pinene	88.9 (88.0–89.7)	44.2 (42.3–46.1)	2.0
β-pinene	88.2 (87.2–89.2)	29.6 (26.2–33.4)	3.0
Camphor	>100	>100	1.0
Borneol	>100	>100	1.0
D-fenchone	>100	61.9 (54.3–70.6)	1.6
β-caryophyllene	60.8 (56.9–65.0)	86.1 (78.3–94.7)	0.7
α and β thujone	>100	17.3 (11.3–26.3)	5.8
4-terpinenol	>100	41.5 (33.9–50.7)	2.4
Camphene	74.8 (66.3–84.2)	24.0 (21.9–26.2)	3.1
Metronidazole	>100	1.0 (0.8–1.1)	100.0

[a]CC50 (μg/ml), concentration needed to produce 50% Vero cell mortality; [b]IC50 (μg/ml), concentration needed to produce 50% trophozoite mortality [c]SI, Selectivity index.

(SI = 1.68), and D-fenchone (SI = 1.62). β-caryophyllene was more toxic for Vero cells than for *T. gallinae* trophozoites and consequently the SI was lower than 1, excluding it for AT purposes. Besides, α and β-thujones were also excluded because they are potent neurotoxic substances (31), although they did not show cytotoxic effect on Vero cells.

Discussion

Several anti-trichomonas EOs, extracts and compounds from plants have been tested against trichomonads, mainly against the human pathogen *T. vaginalis*. Among them, the Lamiaceae family with more than 230 genera, usually aromatic, and the Asteraceae family, with worldwide distribution and more than 1,600 genera, stand out (32). Species from *Lavandula* and *Salvia* (24, 33), *Artemisia* (12), and *Thymus* (34) have been more extensively explored with these parasites. In our study, the best results were obtained from *L. luisieri* (both populations) while lower activity was observed with other *Lavandula* species or varieties, such as *L. angustifolia* or *L. x intermedia*, which displayed activity against *Giardia*, *Hexamita* or *T. vaginalis* in other studies (33). These slight disagreement between the studies could be due to differences in the composition, since it may vary with the diverse conditions of growing, climate or part of the plant collected, but also to the selected methodology employed in the present study.

Also, a remarkable activity was observed with EOs from *Salvia* (*S. sclarea*, *S. hibrida* and *S. officinalis*) and *Thymus* (*T. vulgaris* and *T. zygis*) species, which agrees with the results obtained from other authors testing AT activity (32, 35). Within the list of our best AT active EOs, *Origanum* and *Satureja* species (*O. vulgare* and *O. majorana* and *S. montana*) are included. There are no other anti-trichomonads assays with these two genera, but some authors demonstrated their activity against other protozoa such as *Leishmania* and *Giardia* (35, 36), as well as with some fungi and bacteria (37, 38).

Satisfactory results were also obtained in our study from *R. officinalis* and *M. suaveolens*, the former plant being mentioned in one study with moderate activity against *T. gallinae* (22) and presenting activity against *Plasmodium falciparum* in another study (35). Although the AT activity was good, they were over the cutoff point value in our study (IC_{50} < 200 μg/ml), and for that reason they were not included in later experiments.

Other Asteraceae from the genus *Tanacetum* showed anti-trichomonal effect in previous studies (32), but in our case, only *D. graveolens* displayed moderate results at intermediate doses. Due to the lower AT activity, we did not include any of the Asteraceae EOs in further analysis.

Many natural products assayed against trichomonads from the Lamiaceae are EOs, while compounds from other plants were extracted employing other methods, such as ethanolic, methanolic or alkaloid extraction, as examples. Among the extracts tested against *T. gallinae* trophozoites, many needed high amounts of extract to obtain a good AT activity, such as the aqueous garlic (*Allium sativum*) extract (16), and alcoholic extracts of *Lycopus europaeus* and *Pulicaris dysenterica* (21), *Quercus persica*, *Artemisia annua*, *Myrtus commuis*, *Zataria multiflora*, *R. officinalis*, *Allium sativum* (22) and *Harungana madagascariensis* (23). Others showed some kind of toxicity, such as the alkaloid extract of *Murraya koenigii* (17). Finally, some of the previously cited assayed extracts were not fully characterized, the major components were not described, or the potential toxic effects were not tested (22), and for these reasons and the differences in composition, we could not include them in the comparison with the result of the present study.

Regarding AT active EOs, four plants have been tested against *T. gallinae* so far, *Dinettia tripetala* (Annonaceae), *Artemisia sieberi* (Asteraceae), *Pelargonium roseum* (Geraniaceae) and *Cymbopogon flexuosus* (Poaceae) (12–15). Except *C. flexuosus* (14), that did not share components with the Lamiaceae tested, the other plants EOs shared components with the ones evaluated by us and will be discussed further.

Some of the common compounds were not highly active against trichomonads when tested alone in the experiments conducted in the present study. For example, linalool was

present in the EO composition of *P. roseum* and *D. tripetala*, two plants with AT activity *in vitro* and *in vivo* (13, 15). Although linalool has been suggested as having activity against *Trichomonas*, under our conditions, linalool was not an active AT compound, and the activity of those EOs could be due to other main components, beta-citronellol, geraniol in *P. roseum* EO (13), 2-phenylnitroethane in *D. tripetala* EO (15), ocimene, camphor, linalyl acetate, borneol, 1-8-cineol, and α-pinene in the ethanolic extracts of *L. angustifolia* (24), or even to synergistic effect between them. Besides, linalool showed a positive correlation with the IC_{50} in our study, indicating that those EOs with higher amounts of linalool had lower AT activity. Besides linalool, other compounds with scarce AT activity in our study, but present in the composition of active AT EOs or extract, are camphor and 1,8-cineol in *A. sieberi* EO (12) or the ethanolic extract of *L. angustifolia* (24). In the same way that linalool, 1,8 cineole had an inverse correlation with AT activity.

Thujones, mainly α and β thujones, are the most active anti-*Trichomonas* compounds in our study. These compounds are present also in the composition of *A. sieberi* EOs (12), which was a suitable candidate to treat *T. gallinae*, according to *in vitro* and *in vivo* studies. Although the authors did not report toxicity in the *in vivo* experiment, caution should be taken with these compounds since they are recognized as neurotoxic (31).

Camphene was one of the most active against *T. gallinae* when tested under our conditions. This compound was present in high amounts (higher than 5%) in the EO from *Salvia hibrida*, one of the most active EO tested in the present study, and the abundance of this compound was higher in the EO extracted by SD (7.6%, the most active of both EOs) than the EO extracted by HD (2.8%, the least active of both EOs). Camphene was also present as a major component of *A. sieberi* EO, which was highly active against *T. gallinae* both, *in vivo* and *in vitro* (12). Camphene was slightly cytotoxic for Vero cells, but it might be useful if adjusting the dose according to the SI, since it was the highest one, excepting the potential toxic thujones.

Two compounds are included in the composition of highly active extracts against trichomonads assayed by other authors and the present study: linalyl acetate and α-pinene. They were between the main components of the AT active ethanolic extract of *L. angustifolia* (24) and EOs from *S. sclarea*, *O. virens*, and *T. zygis*. Linalyl acetate is a suitable candidate as anti-trichomonal, since the IC_{50} for *T. gallinae* trophozoites was low (32.2), and the SI high (3.1), and no toxicity was found in Vero cells. Besides, in the *S. sclarea* EOs, linalyl acetate appears with a concentration of more than double in the HD extract (31.20% in HD vs. 14.48% in SD), which could explain the higher activity of the EO extracted by HD *vs*. the EO extracted by SD. On the other hand, α-pinene was present in considerable amounts in *S. hibrida* EO extracted by SD (6.3%), which was more active than the *S. hibrida* EO extracted by HD (4.3%). The anti-trypanosomatid capacity of some EOs, including *Leishmania major* and *Trypanosoma brucei*, was also attributed to α-pinene (35, 39).

Regarding β-pinene, it has been proven as an active anti-*T. vaginalis* compound in another study (32). Within the major compounds of the *Salvia* species evaluated, β-pinene were found in higher concentration in the extracts of *S. officinalis* and *S. hibrida* obtained by SD, which may explain the higher activity, compared to HD extracts. We must keep in mind the slight toxicity of the compound, but β-pinene is the third compound with better AT activity, and for that reason we still consider that both, α and β-pinenes, are good candidates as anti-trichomonads pure compounds.

There are three compounds that appeared with high abundance in several of the most active EOs evaluated in our study: p-cymene, γ-terpinene, and thymol, which were positively correlated with the AT activity. These three compounds are more abundant in EOs from *T. vulgaris* and *T. zygis* extracted by HD, which displayed higher activity when compared with the EOs extracted by SD. These compounds are also included among the major components of both species of *Origanum*, *O. majorana* and *O. vulgaris*. The EO of *O. majorana* extracted by SD, which displayed higher AT activity, had higher abundance of thymol and p-cymene, but lower amount of γ-terpinene. We found a similar situation with EOs from *O. vulgare*, but, in any case, IC_{50} from all these EOs were similar, both, for *O majorana* (IC_{50} = 139.7 for EO by SD *vs*. IC_{50} = 158.8 for EO by HD) and for *O. virens* (IC_{50} = 175.4 for EO by SD *vs*. IC_{50} = 197.9 for EO by HD). The compounds were also present at high concentration in the EOs from S. *montana*, although the proportions were higher in the less active EO (extracted by HD). Maybe the higher concentration of carvacrol and β-caryophyllene in the EO from *S. montana* extracted by SD may act synergistically with the other three compounds, as it has been observed in previous studies (40). Two of these compounds, p-cymene and γ-terpinene have also shown activity against *T. vaginalis* (38, 41), and their combination together with thymol in the most active EOs is frequent, possibly acting in a synergistically manner, at it has been previously proven with other protozoa (40). The activity of these compounds have been demonstrated against other protozoa as well, such as p-cymene against *Plasmodium falciparum* (40) and thymol against *T. brucei* and *T. cruzi* (35). There is a high agreement that these three compounds are good AT compounds considering different studies and authors.

In other studies, caryophyllene oxide and β-caryophyllene were found active against *T. vaginalis* (32). However, under our conditions, they displayed a slight activity against *T. gallinae*, and for that reason they are not included within the list of better anti-*T. gallinae* compounds in the present study. The EO from *S. officinalis* extracted SD showed better AT activity, and higher abundance of β-caryophyllene. Also, the EO from *S. officinalis* extracted by HD had higher abundance of 1,8-cineole, a compound that is inversely correlated with the anti-*T. gallinae*

activity in our conditions. Maybe antagonistic interactions could be acting between β-caryophyllene and 1,8-cineole.

According to our correlation analyses, assays employing α-terpinene could also be of interest and should be further studied in future assays. Also, Germacrene D, lavandulol, trans-α-necrodyl acetate, and an unidentified compound were present at percentages higher than 5% in the most active EOs tested in the present study, *L. luisieri* "2" extracted by SD. Lavandulol showed a negative correlation with AT activity and therefore discarded for future studies. Trans-α-necrodyl acetate is another interesting compound to evaluate due to its highly abundance (18%) in the most active EO (*L. luisieri* "2" by SD). However, it was not significatively correlated with the IC_{50} of the EOs, which could be due to absence of this compound in other plants EOs.

Comparing the chemical structures of the tested terpenes it is evident that oxidation of the double bound $\Delta^{4,5}$ of β-caryophyllene to produce caryophyllene oxide reduced both cytotoxic and AT effects. For monoterpenes, the double methylation of C7 in compounds with a bicycle-heptane structure decreases the AT activity, whereas the acetylation of the hydroxyl group in C3 for linalool increases the AT effects. Also, the position of the hydroxyl groups in the monoterpene structure affects the AT activity as can be seen by the variations between the activity of 4-terpineol and α- terpineol or between carvacrol and thymol.

Although there were a larger number of highly active EOs extracted by SD (n = 9/13) than by HD, it is difficult to recommend one or another method of extraction, since some of the better AT compounds were enriched by SD or HD in a non-consistent manner (p-cymene, linalyl acetate and γ-terpinene), while trans-α-necrodyl acetate, and β pinene were always extracted in higher proportions in EOs obtained by SD and camphene in EOs obtained by HD. Thymol was extracted in higher amounts in EOs extracted by HD with one exception, the EO from *O. majorana*, which surprisingly displayed 32% in the EO extracted by SD and was absent In the EO extracted by HD. However, interaction between the richness of the compounds can occur during the extraction process, making difficult the decision of which method employ.

Conclusions

All the tested EOs from Lamiaceae and Asteraceae, except two, displayed good anti-trichomonal activity, showing the highest activity EOs from *L. luisieri*, *S. officinalis*, *S. hibrida*, *S. sclarea*, *T. vulgaris*, *T. zygis*, *O. majorana*, and *S. montana*.

Among the tested compounds in this study, six were selected as good candidates as AT drugs based on the absence of toxicity in cell cultures and the anti-trichomonad activity *in vitro*: linalyl acetate, thymol, 4-terpinenol, γ-terpinene, p-cymene, and D-fenchone. Three of them also showed a good correlation between the activity of the EOs and their abundance in the EO's composition: thymol, γ-terpinene, and p-cymene. Considering all the analysis conducted, their abundance in the selected plants EOs, the cytotoxic analysis and the AT activity, we propose these compounds as good anti-trichomonads candidates. Their activity could be increased with chemical modifications. Other compounds with high AT activity were α and β-pinenes, but their toxicity should be further studied.

However, although in most cases, the majority compounds of the EOs account for their activity, in some cases the antitrichomonal activity of the compounds is lower than that of the EOs, which could be due to their complex composition, where synergistic or antagonistic relationships occur between the components. The combination of various products could be of interest.

Data availability statement

The original contributions presented in the study are included in the article/Supplementary material, further inquiries can be directed to the corresponding author/s.

Author contributions

Conceptualization: AG-C, RM-D, MB, and MG-M. Data curation, supervision, writing, reviewing, and editing: AG-C, MB, and MG-M. Formal analysis: ID-C, MB, AG-C, and MG-M. Funding acquisition: AG-C, RM-D, and MG-M. Investigation: ID-C, IA-C, SA, and JN-R. Methodology: ID-C, IA-C, SA, JN-R, AG-C, MB, and MG-M. Resources: AG-C, JN-R, RM-D, MB, and MG-M. MG-M. Writing—original draft: ID-C and MG-M. All authors contributed to the article and approved the submitted version.

Funding

This work has been partially financed by Grants PR108/20-08 (Santander-UCM), PID2020-114207RB-I00 (Spanish Ministry of Science and innovation), ERASMUS+ European Hub on New Challenges in the Field of Essential Oils (EOHUB) and PID2019-106222RB-C31/SRA (State Research Agency, 10.13039/501100011033).

Acknowledgments

This article is dedicated to RM-D who sadly passed away in 2021. We want to thank Rubén Muñoz for his kind assistance in conducting identification of chemical components of essential oils.

Conflict of interest

The authors declare that the research was conducted in the absence of any commercial or financial relationships that could be construed as a potential conflict of interest.

Publisher's note

All claims expressed in this article are solely those of the authors and do not necessarily represent those of their affiliated organizations, or those of the publisher, the editors and the reviewers. Any product that may be evaluated in this article, or claim that may be made by its manufacturer, is not guaranteed or endorsed by the publisher.

Supplementary material

The Supplementary Material for this article can be found online at: https://www.frontiersin.org/articles/10.3389/fvets.2022.981763/full#supplementary-material

References

1. Amin A, Bilic I. Liebhart Dieter, Hess M. Trichomonads in birds—a review. *Parasitol.* (2014) 141:733–47. doi: 10.1017/S0031182013002096

2. Lumeij JT, Zwijnenberg RJG. Failure of nitro-imidazole drugs to control trichomoniasis in the racing pigeon (*Columba livia domestica*). *Avian Pathol.* (1990) 19:165–6. doi: 10.1080/03079459008418665

3. Franssen FFJ, Lumeij JT. In vitro nitroimidazole resistance of *Trichomonas gallinae* and successful therapy with an increased dosage of ronidazole in racing pigeons (*Columba livia domestica*). *J Vet Pharmacol Therap.* (1992) 15:409–15. doi: 10.1111/j.1365-2885.1992.tb01032.x

4. Munoz E, Castella J, Gutierrez JF. In vivo and in vitro sensitivity of *Trichomonas gallinae* to some nitroimidazole drugs. *Vet Parasitol.* (1998) 78:239–46. doi: 10.1016/S0304-4017(98)00164-2

5. Tabari MA, Pozniak B, Youssefi MR, Roudaki Sarvandani MR, Giorgi M. Comparative pharmacokinetics of metronidazole in healthy and *Trichomonas gallinae* infected pigeons (*Columba livia*, var. domestica). *British Poultry Sci.* (2021) 62:485–91. doi: 10.1080/00071668.2021.1881043

6. McKeon T, Dunsmore J, Raidal SR. *Trichomonas gallinae* in budgerigars and columbid birds in Perth, Western Australia. *Aust Vet J.* (1997) 75:652–5. doi: 10.1111/j.1751-0813.1997.tb15363.x

7. Zimre-Grabensteiner E, Arshad N, Amin A, Hess M. Genetically different clonal isolates of *Trichomonas gallinae*, obtained from the same bird, can vary in their drug susceptibility, an *in vitro* evidence. *Parasitol Int.* (2011) 60:213–5. doi: 10.1016/j.parint.2011.02.003

8. Rouffaer LO, Adriaensen C, de Boeck C, Claerebout E, Martel A. Racing pigeons: a reservoir for nitro-imidazole–resistant *Trichomonas gallinae*. *J Parasitol.* (2014) 100:360–3. doi: 10.1645/13-359.1

9. Commission Regulation (EC) no 1798/95 of 25 July 1995 amending Annex IV to Council Regulation (EEC) No 2377/90 laying down a Community procedure for the establishment of maximum residue limits of veterinary medicinal products in foodstuffs of animal origin. *Off J.* (1995) L174:20–21.

10. Aziz ZAA, Ahmad A, Setapar SHM, Karakucuk A, Azim MM, Lokhat D, et al. Essential oils: extraction techniques, pharmaceutical and therapeutic potential—a review. *Curr Drug Metab.* (2018) 19:1100–10. doi: 10.2174/1389200219666180723144850

11. Ramsey JT, Shropshire BC, Nagy TR, Chambers KD Li Y, Korach KS. Essential oils and health. *Yale J Biol Med.* (2020) 93:291–305.

12. Youssefi MR, Tabari MA, Moghadamnia AA. *In vitro* and *in vivo* activity of *Artemisia sieberi* against *Trichomonas gallinae*. *Iranian J Vet Res.* (2017) 18:25.

13. Tabari MA, Youssefi MR. In vitro and in vivo evaluations of *Pelargonium roseum* essential oil activity against *Trichomonas gallinae*. *Avicenna J Phytomed.* (2018) 8:136.

14. Baccega B, Wahast Islabão Y, Brauner de Mello A, Obelar Martins F, Caetano dos Santos C, Ferreira Ourique A, et al. *In vitro* and *in vivo* activity of the essential oil and nanoemulsion of *Cymbopogon flexuosus* against *Trichomonas gallinae*. *Avicenna J Phytomed.* (2021) 11:32-34.

15. Gbolade AA, Arcoraci T, D'Arrigo M, Olorunmola FO, Biondi DM, Ruberto G. Essential Oils of *Dennettia tripetala* Bak. f stem bark and leaf – constituents and biological activities. *Nat Prod Commun.* (2008) 3:1925–30. doi: 10.1177/1934578X0800301127

16. Seddiek SA, El-Shorbagy MM, Khater HF, Ali AM. The antitrichomonal efficacy of garlic and metronidazole against *Trichomonas gallinae* infecting domestic pigeons. *Parasitol Res.* (2014) 113:1319–29. doi: 10.1007/s00436-014-3771-6

17. Adebajo AC, Ayoola OF, Iwalewa EO, Akindahunsi AA, Omisore NOA, Adewunmi CO, et al. Anti-trichomonal, biochemical and toxicological activities of methanolic extract and some carbazole alkaloids isolated from the leaves of *Murraya koenigii* growing in Nigeria. *Phytomed.* (2006) 13:246–54. doi: 10.1016/j.phymed.2004.12.002

18. Adebajo AC, Iwalewa EO, Obuotor EM, Ibikunle GF, Omisore NO, Adewunmi CO, et al. Pharmacological properties of the extract and some isolated compounds of *Clausena lansium* stem bark: Anti-trichomonal, antidiabetic, anti-inflammatory, hepatoprotective and antioxidant effects. *J Ethnopharmacol.* (2009) 122:10–9. doi: 10.1016/j.jep.2008.11.015

19. Tabari MA, Youssefi MR, Moghadamnia AA. Antitrichomonal activity of *Peganum harmala* alkaloid extract against trichomoniasis in pigeon (*Columba livia domestica*). *British Poultry Sci.* (2017) 58:236–41. doi: 10.1080/00071668.2017.1280725

20. Ibikunle GF, Adebajo AC, Famuyiwa FG, Aladesanmi AJ, Adewunmi CO. *In-Vitro* Evaluation of Anti-Trichomonal Activities of *Eugenia Uniflora* Leaf. *Afr J Tradit, Complement Altern Med.* (2011) 8:170. doi: 10.4314/ajtcam.v8i2.63205

21. Nikpay A, Soltani M. In vitro anti-parasitic activities of *Pulicaria dysenterica* and *Lycopus europaeus* methanolic extracts against *Trichomonas gallinae*. *J Herbmed Pharmacol.* (2018) 7:112–8. doi: 10.15171/jhp.2018.19

22. Badparva E, Badparva S, Badparva M, Kheirandish F. Comparing effect of some herbal medicines extract with metronidazole for treatment of trichomoniasis in birds. *Der Pharma Chemica.* (2016) 8:241–4.

23. Iwalewa EO, Omisore NO, Adewunmi CO, Gbolade AA, Ademowo OG, Nneji C, et al. Anti-protozoan activities of *Harungana madagascariensis* stem bark extract on trichomonads and malaria. *J Ethnopharmacol.* (2008) 117:507–11. doi: 10.1016/j.jep.2008.02.019

24. Malekifard F, Tavassoli M, Alimoradi M. *In vitro* assessment of anti-*Trichomonas* effects of *Zingiber officinale* and *Lavandula angustifolia* alcoholic extracts on *Trichomonas gallinae*. *Vet Res Forum.* (2021) 12:95–100.

25. Friedman M, Tam CC, Cheng LW, Land KM. Anti-trichomonad activities of different compounds from foods, marine products, and medicinal plants: a review. *BMC Complement Med Ther.* (2020) 20:271–89. doi: 10.1186/s12906-020-03061-9

26. European Pharmacopoeia. Available online at: http://www.edqm.eu/en/Homepage-628.html

27. Guzmán M, González-Coloma A, Andrés M Fe, Navarro-Rocha J, Martínez-Díaz RA. Biological evaluation of essential oils from selected medicinal plants and their main components against *Phytomonas davidi* (Kinetoplastea: Trypanosomatidae). *Chem Biodivers.* (2020) 17:e2000521. doi: 10.1002/cbdv.202000521

28. Julio LF, González-Coloma A, Burillo J, Diaz CE, Andrés MF. Nematicidal activity of the hydrolate byproduct from the semi industrial vapor pressure extraction of domesticated *Artemisia absinthium* against *Meloidogyne javanica*. *Crop Prot.* (2017) 94:33–7. doi: 10.1016/j.cropro.2016.12.002

29. Díaz-Navarro M, Bolívar P, Andrés MF, Gómez-Muñoz MT, Martínez-Díaz RA, Valcárcel F, et al. Antiparasitic Effects of Potentially Toxic Beetles

(Tenebrionidae and Meloidae) from Steppe Zones. *Toxins*. (2021) 13:489. doi: 10.3390/toxins13070489

30. González-Coloma A, Guadaño A, de Inés C, Martínez-Díaz R, Cortes D. Selective action of acetogenin mitochondrial complex I inhibitors. *Z Naturforsch C J Biosci*. (2002) 57:1028–34. doi: 10.1515/znc-2002-11-1213

31. Pelkonen O, Abass K, Wiesner J. Thujone and thujone-containing herbal medicinal and botanical products: toxicological assessment. *Regul Toxicol Pharmacol*. (2013) 65:100–7. doi: 10.1016/j.yrtph.2012.11.002

32. Mehriardestani M, Aliahmadi A, Toliat T, Rahimi R. Medicinal plants and their isolated compounds showing anti-*Trichomonas vaginalis*- activity. *Biomed Pharmacother*. (2017) 88:885–93. doi: 10.1016/j.biopha.2017.01.149

33. Moon T, Wilkinson JM, Cavanagh HMA. Antiparasitic activity of two *Lavandula* essential oils against *Giardia duodenalis*, *Trichomonas vaginalis* and *Hexamita inflata*. *Parasitol Res*. (2006) 99:722–8. doi: 10.1007/s00436-006-0234-8

34. Garza-González JN, Vargas-Villarreal J, Verde-Star MJ, Rivas-Morales C, Oranday-Cárdenas A, Hernandez-García ME, et al. Antiprotozoal activity of a *Thymus vulgaris* methanol extract and its fractions. *Health*. (2017) 09:1081–94. doi: 10.4236/health.2017.97079

35. Monzote L, Alarcón O, Setzer WN. Antiprotozoal activity of essential oils. *Agric Conspec Sci*. (2012) 77:167–75.

36. Jafari F, Ghavidel F, Zarshenas MM, A. Critical Overview on the Pharmacological and Clinical Aspects of Popular *Satureja* Species. *J Acupunct Meridian Stud*. (2016) 9:118–27. doi: 10.1016/j.jams.2016.04.003

37. Cavar S, Maksimović M, Šolić ME, Jerković-Mujkić A, Bešta R. Chemical composition and antioxidant and antimicrobial activity of two *Satureja* essential oils. *Food Chem*. (2008) 111:648–53. doi: 10.1016/j.foodchem.2008.04.033

38. Azimi H, Fallah-Tafti M, Karimi-Darmiyan M, Abdollahi M, A. comprehensive review of vaginitis phytotherapy. *Pak J Biol Sci*. (2011) 14:960–6. doi: 10.3923/pjbs.2011.960.966

39. Costa S, Cavadas C, Cavaleiro C, Salgueiro L, do Céu Sousa M. In vitro susceptibility of *Trypanosoma brucei brucei* to selected essential oils and their major components. *Exp Parasitol*. (2018) 190:34–40. doi: 10.1016/j.exppara.2018.05.002

40. Guardo NI, Paula S, González-Coloma A, Burillo J, Martínez-Díaz, RA. Trypanocidal effects of essential oils from selected medicinal plants synergy among the main components. *Nat Prod Commun*. (2017) 12:709–12. doi: 10.1177/1934578X1701200516

41. Marchese A, Arciola CR, Barbieri R, Silva AS, Nabavi SF, Tsetegho Sokeng AJ, et al. Update on Monoterpenes as Antimicrobial Agents: A Particular Focus on p-Cymene. *Materials*. (2017) 10:947. doi: 10.3390/ma10080947

frontiers | Frontiers in Veterinary Science

TYPE Original Research
PUBLISHED 11 October 2022
DOI 10.3389/fvets.2022.975238

OPEN ACCESS

EDITED BY
Simona Gabrielli,
Sapienza University of Rome, Italy

REVIEWED BY
Hüseyin Can,
Ege University, Turkey
Luca Villa,
University of Milan, Italy

*CORRESPONDENCE
Feng-Cai Zou
zfc1207@vip.163.com
Jun-Jun He
hejunjun617@163.com

†These authors have contributed equally to this work

SPECIALTY SECTION
This article was submitted to Parasitology, a section of the journal Frontiers in Veterinary Science

RECEIVED 22 June 2022
ACCEPTED 23 September 2022
PUBLISHED 11 October 2022

CITATION
Hu X-H, Xie S-C, Liang Q-L, Sun L-X, Li Z, Yang J-F, Zhu X-Q, Zou F-C and He J-J (2022) Seroprevalence and risk factors of *Toxoplasma gondii* and *Neospora caninum* infection in black goats in Yunnan Province, Southwestern China. *Front. Vet. Sci.* 9:975238. doi: 10.3389/fvets.2022.975238

Seroprevalence and risk factors of *Toxoplasma gondii* and *Neospora caninum* infection in black goats in Yunnan Province, Southwestern China

Xiao-Hui Hu[1,2,3†], Shi-Chen Xie[2,4†], Qin-Li Liang[3], Li-Xiu Sun[4], Zhao Li[5], Jian-Fa Yang[1], Xing-Quan Zhu[1,2], Feng-Cai Zou[1*] and Jun-Jun He[1*]

[1]Key Laboratory of Veterinary Public Health of Yunnan, College of Veterinary Medicine, Yunnan Agricultural University, Kunming, China, [2]College of Veterinary Medicine, Shanxi Agricultural University, Taigu, China, [3]State Key Laboratory of Veterinary Etiological Biology, Key Laboratory of Veterinary Parasitology of Gansu, Lanzhou Veterinary Research Institute, Chinese Academy of Agricultural Sciences, Lanzhou, China, [4]Hunan Provincial Key Laboratory of Protein Engineering in Animal Vaccines, College of Veterinary Medicine, Hunan Agricultural University, Changsha, China, [5]State Key Laboratory of Conservation and Utilization of Bio-Resources in Yunnan and Center for Life Science, School of Life Sciences, Yunnan University, Kunming, China

Toxoplasma gondii and *Neospora caninum* are two obligate intracellular protozoan parasites that can cause reproductive failure and production losses. To date, there is no data of *T. gondii* and *N. caninum* seroprevalence in black goats in Yunnan Province, southwestern China. In the present study, a total of 734 serum samples were collected from black goats in four different counties of Yunnan Province. 734 and 590 serum samples were examined for antibodies against *T. gondii* and *N. caninum* by using MAT and indirect ELISA, respectively. A total of 123 and 76 samples were *T. gondii*-positive and *N. caninum*-positive, respectively. The overall seroprevalence of *T. gondii* in black goats was 16.76% (123/734, 95% CI: 14.06–19.46) with the titer ranged from 1:25 to 1:3200. The seroprevalence of *N. caninum* was 12.88% (76/590, 95% CI: 10.18–15.58). There was significant difference in seroprevalence of *N. caninum* in different regions ($P < 0.01$, $\chi^2 = 30.63$) and age groups ($P < 0.05$, $\chi^2 = 11.85$). Significant differences in seroprevalence of *T. gondii* were observed in different regions ($P < 0.05$, $\chi^2 = 9.21$) and different gender groups ($P < 0.01$, $\chi^2 = 12.29$). Results of seroprevalence of *T. gondii* and *N. caninum* indicated that *T. gondii* and *N. caninum* were prevalent parasites in black goats in Yunnan Province. This is the first report of seroprevalence of *T. gondii* and *N. caninum* in black goats in Yunnan Province. The results of this study indicated that some measures should be taken to control these two parasites and to reduce economic losses to the livestock industry in Yunnan Province.

KEYWORDS

black goats, Southwestern China, *Toxoplasma gondii*, *Neospora caninum*, seroprevalence, risk factors

Introduction

Toxoplasma gondii and *Neospora caninum* are two obligate intracellular protozoan parasites infecting many animals. In addition, *T. gondii* is implicated in reproductive disorders in small ruminants, whereas *N. caninum* is considered an important pathogen causing abortion in dairy cows (1). Both parasites have a wide range of intermediate hosts including cattle, goats, sheep, other domestic and wild animals. Cats and dogs are the definitive hosts of *T. gondii* and *N. caninum*, respectively (1, 2). Animals can be infected by *T. gondii* through consumption of raw meat contained tissue cysts or ingestion of oocysts excreted by felines, and by vertical or transplacental transmission in intermediate hosts (3). In small ruminants, primary infection during pregnancy leads to serious congenital damage, resulting in abortion or stillbirth and negative economic impacts (4). A recent systematic review indicated that the global seroprevalence of *T. gondii* in goats was 27.49% (15,206/55,317, 95% CI: 24.15–30.95) (5). Despite goat is an important economic source of meat, fiber and milk in some countries worldwide, but a recent study indicated that there is still a higher potential to transmit *T. gondii* to humans by consumption of raw or undercooked meat, even small serving sizes (5 g) (6). To date, there was only one commercially available vaccine against *T. gondii* in sheep, but it has been discontinued due to self-limitation (3, 7). The average *T. gondii* seroprevalence in goats in China was 17.56% (3,260/18,556, 95% CI: 17.02–18.12) (8).

Similar to *T. gondii*, *N. caninum* has also been widely concerned and studied since it was first reported in 1984 (9). *N. caninum* can be transmitted horizontally and vertically in herds (10). *N. caninum* is considered as a major cause of abortion in cattle, particularly in dairy cattle, and studies revealed that 12% to 42% of aborted fetuses from dairy cattle were infected with *N. caninum* (1). Furthermore, goats would abort infectious fetuses when they were inoculated with *N. caninum* during pregnancy, and a meta-analysis revealed that the prevalence of *N. caninum* in aborted fetuses of goats was 7% worldwide (10, 11). Its zoonotic potential remains unknown because no evidence indicates that humans have been infected with *N. caninum* successfully (12, 13). The *N. caninum* seroprevalence in goats was estimated to be 5.99% (1,332/22,234, 95% CI: 4.38–7.83) worldwide (14). Because of *N. caninum* infection, the economic loss of beef and milk industries is approximate 1 billion US dollars annually (15).

Toxoplasmosis and neosporosis are cosmopolitan parasitic diseases and result in economic losses and reproductive reduction of the herds (1). China has the largest population of goats, and black goats are the most important economic goats in Yunnan Province, southwestern China. High density and diversity of domestic and wild animals might result in a high transmission risk of *T. gondii* and *N. caninum* in Yunnan Province. But knowledge on the seroprevalence of *T. gondii* and *N. caninum* in black goats in Yunnan Province is lacking. Therefore, the objectives of this study were to examine the seroprevalence of *T. gondii* and *N. caninum* and analyze the risk factors associated with their positivity in black goats in Yunnan Province.

Materials and methods

The investigation site and serum samples

Yunnan Province (97°31′ to 106°11′E, 21°8′ to 29°15′N), located in southwestern China, has a vast territory with diverse and unique natural resources. Yunnan Province has a subtropical monsoon climate, with an average annual temperature of 5 to 24°C and over 1000 mm of annual precipitation in most areas (http://www.yn.gov.cn/yngk/). After obtaining the permission of the farm owners or managers, 734 serum samples were collected from black goats in Wuding county ($n = 479$), Yongsheng county ($n = 90$), Ninglang county ($n = 100$) and Mengla county ($n = 65$) in Yunnan Province (Figure 1) from August to September, 2017. Approximately 5 mL of blood from each goat was sampled by jugular puncture in a tube without anticoagulant and stored at 4°C for 2 h, then centrifuged at 3,000 rpm for 10 min to collect serum samples, and all serum samples were stored at -20°C freezer until use.

Serological examination

Modified agglutination test (MAT), the efficient method for diagnosis of toxoplasmosis (3), was used to detected the antibodies against *T. gondii* in this study. The antigen (formalin fixed tachyzoites) used in the experiment were kindly provided by Dr. Jitender P. Dubey (ARS, USDA). The MAT experiment was performed as described previously (16). Briefly, 2 μL serum sample was added to the first well of 96-well U bottomed reaction plate, then was diluted two-fold starting from 1:25 to 1:3,200. 25 μL antigen mixture was added to each well and the plates were incubated at 37°C for 12 h. The negative and positive control were contained in each plate. The serum with titer of 1:25 or higher was considered *T. gondii*-positive. The specific *N. caninum* antibodies were detected using an indirect ELISA kit (ID Screen® *Neospora caninum* Indirect Multi-Species kit, ID VET, Montpellier, France) following the manufacturer's instructions. The kit has a high specificity and sensitivity (17). Positive and negative controls were set in each ELISA detection. The optical density (OD) was measured at 450 nm using microplate reader. The results were expressed as the ratio of absorbance of detected sample to the absorbance of

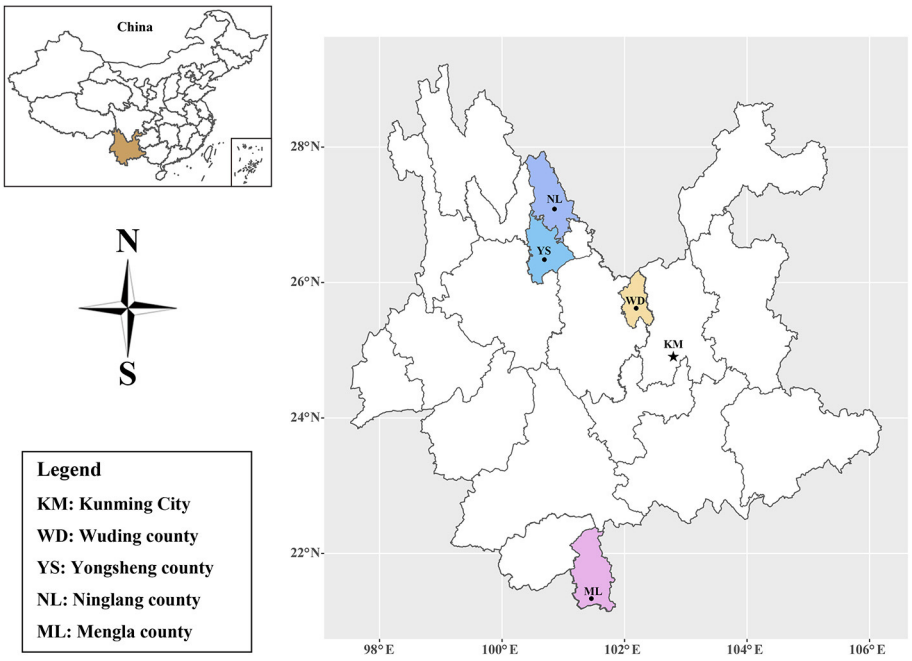

FIGURE 1
Distribution map of the sampling sites in Yunnan Province, Southwestern China.

the positive control following the formula: S/P = $OD_{sample} - OD_{negative\ control}$ / $OD_{positive\ control} - OD_{negative\ control}$. The samples with S/P % ≥50% were judged as positive.

Statistical analysis

Chi-square (χ^2) tests in SPSS software (release 23.0 standard version; SPSS, Inc., Chicago) were used for analyzing the variables (region, gender and age) associated with *T. gondii* and *N. caninum* infection. The variable with $P < 0.05$ was considered statistically significant. Results are presented as adjusted odds ratios (OR) with 95% confidence intervals (95% CI).

Results

The seroprevalence of *T. gondii* and *N. caninum* in black goats

In the present study, the overall seroprevalence of *T. gondii* and *N. caninum* in black goats was 16.76% (95% CI: 14.06–19.46) (Table 1) and 12.88% (95% CI: 10.18–15.58) (Table 2), respectively. Regarding the four study regions, the goats in Wuding county has the lowest seroprevalence of both *T. gondii* (13.78%, 66/479) and *N. caninum* (8.57%, 33/385), whereas the highest seroprevalence of *T. gondii* and *N. caninum* was detected in goats in Yongsheng county (24.44%, 22/90) and Ninglang county (33.33%, 18/54), respectively. Between gender groups, higher seroprevalence of *T. gondii* and *N. caninum* was detected in female goats, with 20.58% (93/452) and 14.80% (53/358), respectively. In addition, the highest seroprevalence of *T. gondii* was detected in goats aged more than 3 years (26.32%, 20/76); however, the seroprevalence of *N. caninum* in goats older than 3 years of age (14.71%, 10/68) was close to that of goats 1 to 2 years old (14.84%, 42/283), and both were significantly higher than that in goats of <1 year old (1.96%, 1/51).

Risk factors analysis

Statistical analysis showed that the seroprevalence of *T. gondii* in female goats was 20.58% (93/452), which was significantly higher than that in male goats (10.64%, 30/282) ($\chi^2 = 12.29$, df = 1, $P < 0.001$). There was statistically significant difference in seroprevalence of *T. gondii* among four study regions ($\chi^2 = 9.21$, df = 3, $P < 0.05$); but no statistically significant difference in *T. gondii* seroprevalence was observed between goats of different age groups ($\chi^2 = 5.81$, df = 1, $P = 0.21$) (Table 1). Moreover, statistically significant difference in seroprevalence of *N. caninum* was observed among different counties ($\chi^2 = 3.64$, df = 3, $P < 0.001$) and different age groups ($\chi^2 = 11.85$, df = 1, $P < 0.05$); whereas no statistically significant difference in *N. caninum* seroprevalence was found between the two genders ($\chi^2 = 3.00$, df = 1, $P = 0.083$).

TABLE 1 Seroprevalence of *Toxoplasma gondii* in black goats in Yunnan Province, Southwestern China.

Factor	Category	Tested No.	Positive No.	Prevalence (%)	95% CI (%)	OR (95%)	*P*-value
Region	Wuding	479	66	13.78	10.69–16.87	Reference	0.027
	Yongsheng	90	22	24.44	15.56–33.32	2.03 (1.17–3.50)	
	Mengla	65	14	21.54	11.55–31.53	1.72 (0.90–3.28)	
	Ninglang	100	21	21.00	13.02–28.98	1.66 (0.96–2.87)	
Gender	Male	282	30	10.64	7.04–14.24	Reference	0.000
	Female	452	93	20.58	16.85–24.31	2.18 (1.40–3.39)	
Age	0<year<1	53	7	13.21	4.09–22.33	Reference	0.214
	1≤ year<2	356	57	16.01	12.20–19.82	1.25 (0.54–2.91)	
	2≤ year<3	230	36	15.65	10.95–20.35	1.22 (0.51–2.91)	
	year ≥3	76	20	26.32	16.42–36.22	2.35 (0.91–6.04)	
	year = unknown	19	3	15.79	0.61–32.19	1.23 (0.28–5.34)	
Total		734	123	16.76	14.06–19.46		

TABLE 2 Seroprevalence of *Neospora caninum* in black goats in Yunnan Province, Southwestern China.

Factor	Category	Tested No.	Positive No.	Prevalence (%)	95% CI (%)	OR (95%)	*P*-value
Region	Wuding	385	33	8.57	5.77–11.37	Reference	0.000
	Yongsheng	91	12	13.19	6.24–20.14	1.62 (0.80–3.28)	
	Mengla	60	13	21.67	11.25–32.09	2.95 (1.45–6.00)	
	Ninglang	54	18	33.33	20.76–45.90	5.33 (2.73–10.41)	
Gender	Male	232	23	9.91	6.07–13.75	Reference	0.083
	Female	358	53	14.80	11.12–18.48	1.58 (0.94–2.66)	
Age	0<year<1	51	1	1.96	1.84–5.76	Reference	0.018
	1≤ year<2	283	42	14.84	10.70–18.98	8.71 (1.17–64.80)	
	2≤ year<3	184	21	11.41	6.82–16.00	6.44 (0.85–49.10)	
	year ≥3	68	10	14.71	6.29–23.13	8.62 (1.07–69.71)	
	year = unknown	4	2	50.00	1.00–99.00	50.0 (3.09–810.5)	
Total		590	76	12.88	10.18–15.58		

Discussion

Toxoplasmosis is a widely distributed zoonosis, both toxoplasmosis and neosporosis are two major causes of reproductive losses in small ruminants (18). In this study, we examined the seroprevalence of *T. gondii* and *N. caninum* in black goats in Yunnan Province, southwestern China, revealing the presence and relatively high seroprevalence of both parasites in study areas.

In the present study, the overall *T. gondii* seroprevalences in the examined black goats in Yunnan Province was 16.76%. A recent systematic review revealed that the seroprevalence of *T. gondii* in goats worldwide from 2000 to 2020 was 27.49%; of which, the highest and lowest seroprevalence of *T. gondii* in goats was detected in central America (62.15%) and Asia (20.74%), respectively (5). The seroprevalence of *T. gondii* in black goats in Yunnan Province detected in this study was higher than that in goats in Myanmar (11.39%, 32/281) (19), Korea (5.08%, 31/610) (20), Hunan Province (11.61%, 124/1,068) (21), Hubei Province (13.40%, 807/6,021) (22) and Shaanxi Province (14.11%, 106/751) (23) of China. But the *T. gondii* prevalence in black goats was lower than that in India (42.47%, 189/445) (24), Pakistan (42.83%, 227/530) (25), Mongolia (32.00%, 345/1,078) (26), Taiwan Province (32.22%, 203/630) (27) and Qinghai Province (29.54%, 192/650) of China (28). The seroprevalence of *T. gondii* detected in black goats in Yunnan Province in this study was similar to that detected in goats in Bangladesh (16.00%, 48/300) (29), and Yunnan Province (17.60%, 69/392) of China (30). The difference in *T. gondii* seroprevalence among difference regions may be related to different climate conditions, rearing conditions and breed variations.

The results of the present study demonstrated that there was significant difference in *T. gondii* seroprevalence of black goats from different geographical regions ($P < 0.05$) (Table 1). The difference may be caused by terrain and climate differences in Yunnan Province that has abundant rainfall and numerous

lakes, and the annual average temperatures range from 5 to 24°C with humid climate. These environmental factors could be beneficial to the sporulation, viability and spread of *T. gondii* oocysts (31). Previous studies indicated that annual temperature and rainfall could facilitate the survival of the environmental *T. gondii* oocysts, and seasonally or permanently pasture goats as well as increases the contact between goats and the oocysts (32–34).

The majority of the black goats examined in this study were free-ranged, which could increase the risk of *T. gondii* infection *via* frequent contact with other free-ranged animals. The high seroprevalence of *T. gondii* in black goats in this study may due to the presence of cats in the farms (35, 36). Cats are the definitive host of *T. gondii*, and oocysts of *T. gondii* are shed *via* feces. The ruminants may be infected by ingesting oocysts (37).

In the present study, the highest *T. gondii* seroprevalence was found in black goats aged 3 years and more (26.32%), with seropositive rate 2.35 times higher than lambs aged lower than 1 year (95% CI = 0.91–6.04). This result is consistent with previous reports that younger goats had lower seropositivity than old goats (24, 36). In contrast, age as a significant risk factor of toxoplasmosis in older animals of ruminant species (i.e., cattle, sheep and goat) comparing to younger animals was observed in several studies (38, 39). Spišák et al. (40) found that the *T. gondii* prevalence in older goats (over 6 years of age) in Slovakia was 4.3 times higher than goats of up to 3 years age. Similar association between the *T. gondii* seroprevalence and age has also been observed in cattle, sheep, goats and pigs in Portugal (41). Furthermore, a recent meta-analysis demonstrated that goats older than 1 year of age were at higher risk of being infected with *T. gondii*, because long-term exposure to the pasture increases the opportunity of ingesting oocysts (5). The results of the present study indicated that *T. gondii* infection was common in black goats in Yunnan Province (Table 1).

A recent systematic review reported that higher *T. gondii* prevalence was observed in female goats than that in males (OR = 1.43; 95% CI = 1.23–1.65) (5). In this study, the seroprevalence of *T. gondii* in female goats was 2.18 times higher than that in male goats (Table 2) (95% CI = 1.40–3.39; $P < 0.01$). This result was consistent with previous studies in sheep and goats in which male animals had a lower *T. gondii* prevalence than the females (42, 43). Some studies inferred that higher seroprevalence in females might be associated with their longer life for milk production and reproduction, whereas males are slaughtered for meat supply at an earlier age (24, 44). In addition, a previous study indicated that hormone differences may increase their susceptibility to *T. gondii* (45).

In this study, the overall seroprevalence of *N. caninum* in black goats was 12.88% (Table 2), which was higher than that in goats in Poland (9.00%, 95/1,060) (46), Pakistan (9.15%, 13/142) (47), Argentina (6.65%, 106/1,594) (48), south America (6.35%, 25/394) (49), Spain (6.00%, 3/50) (32), Brazil (4.58%, 30/655) (50), Turkey (3.21%, 8/249) (51), Romania (2.34%, 12/512) (52), Greece (6.93%, 26/375) (18) and Jordan (1.99%, 6/302) (53). However, it was lower than that in the Czech Republic (18.57%, 13/70) (35). Growing evidences indicated that the risk of infection for *N. caninum* is linked to the age of the hosts, rearing system, worming, the time of exposure to the parasite and the contact with dogs around the farms and history of abortion (18, 54). Also, goat breeds, climatic conditions, feeding and management conditions might contribute to the different seroprevalence of *N. caninum* in black goats in Yunnan Province, and more studies are warranted to investigate the potential association. In addition, previous studies have reported that many birds (e.g., domestic chickens and many wild birds) can act as intermediate hosts of *N. caninum* and can transmit the pathogen after being preyed upon by dogs when they are foraging on the ground, thus facilitating the spread of the *N. caninum* (55–57). However, the potential role played by birds in the transmission of *N. caninum* in Yunnan Province needs further study in the future.

In this study, the region and age factors were significantly related to *N. caninum* infection in black goats ($P < 0.05$). The seroprevalence of *N. caninum* in black goats aged 0–1 years (1.96%) was significantly lower than those in 1–2 years group (14.84%) and 2–3 years group (11.41%). These results were consistent with a previous report (41). Regarding the age groups, adult black goats showed the higher *N. caninum* seroprevalence than lambs, which is consistent with the results that adult cattle and heifers/steers have higher infection rate than calves, due to the increasing chances in postnatal oocyst infection with age (58). Similar to our results, the lowest *N. caninum* seroprevalence was also found in yaks of the 0–1 year group (59). However, two previous reports indicated that no statistically significant difference was observed in *N. caninum* seroprevalence between cattle of different age groups, but the *N. caninum* seroprevalence was strongly linked with the factors of abortion, parity number, gestation number and number of lactations (60, 61). Thus, a comprehensive study should be performed in the future to elucidate the important role of age in *N. caninum* epidemiology. With respect to regions, the present study found that there was significant difference in *N. caninum* seroprevalence among different study areas ($P < 0.001$). We speculated that rearing system, management measures, presence of dogs, and even the history of abortion in goats in the study areas may contribute to the difference in seroprevalence. Nevertheless, the region factor is a complex of multi-subfactors, including climatic, environmental factors. In Italy, the climatic and environmental factors were determined to influence the *N. caninum* distribution in cattle by geographical information system (GIS) and remote sensing (RS) technology (58). Additionally, Villa et al. (62) found a correlation between the geographic distance of the sampling sites and genetic distance of *N. caninum*, further explaining the possible reasons for the seroprevalence difference among different regions. In our investigation, no statistically significant difference in *N.*

caninum seroprevalence was observed between black goats of different genders ($P = 0.083$). Similar to our findings, Shireen et al. (63) indicated that there was no significant correlation between *N. caninum* and gender in small ruminants in Egypt.

In the present study, the co-infection rate of *T. gondii* and *N. caninum* in black goats was 4.44% (26/585), which was similar to the across-infection rate of *T. gondii* and *N. caninum* previous detected in black-bone sheep and goats in Yunnan Province (3.63%, 17/468) (64). Also, it was slightly lower than that in Qinghai Province, where the co-infection rate of *T. gondii* and *N. caninum* was 5.23% in goats and 6.5% in sheep (28). Sampling sizes, grazing practices, the presence of dogs and cats may be the important factors that contribute to co-infection of *N. caninum* and *T. gondii* (1, 65). However, based on an *in vitro*, immunological and serological experimental study, researches indicated that there is no exclusivity of infection and co-infection is a random event (66).

Conclusion

The present study examined the seroprevalence of *T. gondii* and *N. caninum* infection in black goats in Yunnan Province by using MAT and indirect ELISA methods. The overall seroprevalences of *T. gondii* and *N. caninum* in black goats were 16.76 and 12.88%, respectively. Region and gender were significantly associated with *T. gondii* infection in black goats, while region and age were significantly associated with *N. caninum* seroprevalence in black goats. The results of the present study demonstrated that *T. gondii* and *N. caninum* were highly prevalent in black goats in Yunnan Province. Therefore, integrated measures should be taken to prevent and control infection of black goats with these two parasites.

Data availability statement

The original contributions presented in the study are included in the article/supplementary material, further inquiries can be directed to the corresponding authors.

Ethics statement

The animal study was reviewed and approved by Animal Ethics and Welfare Committee of Yunnan Agricultural University.

Author contributions

J-JH, F-CZ, and X-QZ designed the study and revised the manuscript. X-HH and S-CX performed the experiments, analyzed the data, and wrote the manuscript. Q-LL, L-XS, ZL, and J-FY participated in implementation of the study. All authors read and approved the final version of the manuscript.

Funding

Project support was provided by the Yunnan Expert Workstation (Grant No. 202005AF150041), the Veterinary Public Health Innovation Team of Yunnan Province (Grant No. 202105AE160014), the Fund for Shanxi 1331 Project (Grant No. 20211331-13) and the Agricultural Science and Technology Innovation Program (ASTIP) (Grant No. CAAS-ASTIP-2016-LVRI-03). The funders had no role in the design of the study; in the collection, analyses, or interpretation of data; in the writing of the manuscript, or in the decision to publish the results.

Conflict of interest

The authors declare that the research was conducted in the absence of any commercial or financial relationships that could be construed as a potential conflict of interest.

Publisher's note

References

1. Lindsay DS, Dubey JP. Neosporosis, toxoplasmosis, and sarcocystosis in ruminants: an update. *Vet Clin North Am Food Anim Pract.* (2020) 36:205–22. doi: 10.1016/j.cvfa.2019.11.004

2. Miller NL, Frenkel JK, Dubey JP. Oral infections with *Toxoplasma* cysts and oocysts in felines, other mammals, and in birds. *J Parasitol.* (1972) 58:928–37. doi: 10.2307/3286588

3. Dubey JP. The history of *Toxoplasma gondii*–the first 100 years. *J Eukaryot Microbiol.* (2008) 55:467–75. doi: 10.1111/j.1550-7408.2008.00345.x

4. Ducournau C, Moire N, Carpentier R, Cantin P, Herkt C, Lantier I, et al. Effective nanoparticle-based nasal vaccine against latent and congenital toxoplasmosis in sheep. *Front Immunol.* (2020) 11:2183. doi: 10.3389/fimmu.2020.02183

5. Rodrigues AA, Reis SS, Moraes EDS, Do Nascimento Araujo EMA, Zanine AM, Nascimento TVC, et al. A systematic literature review and meta-analysis of *Toxoplasma gondii* seroprevalence in goats. *Acta Trop.* (2022) 230:106411. doi: 10.1016/j.actatropica.2022.106411

6. Dubey JP, Murata FHA, Cerqueira-Cezar CK, Kwok OCH. Public health and economic importance of *Toxoplasma gondii* infections in goats: the last decade. *Res Vet Sci.* (2020) 132:292–307. doi: 10.1016/j.rvsc.2020.06.014

7. Buxton D, Innes EA. A commercial vaccine for ovine toxoplasmosis. *Parasitology*. (1995) 110:S11–6. doi: 10.1017/S003118200000144X

8. Dong H, Su R, Lu Y, Wang M, Liu J, Jian F, et al. Prevalence, risk factors, and genotypes of *Toxoplasma gondii* in food animals and humans (2000-2017) from China. *Front Microbiol.* (2018) 9:2108. doi: 10.3389/fmicb.2018.02108

9. Bjerkas I, Mohn SF, Presthus J. Unidentified cyst-forming sporozoon causing encephalomyelitis and myositis in dogs. *Z Parasitenkd.* (1984) 70:271–4. doi: 10.1007/BF00942230

10. Nayeri T, Sarvi S, Moosazadeh M, Daryani A. The global prevalence of *Neospora caninum* infection in sheep and goats that had an abortion and aborted fetuses: a systematic review and meta-analysis. *Front Vet Sci.* (2022) 9:870904. doi: 10.3389/fvets.2022.870904

11. Lindsay DS, Rippey NS, Powe TA, Sartin EA, Dubey JP, Blagburn BL. Abortions, fetal death, and stillbirths in pregnant pygmy goats inoculated with tachyzoites of *Neospora caninum*. *Am J Vet Res.* (1995) 56:1176–80.

12. Dubey JP. Review of *Neospora caninum* and neosporosis in animals. *Korean J Parasitol.* (2003) 41:1–16. doi: 10.3347/kjp.2003.41.1.1

13. Petersen E, Lebech M, Jensen L, Lind P, Rask M, Bagger P, et al. *Neospora caninum* infection and repeated abortions in humans. *Emerg Infect Dis.* (1999) 5:278–80. doi: 10.3201/eid0502.990215

14. Rodrigues AA, Reis SS, Sousa ML, Moraes EDS, Garcia JL, Nascimento TVC, et al. A systematic literature review and meta-analysis of risk factors for *Neospora caninum* seroprevalence in goats. *Prev Vet Med.* (2020) 185:105176. doi: 10.1016/j.prevetmed.2020.105176

15. Reichel MP, Alejandra Ayanegui-Alcerreca M, Gondim LF, Ellis JT. What is the global economic impact of *Neospora caninum* in cattle—the billion dollar question. *Int J Parasitol.* (2013) 43:133–42. doi: 10.1016/j.ijpara.2012.10.022

16. Qin SY, Zhang XX, Cong W, Zhou DH, Wang JL, Yin MY, et al. Seroprevalence and risk factors of *Toxoplasma gondii* infection in domestic sika deer (*Cervus nippon*) in northeastern China. *Acta Trop.* (2014) 140:184–7. doi: 10.1016/j.actatropica.2014.08.021

17. Alvarez-Garcia G, Garcia-Culebras A, Gutierrez-Exposito D, Navarro-Lozano V, Pastor-Fernandez I, Ortega-Mora LM. Serological diagnosis of bovine neosporosis: a comparative study of commercially available ELISA tests. *Vet Parasitol.* (2013) 198:85–95. doi: 10.1016/j.vetpar.2013.07.033

18. Diakoua A, Papadopoulos E, Panousis N, Karatzias C, Giadinis N. *Toxoplasma gondii* and *Neospora caninum* seroprevalence in dairy sheep and goats mixed stock farming. *Vet Parasitol.* (2013) 198:387–90. doi: 10.1016/j.vetpar.2013.09.017

19. Bawm S, Maung WY, Win MY, Thu MJ, Chel HM, Khaing TA, et al. Serological survey and factors associated with *Toxoplasma gondii* infection in domestic goats in Myanmar. *Scientifica (Cairo).* (2016) 2016:4794318. doi: 10.1155/2016/4794318

20. Jung BY, Gebeyehu EB, Lee SH, Seo MG, Byun JW, Oem JK, et al. Detection and determination of *Toxoplasma gondii* seroprevalence in native Korean goats (*Capra hircus coreanae*). *Vector Borne Zoonotic Dis.* (2014) 14:374–7. doi: 10.1089/vbz.2013.1452

21. Li F, Wang SP, Wang CJ, He SC, Wu X, Liu GH. Seroprevalence of *Toxoplasma gondii* in goats in Hunan province, China. *Parasite.* (2016) 23:44. doi: 10.1051/parasite/2016053

22. Luo HQ, Li K, Zhang H, Wu B, Wang J, Shahzad M, et al. Seroepidemiology of *Toxoplasma gondii* and *Neospora caninum* infections in goats in Hubei province, China. *Trop Biomed.* (2016) 33:285–89.

23. Zhao GH, Zhang MT, Lei LH, Shang CC, Cao DY, Tian TT, et al. Seroprevalence of *Toxoplasma gondii* infection in dairy goats in Shaanxi province, northwestern China. *Parasit Vectors.* (2011) 4:47. doi: 10.1186/1756-3305-4-47

24. Bachan M, Deb AR, Maharana BR, Sudhakar NR, Sudan V, Saravanan BC, et al. High seroprevalence of *Toxoplasma gondii* in goats in Jharkhand state of India. *Vet Parasitol Reg Stud Reports.* (2018) 12:61–8. doi: 10.1016/j.vprsr.2018.02.004

25. Ahmed H, Malik A, Arshad M, Mustafa I, Khan MR, Afzal MS, et al. Seroprevalence and spatial distribution of toxoplasmosis in sheep and goats in north-eastern region of Pakistan. *Korean J Parasitol.* (2016) 54:439–46. doi: 10.3347/kjp.2016.54.4.439

26. Pagmadulam B, Myagmarsuren P, Yokoyama N, Battsetseg B, Nishikawa Y. Seroepidemiological study of *Toxoplama gondii* in small ruminants (sheep and goat) in different provinces of Mongolia. *Parasitol Int.* (2020) 74:101996. doi: 10.1016/j.parint.2019.101996

27. Chiang SH, Huang HH, Chou CC, Chu CS, Shih WL, Lai JM, et al. Epidemiological survey of *Toxoplasma gondii* and *Neospora caninum* infections in dairy goats in central-southern Taiwan. *J Vet Med Sci.* (2020) 82:1537–44. doi: 10.1292/jvms.20-0116

28. Liu ZK, Li JY, Pan H. Seroprevalence and risk factors of *Toxoplasma gondii* and *Neospora caninum* infections in small ruminants in China. *Prev Vet Med.* (2015) 118:488–92. doi: 10.1016/j.prevetmed.2014.12.017

29. Sah RP, Talukder MH, Rahman A, Alam MZ, Ward MP. Seroprevalence of *Toxoplasma gondii* infection in ruminants in selected districts in Bangladesh. *Vet Parasitol Reg Stud Reports.* (2018) 11:1–5. doi: 10.1016/j.vprsr.2017.10.008

30. Zou F, Yu X, Yang Y, Hu S, Chang H, Yang J, et al. Seroprevalence and risk factors of *Toxoplasma gondii* infection in buffaloes, sheep and goats in Yunnan province, southwestern China. *Iran J Parasitol.* (2015) 10:648–51.

31. Djokic V, Klun I, Musella V, Rinaldi L, Cringoli G, Sotiraki S, et al. Spatial epidemiology of *Toxoplasma gondii* infection in goats in Serbia. *Geospat Health.* (2014) 8:479–88. doi: 10.4081/gh.2014.37

32. Diaz P, Cabanelas E, Diaz-Cao JM, Vina M, Bejar JP, Perez-Creo A, et al. Seroprevalence of *Toxoplasma gondii* and *Neospora caninum* in goats from north-western Spain. *Ann Agric Environ Med.* (2016) 23:587–90. doi: 10.5604/12321966.1226851

33. Gazzonis A, Villa L, Manfredi M, Zanzani S. Spatial analysis of infections by *Toxoplasma gondii* and *Neospora caninum* (Protozoa: Apicomplexa) in small ruminants in northern Italy. *Animals (Basel).* (2019) 9:916. doi: 10.3390/ani9110916

34. Condoleo R, Musella V, Maurelli MP, Bosco A, Cringoli G, Rinaldi L. Mapping, cluster detection and evaluation of risk factors of ovine toxoplasmosis in southern Italy. *Geospat Health.* (2016) 11:432. doi: 10.4081/gh.2016.432

35. Bartova E, Kobedova K, Lamka J, Kotrba R, Vodicka R, Sedlak K. Seroprevalence of *Neospora caninum* and *Toxoplasma gondii* in exotic ruminants and camelids in the Czech Republic. *Parasitol Res.* (2017) 116:1925–29. doi: 10.1007/s00436-017-5470-6

36. Rahman M, Azad MT, Nahar L, Rouf SM, Ohya K, Chiou SP, et al. Age-specificity of *Toxoplasma gondii* seroprevalence in sheep, goats and cattle on subsistence farms in Bangladesh. *J Vet Med Sci.* (2014) 76:1257–9. doi: 10.1292/jvms.14-0171

37. Hide G, Gerwash O, Morley EK, Williams RH, Hughes JM, Thomasson D, et al. Does vertical transmission contribute to the prevalence of toxoplasmosis? *Parassitologia.* (2007) 49:223–6.

38. Tzanidakis N, Maksimov P, Conraths FJ, Kiossis E, Brozos C, Sotiraki S, et al. *Toxoplasma gondii* in sheep and goats: seroprevalence and potential risk factors under dairy husbandry practices. *Vet Parasitol.* (2012) 190:340–8. doi: 10.1016/j.vetpar.2012.07.020

39. Gazzonis AL, Zanzani SA, Villa L, Manfredi MT. *Toxoplasma gondii* infection in meat-producing small ruminants: meat juice serology and genotyping. *Parasitol Int.* (2020) 76:102060. doi: 10.1016/j.parint.2020.102060

40. Spišák F, Turčeková L, Reiterová K, Špilovská S, Dubinský P. Prevalence estimation and genotypization of *Toxoplasma gondii* in goats. *Biologia.* (2010) 65:670–74. doi: 10.2478/s11756-010-0070-2

41. Lopes AP, Dubey JP, Neto F, Rodrigues A, Martins T, Rodrigues M, et al. Seroprevalence of *Toxoplasma gondii* infection in cattle, sheep, goats and pigs from the north of Portugal for human consumption. *Vet Parasitol.* (2013) 193:266–9. doi: 10.1016/j.vetpar.2012.12.001

42. Gebremedhin EZ, Agonafir A, Tessema TS, Tilahun G, Medhin G, Vitale M, et al. Seroepidemiological study of ovine toxoplasmosis in east and west Shewa Zones of Oromia Regional State, Central Ethiopia. *BMC Vet Res.* (2013) 9:117. doi: 10.1186/1746-6148-9-117

43. Teshale S, Dumetre A, Darde ML, Merga B, Dorchies P. Serological survey of caprine toxoplasmosis in Ethiopia: prevalence and risk factors. *Parasite.* (2007) 14:155–9. doi: 10.1051/parasite/2007142155

44. Fortes MS, Lopes-Mori FMR, Caldart ET, Constantino C, Evers F, Pagliari S, et al. Caprine toxoplasmosis in Southern Brazil: a comparative seroepidemiological study between the indirect immunofluorescence assay, the enzyme-linked immunosorbent assay, and the modified agglutination test. *Trop Anim Health Prod.* (2018) 50:413–19. doi: 10.1007/s11250-017-1450-1

45. Dubey JP, Lappin MR (2005). *Infectious Diseases of Dogs and Cats*. St. Louis: Saunders-Elsevier.

46. Czopowicz M, Kaba J, Szalus-Jordanow O, Nowicki M, Witkowski L, Frymus T. Seroprevalence of *Toxoplasma gondii* and *Neospora caninum* infections in goats in Poland. *Vet Parasitol.* (2011) 178:339–41. doi: 10.1016/j.vetpar.2011.01.039

47. Nasir A, Ashraf M, Khan MS, Javeed A, Yaqub T, Avais M, et al. Prevalence of *Neospora caninum* antibodies in sheep and goats in Pakistan. *J Parasitol.* (2012) 98:213–5. doi: 10.1645/GE-2863.1

48. Moore DP, Yaniz M, Odeón A, Ca No D, Leunda MR, Späth E, et al. Serological evidence of *Neospora caninum* infections in goats from La Rioja Province, Argentina. *Small Ruminant Res.* (2007) 73:256–8. doi: 10.1016/j.smallrumres.2006.10.019

49. Moore DP. Neosporosis in South America. *Vet Parasitol.* (2005) 127:87–97. doi: 10.1016/j.vetpar.2004.10.001

50. Topazio JP, Weber A, Camillo G, Vogel FF, Machado G, Ribeiro A, et al. Seroprevalence and risk factors for *Neospora caninum* in goats in Santa Catarina State, Brazil. *Rev Bras Parasitol Vet.* (2014) 23:360–6. doi: 10.1590/S1984-29612014062

51. Zhou M, Cao S, Sevinc F, Sevinc M, Ceylan O, Liu M, et al. Enzyme-linked immunosorbent assays using recombinant TgSAG2 and NcSAG1 to detect *Toxoplasma gondii* and *Neospora caninum*-specific antibodies in domestic animals in Turkey. *J Vet Med Sci.* (2017) 78:1877–81. doi: 10.1292/jvms.16-0234

52. Iovu A, Gyorke A, Mircean V, Gavrea R, Cozma V. Seroprevalence of *Toxoplasma gondii* and *Neospora caninum* in dairy goats from Romania. *Vet Parasitol.* (2012) 186:470–4. doi: 10.1016/j.vetpar.2011.11.062

53. Abo-Shehada MN, Abu-Halaweh MM. Flock-level seroprevalence of, and risk factors for, *Neospora caninum* among sheep and goats in northern Jordan. *Prev Vet Med.* (2010) 93:25–32. doi: 10.1016/j.prevetmed.2009.08.004

54. Rodrigues AA, Reis SS, Da Silva Moraes E, Do Nascimento Souza Filho JG, Dos Santos Reis MH, Martins TA, et al. Seroprevalence and risk factors for *Neospora caninum* and *Toxoplasma gondii* in goats of Maranhao State, Brazil. *Vet Parasitol Reg Stud Reports.* (2021) 26:100634. doi: 10.1016/j.vprsr.2021.100634

55. Darwich L, Cabezon O, Echeverria I, Pabon M, Marco I, Molina-Lopez R, et al. Presence of *Toxoplasma gondii* and *Neospora caninum* DNA in the brain of wild birds. *Vet Parasitol.* (2012) 183:377–81. doi: 10.1016/j.vetpar.2011.07.024

56. Gazzonis AL, Villa L, Lubian E, Ressegotti S, Grilli G, Raimondi S, et al. Molecular survey on *Toxoplasma gondii* and *Neospora caninum* infection in wild birds of prey admitted to recovery centers in Northern Italy. *Microorganisms.* (2021) 9:736. doi: 10.3390/microorganisms9040736

57. de Barros LD, Miura AC, Minutti AF, Vidotto O, Garcia JL. *Neospora caninum* in birds: a review. *Parasitol Int.* (2018) 67:397–402. doi: 10.1016/j.parint.2018.03.009

58. Rinaldi L, Fusco G, Musella V, Veneziano V, Guarino A, Taddei R, et al. *Neospora caninum* in pastured cattle: determination of climatic, environmental, farm management and individual animal risk factors using remote sensing and geographical information systems. *Vet Parasitol.* (2005) 128:219–30. doi: 10.1016/j.vetpar.2004.12.011

59. Meng QF, Yao GZ, Qin SY, Wu J, Zhang XC, Bai YD, et al. Seroprevalence of and risk factors for *Neospora caninum* infection in yaks (*Bos grunniens*) in China. *Vet Parasitol.* (2017) 242:22–3. doi: 10.1016/j.vetpar.2017.05.022

60. Villa L, Gazzonis AL, Fumagalli E, Zanzani SA, Manfredi MT. The utility of serological analysis for *Neospora caninum* infection in dairy cattle farms management: serological investigation and evaluation of the effects on reproductive and productive performances in two study herds in Northern Italy. *Animals (Basel).* (2022) 12:786. doi: 10.3390/ani12060786

61. Pfeiffer DU, Williamson NB, Reichel MP, Wichtel JJ, Teague WR, A. longitudinal study of *Neospora caninum* infection on a dairy farm in New Zealand. *Prev Vet Med.* (2002) 54:11–24. doi: 10.1016/S0167-5877(02)00011-9

62. Villa L, Maksimov P, Luttermann C, Tuschy M, Gazzonis AL, Zanzani SA, et al. Spatial distance between sites of sampling associated with genetic variation among *Neospora caninum* in aborted bovine foetuses from northern Italy. *Parasit Vectors.* (2021) 14:47. doi: 10.1186/s13071-020-04557-6

63. Aboelwafa SS, Ali AO, Hamada R, Mahmoud HY. Seroprevalence of *Toxoplasma gondii* and *Neospora caninum* in small ruminants in Luxor, Egypt. *Adv Animal Vet Sci.* (2021) 10:412–20. doi: 10.17582/journal.aavs/2022/10.2.412.420

64. Sun LX, Liang QL, Nie LB, Hu XH Li Z, Yang JF, et al. Serological evidence of *Toxoplasma gondii* and *Neospora caninum* infection in black-boned sheep and goats in southwest China. *Parasitol Int.* (2020) 75:102041. doi: 10.1016/j.parint.2019.102041

65. Dubey JP, Schares G. Neosporosis in animals–the last five years. *Vet Parasitol.* (2011) 180:90–108. doi: 10.1016/j.vetpar.2011.05.031

66. Hughes JM, Williams RH, Morley EK, Cook DA, Terry RS, Murphy RG, et al. The prevalence of *Neospora caninum* and co-infection with *Toxoplasma gondii* by PCR analysis in naturally occurring mammal populations. *Parasitology.* (2006) 132:29–36. doi: 10.1017/S0031182005008784

frontiers | Frontiers in Veterinary Science

TYPE Original Research
PUBLISHED 13 October 2022
DOI 10.3389/fvets.2022.1033380

OPEN ACCESS

EDITED BY
Damer Blake,
Royal Veterinary College (RVC),
United Kingdom

REVIEWED BY
Ifeoma Nancy Nzelu,
Federal University of Agriculture
Makurdi (FUAM), Nigeria
Alice Vismarra,
University of Parma, Italy

*CORRESPONDENCE
Luís F. P. Gondim
pita@ufba.br

SPECIALTY SECTION
This article was submitted to Parasitology,
a section of the journal
Frontiers in Veterinary Science

RECEIVED 31 August 2022
ACCEPTED 22 September 2022
PUBLISHED 13 October 2022

CITATION
Rezende-Gondim MM, da Silva AV, Dubey JP, Schares GRM and Gondim LFP (2022) Immunomagnetic separation of *Toxoplasma gondii* and *Hammondia* spp. tissue cysts generated in cell culture.
Front. Vet. Sci. 9:1033380.
doi: 10.3389/fvets.2022.1033380

Immunomagnetic separation of *Toxoplasma gondii* and *Hammondia* spp. tissue cysts generated in cell culture

Mariana M. Rezende-Gondim[1], Aristeu V. da Silva[2], Jitender P. Dubey[3], Gereon R. M. Schares[4] and Luís F. P. Gondim[1]*

[1]Departamento de Anatomia, Patologia e Clínicas, Escola de Medicina Veterinária e Zootecnia, Universidade Federal da Bahia, Salvador, Bahia, Brazil, [2]Departamento de Biologia, Universidade Estadual de Feira de Santana, Feira de Santana, Bahia, Brazil, [3]United States Department of Agriculture, Agricultural Research Service, Beltsville Agricultural Research Center, Animal Parasitic Diseases Laboratory, Beltsville, MD, United States, [4]Friedrich-Loeffler-Institut, Federal Research Institute for Animal Health, Institute of Epidemiology, National Reference Centre for Toxoplasmosis, Greifswald-Insel Riems, Germany

Toxoplasma gondii is commonly transmitted among animals and humans by ingestion of infected animal tissues or by consumption of food and water contaminated with environmentally-resistant oocysts excreted by cats. Tissue cysts and oocysts have different walls, whose structures and compositions are poorly known. Herein, we describe an immunomagnetic separation (IMS) method that was successfully used for purification of *T. gondii* tissue cysts generated in cell culture. We used an IgG monoclonal antibody (mAb) that reacts against antigens in tissue cyst walls. Many *in vitro* produced cysts were obtained by this IMS; >2,000 *T. gondii* cysts were isolated from a single culture flask of 25 cm^2. Tissue cysts from two *Hammondia* spp., *H. hammondi*, and *H. heydorni*, produced in cell culture were also separated using this method. As a reference, purification of tissue cysts by Percoll gradients was used. Percoll was able to separate *T. gondii* tissue cysts produced in mice but was not suitable for purifying *T. gondii* tissue cysts produced *in vitro*. The IMS described here should favor proteomic studies involving tissue cysts of *T. gondii*.

KEYWORDS

monoclonal antibody, tissue cyst wall, *Toxoplasma gondii*, *Hammondia hammondi*, *Hammondia heydorni*, immunomagnetic

Introduction

Toxoplasma gondii is a globally distributed protozoan parasite, which can infect almost all warm-blooded animals, including humans (1). The two parasite stages involved in its oral horizontal transmission are tissue cysts (TC) and oocysts. Tissue cysts are formed in brain, muscles and other organs of mammalian and avian hosts; they may contain thousands of bradyzoites (2). Animals and humans are mainly infected by consuming TC in raw or undercooked animal tissues and oocysts in contaminated food or water. Other ways of transmission include transplacental infection, organ transplantation, blood transfusion, and accidental inoculation using needles, but the infection by ingestion of oocysts and TC are believed to occur more often (3).

Currently, there is no effective way to eliminate TC in live animals. Tissue cysts possess walls, whose composition and structures are poorly known. The TC wall is formed by a combination of molecules from the host cell and by proteins secreted by the parasite, that confers both resistance to the TC, as well as helps the parasite to evade the host immune system (4, 5). Several proteins have been identified in the TC wall, including a 65KDa protein abundant in its matrix (6), the CST1 protein, which is associated to the integrity of *in vivo* produced TC (7), and BCP1, which is also essential to cyst wall formation (8). A study using a promiscuous biotin ligase allowed the identification of previously described cyst wall proteins of *T. gondii*, as well as undescribed ones (9).

A crucial step to better understand the composition of the TC wall of *T. gondii* is to obtain purified TC. A monoclonal antibody (mAb) initially established to bind oocysts and designated K8/15-15 was shown to also bind to TC walls of *T. gondii* (10). In addition, this mAb also binds to cyst walls of related coccidia, including *Neospora caninum*, *Hammondia hammondi*, and *Hammondia heydorni* (10). In the present study, we describe an immunomagnetic separation (IMS) method to obtain purified TC of *T. gondii*. In addition, the IMS was also qualitatively tested to capture *in vitro* produced TC of *H. hammondi* and *H. heydorni*.

Materials and methods

Study design

An IMS method was developed focusing the purification of *T. gondii* cysts produced in cell culture. The method was initially tested using *T. gondii* tissue cysts produced in mice, as well as *in vitro* generated cysts of *Hammondia* spp., which became available from a previous experiment (10). Subsequently, the IMS method was tested in different conditions (direct and indirect capture at two different temperatures) using *T. gondii* cysts generated in cell culture (Figure 1). Parasites were grown as tachyzoites in Monkey Kidney cells (Marc-145) and submitted to stress conditions to induce cyst formation. *In vitro* generated TC were tested by IMS and the captured cysts were quantified. Non-specific binding of host cells was tested with the magnetic beads and mAb. Purification of *in vitro* produced cysts was also attempted by Percoll gradients.

Cell culture and *in vitro* production of cysts

Monkey kidney cells (Marc-145) (ATCC® CRL-12231) were selected for this study, as these cells have been shown to resist to stress conditions during cell culture for *in vitro* production of *N. caninum* cysts (11). Marc-145 cells were cultured in RPMI medium supplemented with 1% antibiotic/antimycotic solution (100 units/mL of penicillin, 100 µg/mL of streptomycin and 0.25 µg/mL of amphotericin B) (Gibco®, Carlsbad, USA) and 5% of inactivate bovine serum (Invitrogen/Gibco®, Auckland, NZ), at 37°C in a humidified incubator containing 5% CO_2.

For *T. gondii in vitro* cyst production, 7×10^5 Marc-145 cells were placed in 25 cm^2 flasks and after 48 h, 7×10^6 tachyzoites of a chicken isolate of the parasite (TgCkBr284) (12, 13) were added to the flask; 24 h after infection, cultures were transferred to an incubator with no CO_2 supply. Culture medium was replaced by alkalinized medium (pH 8.1) by adding 1M NaOH (18). Alkalinized medium was replaced every 24 h for four consecutive days. Cell monolayers were trypsinized, and after detachment of the cells from the flask surface, trypsin was blocked by adding 2 ml of fresh medium (RPMI with 1% antibiotic/antimycotic and 5% of inactivate bovine serum). The content from each flask was transferred to a 15 ml-tube. Aliquots were collected from each tube and placed on teflon-coated slides for immunofluorescence examination. These *in vitro* produced cyst suspensions were named "pre-capture" samples. The 15 ml-tubes were centrifuged (300 *g*, at 24°C, no brake), the supernatant discarded and the sediment used for IMS.

Magnetic beads and magnetic particle separator

Magnetic beads with diameters of 4.5 µm and coated with goat anti-mouse IgG (Dynabeads®, Invitrogen by Life Technologies) were used. The antibodies attached to these beads can react with the heavy chain of mouse IgG. The minimal volume of beads per reaction suggested by the manufacturer is 25 µl (~1×10^7 beads). However, we used 5 µl (~2×10^6 beads) or 10 µl (~4×10^6 beads) of the original bead suspension per reaction. In case of the production of 2,500 cysts in a culture flask, using 5 µl of beads would result in 800 of beads for each cyst of *T. gondii*. A magnetic particle separator (MPS) (MPG® 3-in-1 MPS®, Lincoln Park, USA) which contains inserts for tubes of 1.5, 15, and 50 ml was used to bind beads.

Washing and coupling magnetic beads to the monoclonal antibody K8/15-15

The method used to couple the mAb to anti-mouse IgG magnetic beads was executed similarly as suggested by the manufacturer but was slightly modified and adapted for 1.5 ml tubes. The original 5-ml vial containing the beads (4×10^8 beads/ml) was vortexed for 40 s, and 25 µl (~1×10^7 beads) were transferred to a 1.5-ml centrifuge tube. The beads were suspended in 1 ml of an isolation buffer (PBS free of Ca^{2+} and

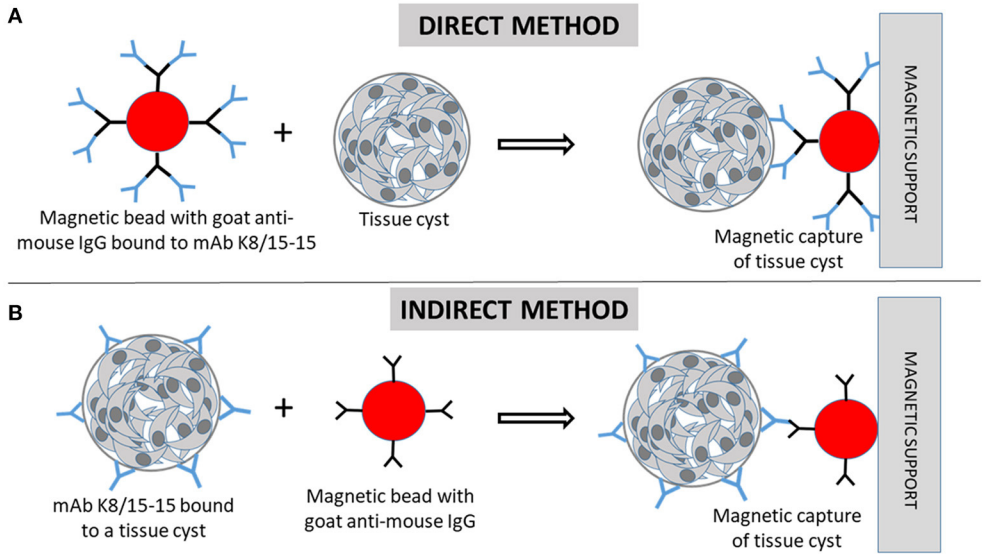

FIGURE 1
Immunomagnetic separation of *Toxoplasma gondii* tissue cysts (TC). **(A)** In the direct capture, magnetic beads coated with goat anti-mouse IgG are firstly incubated with the monoclonal antibody (mAb) K8/15-15. Then, the cell suspension containing TC are incubated with the beads. **(B)** In the indirect method, the cell suspension containing tissue cysts are firstly incubated with the mAb, followed by incubation with the magnetic beads. **(A,B)** The beads bound to TC are magnetically captured by the magnetic support (magnetic cell separator).

Mg^{2+} with 0.1% BSA and 2 mM EDTA, pH 7.4) and placed on a magnetic particle separator (MPS) for 1 min. The supernatant was discarded using an aspiration pump while the tube was still on the MPS. The tube was removed from the MPS, and the beads resuspended with 25 µl of isolation buffer.

Two hundred µl of the mAb K8/15-15 (hybridoma supernatant) at 1:10 or 1:5 dilutions in isolation buffer was homogenized with the beads (25 µl) and incubated at 7°C in a mixer with gentle titling of the tubes every 3–4 min. The tube was placed on the MPS for 1 min and the supernatant aspirated and discarded while the tube was on the MPS. The tube was removed from the MPS, and 1.5 ml of isolation buffer was added to wash the excess of unbound antibodies. The supernatant was removed while the tube was attached to the MPS by using a suction device. The washing step was repeated once. The tube was removed from the MPS, and the beads suspended with 1 ml of isolation buffer. This suspension containing the beads coupled to the mAb was stored at 4°C. At the end of the mAb-beads coupling procedure, the volume of beads in 1 ml was 6.4×10^6, which was divided in fractions of 200 µl (1.26×10^6 beads per aliquot) for subsequent experiments.

IMS of tissue cysts produced in mice and cysts of related coccidia

Two C57 mice were each intraperitoneally inoculated with two tissue cysts of the ME-49 strain of *T. gondii*. Four months later, the mice were euthanized, and their brains aseptically removed. The two mice were used in a previous experiment (10), approved by the Landesamt für Landwirtschaft, Lebensmittelsicherheit und Fischerei of the German Federal State of Mecklenburg-Vorpommern. Each mouse brain was homogenized in 600–800 µl of PBS/T (0.05% Tween 20) using a glass tissue grinder and TC quantified by microscopically counting three aliquots of 10 µl of the brain suspension on a glass slide with a coverslip at 200 × magnification. The TC were concentrated by Percoll gradients in 15-ml plastic centrifuge tubes, as previously described (14, 15). In brief, 10 ml of PBS/T (0.05% Tween 20) were added to 1 ml of the brain suspension. Then, 1.5 ml of 30% Percoll in PBS/T and 1.5 ml of 90% Percoll in PBS/T were consecutively underlayered to the bottom of the brain suspension. The tube was centrifuged at 1,500 *g* at 4°C for 15 min. The entire content of the 30 and 90% Percoll gradients were collected, added to a 50 ml centrifuge tube, and the tube filled with PBS to the top. The tube was centrifuged for 1,200 *g* for 10 min at 4°C, the supernatant discarded, and the sediment resuspended with 200 µl of PBS.

The TC, which had been purified by Percoll gradients, were mixed with 200 µl of isolation buffer. Each fraction of tissue cysts was added to a 1.5-ml tube containing 200 µl of the magnetic beads coupled with the mAb K8/15-15. The tube was incubated for 20 min at 7°C in an automated mixer. Each tube was placed in the MPS for 2 min and while it was there, the supernatant was discarded by aspiration. The tube was removed from the MPS, and 1 ml of isolation buffer was added. The solution was

pipetted 2–3 times and the tube placed in the MPS for 2 min. The supernatant was aspirated and discarded. This washing step was repeated twice. The tube was removed from the MPS, and the beads suspended with 100 μl of PBS. An aliquot of 10 μl was observed at a Nikon Eclipse-Ti microscope at 200, 400, and 600× magnifications. The images were evaluated using phase contrast microscopy.

Cysts of *H. hammondi* and *H. heydorni* were generated in a finite bovine embryo heart cell line (KH-R; Friedrich-Loeffler-Institut, cell line No. RIE 090), as previously described (10). In brief, supernatants of the 25 cm^2-flasks containing *H. hammondi* and *H. heydorni* cultures were individually aspirated and centrifuged at 200 *g* for 10 min. The sediment was suspended with 200 μl of isolation buffer and added to 400 μl of magnetic beads coupled to the mAb K8/15-15. The material was incubated at room temperature for 30 min in continuous agitation, and after this step, placed on the MPS. The supernatant was discarded, and the beads were re-suspended in 100 μl of isolation buffer. Two aliquots of 10 μl each were observed at the microscope. A sample of *H. heydorni* cysts was examined by immunofluorescence, but instead of a FITC anti-mouse IgG conjugate, an anti-mouse IgG coupled with a red fluorochrome was employed (Alexa fluor 555, Invitrogen).

IMS of *in vitro* produced cysts

IMS for *in vitro* produced cysts of *T. gondii* was tested by direct and indirect methods, each one evaluated in two reaction temperatures (4 and 24°C), in total four tests. These tests were also examined using non-infected host cells (prior and post-immunomagnetic capture) to test the specificity of the method. The cells were counted in a Neubauer chamber.

Direct capture of *in vitro* produced cysts (tests 1 and 2)

The mAb K8/15-15 was diluted 1:10 in isolation buffer (200 μl) and was incubated with 20 μl of washed magnetic beads in a tube of 1.5 ml. The tube was agitated at 4°C (test 1) or 24°C (test 2) for 40 min using an automated mixer, followed by placement of the tube on the MPS for 1 min. Then, the supernatant was collected and discarded, and the tube removed from the MPS. Isolation buffer (1.5 ml) was added to the tube, which was placed again for 1 min on the MSP. The supernatant was collected and discarded. This step of addition and removal of isolation buffer was repeated as above, and the beads were finally suspended in 1 ml of isolation buffer and stored in a sterile 1.5 ml tube at 4°C.

Pellets containing non-infected Marc-145 cells and *in vitro* produced cysts of *T. gondii* were each mixed with 250 μl of isolation buffer and 250 μl of magnetic beads coupled to mAb K8/15-15. Each suspension was placed in a 1.5 ml tube. The tubes were agitated at 4°C (test 1) or 24°C (test 2) for 20 min using an automated mixer, then, placed on MPS for 2 min. The supernatant was collected and discarded, and the magnetically attached content was saved. The tubes were removed from the MPS, and 1 ml of isolation buffer was gently added to the tube. The content was homogenized by gently pipetting the solution for three times. The tubes were placed again on the MPS for 1 min, then, the supernatant with non-attached content was collected and discarded. The tubes were submitted for an additional round of washing by adding and removing isolation buffer and using the MPS. After washing, the attached structures were homogenized with 100 μl of PBS and 30 μl from each tube were placed on three wells of teflon-coated slides for immunofluorescence evaluation.

Indirect capture of *in vitro* produced cysts (tests 3 and 4)

Pellets containing non-infected Marc-145 cells and *in vitro* produced cysts of *T. gondii* were each vortexed with 500 μl of isolation buffer and 5 μl of mAb K8/15-15. Each tube was agitated at 4°C (test 3) or 24°C (test 4) for 10 min using an automated mixer, then, 1 ml of isolation buffer was added to each tube, followed by centrifugation (400 g, 4 or 24°C, no brake) for 10 min. After centrifugation, the supernatant was discarded, and each pellet was suspended with 200 μl of isolation buffer and 5 μl of washed beads. The tubes were agitated using an automated mixer at 4°C (test 3) or 24°C (test 4) for 20 min. Then, 1 ml of isolation buffer was added to each tube, followed by placement of the tubes on the MPS for 2 min. The tubes were removed from the MPS, and 1 ml of isolation buffer was gently added to the tube. The content was re-suspended by gently pipetting the solution for three times. The tubes were placed again on the MPS for 1 min, then, the supernatant with non-attached content was collected and discarded. The tubes were submitted for an additional round of washing by adding and removing isolation buffer and using the MPS. After washing, the remaining material was homogenized with 100 μl of PBS and 30 μl of the content from each tube were placed on three wells of teflon-coated slides for immunofluorescence evaluation.

Separation attempt of *in vitro* produced cysts using percoll gradients

TC of *T. gondii* were generated *in vitro* as described elsewhere in this study. Host cells containing cysts of the parasite grown on a 25-cm^2 culture flask were trypsinized, blocked by adding 2 ml of fresh medium and the washed content (1 ml) transferred to a 15-ml tube. The 1 ml solution containing cysts in host cells was homogenized with 10 ml of PBS-Tween (0.05% of

Tween). Separation of cysts by Percoll gradients were conducted identically as the use of Percoll for separation of cysts produced *in vivo*. The final target fraction was resuspended with 200 µl of PBS and observed by light microscopy.

Immunofluorescence

Teflon-coated slides containing 12 wells of 5 mm diameter each were used in immunofluorescence reactions. Wells were filled with suspensions of 10 µl of host cells containing *T. gondii* cysts before capture using antibody-coated glass beads (pre-capture) and after IMS (post-capture). The slide was dried for 15 min at 37°C and stored at −20°C until analysis. For immunofluorescence reaction, the slide was fixed in cold acetone for 5 min, immersed in PBS for 10 min and dried at room temperature. The primary antibody (mAb K8/15-15), diluted at 1:2 in PBS, was added to each well and the slide was incubated in a humid chamber at 37°C for 30 min. After incubation, the slide was immersed in a washing buffer (Na_2CO_3 25 mM, $NaHCO_3$ 100 mM and NaCl 35 mM, pH 9.0) for 10 min, followed by a washing in PBS for 10 min. The slide was dried at room temperature and the secondary antibody (FITC anti-mouse IgG, Sigma Aldrich, USA) was applied at 1:50 dilution and 0.05% of Evans blue. Cysts generated in cell culture of *T. gondii* and *Hammondia heydorni* were also tested as described above, but using a rabbit anti-BAG1 (16) as a primary antibody, and Alexafluor (Alexa 488) donkey anti-rabbit-IgG (1:500) as a secondary antibody. Slides were incubated in a dark and humid chamber for 30 min and washed as described for the primary antibody. Slides were dried at room temperature and mounted with glycerin (90% glycerol and 10% of PBS) and coverglass. Reactions were analyzed at a Nikon microscope and Nikon NIS-Elements software.

Statistical analysis

Immunomagnetic capture for *in vitro* produced cysts was performed in quadruplicates, resulting in a total of 16 culture flasks for tests 1, 2, 3, and 4. The number of fluorescent cysts in three wells (total of 30 µl) was counted for each flask, and the total number of cysts per flask was extrapolated for the 100 µl solution. The cyst/host cells ratio was determined by counting the labeled cysts and host cells in five microscopic fields (600 × magnification) of each well. Pre-capture and post-capture samples was evaluated in triplicate, resulting in a total of 96 samples. The cyst/host cells ratio was determined for the pre-capture samples. The Kruskal-Wallis test was employed to compare tests 1, 2, 3, and 4 in each pre- and post-capture samples. Differences were considered statistically significant if $p < 0.05$.

Results

IMS of *in vitro* produced cysts of *T. gondii*

The post-capture samples were examined by microscopic evaluation of all fields on the entire well of the slide (Table 1). The cyst/host cell ratio for pre-capture samples were obtained after evaluation by immunofluorescence of five microscopic fields using 600 × magnification. The captured cysts exhibited fluorescence in their cyst walls and magnetic beads were attached to them. Reactions were also tested using rabbit serum to BAG1 which label bradyzoites inside the cyst (Figure 2).

IMS of *T. gondii* tissue cysts produced in mice

Tissue cysts ($n = 1{,}160$) were obtained from two chronically infected mice. About 50% of the tissue cysts were recovered after purification using Percoll gradients. The resultant suspension

TABLE 1 Immunomagnetic separation of *in vitro* produced cysts of *Toxoplasma gondii* by the direct and indirect methods using two reaction temperatures.

	Number of cysts captured per flask			
	Direct at 4°C	Direct at 24°C	Indirect at 4°C	Indirect at 24°C
	320	620	584	2,481
	330	834	396	1,590
	161	557	541	1,775
	518	570	396	2,762
Mean	332.25*	645.25	479.25	2,152*

Direct = magnetic beads anti-mouse IgG are coupled to the murine monoclonal antibody K8/15-15, and then, incubated with cyst-host cell suspension; Indirect = cyst-host cell suspension was incubated with the murine monoclonal antibody K8/15-15, and then, incubated with the magnetic beads anti-mouse IgG.
*To indicate statistically significant differences.

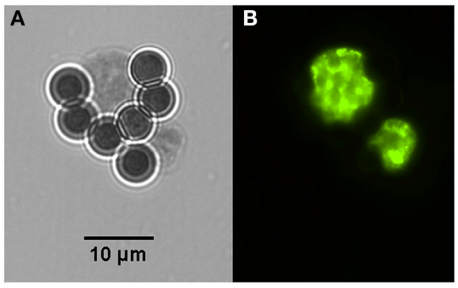

FIGURE 2
Two *in vitro* produced tissue cysts of *Toxoplasma gondii* bound to magnetic beads containing the monoclonal antibody K8/15-15. **(A)** One of the cysts has about the size of the magnetic bead, which has 4.5 µm in diameter. **(B)** Bradyzoites inside the captured cysts were labeled by immunofluorescence using a rabbit serum to the bradyzoite antigen BAG-1.

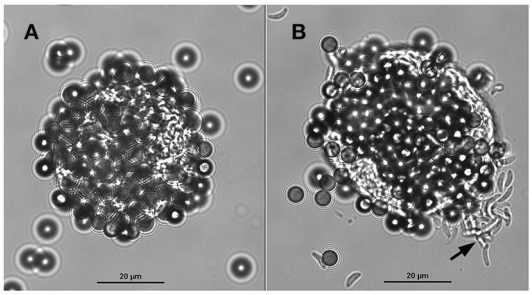

FIGURE 3
A tissue cyst of *Toxoplasma gondii* derived from mouse brain bound to magnetic beads containing the monoclonal antibody K8/15-15. **(A)** The beads cover most of the tissue cyst surface. **(B)** The same tissue cyst shown in A was mechanically ruptured by pushing the coverslip against the glass slide; note that some beads were detached from the cyst wall and numerous bradyzoites (black arrow) were released from the tissue cyst.

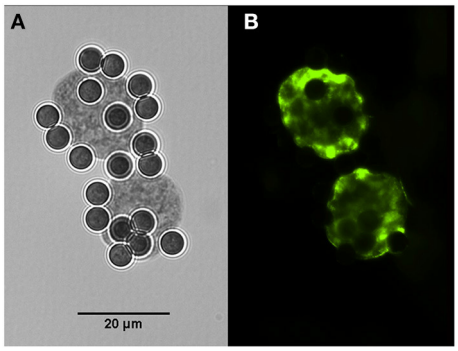

FIGURE 4
Cysts of *Hammondia heydorni* produced in cell culture and captured by magnetic beads containing the monoclonal antibody K8/15-15. **(A)** The captured cyst observed in bright field. **(B)** Immunofluorescence using a rabbit serum to the bradyzoite antigen BAG-1.

with purified tissue cysts (n = 500–600) contained ~9 mouse erythrocytes per tissue cyst. After incubation with the mAb-coupled beads, the final bead suspension was resuspended with 100 or 200 µl of PBS to facilitate the microscopical visualization of cyst-beads complexes. The surfaces of the tissue cysts were completely covered by the magnetic beads. To better visualize the tissue cysts which were covered by magnetic beads, and to ensure that they were indeed tissue cysts and not artifacts, the coverslip was mechanically pressed against the glass slide. The pressure on the coverslip caused the removal of part of the beads from the cyst wall and rupture the cyst, inducing the release of bradyzoites (Figure 3). No mouse erythrocytes were observed among the suspension. No further treatment was performed to separate tissue cysts from magnetic beads. For this reason, captured tissue cysts were not quantified.

IMS of *H. hammondi* and *H. heydorni* cysts

Cysts of *H. hammondi* and *H. heydorni* were obtained from supernatants of bovine heart cells (KH-R) infected with sporozoites of the parasites. After IMS, magnetic beads attached to cysts of both parasites were suspended in 100 µl solutions. Aliquots of 10 µl contained ~7–10 cysts, which varied in dimensions. Immunofluorescence was performed using captured cysts of *H. heydorni* (Figure 4).

All IMS methods (tests 1, 2, 3, and 4) employed in the current study showed significant increases of the cyst/host cell ratio, reaching a maximum increase of 3.78 times using test 4 (Figure 5A). Statistical difference was observed between test 4 and test 1; however, there was no statistical difference among tests 2, 3, and 4. The median of cysts isolated in each test (4 flasks per test) corresponded to 305 (test 1), 610 (test 2), 480 (test 3), and 2,170 (test 4). Non-specific capture was also examined and was based on the binding of magnetic beads to non-infected host cells (Marc-145). In all tests some degree of non-specific binding was observed. In test 3, a higher number of host cells was captured in comparison with test 4 (Figure 5B). The duration of the test for the indirect and direct method were 1 h and 1 h 10 min, respectively.

Percoll separation of *in vitro* produced cysts of *T. gondii*

The final 200 µl suspension obtained between after Percoll separation was observed by light microscopy and contained rare cells with cyst-like structures. The cysts did not migrate to the expected fractions (30 and 90% Percoll). Microscopic examination of aliquots of the top layer, which is expected to contain cell debris, revealed host cells with cyst-like structures (parasitophorous vacuoles filled with zoites); it shows that cysts produced in cell culture presented similar densities (low density) as non-infected cells (Marc-145), and for this reason, did not migrate to 30 and 90% Percoll gradients.

Discussion

We reported here an IMS method for isolation of tissue cysts of *T. gondii* using a murine IgG-mAb. The mAb-attached magnetic beads were demonstrated to bind to cyst walls of the parasite. To our knowledge, this is the first IMS method targeted for intact tissue cysts of *T. gondii*. The same mAb-attached beads also successfully captured cysts of *H. hammondi* and *H. heydorni* produced in cell culture.

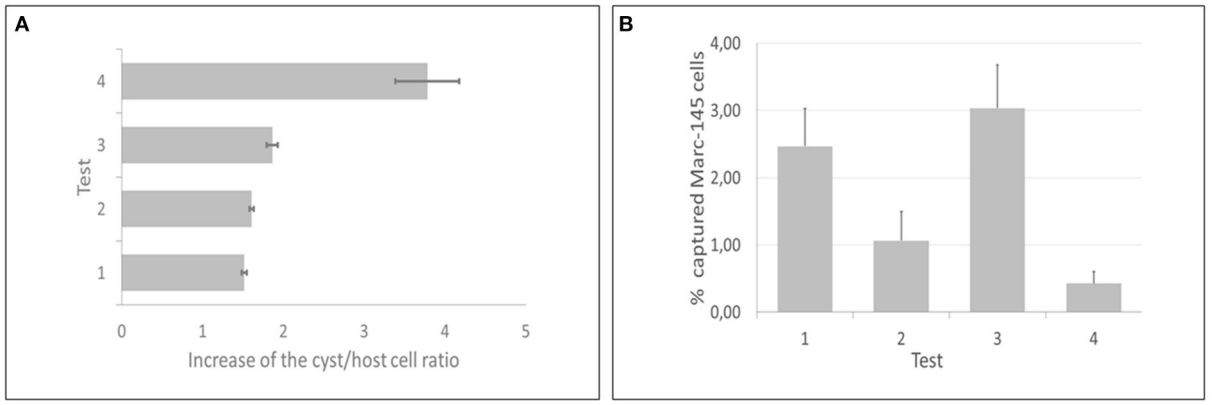

FIGURE 5
Direct and indirect immunomagnetic separation methods for *in vitro* produced cysts of *Toxoplasma gondii* were each tested at two reaction temperatures (4 and 24°C). **(A)** Test 4 (indirect capture at 24°C) presented the best performance, as the cyst/host cell ratio had a maximum increase of 3.78 times. **(B)** Test 3 (indirect capture at 4°C) showed the highest non-specific binding, contrasting with test 4, that showed the lowest non-specific binding.

A previous IMS method was developed for purification of *T. gondii* cyst wall using lysed tissue cysts from *in vivo* or *in vitro* produced cysts (17); the authors used magnetic beads coupled to *Dolichos biflorans* lectin (DBA), as DBA had been shown to bind to a cyst wall protein called CST1 (18). Three IMS methods have been developed, so far, to detect *T. gondii* oocysts or sporocysts in contaminated samples. In the first method, the authors conducted an indirect binding using an IgM mAb targeted to the oocyst wall of *T. gondii* (19); however, when this method was tested with turbid water containing debris, non-specific binding of debris to the coupled magnetic beads was observed. Another IMS was attempted with a different mAb-IgM directed to the sporocyst wall of *T. gondii* (20); in this method a direct binding was employed, i.e., the magnetic beads were firstly coupled to the mAb, followed by addition of the test sample. For this test, sonication of the test sample is needed, as sporocysts must be released from oocysts before adding the magnetic beads (20); sporocysts of related coccidia, such as *N. caninum* and *Hammondia* sp., are bound by the mAb, what required additional analysis of the samples by PCR (20). The third IMS consisted of an improvement of the previous methods and was based on the use of an IgM-mAb covalently bound to magnetic beads coupled to qPCR (21). This method showed promising results for detection of oocysts in contaminated fruits.

To our knowledge, no reported IMS method has been applied for intact tissue cysts of *T. gondii*. The IMS developed here, based on a murine IgG-mAb, can capture significant numbers of *T. gondii* cysts using a single culture flask of 25 cm^2. Moreover, this IMS is also applicable to separate cysts of related coccidia, such as *H. hammondi* and *H. heydorni*, which have been used in comparative proteomic/genomic studies with *T. gondii* (22, 23). In the present work, the IMS was qualitatively tested with *T. gondii* tissue cysts produced in mice, as these cysts became available from a previous experiment (10). The major focus of this study was IMS using *T. gondii* cysts generated in cell culture. The method resulted in expressive numbers of separated cysts (>2,000) produced in cell culture and represents a promising technique for studies involving tissue cysts.

Tissue cysts of *T. gondii* have been separated for decades using Percoll gradients (24). A great recovery of tissue cysts was achieved with this method, which has been performed in different versions and applied to isolate tissue cysts from other animal species, besides mice (14, 15). The isolated cysts obtained by Percoll gradients are quite pure, with some contamination with red blood cells. An improved Percoll separation method resulted in a pure fraction of tissue cysts with no erythrocyte contamination (25). In the present work, we used Percoll gradients, which successfully allowed the separation of tissue cysts produced in mice. When we applied the same method for *in vitro* generated tissue cysts, the cysts did not migrate to the expected gradient. The density of these cysts derived from cell culture was probably lower than those produced in mice. A similar finding was reported by others (25), who observed that the use of Percoll gradients is not indicated for separation of cysts from mutant strains; these cysts are more fragile than typical ones, so they may not resist to the separation protocol or are not able to reach the expected gradient. We have not tested the density of cyst derived from cell culture, but as these cysts are produced in 4 days, they should be more fragile and present a lower density than those developed in mice.

The IMS for *T. gondii* tissue cyst in the current work was tested using direct and indirect methods, each one evaluated at two temperatures. The indirect method, which consisted of the addition of the mAb to the cell suspension, followed by inclusion of the magnetic beads to the reaction, showed the best performance. The cyst/host cell ratio was significantly increased by using the indirect method at a reaction temperature of 24°C. Although the indirect method at 24°C (test 4) did not

statistically differed from the indirect method at 4°C (test 3), the latter one (test 3) showed a significant non-specific binding to Marc-145 cells. The direct method requires a longer initial incubation time (antibody plus magnetic beads) when compared with the incubation time (antibody plus target cell) of the indirect method. Therefore, the duration to perform the direct method was longer than the indirect one.

The mAb used here is of IgG class, what seems to minimize non-specific binding of the mAb to host cells or cell debris. Some additional experimental controls that were not included in our study, such as the use of magnetic beads uncoupled to mAb K8/15-15 to test non-specific binding of the beads to tissue cysts would certainly enrich the results obtained here. During the IMS for tissue cysts, caution should be taken to wash the complex bead-tissue cysts, as tissue cysts generated in cell culture are more fragile than those generated in mice. Instead of vortexing, the complexes should be washed by pipetting the sample using 1 ml-automatic pipettes.

In conclusion, we developed an IMS method based on the use of an IgG mAb targeted to tissue cyst walls of *T. gondii*. We could isolate significant numbers of cysts produced in cell culture. The method reported here should facilitate identification of molecules on the walls of *T. gondii* and related parasites. Moreover, it represents a promising alternative for using *in vivo* generated cysts, reducing the need of animal experiments.

Data availability statement

The original contributions presented in the study are included in the article/supplementary material, further inquiries can be directed to the corresponding author.

Ethics statement

The animal study was reviewed and approved by Landesamt für Landwirtschaft, Lebensmittelsicherheit und Fischerei of the German Federal State of Mecklenburg-Vorpommern.

Author contributions

MR-G: conducted the experiments, analyzed the results, and wrote of the manuscript. AS: performed the statistics and revised the manuscript. JD: provided samples and revised the manuscript. GS and LG: designed the experiment, provided financial support, and revised the manuscript. All authors approved the final version of the submitted manuscript.

Funding

MR-G was recipient of a fellowship by Coordenação de Aperfeiçoamento de Pessoal de Nível Superior (CAPES). This work was financially supported by Fundação de Amparo à Pesquisa do Estado da Bahia (FAPESB) under the Grant Number APP0053/2016. LG and AS are recipients of research productivity fellowships by Conselho de Desenvolvimento Científico e Tecnológico (CNPq). The generation of the mAb was partially funded by the German Federal Ministry of Education and Research (Toxonet01 and Toxonet02; funds to GS; 01KI0765 and 01KI1002F).

Conflict of interest

The authors declare that the research was conducted in the absence of any commercial or financial relationships that could be construed as a potential conflict of interest.

Publisher's note

References

1. Hill DE, Chirukandoth S, Dubey JP. Biology and epidemiology of *Toxoplasma gondii* in man and animals. *Anim Health Res Rev.* (2005) 6:41–61. doi: 10.1079/AHR2005100

2. Dubey JP, Lindsay DS, Speer CA. Structures of *Toxoplasma gondii* tachyzoites, bradyzoites, and sporozoites and biology and development of tissue cysts. *Clin Microbiol Rev.* (1998) 11:267–99. doi: 10.1128/CMR.11.2.267

3. Robert-Gangneux F, Darde ML. Epidemiology of and diagnostic strategies for toxoplasmosis. *Clin Microbiol Rev.* (2012) 25:264–96. doi: 10.1128/CMR.05013-11

4. Tu V, Yakubu R, Weiss LM. Observations on bradyzoite biology. *Microbes Infect.* (2018) 20:466–76. doi: 10.1016/j.micinf.2017.12.003

5. Tomita T, Sugi T, Yakubu R, Tu V, Ma Y, Weiss LM. Making home sweet and sturdy: *Toxoplasma gondii* Ppgalnac-ts glycosylate in hierarchical order and confer cyst wall rigidity. *Mbio.* (2017) 8:e02048–16. doi: 10.1128/mBio.02048-16

6. Parmley SF, Yang S, Harth G, Sibley LD, Sucharczuk A, Remington JS. Molecular characterization of a 65-kilodalton *Toxoplasma gondii* antigen expressed abundantly in the matrix of tissue cysts. *Mol Biochem Parasitol.* (1994) 66:283–96. doi: 10.1016/0166-6851(94)90155-4

7. Tomita T, Bzik DJ, Ma YF, Fox BA, Markillie LM, Taylor RC, et al. The *Toxoplasma gondii* cyst wall protein Cst1 is critical for cyst wall integrity and promotes bradyzoite persistence. *PLoS Pathog.* (2013) 9:e1003823. doi: 10.1371/journal.ppat.1003823

8. Milligan-Myhre K, Wilson SK, Knoll LJ. Developmental change in translation initiation alters the localization of a common microbial protein necessary for *Toxoplasma* chronic infection. *Mol Microbiol.* (2016) 102:1086–98. doi: 10.1111/mmi.13538

9. Tu V, Tomita T, Sugi T, Mayoral J, Han B, Yakubu RR, et al. The *Toxoplasma gondii* cyst wall interactome. *mBio*. (2020) 11:e02699–19. doi: 10.1128/mBio.02699-19

10. Gondim LF, Wolf A, Vrhovec MG, Pantchev N, Bauer C, Langenmayer MC, et al. Characterization of an IgG monoclonal antibody targeted to both tissue cyst and sporocyst walls of *Toxoplasma gondii*. *Exp Parasitol.* (2016) 163:46–56. doi: 10.1016/j.exppara.2016.01.014

11. Risco-Castillo V, Fernandez-Garcia A, Ortega-Mora LM. Comparative analysis of stress agents in a simplified *in vitro* system of *Neospora caninum* bradyzoite production. *J Parasitol.* (2004) 90:466–70. doi: 10.1645/GE-3298

12. Gonçalves IN, Uzêda RS, Lacerda GA, Moreira RR, Araujo FR, Oliveira RH, et al. Molecular frequency and isolation of cyst-forming coccidia from free ranging chickens in Bahia state, Brazil. *Vet Parasitol.* (2012) 190:74–9. doi: 10.1016/j.vetpar.2012.05.007

13. Rocha DS, Nilsson MG, Maciel BM, Pena HFJ, Alves BF, Silva AV, et al. Genetic diversity of *Toxoplasma gondii* isolates from free-range chickens in Bahia, Brazil. *J Parasitol.* (2018) 104:377–82. doi: 10.1645/18-9

14. Blewett DA, Miller JK, Harding J. Simple technique for the direct isolation of *Toxoplasma* tissue cysts from fetal ovine brain. *Vet Rec*. (1983) 112:98–100. doi: 10.1136/vr.112.5.98

15. Buchholz KR, Fritz HM, Chen X, Durbin-Johnson B, Rocke DM, Ferguson DJ, et al. Identification of tissue cyst wall components by transcriptome analysis of *in vivo* and *in vitro Toxoplasma gondii* bradyzoites. *Eukaryot Cell.* (2011) 10:1637–47. doi: 10.1128/EC.05182-11

16. McAllister MM, Parmley SF, Weiss LM, Welch VJ, McGuire AM. An immunohistochemical method for detecting bradyzoite antigen (Bag5) in *Toxoplasma gondii*-infected tissues cross-reacts with a *Neospora caninum* bradyzoite antigen. *J Parasitol.* (1996) 82:354–5. doi: 10.2307/3284181

17. Zhang YW, Halonen SK, Ma YF, Tanowtiz HB, Weiss LM. A purification method for enrichment of the *Toxoplasma gondii* cyst wall. *J Neuroparasitol.* (2010) 1:N101001. doi: 10.4303/jnp/N101001

18. Zhang YW, Halonen SK, Ma YF, Wittner M, Weiss LM. Initial characterization of Cst1, a *Toxoplasma gondii* cyst wall glycoprotein. *Infect Immun.* (2001) 69:501–7. doi: 10.1128/IAI.69.1.501-507.2001

19. Dumetre A, Darde ML. Immunomagnetic Separation of *Toxoplasma gondii* Oocysts using a monoclonal antibody directed against the oocyst wall. *J Microbiol Methods.* (2005) 61:209–17. doi: 10.1016/j.mimet.2004.11.024

20. Dumetre A, Darde ML. Detection of *Toxoplasma gondii* in water by an immunomagnetic separation method targeting the sporocysts. *Parasitol Res.* (2007) 101:989–96. doi: 10.1007/s00436-007-0573-0

21. Hohweyer J, Cazeaux C, Travaille E, Languet E, Dumetre A, Aubert D, et al. Simultaneous detection of the protozoan parasites *Toxoplasma*, *Cryptosporidium* and *Giardia* in food matrices and their persistence on basil leaves. *Food Microbiol.* (2016) 57:36–44. doi: 10.1016/j.fm.2016.01.002

22. Walzer KA, Wier GM, Dam RA, Srinivasan AR, Borges AL, English ED, et al. *Hammondia hammondi* harbors functional orthologs of the host-modulating effectors Gra15 and Rop16 but is distinguished from *Toxoplasma gondii* by a unique transcriptional profile. *Eukaryot Cell.* (2014) 13:1507–18. doi: 10.1128/EC.00215-14

23. Sokol SL, Primack AS, Nair SC, Wong ZS, Tembo M, Verma SK, et al. Dissection of the *in vitro* developmental program of *Hammondia hammondi* reveals a link between stress sensitivity and life cycle flexibility in *Toxoplasma gondii*. *eLife.* (2018) 7:36491. doi: 10.7554/eLife.36491

24. Cornelissen AW, Overdulve JP, Hoenderboom JM. Separation of *Isospora* (*Toxoplasma*) *gondii* cysts and cystozoites from mouse brain tissue by continuous density-gradient centrifugation. *Parasitology*. (1981) 83:103–8. doi: 10.1017/S0031182000050071

25. Watts EA, Dhara A, Sinai AP. Purification *Toxoplasma gondii* tissue cysts using Percoll gradients. *Curr Protoc Microbiol.* (2017) 45:20C 2 1–C 2 19. doi: 10.1002/cpmc.30

frontiers | Frontiers in Veterinary Science

TYPE Original Research
PUBLISHED 09 January 2023
DOI 10.3389/fvets.2022.934197

OPEN ACCESS

EDITED BY
Alessia Libera Gazzonis,
University of Milan, Italy

REVIEWED BY
Elizabeth Ferrer,
University of Carabobo, Venezuela
Marisela Hernández,
National Autonomous University of Mexico, Mexico

*CORRESPONDENCE
Biying Zhou
✉ 1458030871@qq.com

SPECIALTY SECTION
This article was submitted to Parasitology, a section of the journal Frontiers in Veterinary Science

RECEIVED 02 May 2022
ACCEPTED 07 December 2022
PUBLISHED 09 January 2023

CITATION
Li L, He W, Fan X, Liu M, Luo B, Yang F, Jiang N, Wang L and Zhou B (2023) Proteomic analysis of *Taenia solium* cysticercus and adult stages. *Front. Vet. Sci.* 9:934197. doi: 10.3389/fvets.2022.934197

Proteomic analysis of *Taenia solium* cysticercus and adult stages

Lizhu Li, Wei He, Xianmin Fan, Meichen Liu, Bo Luo, Fengjiao Yang, Nan Jiang, Lingjun Wang and Biying Zhou*

Department of Parasitology, School of Basic Medical Sciences, Zunyi Medical University, Zunyi, China

Taenia solium (*T. solium*) cysticercosis is a neglected parasitic zoonosis that occurs in developing countries. Since *T. solium* has a complex life cycle that includes eggs, oncospheres, cysticerci, and adults, presumably many proteins are produced that enable them to survive and establish an infection within the host. The objectives of this study were to perform a comparative proteomic analysis of two ontogenetic stages of *T. solium* (cysticerci and adult) and to analyze their differential expression of proteins. Methods proteins were separated by High Performance Liquid Chromatography (HPLC) fractionation, and protein samples were also digested in liquid and identified by liquid chromatography tandem mass spectrometry (LC-MS/MS); the differentially expressed proteins were then processed by a bioinformatics analysis and verified by parallel reaction monitoring (PRM). Results we identified 2,481 proteins by label-free quantitative proteomics. Then differentially expressed proteins were screened under P values < 0.05 and 2 fold change, we found that 293 proteins up-regulated and 265 proteins down-regulated. Discussion through the bioinformatics analysis, we analyzed the differences types and functions of proteins in the *Taenia solium* and cysticercus, the data will provide reference value for studying the pathogenic mechanism of the two stages and the interaction with the host, and also support for further experimental verification.

KEYWORDS

cysticercus, host-parasite interaction, mass spectrometry proteomic analysis, *Taenia solium*, parallel reaction monitoring

Introduction

Cysticercosis is caused by the larvae (cysticercus) of *Taenia solium* and is one of the 20 neglected tropical diseases according to the World Health Organization (WHO) (1). The life cycle of *T. solium* is complex, however, requiring the parasitism of two kinds of mammals, namely, pigs and humans, which serve as intermediate hosts, whereas only the latter are the final hosts. The transmission of *T. solium* from a tapeworm carrier occurs *via* the shedding of eggs in feces, followed by their ingestion by hosts (e.g., pigs and humans) and subsequent development into cysticercus (2).

In the past 10 years, vaccines and drugs have been jointly administered to pigs followed by strategic deworming treatments of infected humans (3). Because of the

complex life cycle of tapeworms, they have developed strategies to protect themselves at each specific stage, thus providing favorable conditions for their survival. For example, the activity of its metabolic enzymes is related to growth and development. In addition, cestodes have evolved specific detoxification pathways to absorb nutrients from the host as a source of their metabolic energy (4). The adult stage causes *T. solium* taeniasis in humans, and the larval stage (cysticerci) causes porcine and human cysticercosis. It can cause neurocysticercosis and seizures (5). *T. solium* cysts are known to induce persistent infections that can last for decades in humans. Establishing such long-term infections requires modulating the host immune system for a long period of time and suggests the existence of a vast array of immunoregulatory mechanisms (6, 7). This is associated with the exposure and intensity of infection as well as the developmental stage of the parasite and induced immune response. It may also be related to the inhibitory effect of T regulatory cells (8–10). Until now, however, it is unknown which parasitic molecules are responsible for these effects.

Mass spectrometry-based proteomics can detect and compare thousands of proteins on a large scale, contributing to the understanding of the functional role of proteins in biological systems. Proteomics of worms had been shown to understand their biology/pathogenesis, diagnostic biomarkers, new drug targets, or potential vaccine candidates. Several reports that investigated the proteome of *T. solium* across its developmental stages have discovered that cytoskeleton, actin, and paramyosin can be used as targets for applied research on cysticercosis vaccines and potential diagnostic antigens (e.g., enolase, calcium-binding protein, small molecule shock protein, 14-3-3 protein, tropomyosin α, α-1 tubulin, β tubulin, annexin B1, and cAMP cyclic adenylate protein-dependent kinase) (11–14). However, we expect to increase our knowledge of their pathogenesis through the *T. solium* and cysticercus proteomes.

Accordingly, in this study, we sought to compare the proteomes of two consecutive developmental stages, finding both similarities and differences between *T. solium* adults and larvae. These differences in protein activity may be crucial for influencing the parasite's invasion, survival, immune evasion, and worm development. The major goal of our study is to provide data to support experiments to understand the pathogenic mechanisms of *T. solium* adults and larvae.

Materials and methods

Parasites

A whole adult *T. solium* was obtained from a patient with taeniasis from a taeniasis-endemic area in Yajiang, Ganzi, Sichuan Province. To generate *T. solium* larvae, each healthy piglet was infected by feeding 5 pieces of mature gravid proglottids from the worm at the Animal Experimental Center of Zunyi Medical University. There were 12 piglets in this infection experiment, including 10 piglets in the infection group and 2 piglets in the control group. The healthy piglets were confirmed to be pathogen-free before infection and raised under standard conditions (15). The infected piglets were euthanized 2–3 months postinfection, and *Cysticercus cellulosae* were harvested from the muscle tissue. After obtaining the parasite, we observed its structure under a microscope.

Protein extraction

The *T. solium* was washed 3 times with phosphate-buffered saline (PBS), cut into pieces using scissors, ground and divided into 1.5 ml centrifuge tubes, and centrifuged at 4°C and 12,000 r/min for 5 min, and the supernatant was collected. The *C. cellulosae* were collected and washed three times with physiological saline and PBS, and then homogenized in a homogenizer (70 Hz/s, 10 s/time) at 4°C until completely lysed. The supernatants were collected, and their protein concentration was measured using a Bradford protein assay kit (Beyotime, China) according to the manufacturer's instructions and stored at −80°C until further use.

Each protein sample was first ground with liquid nitrogen into cell powder and then transferred into a 5-ml centrifuge tube. Next, four volumes of lysis buffer (8 M urea; Sigma, China) and 1% protease inhibitor (Calbiochem, Germany) were added to the cell powder, followed by sonication three times on ice using a high-intensity ultrasonic processor (Scientz); the remaining debris was removed by centrifugation at 12,000 *g* for 10 min at 4°C. Finally, the supernatant was collected and the protein concentration was determined using a BCA kit (Beyotime, China) according to the manufacturer's instructions.

Trypsin digestion

The protein solution was added with dithiothreitol to a final concentration of 5 mM and incubated for 30 min at 56°C. Then, iodoacetamide was added to a final concentration of 11 mM and incubated for 15 min at room temperature in the dark. Finally, the urea concentration of the sample was diluted to less than 2 M. Trypsin was added at a mass ratio of 1:50 (trypsin: protein) and digested overnight at 37°C. The trypsin was added at a mass ratio of 1:100 and was digested for 4 h and continued for 4 h.

HPLC fractionation

The tryptic peptides were separated into fractions by high pH reverse-phase HPLC, using a Thermo Betasil C18 column (5-μm particles, 10-mm inner diameter, 250-mm length). Briefly, peptides were first separated by a gradient spanning 8 to

32% acetonitrile (pH 9.0) over 60 min, which generated sixty fractions. Then, these peptides were pooled into six fractions and dried by vacuum centrifuging.

LC-MS/MS analysis

The tryptic peptides were dissolved in 0.1% formic acid (solvent A) and directly loaded onto a homemade reversed-phase analytical column (15-cm length, 75-μm inner diameter.). The gradient consisted of an increase from 6 to 23% solvent B (0.1% formic acid in 98% acetonitrile) over 26 min, followed by 23 to 35% over 8 min and climbing to 80% in 3 min, then holding it at 80% for the last 3 min, all performed at a constant flow rate of 400 nl/min on an EASY-nLC 1000 UPLC system. The peptides were subjected to a nanoelectrospray ionization (NSI) source, followed by tandem mass spectrometry (MS/MS) in a Q ExactiveTM Plus (Thermo) coupled online to the UPLC system. The electrospray voltage applied was 2.0 kV; the m/z scan range was 350 to 1,800 for each full scan, and intact peptides were detected in the Orbitrap at a resolution of 70,000. Peptides were then selected for MS/MS by using an NCE set to 28, with fragments detected in the Orbitrap at a resolution of 17,500. A data-dependent procedure was used, one that alternated between a single MS scan followed by 20 MS/MS scans with a 15.0-s dynamic exclusion. The automatic gain control (AGC) was set to 5E4. The fixed first mass was set to 100 m/z.

Database search

The secondary mass spectrum data were searched using Maxquant (version 1.5.2.8, http://www.maxquant.org/). For the retrieve parameter settings, the database is *Taenia_asiatica*_60517_PR_20190708 (10,328 sequences). Trypsin/P was specified as the cleavage enzyme, permitting up to four missing cleavages. The mass tolerance for precursor ions was set to 20 ppm in the "First search" and 5 ppm in the "Main search," while the mass tolerance for fragment ions was set to 0.02 Da. Carbamidomethyl on Cys was specified as the fixed modification and acetylation modification and oxidation on Met were specified as the variable modifications. The false discovery rate (FDR) was adjusted to <1% and a minimum score for modified peptides was set *a priori* to >40.

Bioinformatics

GO annotation

Gene ontology (GO) annotation (http://www.maxquant.org/) of the parasite's proteome was based on the UniProt-GOA database (http://www.ebi.ac.uk/GOA/). First, each identified protein ID was converted into a UniProt ID and then mapped to the existing GO IDs by protein ID. For those identified proteins that could not be annotated by the UniProt-GOA database, the InterProScan software was used to annotate the GO function of the proteins based on the protein sequence alignment method. Then, all the proteins were, respectively, classified by GO annotation according to their three main categories, namely, biological process (BP), cellular component, and molecular function.

Enrichment of pathways

The Encyclopedia of Genes and Genomes (KEGG, http://www.genome.jp/kaas-bin/kaas_main) database was used to identify enriched pathways by applying a two-tailed Fisher's exact test to test the enrichment of the differentially expressed protein against all the identified proteins. The pathway with a corrected P-value < 0.05 was considered significant. These pathways were classified into hierarchical categories, as recommended on the KEGG website.

Mass spectrometry-based targeted proteomic quantification by parallel reaction monitoring

The tryptic peptides were dissolved in 0.1% formic acid (solvent A) and directly loaded onto a homemade reversed-phase analytical column. The gradient was comprised of an increase from 6 to 23% solvent B (0.1% formic acid in 98% acetonitrile) over 38 min, 23 to 35% in 14 min, and climbing to 80% in 4 min and then holding at 80% for the last 4 min, all at a constant flow rate of 700 nl/min on an EASY-nLC 1,000 UPLC system. The peptides were subjected to an NSI source followed by tandem mass spectrometry (MS/MS) in Q ExactiveTM Plus (Thermo) coupled online to the UPLC system.

The electrospray voltage applied was 2.0 kV. The m/z scan range was 350 to 1,000 for the full scan, and intact peptides were detected in the Orbitrap at a resolution of 35,000. Peptides were then selected for MS/MS using the NCE setting as 27 and the fragments were detected in the Orbitrap at a resolution of 17,500. A data-independent procedure alternated between one MS scan followed by 20 MS/MS scans. AGC was set at 3E6 for full MS and 1E5 for MS/MS. The maximum IT was set at 20 ms for full MS and auto for MS/MS. The isolation window for MS/MS was set at 2.0 m/z.

Results

Protein identification analysis of differentially expressed proteins by LC-MS/MS

According to MS/MS analysis, the total peptide identified was 143,698, the specific peptide was 19,210, and a total of 3,658

TABLE 1 MS/MS spectrum database search analysis summary.

Total spectrum	Matched spectrum	Peptides	Unique peptides	Identified proteins	Quantifiable proteins
942,271	223,234 (23.7%)	30,689	29,761	3,658	2,481

TABLE 2 Differentially expressed protein summary (filtered according to a threshold value of expression fold-change with a *P*-value < 0.05); A = adult, L = larva.

Compared groups	Regulated type	Fold-change > 2
A/L	Upregulated	293
	Downregulated	265

proteins were identified, of which 2,481 contained quantitative information (Tables 1, 2). Relative standard deviation (RSD) was used to estimate repeatability, and a lower RSD ($n = 3$) value increases the accuracy of the repeatability (Figure 1). A corrected *P*-value of 0.05 and minimum fold-change of 2 were set as threshold criteria for determining the significant differential expression of a protein. In comparing the *T. solium* adults and larvae, we found 293 upregulated proteins (adults) and 265 downregulated proteins (cysticerci) (Supplementary Table S1).

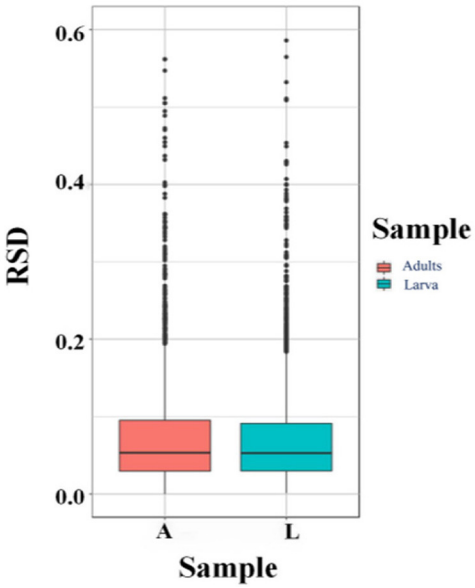

FIGURE 1
Relative standard deviations (RSDs). A, adults; L, Larva (cysticercus).

Protein functional classification based on gene ontology of differentially expressed proteins in *Taenia solium* and cysticercus stage

The identified proteins were classified according to their molecular function, cellular component, and BP. Among these differentially expressed proteins, many were found to be involved in cellular processes, biological regulation, metabolic processes, multicellular organismal processes, developmental processes, and immune system processes. The predominant molecular functions are related to binding (e.g., protein binding) and catalytic activity (hydrolase and oxidoreductase activity). Regarding BPs, the predominant number of proteins is involved in metabolic and cellular processes. For cellular components, our GO results indicated that the identified proteins are primarily associated with cell parts, intracellular, and protein-containing complexes.

The forty downregulated (cysticercus stage) proteins were most enriched in terms of regulation of immune system process at biological function; such as protein kinase C, E3 ubiquitin-protein ligase, SH2 domain-containing protein, annexin, cAMP-dependent protein kinase regulatory, and fatty acid binding protein (Supplementary Table S2). Both annexin and human plasminogen proteins are known for their strong antigenicity, hence, their use as diagnostic antigens. In addition, 25 other proteins involved as immune effectors were found (Supplementary Table S3).

The results revealed that most downregulated proteins were enriched in the regulation of protein localization to membrane, bicarbonate transport, neuroepithelial cell differentiation, and mechanoreceptor differentiation, all under the BP category. The molecular function was enriched for cytoskeletal protein binding and actin binding. The cellular component was enriched in terms of the intracellular vesicle, cytoplasmic vesicle, plasma membrane region, and secretory vesicle (Figure 2A).

The upregulated (adult stage) proteins were mainly enriched in terms of regulation of metabolic processes in biological function (Figure 3A). Most proteins are involved in the metabolic process, of which nineteen of these proteins have been studied in other parasites, all of which are related to the growth, development, and metabolism of parasites, and only 2 proteins are related to immune function (Supplementary Tables S4, S5).

KEGG enrichment of differentially expressed proteins in *Taenia solium* and *cysticercus* stage

In the cysticercus stage, the KEGG enrichments included lysosome, glutathione metabolism, porphyrin

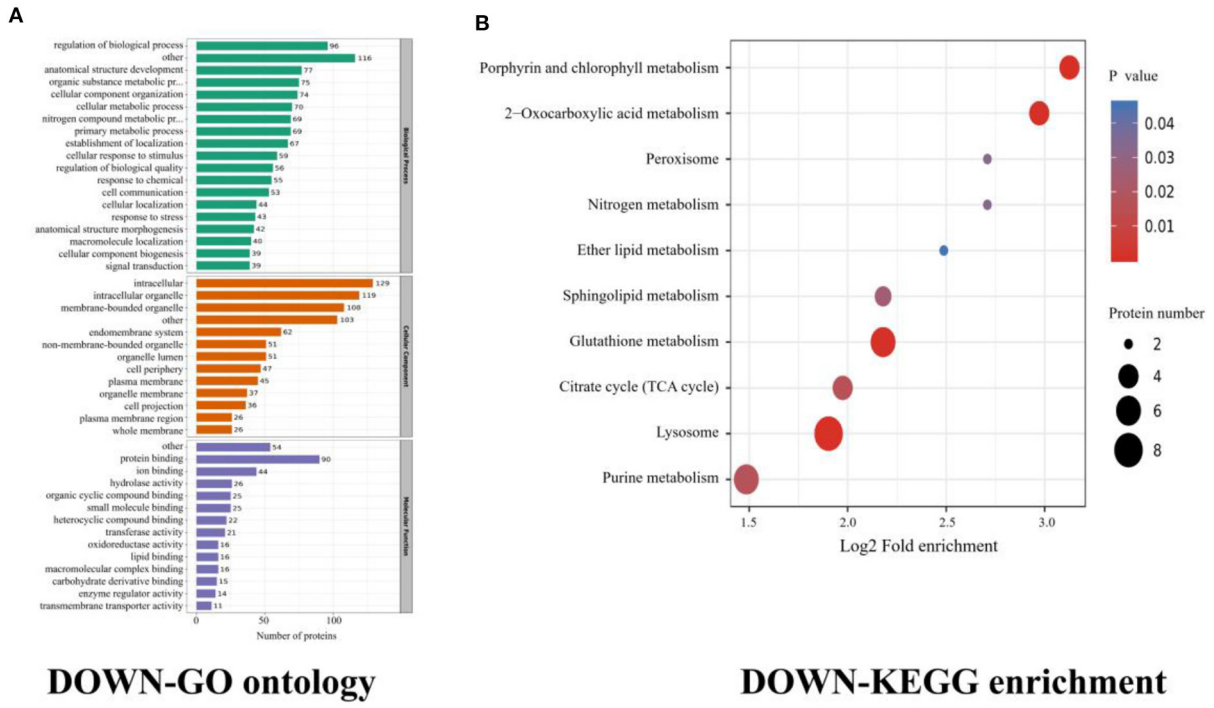

FIGURE 2
Cysticercus (downregulated) proteins GO ontology and KEGG enrichment. **(A)** Gene ontology (GO) of cysticercus, dividing the annotated proteins into 3 categories: cellular component, molecular function, and biological process. The number of genes is expressed as the number of annotation proteins. **(B)** KEGG enrichment analysis of identified proteins in cysticercus.

and chlorophyll metabolisms, and 2-oxocarboxylic acid metabolism (Figure 2B, Table 3). Isocitrate dehydrogenase [NADP], NAD_binding_2 domain-containing protein, 6PGD domain-containing protein, and phospholipid hydroperoxide glutathione were involved in glutathione metabolism; 5-aminolevulinate synthase, porphobilinogen deaminase, coproporphyrinogen III oxidase, and protoporphyrinogen oxidase were involved in porphyrin and chlorophyll metabolisms; isocitrate dehydrogenase [NADP], aconitate hydratase, and citrate synthase were involved in 2-oxocarboxylic acid metabolism; ADP ribosylation factor-binding protein GGA1, beta-galactosidase, Prosaposin a preproprotein, and LITAF domain-containing protein were involved in the lysosome.

In the adult stage, the KEGG enrichments included ribosome, pyrimidine metabolism, and ribosome biogenesis in eukaryotes. There were 18 proteins involved in the ribosome, CTP synthase, PNP_UDP_1 domain-containing protein, and Thymidylat_synt domain-containing protein were associated with pyrimidine metabolism; ribonucleoside-diphosphate reductase subunit and ribonucleoside-diphosphate reductase were involved in glutathione metabolism and pyrimidine metabolism. 39S ribosomal protein L3, 60S ribosomal protein L3, Ribosomal_L2_C domain-containing protein, 40S ribosomal protein S4, Ribosomal protein L11, Ribosomal S15a protein, Ribosomal protein l5, large subunit ribosomal protein l7e, and 39S ribosomal protein L12 were associated with the ribosome biogenesis in eukaryotes (Figure 3B, Table 4).

Differentially expressed protein quantification by mass spectrometry-based targeted proteomics

According to GO annotation and KEGG enrichments, we analyzed 9 out of 20 differentially expressed proteins with PRM instead of traditional western blotting. The quantitative information of PRM protein was calculated according to the ion peak area of the peptide. Four proteins were identified in adults (Figure 4A), namely, S1 motif domain-containing protein, Cullin-1, Protein kinase domain-containing protein, and proliferating cell nuclear antigen. Four proteins were identified in the larvae (Figure 4B), namely, citrate synthase, glutamate synthase, synaptotagmin protein 4, and neurogenic locus notch protein.

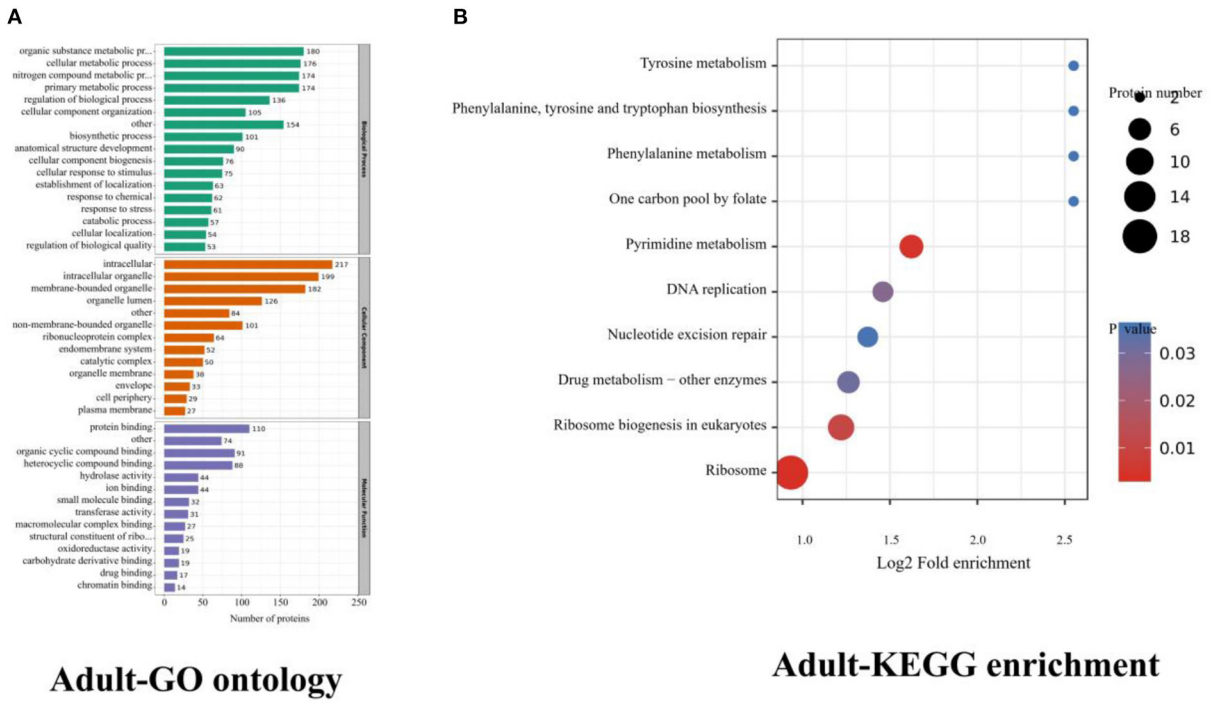

FIGURE 3
Adults (upregulated) proteins GO ontology and KEGG enrichment. **(A)** Gene ontology (GO) of adults, dividing the annotated proteins into 3 categories: cellular component, molecular function, and biological process. The number of genes is expressed as the number of annotation proteins. **(B)** KEGG enrichment analysis of identified proteins in adults.

Discussion

Examination of homologous genes among human *Taenia* tapeworms showed that 11,888 (90.3%) *T. asiatica* genes had homologs in *Taenia saginata* and *T. solium*. However, *T solium* lacks a complete proteomic database, and we performed sequence alignments between the proteins of *T. solium*'s cysticercus and adult stages by comparing them to the *T. asiatica* database—corresponding to specific proteins of this species and searching the library according to the sequence of more than one specific peptide of the protein and analyzed them using bioinformatics. Although the survival of either the cysticercus or adult depends on the energy metabolism in its host, their main energy source, carbohydrates, might be catabolized by aerobic respiration or by two complementary anaerobic pathways, those of lactate fermentation and malate dismutation (4). In addition, both rely on glutathione metabolism to grow and develop in the host. The difference is that adults can also survive through pyrimidine metabolism. Glutathione plays a role in antioxidant defense and in maintaining the reducing environment of the cytosol; many known glutathione-dependent processes are directly related to the specific lifestyle of the parasite. In the *Plasmodium falciparum*, proteins involved in GSH-dependent processes are studied as factors in the pathophysiology of malaria but also as potential drug targets (16). In KEGG enrichment of cysticercus and adults, pyrimidine and purine are the raw materials for the synthesis of DNA and RNA. The parasite itself synthesizes pyrimidine and forms its own set of survival mechanisms, therefore, generating new lead compounds to treat malaria and schistosomes by targeting purine and pyrimidine pathways (17, 18). Glutathione-related enzymes were identified in the proteomics of both adults and larvae, while proteins involved in pyrimidine metabolism were only identified in adults. Pyrimidine metabolic pathway can be used as an idea for the treatment of taeniasis, which also shows the differences in growth and development between adults and larvae.

Analyzing the genomes of four species of tapeworms, the researchers found that there were a large number of genes lost in the genome in order to adapt to parasitic life, but some genes that can increase the survival rate of the parasite were amplified simultaneously. For example, the tapeworm genome lacks genes related to synthesizing fatty acids and cholesterol *de novo* (19, 20). Over time, tapeworms have lost their ability to synthesize essential fats and cholesterol essential for larval development, which they obtain from their hosts. However, there are a large number of lipid elongating enzymes and fatty acid transporter genes, and a large number of fatty acid-binding

TABLE 3 KEGG enrichment of differentially expressed proteins in cysticercus.

KEGG pathway	Protein accession	Protein description	Ratio	*p* value
Lysosome	A0A0R3WB48	ADP ribosylation factor binding protein GGA1 (predicted)	0.356	0.0001596
	A0A0R3W2H9	Peptidase A1 domain-containing protein (predicted)	0.343	3.825E-05
	A0A0R3W9I1	Beta-galactosidase	0.332	3.743E-05
	A0A0R3W6D3	SSD domain-containing protein (predicted)	0.495	0.0001026
	A0A0R3W4P0	Prosaposin a preproprotein (predicted)	0.265	1.792E-06
	A0A0R3VUB5	LITAF domain-containing protein (predicted)	0.496	0.0004954
	A0A0R3WF80	ML domain-containing protein (predicted)	0.152	4.469E-05
	A0A0R3VWZ7	Cathepsin L-like cysteine peptidase (predicted)	0.25	0.0004831
Glutathione metabolism	A0A0R3W597	Sigma-type glutathione S-transferase (predicted)	0.133	2.071E-05
	A0A0R3WGD8	6PGD domain-containing protein (predicted)	0.336	1.574E-05
	A0A0R3WDK3	Phospholipid hydroperoxide glutathione (predicted)	0.376	0.0002813
	A0A0R3W2C6	Glutathione transferase (predicted)	0.233	4.331E-06
	A0A0R3WC84	Isocitrate dehydrogenase [NADP]	0.018	2.789E-07
	A0A0R3VXS3	NAD_binding_2 domain-containing protein (predicted)	0.4	0.00028
Porphyrin and chlorophyll metabolism	A0A0R3WES1	5-aminolevulinate synthase	0.259	0.010716
	A0A0R3W2K4	Porphobilinogen deaminase (predicted)	0.249	4.424E-05
	A0A0R3W1Y3	Coproporphyrinogen III oxidase (predicted)	0.112	8.166E-05
	A0A0R3W877	Protoporphyrinogen oxidase	0.36	2.51E-06
2-Oxocarboxylic acid metabolism	A0A0R3VW15	Aconitate hydratase, mitochondrial	0.27	3.231E-06
	A0A0R3W1A1	Citrate synthase	0.086	1.44E-09
	A0A0R3WA42	Aminotran_1_2 domain-containing protein (predicted)	0.17	0.0002166
	A0A0R3WC84	Isocitrate dehydrogenase [NADP]	0.018	2.789E-07

proteins and apolipoprotein B antigens are expressed, which may be related to the parasite consuming a lot of nutrients in the process of growth and development. These proteins have been identified in the proteomics of both adults and larvae.

The transcriptome is used to study the expression and regulation level of functional gene mRNA, which is highly sensitive to the detection of differentially expressed genes and can more truly reflect the whole process of complex expression regulation of transcriptome. Through the transcriptome analysis of *T. solium* cysticerci, it was found that paramyosin, major egg antigen, cathepsin L-like cysteine proteinase, heat shock protein 70 kDa protein, and H17g or TEG-Tsol surface antigen (21) have the potential to develop worm antigens for immunodiagnosis or vaccine (22). Similar to the results of proteomic analysis, most of the proteins are also involved in cell process, catalytic activity, and binding proteins. The selection of diagnostic antigens was based on the cloning of genes encoding the antigens or the screening of recombinant antigens from the *T. solium* cDNA library, which is relevant to the identification of different regions, developmental stages, and body parts of *T. solium* (21, 23–27). Transcriptome can observe the expression and regulation level of mRNA at different time points and observe the related pathways more intuitively. Proteomics is the identification of the whole protein in the sample and can only observe static proteins in sample preparation. On the basis of the transcriptome, it can have a more comprehensive understanding of the pathogenic mechanism and treatment of C. cellulosae.

Identified proteins in the cysticercus (downregulated)

Through a functional enrichment analysis, we found 25 proteins involving the immune process in the larva. It included known proteins such as thioredoxin peroxidase, calcium-binding protein 39, fatty acid-binding protein FABP2, and protein kinase C. Calcium-binding protein is involved in various regulatory functions of host invasion by parasites, and these mainly include members of the calmodulin family (CAM), the calcineurin B-like (CBL) family, and the calcium-dependent protein kinase (CDPK) family: all of these are highly conserved helix–loop–helix structure, namely, the EF-hand domain. In

TABLE 4 KEGG enrichment of differentially expressed proteins in the adult stage.

KEGG pathway	Protein accession	Protein description	Ratio	*p* value
Ribosome	A0A0R3WCV3	39S ribosomal protein L12 (predicted)	2.028	0.0027817
	A0A0R3VVI0	Ribosomal protein L11 (predicted)	2.117	0.0002648
	A0A0R3W3C5	40S ribosomal protein S4	2.346	1.86E-05
	A0A0R3W4M0	40S ribosomal protein S15 (predicted)	2.16	0.0006813
	A0A0R3VSK8	60S ribosomal protein L3 (predicted)	2.105	1.671E-05
	A0A0R3W1U3	60S ribosomal protein L6 (Fragment) (predicted)	3.029	0.0001604
	A0A0R3VVJ5	Ribosomal S15a protein (predicted)	2.287	4.257E-06
	A0A0R3W373	Large subunit ribosomal protein l7e (predicted)	2.233	0.0010246
	A3F4S0	60S ribosomal protein L18	2.934	8.693E-07
	A0A0R3WDH4	60S ribosomal protein L35a (predicted)	2.078	0.0002394
	A0A0R3W3L7	60S ribosomal protein L36 (predicted)	2.887	0.0007586
	A0A0R3VT58	Ribosomal protein L15	2.288	0.000801
	A0A0R3WC08	Ribosomal_L2_C domain-containing protein (predicted)	2.27	0.0019432
Pyrimidine metabolism	A0A0R3W9Z3	PNP_UDP_1 domain-containing protein (predicted)	6.624	4.536E-09
	A0A0R3W9X3	Ribonucleoside diphosphate reductase subunit (predicted)	25.427	4.19E-06
	A0A0R3W5N1	Purine nucleoside phosphorylase	544.455	0.0002366
	A0A0R3WBK6	Thymidylat_synt domain-containing protein (predicted)	5.608	0.033756
	A0A0R3WB77	Purine nucleoside phosphorylase	11.818	0.0036187
	A0A0R3W2V2	Ribonucleoside-diphosphate reductase	30.579	0.0001017
	A0A0R3WDN1	CTP synthase	2.942	4.126E-05
Ribosome biogenesis in eukaryotes	A0A0R3WAR2	Ribosome biolocus tagsis protein BMS1 (predicted)	5.45	0.036556
	A0A0R3WCI1	rRNA 2 O methyltransferase fibrillarin (predicted)	2.055	4.133E-05
	A0A158R6D7	RNA cytidine acetyltransferase	2.041	0.0182639
	A0A0R3WDJ3	Nuclear valosin containing protein (predicted)	2.264	0.0002803
	A0A0R3W7X6	AAA family ATPase (predicted)	2.651	0.000219
	A0A0R3W830	Ribosomal_L7Ae domain-containing protein (predicted)	2.032	0.0001434
	A0A0R3VW23	OBG-type G domain-containing protein (predicted)	2.274	5.622E-05
	A0A0R3WB31	Nop domain-containing protein (predicted)	2.214	7.687E-05

Plasmodium and *Toxoplasma*, phosphatidylinositol can also be stimulated by ligands binding to surface receptors (such as G-protein binding receptors [GPCR]), to produce calcium signals, thereby stimulating multiple cellular pathways (28). Fatty acid-binding proteins (FABPs) are a family of proteins with binding of triclabendazole (29), anti-oxidant activity, and immunomodulation (30). It is used as a potential drug target in *Echinococcus granulosus* and schistosomiasis (31, 32). Some proteins have been studied for immunity in other parasitic worms. For example, the *Trichinella spiralis* ES product thioredoxin peroxidase-2 induces macrophages toward an M2-like phenotype, both *in vivo* and *in vitro*, and $CD4^+$T cells increased in number after immunization of mice with rTsTPX2 and mediate the expulsion of the worm from the host to protect them, thus suggesting TsTPX2 is a potential vaccine candidate against trichinosis (33). Also, thioredoxin peroxidase was significantly recognized by melioidosis-positive sera in the cysticercus stage, for which strong immunogenic properties render it an anticipated vaccine target (34). Pyruvate kinase is a crucial glycolytic enzyme that has been characterized in *Clonorchis sinensis* (35) and it promotes the development of Th1 and inhibition of dendritic cells (DCs).

Some researchers revealed that fructose-1-6-bisphosphate aldolase (FBPA) proteins of *T. solium* cyst fluid were mainly enriched PI3K-Akt signaling pathways which are thought to play important roles in proliferation, migration, invasion, and drug resistance (36, 37). FBPA is a crucial glycolytic enzyme and a plasminogen-binding protein and is involved in parasitic motion

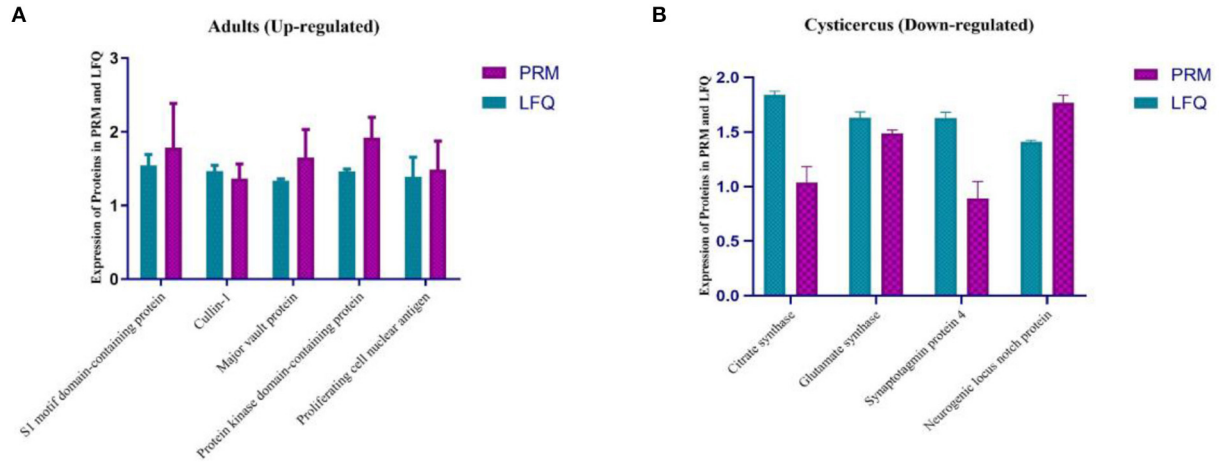

FIGURE 4
(A, B) Differentially expressed protein quantification by mass spectrometry-based targeted proteomics (PRM). PRM, parallel reaction monitoring; LFQ, lab-free quantitation.

and invasion by connecting surface adhesion proteins to the actin-myosin of parasites (38). Specifically, FBPA binds to the surface of the cell membrane, and then binds to plasminogen, using the activity of hydrolyzing surface-related proteins to help invade host cells; hence, it is also considered a potential vaccine candidate or chemotherapy target for *Trichinella spiralis* and *Giardia* infections (39–41).

Furthermore, antigens and immunomodulatory proteins observed in cysticercus are able to play a special mechanism of adaptation at this developmental stage, one that has evolved to evade the host immune system, which is a prerequisite for establishing a successful infection. We have only discussed the known proteins, and there are still several unknown proteins with specific functions that need to be verified.

Identified proteins in the adults (upregulated)

Lacking a digestive tract, *T. solium* instead absorbs nutrients from its host across the body wall. The cortex absorbs all kinds of nutrients by means of diffusion and active transport, and it also has the function of secreting and resisting the destruction of the host's digestive juice. Their main energy source, carbohydrates, can be catabolized by aerobic respiration or by two complementary anaerobic pathways, namely, lactate fermentation and malate dismutation (4). In this study, we found the upregulated proteins, most of the proteins are related to metabolism. Following PRM analysis, we found that the expression of four proteins (S1 motif domain-containing protein, Cullin-1, protein kinase domain-containing protein, and proliferating cell nuclear antigen) was consistently elevated, and several proteins whose functions are lacking in the study of the porcine tapeworm have important values in other parasite fields, which provides us with different insights into the tapeworm. Cullin protein is the most typical ubiquitin ligase family and a key tumor-associated protein, which is able to promote the proliferation of tumor cells and also can be used as a marker and therapeutic target for tumor prognosis. According to the GO analysis, the Cullin protein is also involved in cell cycle progression, signal transduction and transcription, intracellular metabolism, and the corresponding response to stimuli. However, this protein has not been studied in parasites and could be a research target to be verified in the next experiments (42–44). Proliferating cell nuclear antigen (PCNA) is a protein that acts as a processivity factor for DNA polymerase δ in eukaryotic cells and was originally identified as an antigen expressed in the nuclei of cells during the DNA synthesis phase of the cell cycle (45, 46). The major vault protein is a ribonucleoprotein that is highly conserved in lower and higher eukaryotes, and its function is not clear (47). Some studies have found that *Schistosoma mansoni* participates in the adaptation mechanism of parasitic hosts in the process of infection.

Topoisomerase is a critical type of enzyme for overcoming the problem of chromosome topology that arises during DNA replication, transcription, recombination, and mitosis, and they are involved in cell growth, tissue development, and cell differentiation (48–50). These enzymes participate in a variety of DNA metabolic processes; in the parasitic infection, the inhibition of topoisomerase II by different ketone benzene and furan derivatives in cells hinders the basic metabolic process of cells and eventually leads to apoptosis. In view

of the parasite DNA topoisomerase II, these compounds can be used as potential antiparasitic drugs. *Schistosome* parasite miRNA mediates the activity of the frizzled protein (frizzled-related protein 1), which increases liver fibrosis, in that FRZB2 is a secreted frizzled protein-related protein, which can competitively bind to specific frizzled protein receptors to suppress the signal transduction of Wnt, thus affecting the severity of liver fibrosis. The FRZB2 gene knockdown affected *S. japonicum* morphology, development, survival, as well as reproductive capacity (51, 52). *Plasmodium* glyceraldehyde-3-phosphate dehydrogenase functions as a glycolytic enzyme and also as a host plasminogen-binding protein, thereby interacting with the host's fibrinolytic system to establish an important mechanism for a parasite's invasion, growth, and development. At the same time, it can be used as a potential diagnostic biomarker for a variety of parasites, such as *Plasmodium*, *T. solium*, *E. granulosus*, filariasis, *S. mansoni*, and *Babesia microti* (53–57). The distinct mechanisms of cell cycle arrest are associated with the upregulating or downregulating of TbPCNA. Deregulating the intra-parasite levels of TbPCNA is a potential strategy for therapeutically exploiting this target in the bloodstream form of *Trypanosoma brucei*, which shows that PCNA is related to that parasite's growth and development (58).

Adults only survive in the host's intestines and escape the immune response without causing excessive damage to the host. In our study, we found that there are few proteins related to immunity, and most of them are related to growth and development, which also reflects the difference between adults and larvae to the host.

Conclusion

Cysticercosis/taeniosis remains a serious neglected public health problem in many developing countries. Even if there are preventive and therapeutic approaches, we need to be constantly updated it. Proteomics now gives us a broader platform for research. In the previous several years, tremendously useful advances were made in the field of proteomics in terms of rapid and sensitive technologies, which provided greater proteome coverage. We profiled the proteome of *T. solium*'s cysticercus and adult stages. We analyzed the different types and functions of proteins in *T. solium* and cysticercus. The data will provide a reference value for studying the pathogenic mechanism of the two stages and the interaction with the host, as well as support for further experimental verification.

Data availability statement

The datasets presented in this study can be found in online repositories. The names of the repository/repositories and accession number(s) can be found in the article/Supplementary material.

Ethics statement

The animal study was reviewed and approved by Zunyi Medical University's ethical review of experimental animals.

Author contributions

BL and WH completed data curation. FY and LW provided software support. NJ and ML provided experimental methodology. LL drafted the manuscript and drew the figures. BZ checked and modified the manuscript. All authors contributed to the article and approved the submitted version.

Funding

This study was supported by the National Natural Science Foundation of China (Grant No. 81960378); the Guizhou Science and Technology Cooperation Foundation ([2018]1190); and the Youth Science and Technology Talent Growth Project of the Guizhou Educational Department ([2017]187).

Acknowledgments

We thank Jingjie PTM BioLabs (Hangzhou, China) for supporting LFQ and PRM proteomics analysis.

Conflict of interest

The authors declare that the research was conducted in the absence of any commercial or financial relationships that could be construed as a potential conflict of interest.

Publisher's note

Supplementary material

The Supplementary Material for this article can be found online at: https://www.frontiersin.org/articles/10.3389/fvets.2022.934197/full#supplementary-material

References

1. Organization WHO. *Neglected tropical diseases: enhancing safe treatment for more than 1 billion people annually.* (2021).

2. Garcia HH, Gonzalez AE, Evans CA, Gilman RH. Cysticercosis working group in peru. *Taenia solium* cysticercosis. *Lancet.* (2003) 362:547–56. doi: 10.1016/S0140-6736(03)14117-7

3. Lightowlers MW, Donadeu M. Designing a minimal intervention strategy to control *Taenia solium*. *Trends Parasitol.* (2017) 33:426–34. doi: 10.1016/j.pt.2017.01.011

4. Tsai IJ, Zarowiecki M, Holroyd N, Garciarrubio A, Sanchez-Flores A, Brooks KL, et al. The genomes of four tapeworm species reveal adaptations to parasitism. *Nature.* (2013) 496:57–63. doi: 10.1038/nature12031

5. Garcia HH, Rodriguez S, Friedland JS. Cysticercosis working group in peru. Immunology of Taenia solium taeniasis and human cysticercosis. *Parasite Immunol.* (2014) 36:388–96. doi: 10.1111/pim.12126

6. Grewal JS, Kaur S, Bhatti G, Sawhney IM, Ganguly NK, Mahajan RC, et al. Cellular immune responses in human neurocysticercosis. *Parasitol Res.* (2000) 86:500–3. doi: 10.1007/s004360050701

7. Chavarria A, Roger B, Fragoso G, Tapia G, Fleury A, Dumas M, et al. TH2 profile in asymptomatic *Taenia solium* human neurocysticercosis. *Microbes Infect.* (2003) 5:1109–15. doi: 10.1016/S1286-4579(03)00206-5

8. Adalid-Peralta L, Lopez-Roblero A, Camacho-Vazquez C, Najera-Ocampo M, Guevara-Salinas A, Ruiz-Monroy N, et al. Regulatory t cells as an escape mechanism to the immune response in *taenia crassiceps* infection. *Front Cell Infect Microbiol.* (2021) 11:630583. doi: 10.3389/fcimb.2021.630583

9. Prodjinotho UF, Lema J, Lacorcia M, Schmidt V, Vejzagic N, Sikasunge C, et al. Host immune responses during *Taenia solium* neurocysticercosis infection and treatment. *PLoS Negl Trop Dis.* (2020) 14:e0008005. doi: 10.1371/journal.pntd.0008005

10. Verma A, Prasad KN, Cheekatla SS, Nyati KK, Paliwal VK, Gupta RK. Immune response in symptomatic and asymptomatic neurocysticercosis. *Med Microbiol Immunol.* (2011) 200:255–61. doi: 10.1007/s00430-011-0198-x

11. Santivanez SJ, Hernandez-Gonzalez A, Chile N, Oleaga A, Arana Y, Palma S, et al. Proteomic study of activated *Taenia solium* oncospheres. *Mol Biochem Parasitol.* (2010) 171:32–9. doi: 10.1016/j.molbiopara.2010.01.004

12. Victor B, Kanobana K, Gabriel S, Polman K, Deckers N, Dorny P, et al. Proteomic analysis of *Taenia solium* metacestode excretion-secretion proteins. *Proteomics.* (2012) 12:1860–9. doi: 10.1002/pmic.201100496

13. Navarrete-Perea J, Moguel B, Bobes RJ, Villalobos N, Carrero JC, Sciutto E, et al. Protein profiles of *Taenia solium* cysts obtained from skeletal muscles and the central nervous system of pigs: Search for tissue-specific proteins. *Exp Parasitol.* (2017) 172:23–9. doi: 10.1016/j.exppara.2016.11.006

14. da Costa GCV, Peralta RHS, Kalume DE, Alves A, Peralta JM, A. gel-free proteomic analysis of *Taenia solium* and *Taenia crassiceps* cysticerci vesicular extracts. *Parasitol Res.* (2018) 117:3781–90. doi: 10.1007/s00436-018-6080-7

15. Fan XM, Zhang Y, Ouyang RH, Luo B, Li LZ, He W, et al. Cysticercus cellulosae regulates t-Cell responses and interacts with the host immune system by excreting and secreting antigens. *Front Cell Infect Microbiol.* (2021) 11:728222. doi: 10.3389/fcimb.2021.728222

16. Becker K, Rahlfs S, Nickel C, Schirmer RH. Glutathione–functions and metabolism in the malarial parasite *Plasmodium falciparum*. *Biol Chem.* (2003) 384:551–66. doi: 10.1515/BC.2003.063

17. Cassera MB, Zhang Y, Hazleton KZ, Schramm VL. Purine and pyrimidine pathways as targets in *plasmodium falciparum*. *Curr Top Med Chem.* (2011) 11:2103–15. doi: 10.2174/156802611796575948

18. el Kouni, H. M. Pyrimidine metabolism in *schistosomes*: A comparison with other parasites and the search for potential chemotherapeutic targets. *Comp Biochem Physiol B Biochem Mol Biol.* (2017) 213:55–80. doi: 10.1016/j.cbpb.2017.07.001

19. Berriman M, Haas BJ, LoVerde PT, Wilson RA, Dillon GP, Cerqueira GC, et al. The genome of the blood fluke *Schistosoma mansoni*. *Nature.* (2009) 460:352–8. doi: 10.1038/nature08160

20. Frayha GJ. Comparative metabolism of acetate in the taeniid tapeworms *Echinococcus granulosus*, *E. multilocularis* and Taenia hydatigena. *Comp Biochem Physiol B.* (1971) 39:167–70. doi: 10.1016/0305-0491(71)90264-1

21. Parkhouse RM, Bonay P, Gonzalez LM, Ferrer E, Garate T, Aguilar CM, et al. TSOL18/HP6-Tsol, an immunogenic *Taenia solium* oncospheral adhesion protein and potential protective antigen. *Parasitol Res.* (2008) 102:921–6. doi: 10.1007/s00436-007-0853-8

22. Almeida CR, Stoco PH, Wagner G, Sincero TC, Rotava G, Bayer-Santos E, et al. Transcriptome analysis of *Taenia solium* cysticerci using Open Reading Frame ESTs (ORESTES). *Parasit Vectors.* (2009) 2:35. doi: 10.1186/1756-3305-2-35

23. Garrido O, Requena D, Flores Angulo C, Gárate T, Ferrer E. Spliced leader gene cloning from expression library of *Taenia solium* cysticerci. *Salus J.* (2012) 16:13–22. Available online at: http://ve.scielo.org/scielo.php?script=sci_arttext&pid=S1316-71382012000100004&lng=es&tlng=

24. Garrido O, Gárate T, Ferrer E. Sequences analysis of molecules of *Taenia solium* post-transcriptionally processed by trans-splicing. *Bol Malariol Salud Ambient.* (2015) 55:41–51. Available online at: http://ve.scielo.org/scielo.php?script=sci_arttext&pid=S1690-46482015000100003&lng=es&tlng=

25. Ferrer E, Gonzalez LM, Foster-Cuevas M, Cortez MM, Davila I, Rodriguez M, et al. *Taenia solium:* characterization of a small heat shock protein (Tsol-sHSP356) and its possible relevance to the diagnosis and pathogenesis of neurocysticercosis. *Exp Parasitol.* (2005) 110:1–11. doi: 10.1016/j.exppara.2004.11.014

26. Ferrer E, Bonay P, Foster-Cuevas M, Gonzalez LM, Davila I, Cortez MM, et al. Molecular cloning and characterisation of Ts8B1, Ts8B2 and Ts8B3, three new members of the *Taenia solium* metacestode 8 kDa diagnostic antigen family. *Mol Biochem Parasitol.* (2007) 152:90–100. doi: 10.1016/j.molbiopara.2006.12.003

27. Morillo M, Noguera C, Gallego L, Fernandez Z, Mata M, Khattar S, et al. Characterization and evaluation of three new recombinant antigens of *Taenia solium* for the immunodiagnosis of cysticercosis. *Mol Biochem Parasitol.* (2020) 240:111321. doi: 10.1016/j.molbiopara.2020.111321

28. Berridge MJ. Inositol trisphosphate and calcium signalling mechanisms. *Biochim Biophys Acta.* (2009) 1793:933–40. doi: 10.1016/j.bbamcr.2008.10.005

29. Chemale G, Perally S, LaCourse EJ, Prescott MC, Jones LM, Ward D, et al. Comparative proteomic analysis of triclabendazole response in the liver fluke Fasciola hepatica. *J Proteome Res.* (2010) 9:4940–51. doi: 10.1021/pr1000785

30. Cwiklinski K, Dalton JP, Dufresne PJ, La Course J, Williams DJ, Hodgkinson J, et al. The Fasciola hepatica genome: gene duplication and polymorphism reveals adaptation to the host environment and the capacity for rapid evolution. *Genome Biol.* (2015) 16:71. doi: 10.1186/s13059-015-0632-2

31. Vicente B, Lopez-Aban J, Rojas-Caraballo J, del Olmo E, Fernandez-Soto P, Muro A. Protection against Schistosoma mansoni infection using a Fasciola hepatica-derived fatty acid binding protein from different delivery systems. *Parasit Vectors.* (2016) 9:216. doi: 10.1186/s13071-016-1500-y

32. Bélgamo JA, Alberca LN, Pórfido JL, Romero FNC, Rodriguez S, Talevi A, et al. Application of target repositioning and in silico screening to exploit fatty acid binding proteins (FABPs) from *Echinococcus multilocularis* as possible drug targets. *J Comput Aid Mol Des.* (2020) 34:1275–88. doi: 10.1007/s10822-020-00352-8

33. Jin QW, Zhang NZ Li WH, Qin HT, Liu YJ, Ohiolei JA, et al. *Trichinella spiralis* thioredoxin peroxidase 2 regulates protective th2 immune response in mice by directly inducing alternatively activated macrophages. *Front Immunol.* (2020) 11:2015. doi: 10.3389/fimmu.2020.02015

34. Yin C, Luo XN, Wang S, Chen GL, Zeng QY, Cai XP. Prokaryotic expression and biological properties of thioredoxin peroxidase from *Taenia solium*. *Zootechn. Sinica*. (2014) 45:1512–17.

35. Chen T, Jiang H, Sun H, Xie Z, Ren P, Zhao L, et al. Sequence analysis and characterization of pyruvate kinase from Clonorchis sinensis, a 531-kDa homopentamer, implicated immune protective efficacy against clonorchiasis. *Parasit Vectors.* (2017) 10:557. doi: 10.1186/s13071-017-2494-9

36. Gasparri ML, Besharat ZM, Farooqi AA, Khalid S, Taghavi K, Besharat RA, et al. MiRNAs and their interplay with PI3K/AKT/mTOR pathway in ovarian cancer cells: a potential role in platinum resistance. *J Cancer Res Clin Oncol.* (2018) 144:2313–8. doi: 10.1007/s00432-018-2737-y

37. Cui Y, Wang X, Xu J, Liu X, Wang X, Pang J, et al. Proteomic analysis of *taenia solium* cyst fluid by shotgun LC-MS/MS. *J Parasitol.* (2021) 107:799–809. doi: 10.1645/20-65

38. Diaz SA, Martin SR, Grainger M, Howell SA, Green JL, Holder AA. *Plasmodium falciparum* aldolase and the C-terminal cytoplasmic domain of certain apical organellar proteins promote actin polymerization. *Mol Biochem Parasitol.* (2014) 197:9–14. doi: 10.1016/j.molbiopara.2014.09.006

39. Gao X, Bao S, Xing X, Fu X, Zhang Y, Xue H, et al. Fructose-1,6-bisphosphate aldolase of *Mycoplasma bovis* is a plasminogen-binding adhesin. *Microb Pathog.* (2018) 124:230–7. doi: 10.1016/j.micpath.2018.08.032

40. Boucher LE, Bosch J. Structure of *Toxoplasma gondii* fructose-1,6-bisphosphate aldolase. *Acta Crystallogr F Struct Biol Commun.* (2014) 70:1186–92. doi: 10.1107/S2053230X14017087

41. Galkin A, Kulakova L, Melamud E, Li L, Wu C, Mariano P, et al. Characterization, kinetics, and crystal structures of fructose-1,6-bisphosphate aldolase from the human parasite, *Giardia lamblia*. *J Biol Chem.* (2007) 282:4859–67. doi: 10.1074/jbc.M609534200

42. Zhou YH, Xia J, Xu WH, Zhu X, Wu XH, Hua D, et al. Cullin-1 promotes cell proliferation in human breast cancer and is related to diabetes. *Int J Biol Markers.* (2016) 31:e375–81. doi: 10.5301/jbm.5000215

43. Sweeney MA, Iakova P, Maneix L, Shih F-Y, Cho HE, Sahin E, et al. The ubiquitin ligase Cullin-1 associates with chromatin and regulates transcription of specific c-MYC target genes. *Sci Rep.* (2020) 10:13942. doi: 10.1038/s41598-020-70610-0

44. Cheng Q, Yin G. Cullin-1 regulates MG63 cell proliferation and metastasis and is a novel prognostic marker of osteosarcoma. *Int J Biol Markers.* (2017) 32:e202–9. doi: 10.5301/jbm.5000247

45. Bravo R, Frank R, Blundell PA, Macdonald-Bravo H. Cyclin/PCNA is the auxiliary protein of DNA polymerase-delta. *Nature.* (1987) 326:515–7. doi: 10.1038/326515a0

46. Strzalka W, Ziemienowicz A. Proliferating cell nuclear antigen (PCNA) : a key factor in DNA replication and cell cycle regulation. *Ann Bot.* (2011) 107:1127–40. doi: 10.1093/aob/mcq243

47. Das D, Wang YH, Hsieh CY, Suzuki YJ. Major vault protein regulates cell growth/survival signaling through oxidative modifications. *Cell Signal.* (2016) 28:12–8. doi: 10.1016/j.cellsig.2015.10.007

48. Champoux JJ, DNA. Topoisomerases: structure, function, and mechanism. *Annu Rev Biochem.* (2001) 70:369–413. doi: 10.1146/annurev.biochem.70.1.369

49. Vos SM, Tretter EM, Schmidt BH, Berger JM. All tangled up: how cells direct, manage and exploit topoisomerase function. *Nat Rev Mol Cell Biol.* (2011) 12:827–41. doi: 10.1038/nrm3228

50. Heng X, Le W-D. The function of DNA topoisomerase IIβ in neuronal development. *Neurosci Bull.* (2010) 26:411–6. doi: 10.1007/s12264-010-0625-9

51. Wang Y, Fan X, Lei N, He X, Wang X, Luo X, et al. A microrna derived from *schistosoma japonicum* promotes schistosomiasis hepatic fibrosis by targeting host secreted frizzled-related protein 1. *Front Cell Infect Microbiol.* (2020) 10:101. doi: 10.3389/fcimb.2020.00101

52. Mishra A, Vinayagam J, Saha S, Chowdhury S, Chowdhury SR, Jaisankar P, et al. Isobenzofuranone derivatives exhibit antileishmanial effect by inhibiting type II DNA topoisomerase and inducing host response. *Pharmacol Res Perspect.* (2014) 2:e00070. doi: 10.1002/prp2.70

53. Gonzalez-Miguel J, Larrazabal C, Loa-Meson D, Siles-Lucas M, Simon F, Morchon R. Glyceraldehyde 3-phosphate dehydrogenase and galectin from *Dirofilaria immitis* participate in heartworm disease endarteritis via plasminogen/plasmin system. *Vet Parasitol.* (2016) 223:96–101. doi: 10.1016/j.vetpar.2016.04.029

54. Krause RGE, Hurdayal R, Choveaux D, Przyborski JM, Coetzer THT, Goldring JPD. Plasmodium glyceraldehyde-3-phosphate dehydrogenase: A potential malaria diagnostic target. *Exp Parasitol.* (2017) 179:7–19. doi: 10.1016/j.exppara.2017.05.007

55. Tallima H, Montash M, Veprek P, Velek J, JeŽek J, El Ridi R. Differences in immunogenicity and vaccine potential of peptides from *Schistosoma mansoni* glyceraldehyde 3-phosphate dehydrogenase. *Vaccine.* (2003) 21:3290–300. doi: 10.1016/S0264-410X(03)00180-4

56. Pirovich DB, Da'dara AA, Skelly PJ. *Schistosoma mansoni* glyceraldehyde-3-phosphate dehydrogenase enhances formation of the blood-clot lysis protein plasmin. *Biol Open.* (2020) 9:bio050385. doi: 10.1242/bio.050385

57. Liu X, Li H, Deng H, Zheng C, Yan H, Chen Z, et al. Glyceraldehyde-3-phosphate dehydrogenase of babesia microti is a plasminogen- and actin-binding protein. *Front Vet Sci.* (2019) 6:228. doi: 10.3389/fvets.2019.00228

58. Valenciano AL, Ramsey AC, Mackey ZB. Deviating the level of proliferating cell nuclear antigen in *Trypanosoma brucei* elicits distinct mechanisms for inhibiting proliferation and cell cycle progression. *Cell Cycle.* (2015) 14:674–88. doi: 10.4161/15384101.2014.987611

Frontiers in Veterinary Science

Transforms how we investigate and improve animal health

The third most-cited veterinary science journal, bridging animal and human health with a comparative approach to medical challenges. It explores innovative biotechnology and therapy for improved health outcomes.

Discover the latest Research Topics

See more →

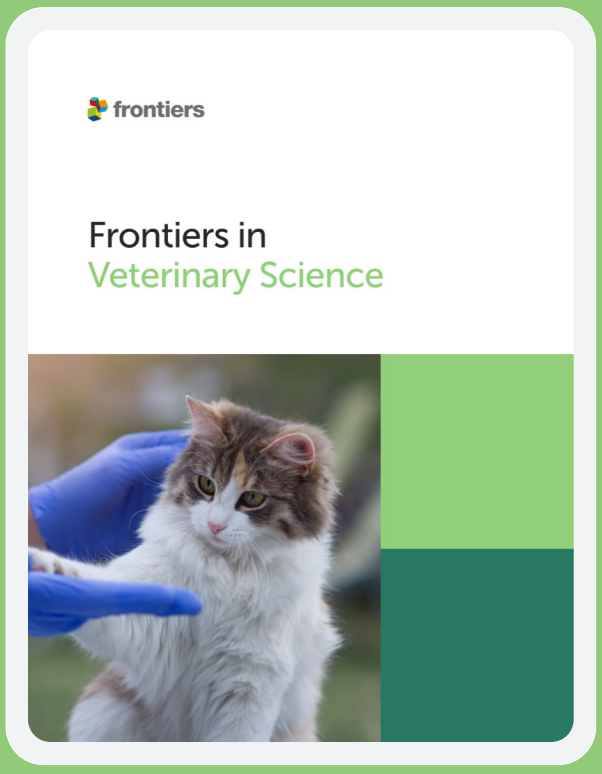

Frontiers

Avenue du Tribunal-Fédéral 34
1005 Lausanne, Switzerland
frontiersin.org

Contact us

+41 (0)21 510 17 00
frontiersin.org/about/contact